

AD-A015 064

INTEGRAL ENGINE INLET PARTICLE SEPARATOR.
VOLUME II. DESIGN GUIDE

Robert J. Duffy, et al
General Electric Company

Prepared for:

Army Air Mobility Research and Development
Laboratory

August 1975

DISTRIBUTED BY:

NTIS

National Technical Information Service
U. S. DEPARTMENT OF COMMERCE

276115

USAAMRDL-TR-75-31B



INTEGRAL ENGINE INLET PARTICLE SEPARATOR

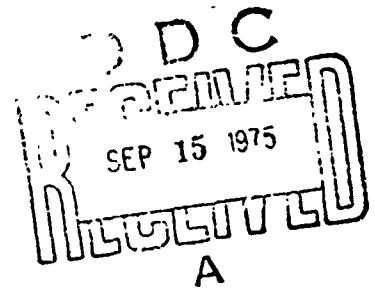
Volume II - Design Guide

General Electric Company
Aircraft Engine Group
Cincinnati, Ohio 45215

ADA 015064

August 1975

Approved for public release;
distribution unlimited.



Prepared for

EUSTIS DIRECTORATE

U. S. ARMY AIR MOBILITY RESEARCH AND DEVELOPMENT LABORATORY

Fort Eustis, Va. 23604

Reproduced by
NATIONAL TECHNICAL
INFORMATION SERVICE
US Department of Commerce
Springfield, VA 22151

**Best
Available
Copy**

EUSTIS DIRECTORATE POSITION STATEMENT

The work reported herein represents the first known systematic investigation of the design variables that influence the performance of integral inlet particle separators. It is expected that the design procedures and performance data described herein will be used in the design of integral inlet particle separators for future Army aircraft gas turbine engines. Appropriate technical personnel of this Directorate have reviewed this report and concur with the conclusions and recommendations contained herein.

Mr. David B. Cale of the Propulsion Technical Area, Technology Applications Division, served as Project Engineer for this effort.

DISCLAIMERS

The findings in this report are not to be construed as an official Department of the Army position unless so designated by other authorized documents.

When Government drawings, specifications, or other data are used for any purpose other than in connection with a definitely related Government procurement operation, the United States Government thereby incurs no responsibility nor any obligation whatsoever, and the fact that the Government may have formulated, furnished, or in any way supplied the said drawings, specifications, or other data is not to be regarded by implication or otherwise as in any manner licensing the holder or any other person or corporation, or conveying any rights or permission, to manufacture, use, or sell any patented invention that may in any way be related thereto.

Trade names cited in this report do not constitute an official endorsement or approval of the use of such commercial hardware or software.

DISPOSITION INSTRUCTIONS

Destroy this report when no longer needed. Do not return it to the originator.

UNCLASSIFIED

SECURITY CLASSIFICATION OF THIS PAGE (When Data Entered)

REPORT DOCUMENTATION PAGE		READ INSTRUCTIONS BEFORE COMPLETING FORM
1 REPORT NUMBER USAAMRDL-TR-75-31B	2 GOVT ACCESSION NO.	3 RECIPIENT'S CATALOG NUMBER
4 TITLE (and Subtitle) INTEGRAL ENGINE INLET PARTICLE SEPARATOR, Volume II - Design Guide		5 TYPE OF REPORT & PERIOD COVERED
		6 PERFORMING ORG. REPORT NUMBER
7 AUTHOR(s) Robert J. Duffy Bernard F. Shattuck		8 CONTRACT OR GRANT NUMBER(s) DAAJ02-73-C-0004
9 PERFORMING ORGANIZATION NAME AND ADDRESS General Electric Company Aircraft Engine Group Cincinnati, Ohio 45215/Lynn, Mass. 01910		10 PROGRAM ELEMENT PROJECT TASK AREA & WORK UNIT NUMBERS 62204A 1G162204AA71 04 001 EK
11 CONTROLLING OFFICE NAME AND ADDRESS Eustis Directorate U.S. Army Air Mobility R&D Laboratory Fort Eustis, Va. 23604		12 REPORT DATE August 1975
		13 NUMBER OF PAGES 236
14 MONITORING AGENCY NAME & ADDRESS (if different from Controlling Office)		15 SECURITY CLASS. (of this report) UNCLASSIFIED
		15a DECLASSIFICATION/DOWNGRADING SCHEDULE
16 DISTRIBUTION STATEMENT (of this Report) Approved for public release; distribution unlimited.		
17 DISTRIBUTION STATEMENT (of the abstract entered in Block 20, if different from Report)		
18 SUPPLEMENTARY NOTES Volume II of a two-volume report		
19 KEY WORDS (Continue on reverse side if necessary and identify by block number) Inlet Particle Separator, Design Guide, Integral, Inertial, Axial, Scroll, Particle Trajectory, Separation Efficiency, Test Specifications		
20 ABSTRACT (Continue on reverse side if necessary and identify by block number) Volume II of this report is a design guide for integral engine inlet separators in the 2 to 15 lb/sec size range. The separators are designed to remove sand, dust, and single foreign objects from the air entering a turboshaft engine. The procedures are based on results of a 30-month program to design and evaluate integral separators in 2, 5, and 15 lb/sec sizes. Also included are procedures developed during the		

DD FORM 1 JAN 73 1473 EDITION OF 1 NOV 65 IS OBSOLETE

UNCLASSIFIED

SECURITY CLASSIFICATION OF THIS PAGE (When Data Entered)

UNCLASSIFIED

SECURITY CLASSIFICATION OF THIS PAGE (When Data Entered)

development of an integral inlet separator for the T700-GE-700 engine.

A definition of a turboshaft engine environment in terms of sand, dust, and foreign objects is included in Appendix A.

Appendix B describes the analysis of individual particle trajectories in separators to predict sand separation efficiency.

Volume I of this report is the final report of the Integral Engine Inlet Protection Device Program. It includes information acquired during the conduct of the program which is not required for the design guide.

UNCLASSIFIED

SECURITY CLASSIFICATION OF THIS PAGE (When Data Entered)

1(a)

TABLE OF CONTENTS

	<u>Page</u>
LIST OF ILLUSTRATIONS.	5
LIST OF TABLES	13
INTRODUCTION	14
Separator Design and Performance.	14
Index to Technical Data	20
PRELIMINARY DESIGN.	23
Definition of Separator Design Requirements.	23
Integrated Design Features.	28
Scaling	36
Foliage Separation.	40
Single Foreign Object	51
Trade-Offs.	51
Materials.	58
Scavenge System	59
AERODYNAMIC DESIGN	68
Flow Path Definition.	68
Swirl Vane Design	86
Deswirl Vane Design	109
Scavenge Vane Design.	126
MECHANICAL DESIGN.	140
Swirl Frame	140
Front Frame	142
Main Frame.	142
Anti-Icing.	145
Manufacturing Considerations.	155
Reliability and Safety.	158
Vulnerability	159
SCROLL SEPARATORS.	160
DESIGN CHECKLIST	172

TABLE OF CONTENTS - Continued

	<u>Page</u>
TEST REQUIREMENTS	175
Test Specifications	175
Components Test	181
REFERENCES.	191
APPENDIXES.	196
A. Important Elements of the Helicopter Environment	196
B. Trajectory Analysis	217
LIST OF SYMBOLS	234

LIST OF ILLUSTRATIONS

<u>Figure</u>		<u>Page</u>
1	T700 Turboshaft Engine With Inlet Separator	15
2	T700 Type Inlet Separator Schematic	16
3	Exploded View of Major Components	16
4	T700 Separator - Cross Section and Parts Identification .	17
5	AC Coarse Efficiency vs g Field	19
6	Particle Trajectory Through Swirl Vanes	20
7	Sand Particle Trajectories	21
8	Percentage of Initial Power vs Pounds of Sand Ingested. .	25
9	2 Lb/Sec T700 Type Separator With PTO Shaft Canted Forward	30
10	2 Lb/Sec T700 Type Separator With PTO Shaft Between Swirl Vaness and Scavenge Air Vanes	31
11	2 Lb/Sec T700 Type Separator With PTO Shaft Canted Aft .	32
12	Air-Oil Separator	35
13	Compressor Inlet Guide Vane	36
14	T700 Type Separator Flow Path for 2 Lb/Sec Engine	38
15	Comparison of Engine Inlet Separators of 2, 5, and 15 Lb/Sec.	39
16	Foliage Sample - Wet Swamp Grass	41
17	Foliage Sample - Semidry Hay	42
18	Foliage Sample - Semidry Leaves	43

LIST OF ILLUSTRATIONS - Continued

<u>Figure</u>		<u>Page</u>
19	Ingested Foliage (Hay) on Struts	44
20	Ingested Foliage (Hay) on Inlet Guide Vanes.	45
21	Foliage Collector	46
22	Ingested Hay on Foliage Collector.	47
23	Foliage Collector Capability - Pressure Loss vs Foliage Ingested (Hay)	48
24	Leaves on Foliage Collector.	49
25	Swamp Grass on Foliage Collector	50
26	Foreign Object Ingestion Test Results - Airflow at De- sign Point	52
27	Foreign Object Ingestion Test Results - Airflow at 40 Percent of Design Point (Idle)	53
28	C-Spec Efficiency vs Pressure Loss	54
29	AC Coarse Efficiency vs Pressure Loss.	55
30	Scavenge Flow Requirements	62
31	Scavenge Blower Design Parameters.	63
32	Blower Configurations.	64
33	Effect of Sand Ingestion on Scavenge Blower Performance.	64
34	Blower Impeller.	66
35	Wear on Blower Aluminum Housing.	67
36	Area Distribution Through Separator Based on Radius.	69
37	L/R ₁ Separator Shape (See Table 6) - T700 Flow Path.	70
38	2 Lb/Sec L/R ₁ Separator Flow Path.	76
39	5 Lb/Sec Swirlless Flow Path With Design 3 Inner Wall.	79

LIST OF ILLUSTRATIONS - Continued

<u>Figure</u>		<u>Page</u>
40	Aero Analysis of 5 Lb/Sec Swirlless Flow Path, Showing Stations.	82
41	Mach Number Distribution for 5 Lb/Sec Separator Model - Vaneless.	84
42	Wall Static Pressure for 5 Lb/Sec Separator Model - Vaneless.	85
43	Area Through Vaneless Separator - Based on $\psi = 0.6$ Flow Mach Number	87
44	C-Spec Efficiency vs Swirl Level.	88
45	AC Coarse Efficiency vs Swirl Level	89
46	Core Pressure Loss vs Swirl Level	90
47	Swirl Vane Clocking Relative to Deswirl Vanes	91
48	2 Lb/Sec Swirl Vane Profile (Reference Table 3)	93
49	Vane Trailing-Edge Thickness as Part of Passage Width	93
50	5 Lb/Sec Thinned Design 3 Vane.	95
51	Design 3 Separator Swirl System	95
52	Vane Pressure - Side Slope.	96
53	Separation Efficiency With AC Coarse Material vs Swirl Level	97
54	15 Lb/Sec Design 3 Trailing-Edge Extension.	99
55	Mach No. Along Wall of 5 Lb/Sec Separator With Swirl Vanes	102
56	Comparison of Rainstep Swirl Angle Prediction With Test Data.	103
57	Flow Field With False Wall.	105
58	Wall Mach Number Distribution for 5 Lb/Sec Separator With Swirl Vanes	106

LIST OF ILLUSTRATIONS - Continued

<u>Figure</u>		<u>Page</u>
59	5 Lb/Sec Separator Model Wall Static Pressures With Swirl Vanes	107
60	Core Swirl Angle With No Deswirl Vanes - 5 Lb/Sec Separator Model	109
61	Deswirl Vane in Separator	111
62	PTO Vane Section.	111
63	Total Pressure Profiles, 2 Lb/Sec Separator.	113
64	Total Pressure Profiles, 5 Lb/Sec Separator	114
65	Total Pressure Profiles, 15 Lb/Sec Separator.	115
66	Schematic of Secondary Flows.	116
67	Deswirl Vane Lean	116
68	Separator Exit Radial Profiles at Design Airflows	117
69	Effect of Changing Flow Path Contour With a Deswirl Vane - 5 Lb/Sec Separator Model With Swirl Vanes	119
70	Separated Region and Linear Deswirl Distribution - 5 Lb/Sec Model With Swirl Vanes	120
71	Wall Mach Number Distribution for 5 Lb/Sec Separator With Flow Path Changes	121
72	Wall Mach Number Distribution for 5 Lb/Sec Separator With Leaned Deswirl Vanes.	122
73	5 Lb/Sec Separator Cambered Plate Circular Arc Deswirl Vane.	123
74	5 Lb/Sec Separator Model With Vane Wall Static Pressures	124
75	Traverse in Front of the Scavenge Vanes at Design Scavenge Flow	127

LIST OF ILLUSTRATIONS - Continued

<u>Figure</u>		<u>Page</u>
76	T700 Separator Traverse in Front of the Swirl Vanes (Slim Duct) - $W_{sa} = 1.32$	128
77	2 Lb/Sec Scroll Pressure Loss	129
78	5 Lb/Sec Scroll Pressure Loss	130
79	15 Lb/Sec Scroll Pressure Loss.	131
80	2 Lb/Sec Separator Off-Design Core Pressure Loss.	132
81	5 Lb/Sec Separator Off-Design Core Pressure Loss.	133
82	15 Lb/Sec Separator Off-Design Core Pressure Loss	133
83	AC Coarse Collection Efficiency vs Scavenge Flow Ratio.	134
84	AC Coarse Efficiency vs Scavenge Flow Ratio - 15 Lb/Sec Model.	134
85	5 Lb/Sec Scroll Vane.	137
86	5 Lb/Sec Model - Scroll Vane Leading Edge Definition	138
87	5 Lb/Sec Inlet Separator Scroll Area Schedule	139
88	Separator Front Frame Cross Section	141
89	Positive or Negative Overlap at Flange Joints	143
90	Mount Support Plates on Separator	143
91	Acceptable Positive Overlap	143
92	T700 Main Frame Oil System.	146
93	T700 Front Engine Mounts.	147
94	Anti-Icing System of Axial Separator.	148
95	Swirl Vane - No Baffle.	151
96	Swirl Vane - With Raffle.	151

LIST OF ILLUSTRATIONS - Continued

<u>Figure</u>		<u>Page</u>
97	Swirl Vane - Centerbody Baffle.	151
98	Swirl Vane - Partition Baffle	151
99	Swirl Vane - Serpentine Flow Path	152
100	Swirl Vane - Film Heating With Baffle	152
101	Swirl Vane - Combination Film and Impingement Heating . .	152
102	Swirl Vane - Combination Film and Impingement Heating . .	152
103	Swirl Vane Anti-Icing Air Discharge Port.	153
104	2 Lb/Sec Turboshaft Engine With Inlet Scroll Separator. .	161
105	Scroll Separator Cleanout - Cross Section	163
106	Scroll Separator Tangential Inlet	165
107	Frictional Resistance In A Smooth Pipe.	169
108	Scroll Separator Pressure Loss Variation With Flow Area .	169
109	Scroll Separator Tested	171
110	2 Lb/Sec Scroll Separator Inlet Rework.	171
111	Schematic of Separator Facility	179
112	Inlet Separator Test Cell	180
113	Cross Section of Typical Separator Model.	183
114	Separator Model Instrumentation	185
A-1	Engine Inlet Sand Concentration CH-3C (Single Rotor) - MCAS, Yuma, Arizona	199
A-2	Engine Inlet Sand Concentration - CH46A (Tandem Rotor) - Patuxent River NATC.	199
A-3	Aircraft Cabin Roof Sand Concentration - HTK (Dual Rotor) - Test Site Unknown	200

LIST OF ILLUSTRATIONS - Continued

<u>Figure</u>		<u>Page</u>
A-4	Aircraft Cabin Roof Sand Concentration - Wesser (Single Rotor) - Ghibli, North Africa	200
A-5	Aircraft Right Rear Wheel Sand Concentration.	201
A-6	Sand Concentration - Australia.	202
A-7	Terrain Particle Size Distribution - Far East	203
A-8	Terrain Particle Size Distribution - United States.	204
A-9	Terrain Particle Size Distribution - Southeast Asia	205
A-10	Particle Size Distribution - Phillips Drop Zone, Yuma, Arizona	206
A-11	Particle Size Distribution - Vehicle Dust Course, Yuma, Arizona	207
A-12	Particle Size Distribution - Lee Drop Zone, Ft. Benning, Georgia	208
A-13	Particle Size Distribution - Southwest Research In- stitute Dust Coarse, San Antonio, Texas	209
A-14	Particle Size Distribution - Standard United States Test Dusts	210
A-15	Foreign Object Damage - Commonly Ingested Items	214
B-1	Typical Separator Flux Plot	220
B-2	Typical Test Sand Particle Size Distribution.	222
B-3	Trajectories of Particle Injected at $\psi = 0.122$	223
B-4	Critical Diameter Distribution for Figure B-3	224
B-5	Local Efficiency Distribution for Figure B-3.	225
B-6	Hidden Splitter Separator Flux Plot	226
B-7	Critical Diameter Distribution for Figure B-6	227

LIST OF ILLUSTRATIONS - Continued

<u>Figure</u>		<u>Page</u>
B-8	Local Efficiency Distribution for Figure B-6.	227
B-9	Trajectories of Particle Injected at $\psi = 0.380$	228
B-10	Critical Diameter Distribution for Figure B-9	229
B-11	Jane Impact Point Crossplot for Figure B-9.	231
B-12	Local Efficiency Distribution for Figure B-9.	231
B-13	Comparison of Predicted and Measured Separation Efficiency	232

LIST OF TABLES

<u>Table</u>		<u>Page</u>
1	Index to Technical Data for 2 Lb/Sec, 5 Lb/Sec, and 15 Lb/Sec Separators	22
2	Oil System Requirements and Volumes	33
3	2 Lb/Sec Separator Testing Summary.	71
4	5 Lb/Sec Separator Testing Summary.	72
5	15 Lb/Sec Separator Testing Summary	73
6	Typical Separator Flow Path	75
7	2 Lb/Sec Separator Flow Path	77
8	5 Lb/Sec Separator Flow Path	80
9	2 Lb/Sec Swirl Vane	94
10	Design 3A 5 Lb/Sec Swirl Vane	98
11	Design 3 New Swirl Vane	100
12	Deswirl Vane Cascade Characteristics.	110
13	5 Lb/Sec Separator Model Deswirl Vane Circular Arc Flat Plate	125
14	Scavenge Exhaust System, Splitter, IGV's and Swirl Frame.	154
15	2 Lb/Sec Scroll Separator Testing Summary	170

INTRODUCTION

SEPARATOR DESIGN AND PERFORMANCE

Aircraft frequently operate in environments (see Appendix A) which can cause engine damage or failure because of the ingestion of foreign matter. The engine may gradually be eroded by sand and dust to the point where its stall margin, power or fuel consumption becomes unacceptable; the engine may catastrophically fail because of ingestion of a wrench, bird, or large piece of ice; or the engine may be shut down by a rag or foliage which cuts off its air supply. In order to avoid the occurrence of events of this kind, foreign material must be prevented from entering the compressor inlet of the engine. This design guide is intended to provide the basis for designing aircraft engine inlet separators which will, to a large extent, accomplish that purpose. The separator designs in this guide are for a turboshaft engine and are all of the axial inertial type in which objects are separated from the compressor airflow without the use of screens or barrier filters. Screens and barrier filters are not recommended for military aircraft because they are very bulky; have high total pressure losses; clog up easily with materials such as rags, grass, or leaves; cannot be anti-iced easily; and, when damaged by foreign objects or weapon fire, can contribute debris which goes directly into the engine.

Figure 1 shows the General Electric T700 engine with an integral inlet separator. Figure 2 shows the separator schematically in three dimensions, and Figure 3 shows the major components in an exploded view. Figure 2 indicates the dust and sand separation technique which is the important function of a separator. Figure 4 is a cross-section schematic which identifies the important elements of a separator. Air (in which there may be entrained sand or dust, single foreign objects, foliage, rags, ice, water, or snow) enters through the inlet swirl vanes (1). The particles in the air either bounce off the swirl vanes toward the outer wall (9) or are forced to move in that direction by the centrifugal force on the particle caused by its angular momentum. The particle acquires angular momentum since it tends to follow the streamlines in the airflow, and the streamlines have a tangential velocity (swirl) induced by the swirl vanes. Particles are also directed toward the outer wall by the shape of the forward part of the inner wall (8). Particles which impinge on the sloping inner wall bounce outwardly, and the inertia of the particles also tends to carry them toward the outer wall. In this way the particles in the air are concentrated near the outer wall, where they enter the scavenge system through the scavenge air vanes (12). The contaminated scavenge air flows from the scavenge vanes into the collection scroll (7), which ducts it to the scavenge blower. From the blower it is sent overboard through a vent. The "clean" air which follows the inner part of the flow path enters the

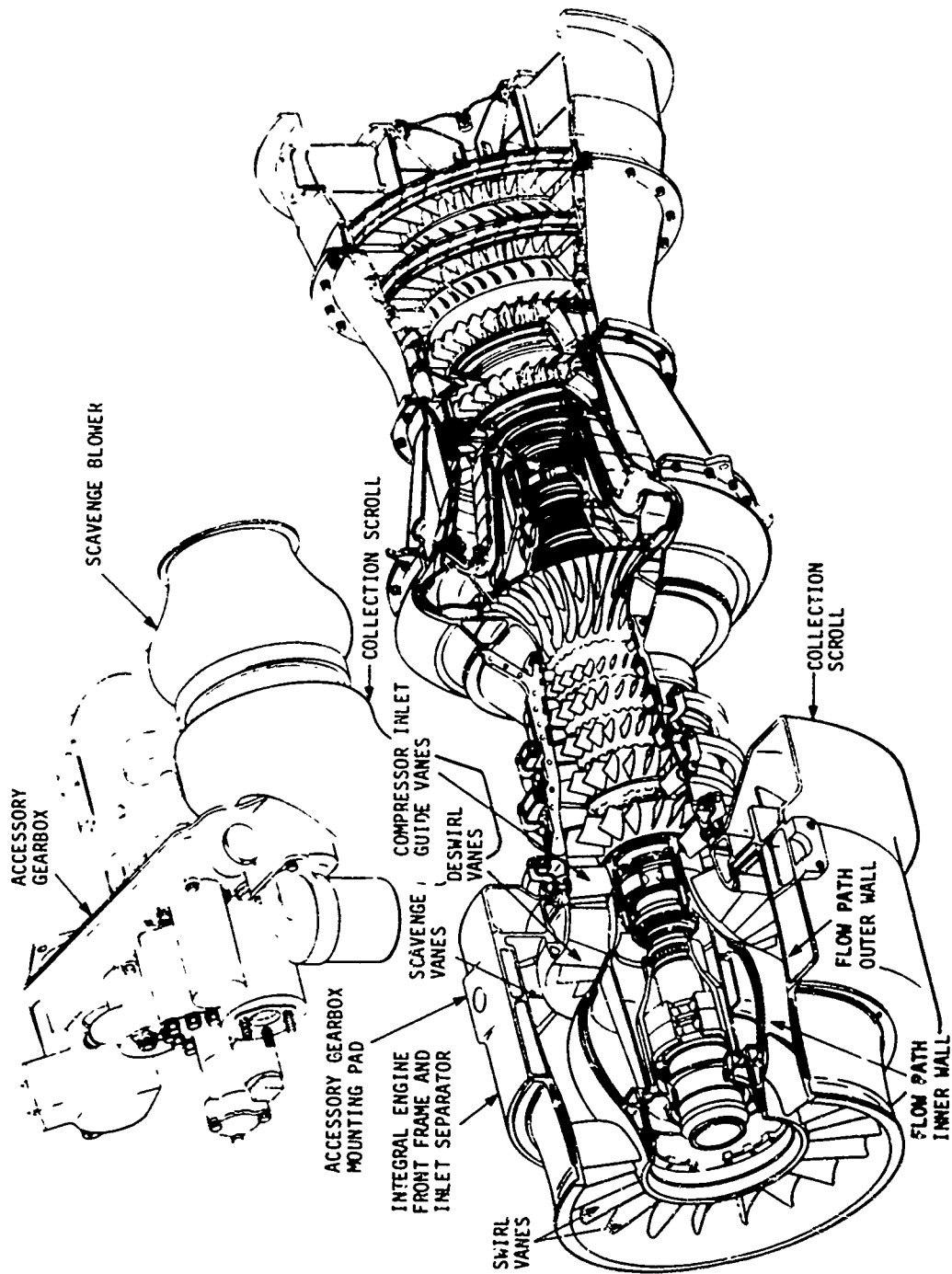


Figure 1. T700 Turboshaft Engine With Inlet Separator.

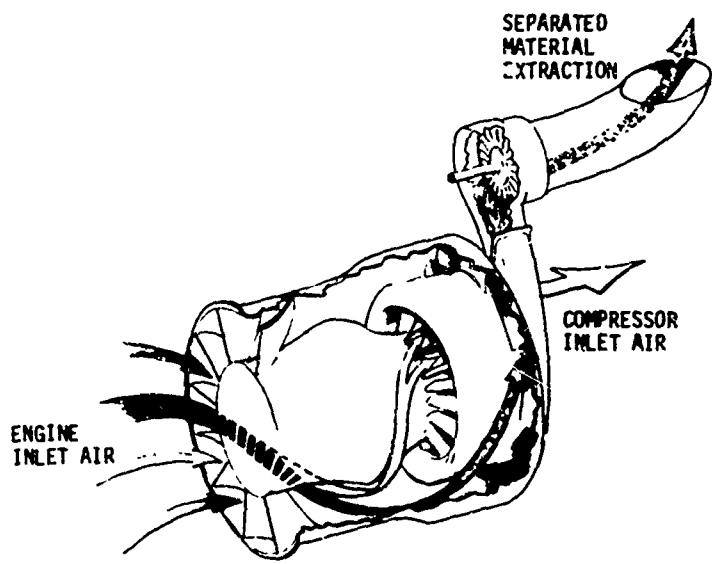


Figure 2. T700 Type Inlet Separator Schematic.

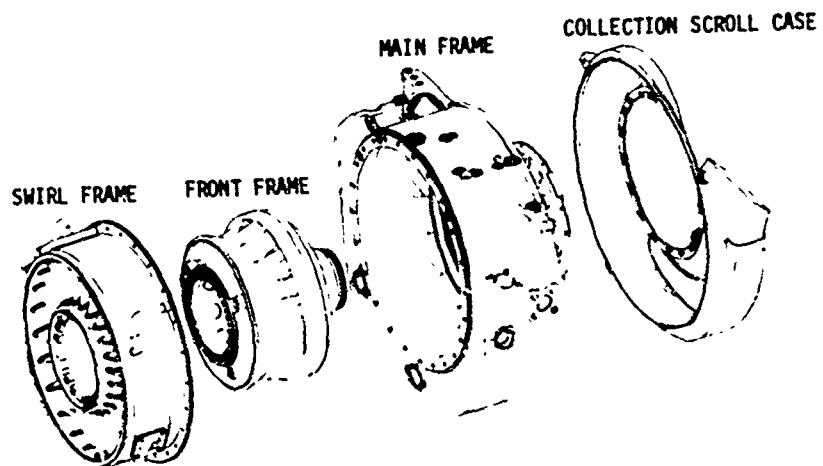
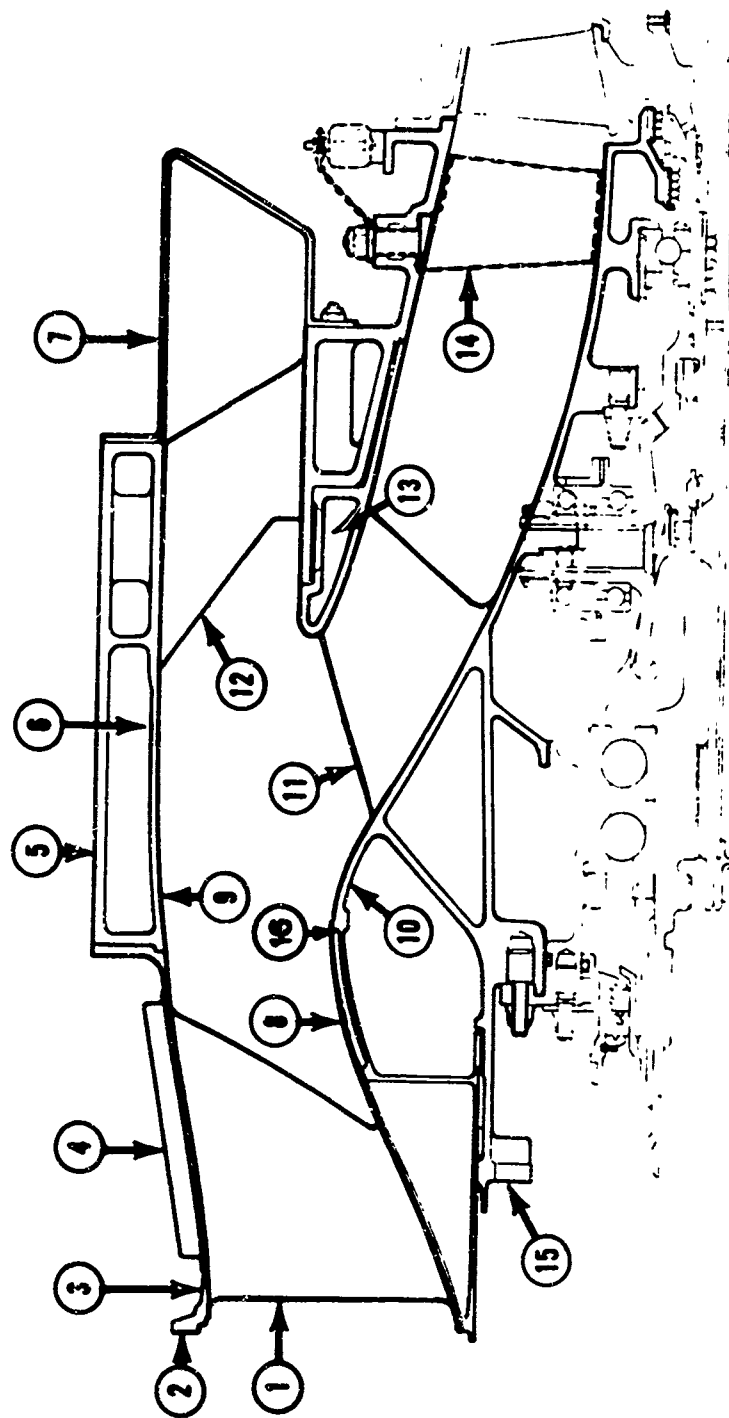


Figure 3. Exploded View of Major Components.



- | | | |
|-------------------------------|---------------------------|---------------------------------|
| 1. INLET SWIRL VANE | 6. OIL TANK | 11. DESWIRL VANE |
| 2. FORWARD QUICK-DISCONNECT | 7. SCAVENGE AIR COLLECTOR | 12. SCAVENGE AIR VANE |
| 3. FLANGE CUSTOMER CONNECTION | 8. INNER WALL | 13. ANTI-ICING AIR PLENUM |
| 4. SWIRL FRAME | 9. OUTER WALL | 14. COMPRESSOR INLET GUIDE VANE |
| 5. ANTI-ICING MANIFOLD | 10. FRONT FRAME | 15. CUSTOMER CONNECTION |
| | | 16. RAINSTEP |

Figure 4. T700 Separator - Cross Section and Parts Identification.

engine through deswirl vanes (11) which remove its angular velocity. From the deswirl vanes the clean engine air flows through the compressor inlet guide vanes (IGV) (14) to the engine. Several other features of an integral engine inlet particle separator are shown in Figure 4. The figure indicates that engine design considerations which affect the separator design include anti-icing, bearing housing, oil tank, engine mounting, accessory gearbox support, customer connections, oil cooling, and mounting for several engine accessories.

The performance of an inlet separator is described by its capacity to remove particles from the engine air and by total pressure losses in the clean engine air and the contaminated scavenge air. The figure of merit for removing particles, usually called separation efficiency, can be defined in different ways, two of which are commonly used. The definition based on weight is

$$\eta_w = (\text{WEIGHT OF SAND SCAVENGED}) / (\text{WEIGHT OF SAND AT SEPARATOR INLET}) \quad (1)$$

The second definition recognizes a penalty for scavenge airflow. It is

$$\eta_c = 1 - (\text{SAND CONCENTRATION AT IGV}) / (\text{SAND CONCENTRATION AT SEPARATOR INLET}) \quad (2)$$

where concentration is (Sand Flow)/(Airflow). The two efficiencies are related by the equation

$$\eta_c = \eta_w - (1 - \eta_w) (\text{SCAVENGE AIRFLOW}) / (\text{COMPRESSOR AIRFLOW}) \quad (3)$$

This equation shows the penalty assessed for scavenge flow, which is usually given as a percentage of the compressor airflow. As a result of trade-off studies and experience, 15 to 20% has become the normal range of scavenge flow. No matter which definition of separator efficiency is used, prediction of separation efficiency for a particular separator design requires a particle trajectory analysis. The analysis is based on a definition of the separator aerodynamic flow field (speed and flow direction). Then a point-by-point calculation of individual particle paths through the flow field is carried out.

A characteristic quantity describing the swirling separator airflow is the "g-field" strength. This quantity is defined as the air tangential velocity (V_θ) squared divided by a reference radius (R).

Separation efficiency is a function of "g-field" strength for a given separator design, as shown in Figure 5; but at the same value of "g-field" strength, different separator designs give different values of separation efficiency.

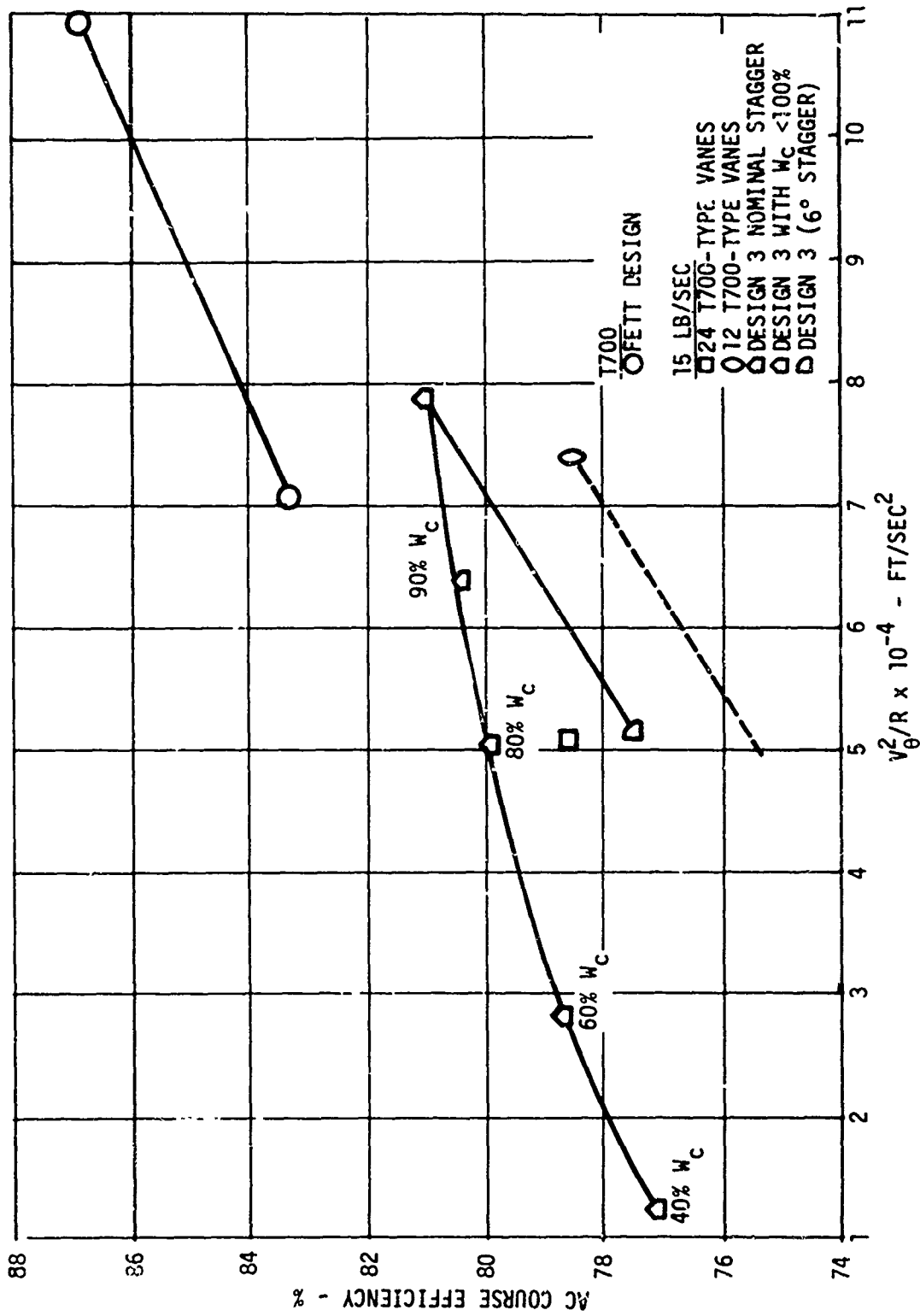


Figure 5. AC Course Efficiency vs g Field.

Particle trajectory analysis must consider particle deflection by the swirl vanes, as shown in Figure 6. Small particles (less than 40μ) are separated primarily by the aerodynamic forces. Large particles (greater than 40μ) are separated by aerodynamic forces and by bouncing off the swirl vanes. This feature is illustrated by the trajectory analysis result shown in Figure 7, where sand particles are shown being deflected off the swirl vanes toward the separator outer diameter. The trajectory paths in Figure 7 have been rotated into the plane of the graph and include the tangential deflection shown in Figure 6.

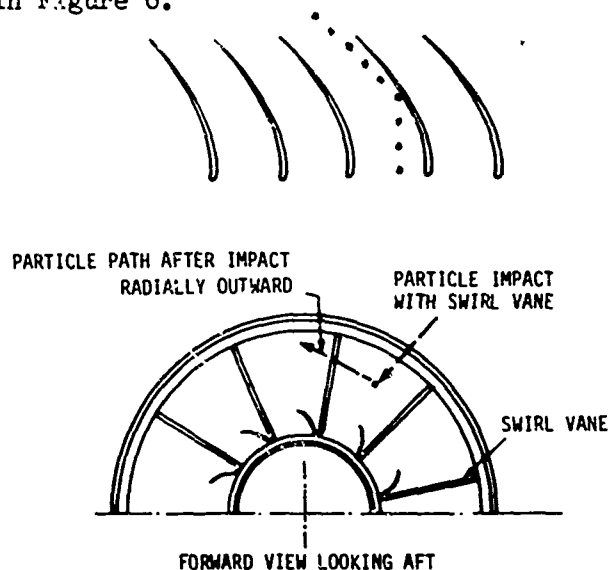


Figure 6. Particle Trajectory Through Swirl Vanes.

It is also possible to design an inertial separator without vanes. In that case particles bounce off the inner flow path. Their design and analysis of vaneless separator is otherwise similar to that of a vaned separator. Reasonable separator efficiencies are achieved by making the splitter radial height in Figure 7 equal to the maximum diameter of the separator inner wall. This is called a "hidden splitter lip" design since the splitter lip can not be seen by looking straight into the separator. This design also benefits from the significant "g-field" established in the meridional plane by the air turning from the hub maximum diameter into the compressor inlet passage.

INDEX TO TECHNICAL DATA

To make this final report as useful as possible, an index to the technical data contained in both volumes of the report is included as Table 1. Table 1 serves a secondary purpose by indicating the parameters which are important to the design of an inlet particle separator.

SAMPLE TRAJECTORIES $\psi = .380$
 $Z = .28$
 $\theta_i = 10^\circ$ (MIDWAY BETWEEN VANES)
 $V_i = 0^\circ$

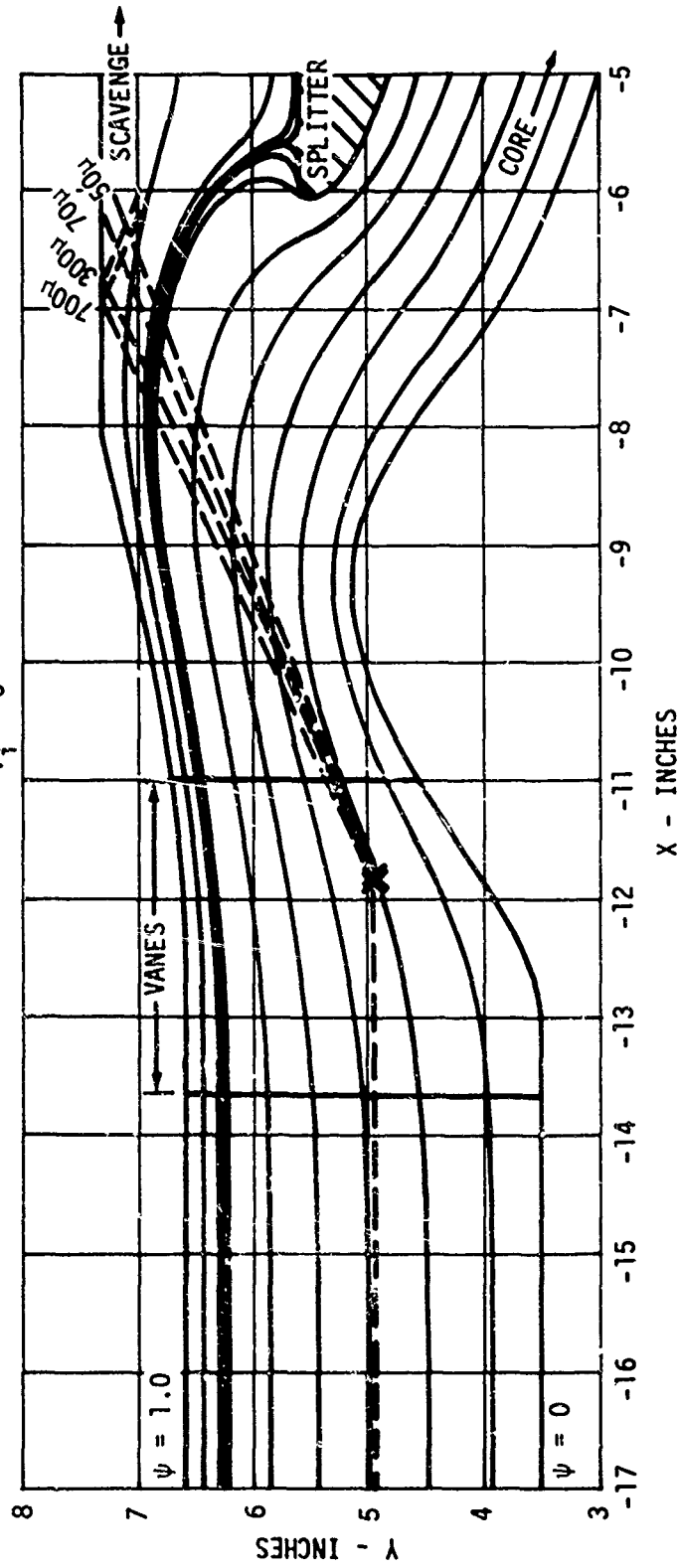


Figure 7. Sand Particle Trajectories.

TABLE 1. INDEX TO TECHNICAL DATA FOR 2-LB/SEC, 5-LB/SEC, AND 15-LB/SEC SEPARATORS
(Volume No. - Page No.)

Parameter	2 Lb/Sec Separators	5 Lb/Sec Separators	15 Lb/Sec Separators
Swirl Vane			
Shape	I-64, II-92, II-97	I-74, II-92, II-97	I-51, I-56, I-57, I-58, I-82, I-84, II-99
Location	II-86	II-86	I-57, I-84, II-86
Solidity	I-64, II-86, II-91, II-92	I-74, II-86, II-91	I-51, I-98, II-86, II-91, II-92
Swirl Vane	I-64, II-19, II-86	I-77, II-19, II-86	I-82, I-87, I-88, I-89, II-19, II-86
Flow Path			
Aerodynamics	I-33, I-63, II-68	I-46, I-73, I-77, II-68	I-56, I-84, II-68
Separator Efficiency	I-64, II-68	I-73, I-74, II-68	I-82, I-83, I-84, I-85, I-92, II-68
Scavenge Flow Ratio	I-66, II-18, II-129, II-132 II-134	I-75, II-18, II-130, II-133, II-134	I-95, I-96, I-98, II-18, II-131, II-133, II-134
Deswirl Vane			
Shape	II-109	II-109	II-109
Location	II-112, II-109	II-112, II-132, II-109	II-112, II-109
Solidity	I-64	II-112	II-112
Scroll Vanes	I-64, II-126	I-76, II-126	II-126

PRELIMINARY DESIGN

DEFINITION OF SEPARATOR DESIGN REQUIREMENTS

Aerodynamics

Before an inlet particle separator detail design is initiated, it is necessary to determine what level of protection from the various kinds of inlet debris is required and what the cost will be. This may be defined by customer requirements or it may result from a trade-off between separator performance and factors such as cost, weight, power, fuel consumption penalties, and reliability. Data from Appendix A can be used to determine the amount of sand that the engine would be expected to ingest during its operating life in the proposed application.

Next, the engine to be protected is compared with engines that have experienced controlled sand ingestion tests. Using these engines as a guide, it is possible to assess the new engine's capability to withstand sand ingestion. Factors to be considered are:

1. Material differences between critical components of known engine and proposed separator engine.
2. Rotor tip speed.
3. Rotor and stator leading edge radii.
4. Compressor and turbine clearances and land material.
5. Turbine operating temperature and cooling schemes.
6. Effect of compressor and turbine deterioration on cycle performance.
7. Combustor design (reverse flow combustors of sufficient flame temperature have a tendency to melt ingested sand, causing fused globules of sand material to accumulate on the turbine).¹
8. IR suppressor design, if any, and its susceptibility to clogging, coating erosion, or other damage due to sand ingestion.

Using the above information, an estimate can be made of the amount of sand that the engine can ingest before excessive power loss² occurs. Excessive power loss may be defined by the engine specification or, if not, could be based on T₅ or some aircraft mission. Over 10% power loss is usually considered excessive.

One method of making the estimate is to compare the difference between the erosion parameter

$$U^{2.3} \times f_a \times f_d$$

for the proposed engine and the known engine, where U is the blade section tangential velocity, f_a is depth of erosion, based on material and impact angle,³ in mils, and f_d is a normalized severity factor² to account for leading-edge radii.

A typical erosion calculation proceeds as follows for a first-stage compressor rotor blade:

1. Define blade material.
2. Define blade leading-edge radii at all sections to be considered for definition of normalized leading-edge factor from Reference 2.
3. Assume that sand particle velocity is zero at the blade leading edge and use this fact to define the sand impact angle on the blade based on compressor speed and section leading-edge angle. Use a compressor speed corresponding to the power setting at which the ingestion test was run.
4. Tabulate calculation of the erosion parameter as follows:

		<u>(1)</u>			<u>(2)</u>	<u>(3)</u>	<u>(1)x(2)</u>	<u>(1)x(2)x(3)</u>
	Radius Ratio	$U^{2.3}$ (ft/sec $\times 10^{-6}$)	L.E. Angle (deg)	L.E. Dia. (in.)	f_a (mil)	f_d -		
Tip	1.0	20.308	67.3	.0069	2.8	3.7	56.9	210.4
Pitch	.780	12.151	64.5	.0095	2.95	3.3	35.8	118.3
Hub	.545	5.018	56.0	.0154	3.35	2.6	.6.8	43.7

The above table implies that blade hub erosion damage is about 20.8% of tip erosion damage. Field experience for the engine indicates that blade hub chord reduction is 18% of tip chord reduction. Performing the same calculation on the proposed engine and comparing the erosion parameters gives an estimate of the proposed engine's ability to withstand sand erosion.

Power loss is a function of total pounds of sand ingested. Power loss increases as mass average sand particle size increases. Figure 8 shows the results of controlled tests on the same engine design using various particle sizes. There is a general increase in power loss per pound of sand

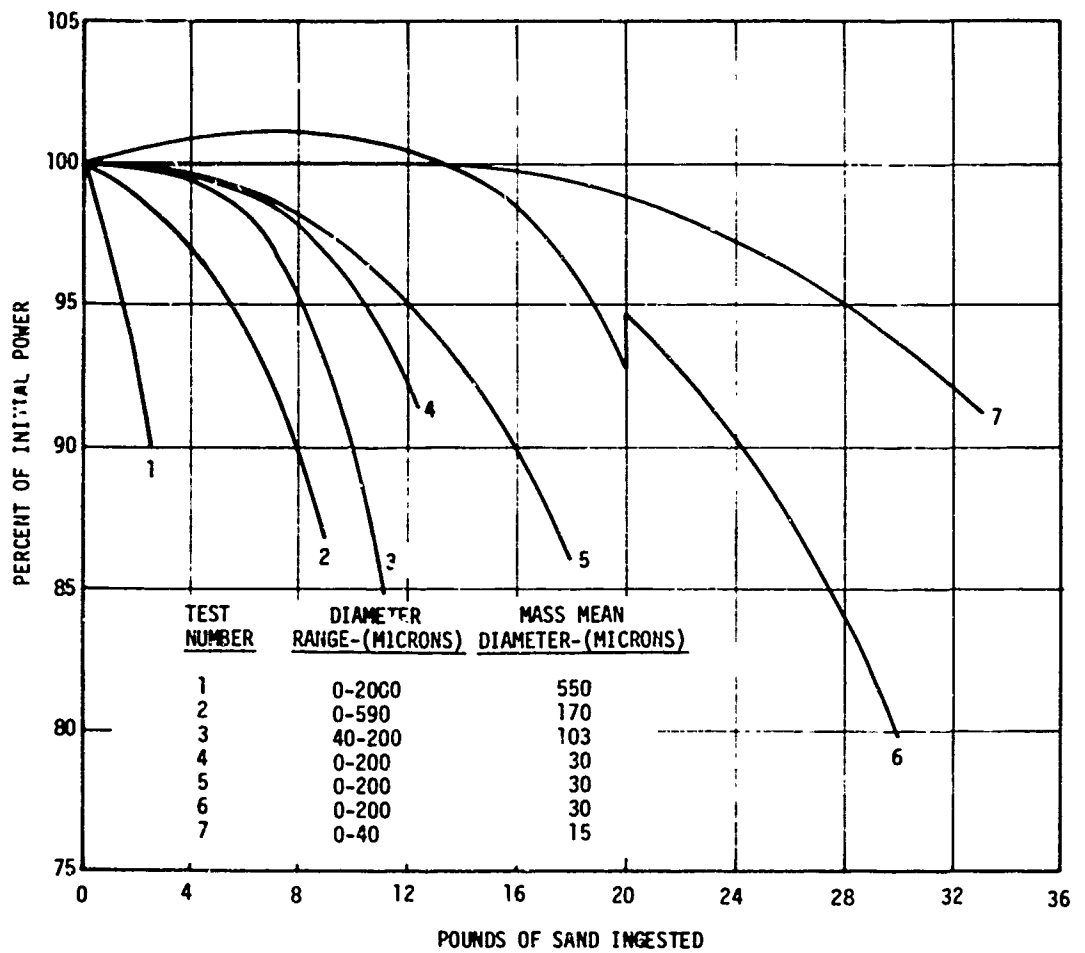


Figure 8. Percentage of Initial Power vs Pounds of Sand Ingested.

as average sand size increases. Therefore, the engine data used in the above estimate should be generated with sand that is approximately the same particle size as the sand that the proposed engine will ingest.

Mechanical

Preliminary mechanical design of an integral inlet separator includes consideration of the following:

1. Separator size and shape.
2. Mechanical integration into the engine.
3. Scavenge exhaust system and its integration with the engine and aircraft.
4. Separator anti-icing.
5. Provisions for services such as oil lines, anti-icing air, and wash manifold.
6. Integration into aircraft installations including customer connections and main engine mounts.
7. Manufacturing methods, weight, size, and cost.
8. Materials, stress concentration, loading, fatigue, and corrosion.
9. Thermal compatibility.
10. Reliability, maintainability, vulnerability, and safety.

Principal Structural Components

Figure 4 shows a typical separator cross section, which usually consists of:

1. Swirl frame (Item 1).
2. Main frame (Item 5).
3. Engine front frame (Item 10).
4. Scavenge air collector (Item 7).
5. Customer structural connections (Items 2 and 15).

In an integral separator many major components and features are integrated into one basic structure. These multipurpose structures require greater study and evaluation than would otherwise be required. As an example, the main frame shown in Figure 4 is not only a structural member but also

serves as an oil tank, has deaeration capability, and provides for an air-oil heat exchanger and scavenge vanes which are structural members. An important consideration in such a part is thermal compatibility. Sudden or steep thermal gradients which may exist in scavenge vanes could result in cracking and failure of the assembly. If oil passes through the vanes, any cracking could result in loss of oil and ultimately in loss of the engine.

Guidelines for Integral Inlet Separator

An integral inlet separator design requires many design studies and trade-offs. Some of the basic requirements which should be included in the preliminary design and trade-off studies for an integral inlet separator are:

1. Decision is required initially on swirlless separator versus a separator having swirl vanes.
2. Correct sizing and design of the oil sump and its components are some of the first items that must be done. These parts determine and influence the size and shape of the flow path.
3. Method of supporting the engine must be established early since this affects the design and structural requirements of the separator.
4. Engine structural loads from operational and maneuver forces must be determined early. Structures must be subassemblies that are capable of being assembled and disassembled easily for inspection and replacement.
5. The separator inlet must be sized to handle core engine air and the extra scavenge air.
6. All separator parts must be able to handle their assigned share of structural loads. In addition, vanes or struts must be optimized for structural and aerodynamic considerations including capability to withstand impacts from single foreign objects without failure or excessive deformation.
7. Scavenge air scroll collector and blower must be capable of withstanding sand, single foreign objects, and bleed air temperatures. Either metal or relatively thick high-temperature plastic should be usable for the scroll collector. Metal reinforcements may be necessary to prevent excessive wear at key locations such as bends.
8. Vanes and/or struts must be large enough for service lines running into the engine sump and for deicing fluids (usually air or oil) where they are used.

9. Since the accessory gearbox (AGB) power takeoff (PTO) shafting and gearing are difficult to incorporate in small sizes, special attention must be provided to avoid excessive strut or vane size.
10. Radial spline and PTO for AGB must be smaller in diameter than the opening through which it must pass.
11. Separator scavenge blower must have a good bearing support for the impeller. An overhanging, grease-lubricated, single bearing shaft is not acceptable.
12. Anti-icing of all separator air flow path surfaces is necessary. This includes all vanes through IGV's, all surfaces, and the scavenge system including the scroll collector.
13. After use, anti-icing air should be dumped into the scavenge system which it will help to anti-ice. Any anti-icing air entering the engine core should be kept to an absolute minimum to prevent heating of the inlet air to the engine core.
14. Anti-icing air should have an ON-OFF control and be regulated to prevent excessive use of bleed air and to prevent overtemperaturing of materials such as aluminum or plastics.
15. Anti-icing air must not be higher in temperature than materials can withstand, assuming a valve failure resulting in continuous anti-icing.
16. Thermal matching of structural parts and assemblies is necessary to prevent cracking or failures due to excessive thermal stresses.
17. An integral engine oil system, contained in the separator, must include provisions for oil:
 - a. Expansion.
 - b. Settling (dwell time).
 - c. Flight maneuver loads (rolling, tilting, etc.).
 - d. Negative "g" operation.
 - e. Deaeration.
 - f. Adequate scavenge pump capacity.
 - g. Cooling (air-oil heat exchange or oil-fuel heat exchange).
 - h. Loss of oil during operation.
 - i. Filling.
 - j. Passage or lines.

INTEGRATED DESIGN FEATURES

To obtain efficient utilization of space and weight, the separator design must be integrated with other engine parts and subsystems, such as the lube

system, accessories, accessory gearbox, PTO, anti-icing of vanes, structural frames, aero-thermo systems, oil-air heat exchanger, and engine mounting. These are all engine parts and subsystems that have a direct influence upon each other, upon the engine, and upon the separator. Inlet particle separators in the 2 to 15 lb/sec size range have similar problems. A brief description of some of the major subsystems and how they relate to the separator design is given in this design guide. Specific information for each new application must be obtained through the detailed design of the separator for the particular engine involved. Scaling or estimating the loads, flows, quantities and volumes for different size engines and for different configurations is very generalized and is intended to be used as a guide and not as replacement for specific information for the particular design.

For separator design based on the axial type integral separator of Figure 2, it is possible that a complete integration of all the subsystems is the wrong approach for a particular engine. It is necessary to consider separators that have separate as well as integrated oil tanks, ejector as well as blower exhaust systems, and ON-OFF as well as continuous scavenge

Accessories, accessory gearboxes, and accessory power requirements must also be considered when designing separators. Although not part of the basic separator design, the size of the accessory power load and the size and location of the PTO shafting, PTO bearings and seals, PTO gearing, power input gearing, and bearings influence separator designs.

A separator design must minimize distances to assure good gearing relationships. Long gear overhangs from thrust bearings cause excessive backlash, gear wear, misalignment, and gear binding in cases of thermal transients. PTO shafting, gearing, and splines are sized on the basis of assumed starter loading and then checked against the total assumed accessory power load when running.

For good aerodynamics and high separation efficiencies in the small size separators (2 to 5 lb/sec) the AGB-PTO shafting goes through the swirl vanes rather than the deswirl vanes. This permits a reduction in the size of the struts in the inlet duct or the compressor inlet and in the scavenge air exhaust. Examples of separators with the AGB-PTO shafting at different locations are shown in Figures 9 through 11.

For preliminary design studies, typical accessory requirements and accessory sizes can be found in Volume 1, Table 2. Actual data on accessory sizes and ratings depend on the particular engine design and its requirements since accessories are not directly or equally scalable. Some accessories such as temperature and pressure sensing equipment are nearly the same size regardless of engine rating. Other accessories such as the blower or lube pump are more nearly scalable.

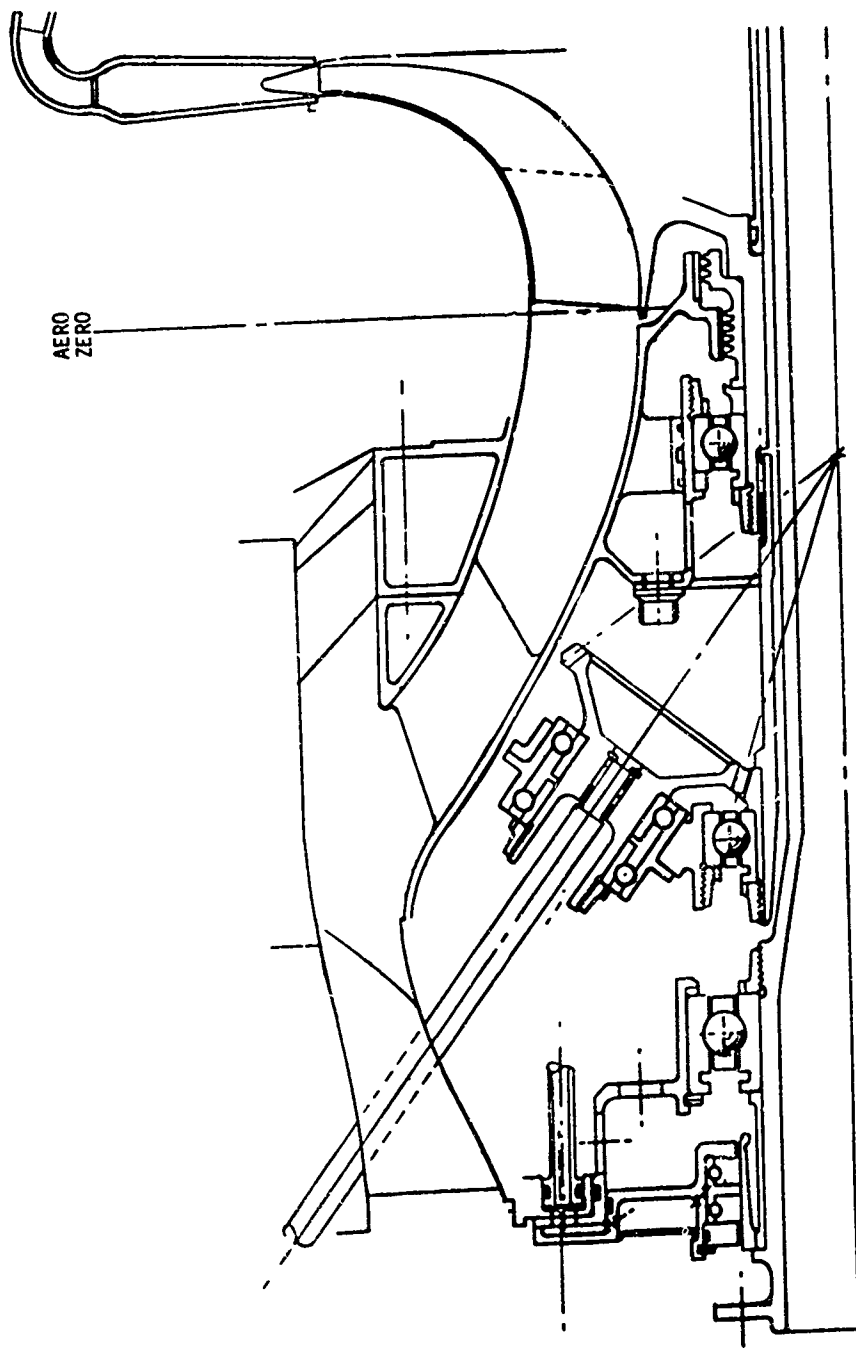


Figure 9. 2 Lb/Sec T700 Type Separator With PT0 Shaft Canted Forward.

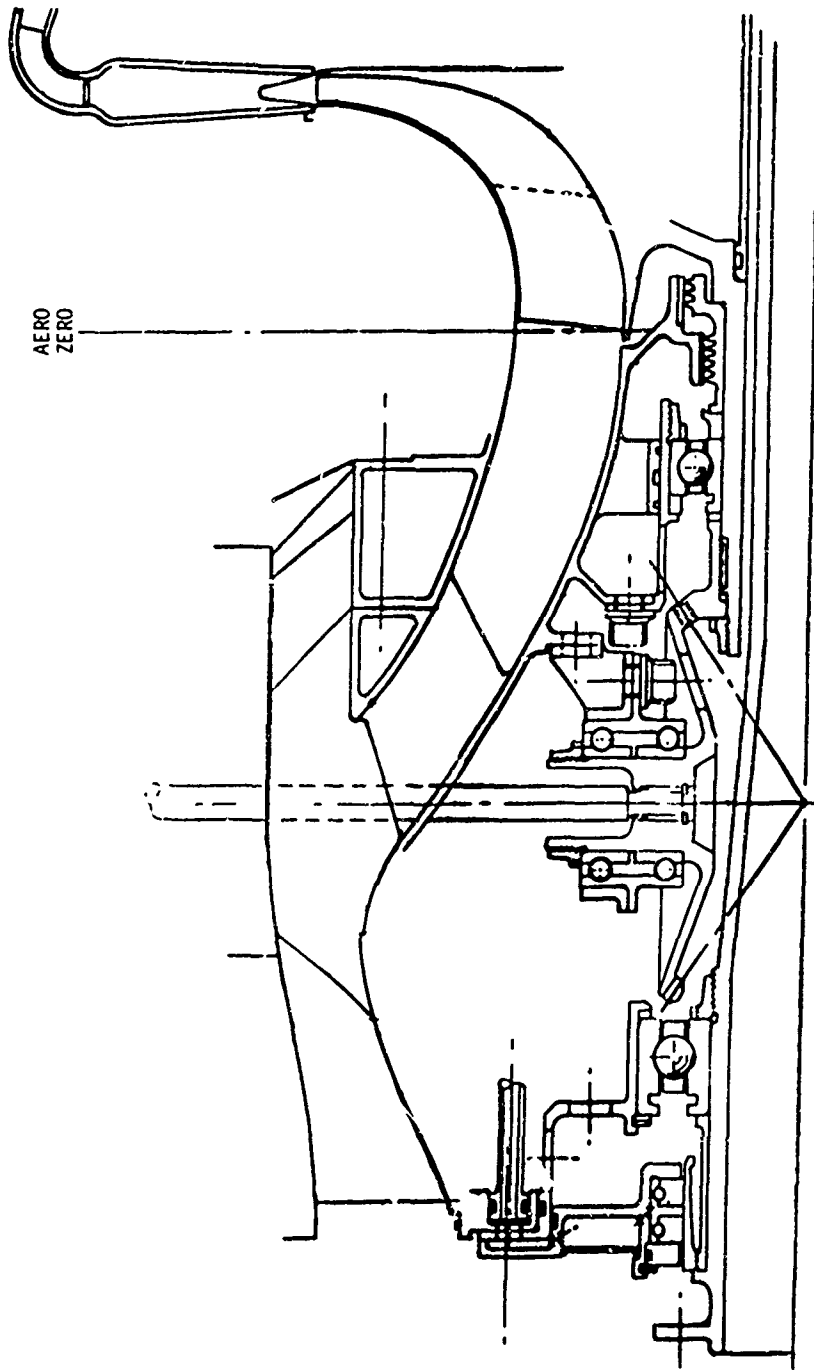


Figure 10. 2 Lb/Sec T700 Type Separator With PTO Shaft Between Swirl Vanes and Scavenge Air Vanes.

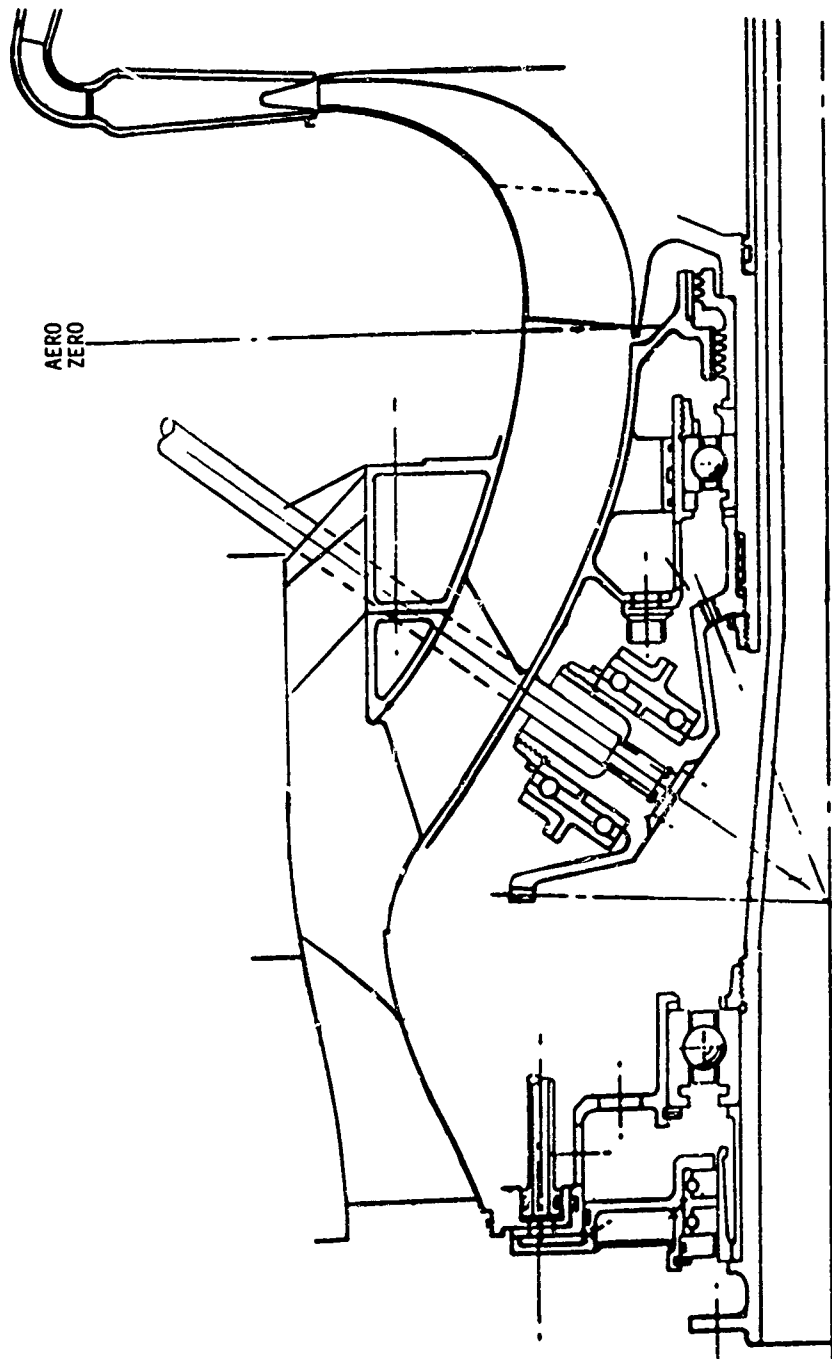


Figure 11. 2 Lb/Sec F700 Type Separator With F70 Shaft Canted Aft.

Oil System

In a similar manner, estimates of oil flows and oil tank capacities were made as a guide only, since each engine has different requirements (see Table 2).

	Engine Size (Airflow, lb/sec)		
	2	5	15
Oil Tank Volume - (gal oil only)	1.2	1.5	2.1
Usable Oil (gal)	.3	.4	.6
Oil Flow (gal./min)	2.5	3.3	4.5
Dwell Time (sec)	20	20	20
Expansion Air Space (%vol.)	--	--	10-25

Integration of the oil system into the separator design allows use of the high-temperature oil to eliminate thermal gradients and the resulting stress in the separator structure.

Front Oil Sump

Oil sump requirements have a major influence upon the size and shape of the separator and its flow path. The oil system and the front oil sump have to be defined and sized very early in the program. Factors to be considered are:

1. Speed of the engine shaft and related parts.
2. Size, speed, torque, location, and lubrication of the main power output shaft and bearings.
3. Size, speed, torque, location, and lubrication of the bearings, gearing, and shafting to provide power to the accessory gearbox.
4. Space for emergency lube system.
5. Amount and method of heat transfer.
6. Space for anti-icing air, service lines.
7. Negative "g" capability.
8. Deaeration of oil.

9. Thermal growth of parts.
10. Bearing design including type, alignment, clearances required, oil lube, and scavenge.
11. Structural assembly (subassemblies).

Space must be allowed between the inner flow path and the sump proper for necessary walls and passageways to carry anti-icing air and oil as required. The sump and inner structure must be built as easy-to-assemble-and-disassemble subassemblies. The rainstep at the inner flow path usually makes a good breakpoint and provides good visibility of internal sump parts, including gearing.

For 2 to 5 lb/sec engine sizes, it is recommended that the radial PTO shaft be located at the front of the gearbox and pass through the swirl vanes radially, rather than at an angle (see Figure 9, 2 lb/sec cross section). This reduces the axial length, minimizes effect on the swirl vane passages, and minimizes size and weight. The splined shaft shown can be removed radially. It should be noted that a full spline is recommended over a square type shaft to carry the load because the latter has misalignment and wear problems. Make sure that the spline is smaller than the opening it has to pass through.

The sump design must also include negative "g" capability provision for angle of climb, angle of descent and roll conditions, deaeration of the oil and positive oil feed to the bearings with a two-jet provision (if possible) to provide good scavenging and heat transfer capability. The sump is sized at least 25% oversize to handle aerated oil. Since the oil sump, oil flow, oil deaeration, and oil tank have common system problems, the integration of the oil system helps to solve these problems in minimum space and with minimum complexity. By allowing oil to dribble down over the inner wall of the outer casing, most of the air is removed from the oil. To obtain greater deaeration, or for an alternate deaeration method, the air-oil separator design shown in Figure 12 is very effective in removing entrained air from the oil. This separator centrifuges the oil by spinning it as a thin film on the inside of a small, tapered cylinder so that the air is pushed out of the oil into the center of the cylinder, which is vented to the air vent system. The spinning oil is ducted out the opposite end of the cylinder. This deaerator is small, 1 to 2 inches in diameter and 2 to 4 inches long, has no moving parts, and is very reliable. It is especially effective when the oil dwell time is small, as occurs in small engines. Air separation efficiencies of 95 to 99.5% are readily attainable with this configuration.

The size, speed, loading and lubrication of the bearings have a direct effect upon the size of the sump, particularly for small engines and engine separators. For almost all applications, the DN of the bearings determines, or is a major factor in, the design. (Note that D is bearing bore diameter

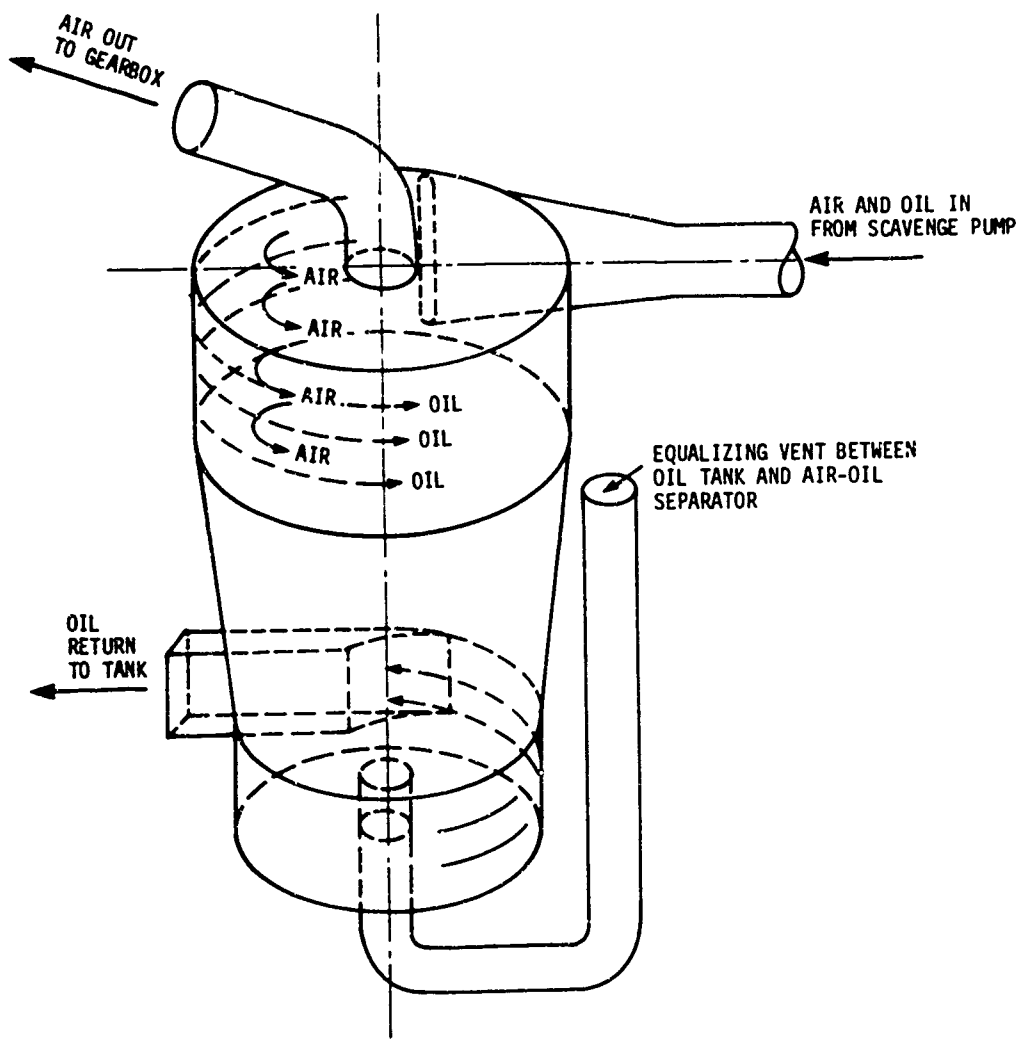


Figure 12. Air-Oil Separator.

in millimeters and N is bearing speed in RPM.) For small bearings, a DN value of 700,000 is acceptable; higher DN's up to 1,500,000 are feasible but with greater risk. Bearing alignment, bearing clearances, and lubrication details such as rate, method, point of introduction, and method and point of scavenge become extremely critical as DN values increase.

Deswirl vanes (Item 11 of Figure 4) can be incorporated into the compressor inlet guide vanes (IGV) as shown in Figure 13. While this feature has not been incorporated in existing separator design, it should be explored as a method of reducing system pressure loss and axial length.

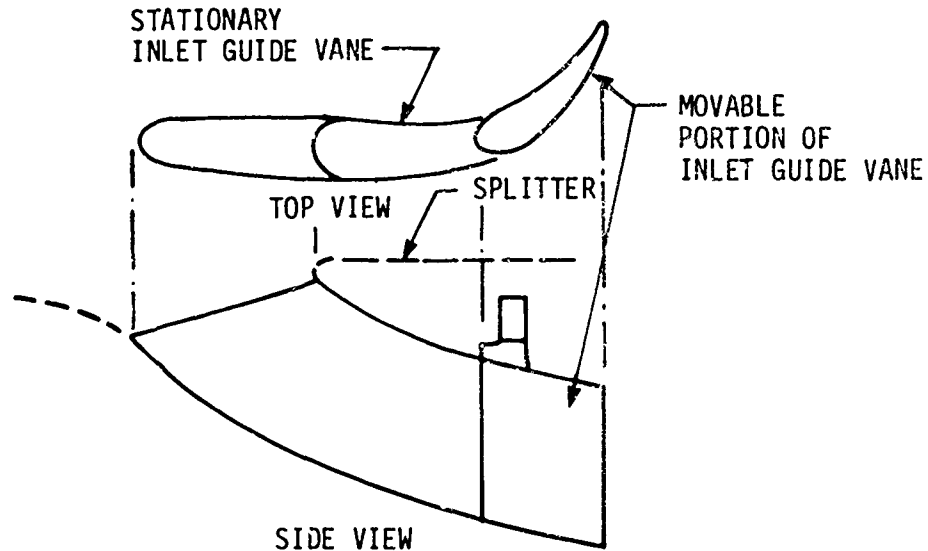


Figure 13. Compressor Inlet Guide Vane.

SCALING

As engine size and engine airflow decrease below 5 lb/sec, the integral separator size gets proportionately larger and larger and is no longer a true mechanical scale-down of the baseline separator configuration. This is due principally to the fact that the oil sump and the AGB-PTO gearing located inside the sump cannot be scaled directly. In addition, relatively larger struts and vanes are required to accommodate anti-icing passages and the PTO shaft. Axial spacing of parts also increases proportionately.

A comparison of a true scale reduction of an axial integral separator flow path for a 2 lb/sec engine size, with a modified scale separator for a 2 lb/sec size, is shown in Figure 14. The modified scale separator is approximately 16% longer and approximately 37% larger in diameter. The difference between the two flow paths is caused by limitations in size of ball bearings, shafting, gearing, seals and other mechanical parts. In addition, the sump must be larger to meet engine flight requirements, such as angle of climb, descent, pitch and roll, "g" loading, and oil deaeration.

A comparison study of engine inlet separators of 2, 5 and 15 lb/sec sizes is shown in Figure 15. Both 5 and 15 lb/sec designs are true scale, and the 2 lb/sec size is the modified scale, larger than true scale.

Examination of the three separator designs of Figure 15 shows the effect of component size. Although there are the same number of gears, bearings, and seals, as these parts get smaller they take up a larger percentage of the available volume.

In scaling to smaller sizes, the PTO shafting is especially difficult to integrate since its size decreases much less rapidly than does the vane or strut through which it passes. The inverse happens as separator sizes are scaled up, so no problem exists for the 15 lb/sec engine separator. Direct scaling of struts and vanes is not usually feasible or possible for the smaller size engine separators. Mechanical sizing of the sump is influenced by the AGB-PTO shafting, bearings and gearing, and for the space required by the front drive power takeoff bearings and shafting. Consequently, vanes and struts for the smaller separator cannot be direct scale. Directly scaled vanes are also too small internally for functional uses such as porting engine oil, housing the AGB-PTO shafting, or housing service lines. At least one oversize swirl vane or strut must be provided for the AGB-PTO radial shafting. This results from a PTO shaft diameter which changes only a small amount with engine airflow variations while the thickness of the vane or strut decreases rapidly as engine sizes decrease.

Detailed information on vane sizes, vane shapes, and number of vanes is given in the section on aerodynamic design and should be used in scaling. Care must be taken, however, to check the size of scaled vanes to be sure that oil lines, radial shafting and passages can go through the vanes.

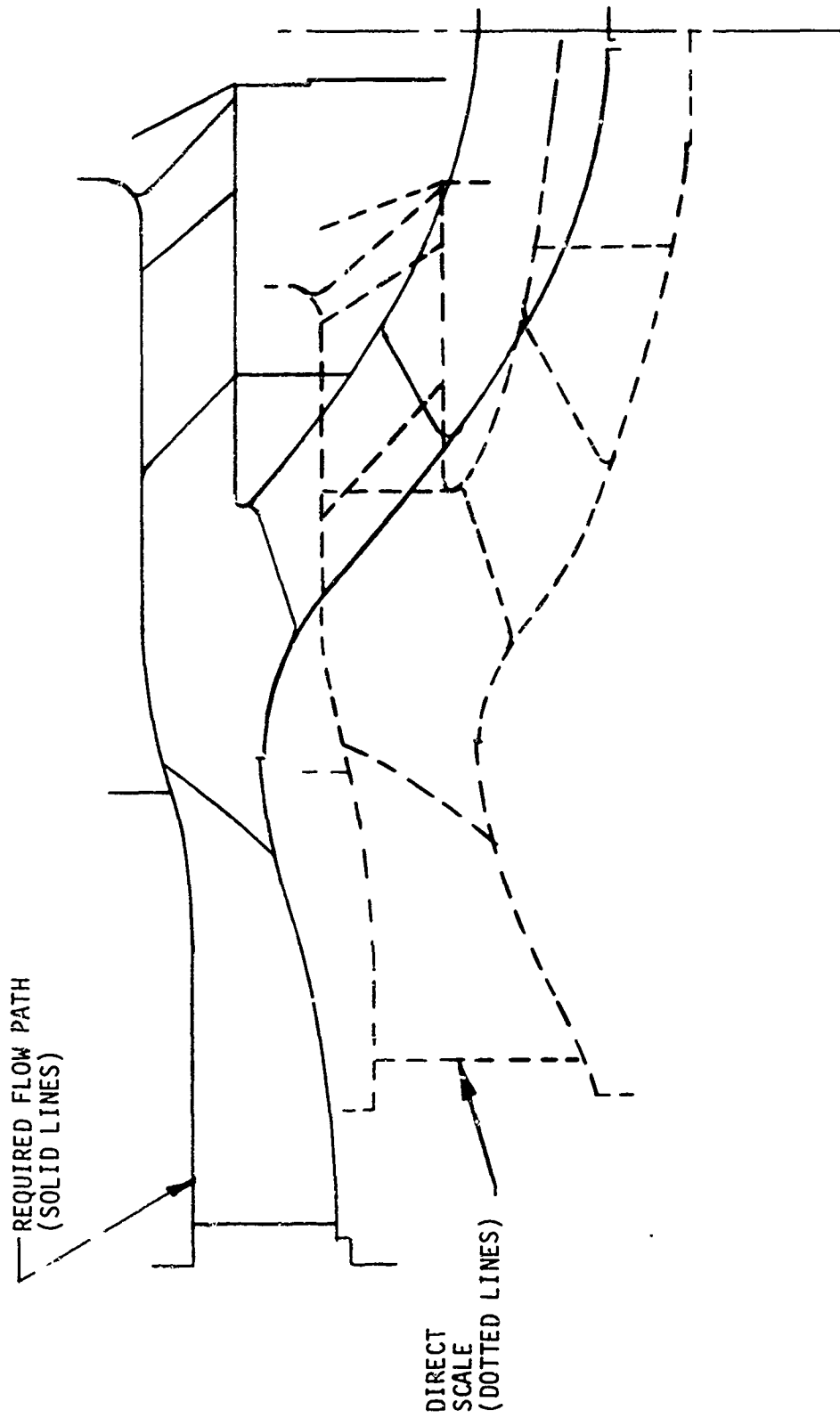
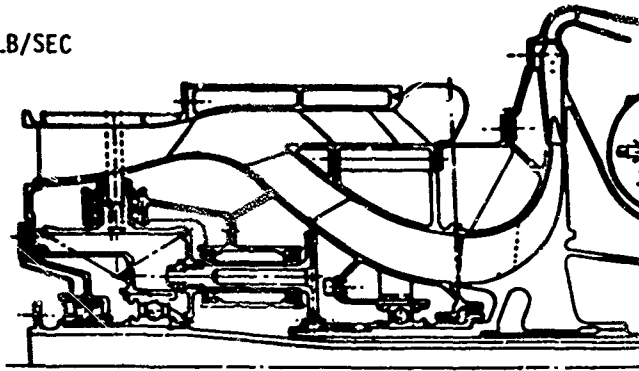
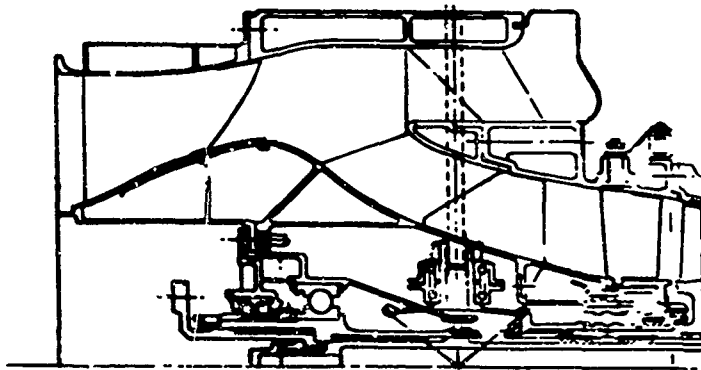


Figure 14. T700 Type Separator Flow Path for 2 Lb/Sec Engine.

2 LB/SEC



5 LB/SEC



15 LB/SEC

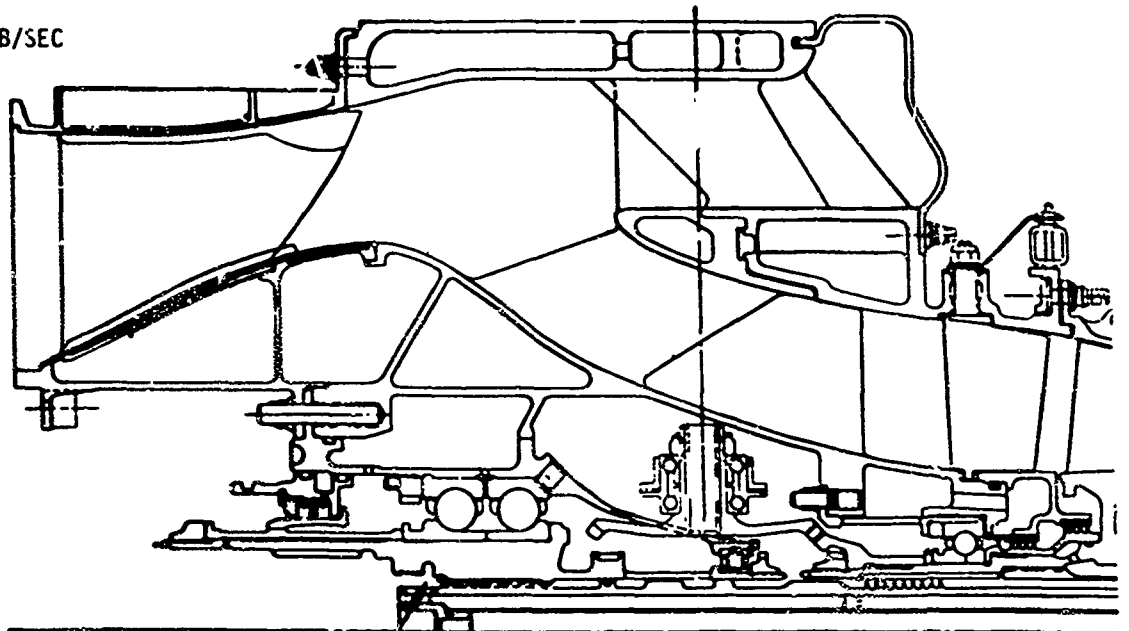


Figure 15. Comparison of Engine Inlet Separators of 2, 5, and 15 Lb/Sec.

FOLIAGE SEPARATION

The ingestion of foliage into a turboshaft engine usually results in clogged compressor inlet guide vanes when a centrifugal separator is used. Events of this kind are undesirable since they may cause engine shutdown as the result of a stall. There should be no damage to the engine from foliage ingestion, but there have been instances of compressor blade failure due to the stall.

Typical examples of foliage used in separator tests are shown in Figures 16, 17, and 18. To determine the effect of foliage ingestion, random-length (4 to 15 in.) hay was fed into a T700 type particle separator with swirl vanes removed. The central hub was supported by five struts in this test. Results indicate that 20% of the hay was collected on the five struts (Figure 19), 20% was scavenged, and 60% entered the gas generator inlet. Most of the hay ingested followed the aerodynamic streamlines. Ingestion of 0.2 lb of hay resulted in the unacceptable condition shown on Figure 20 with 25% pressure loss at the deswirl vane exit. The results of these tests show that if foliage protection is required, it must be provided ahead of all blade rows and struts.

A relatively simple foliage collector, based on the radial spoke inclined screen shown schematically in Figure 21, was designed and tested. There was 5% pressure loss with 0.2 lb of hay ingested. Figure 22 shows conditions after this amount of ingestion. Data from this test is plotted on Figure 23. Leaves and swamp grass were also ingested, with the results shown on Figures 24 and 25. These tests indicate that protection against foliage is possible by a relatively simple system which can be provided in kit form as optional protection to be used when the operational environment permits. The foliage separator designed for this test was an engine part, integral with the particle separator. Therefore, the foliage had to be separated and scavenged. Since very large amounts of foliage could clog the scavenge system, the foliage separator is more effective when designed as a simple "cowcatcher" located ahead of the inlet. The cowcatcher shunts foliage, rags, and large birds overboard, preventing them from entering the engine's inlet system.

Since anti-icing a cowcatcher type of foliage separator is a difficult task, it is enough to make it retractable or easily removable. If it is removable on the ground only, its use is restricted to nonicing conditions. It could be automatically removable in the air and not be anti-iced.

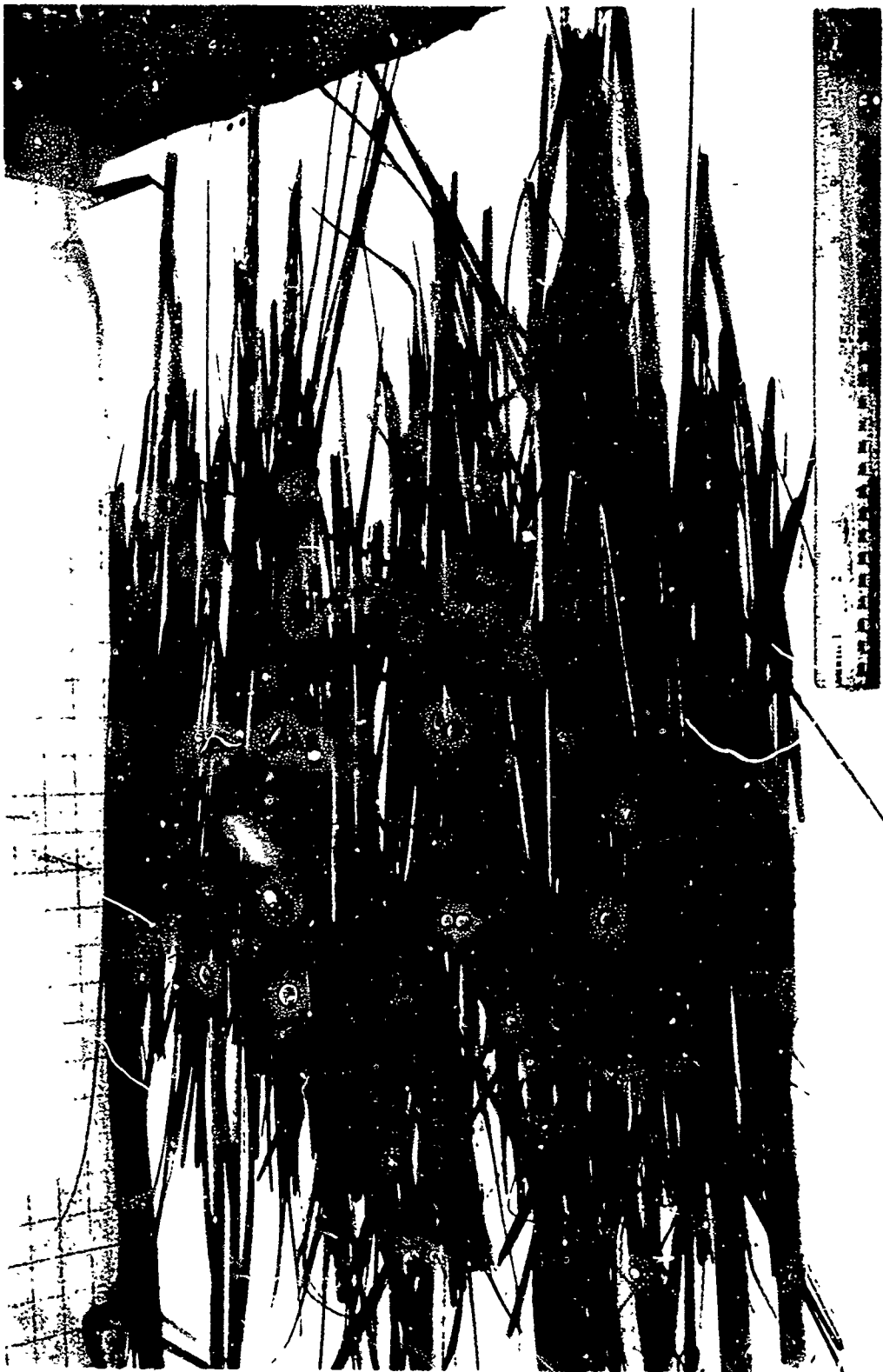


Figure 16. Foliage Sample - Wet Swamp Grass.



Figure 17. Foliage Sample - Semidry Hay.



Figure 18. Foliage Sample - Semidry Leaves.



Figure 19. Ingested Foliage (Hay) on Struts.



Figure 20. Ingested Foliage (Hay) on Inlet Guide Vanes.

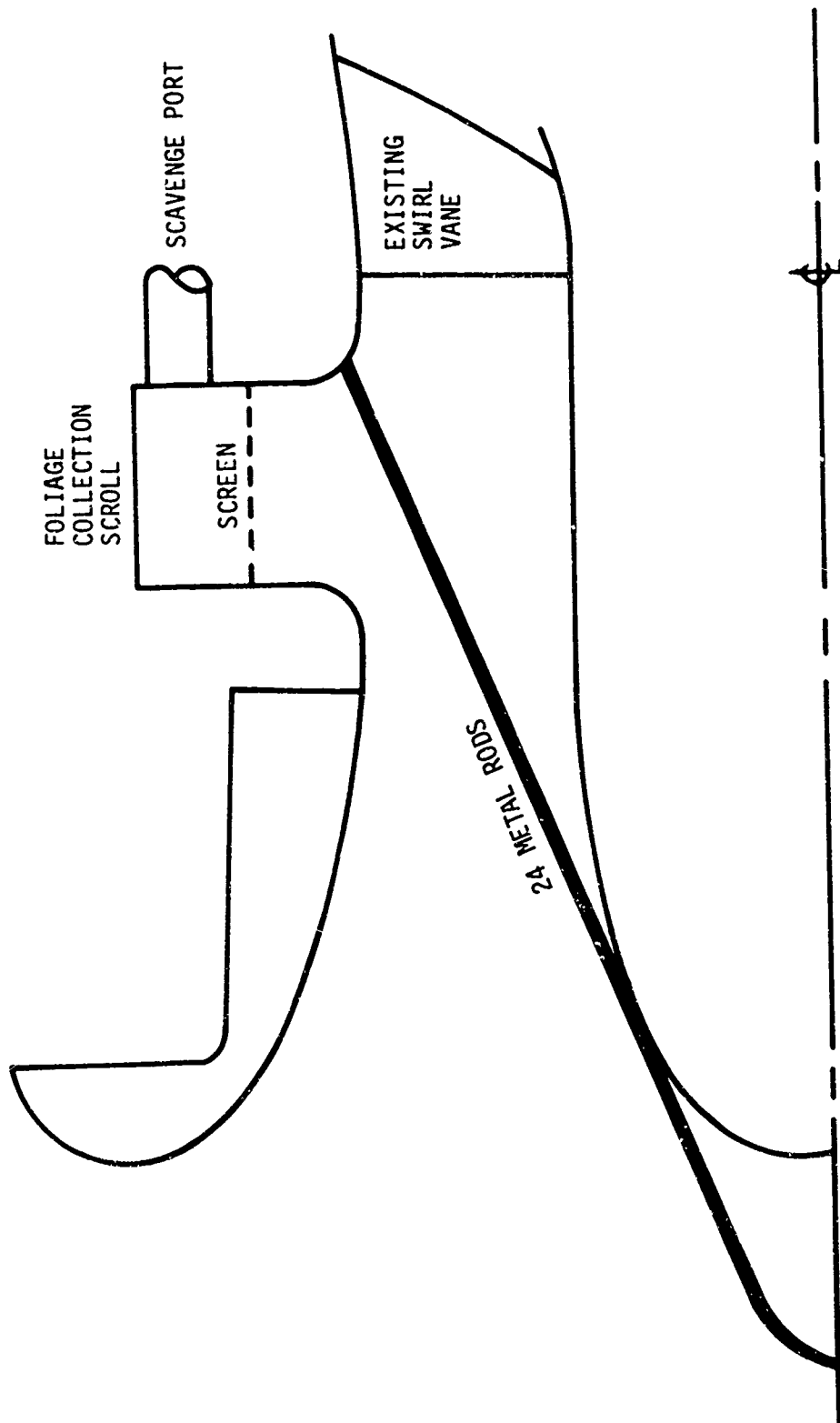


Figure 21. Foliage Collector.



Figure 22. Ingested Hay on Foliage Collector.

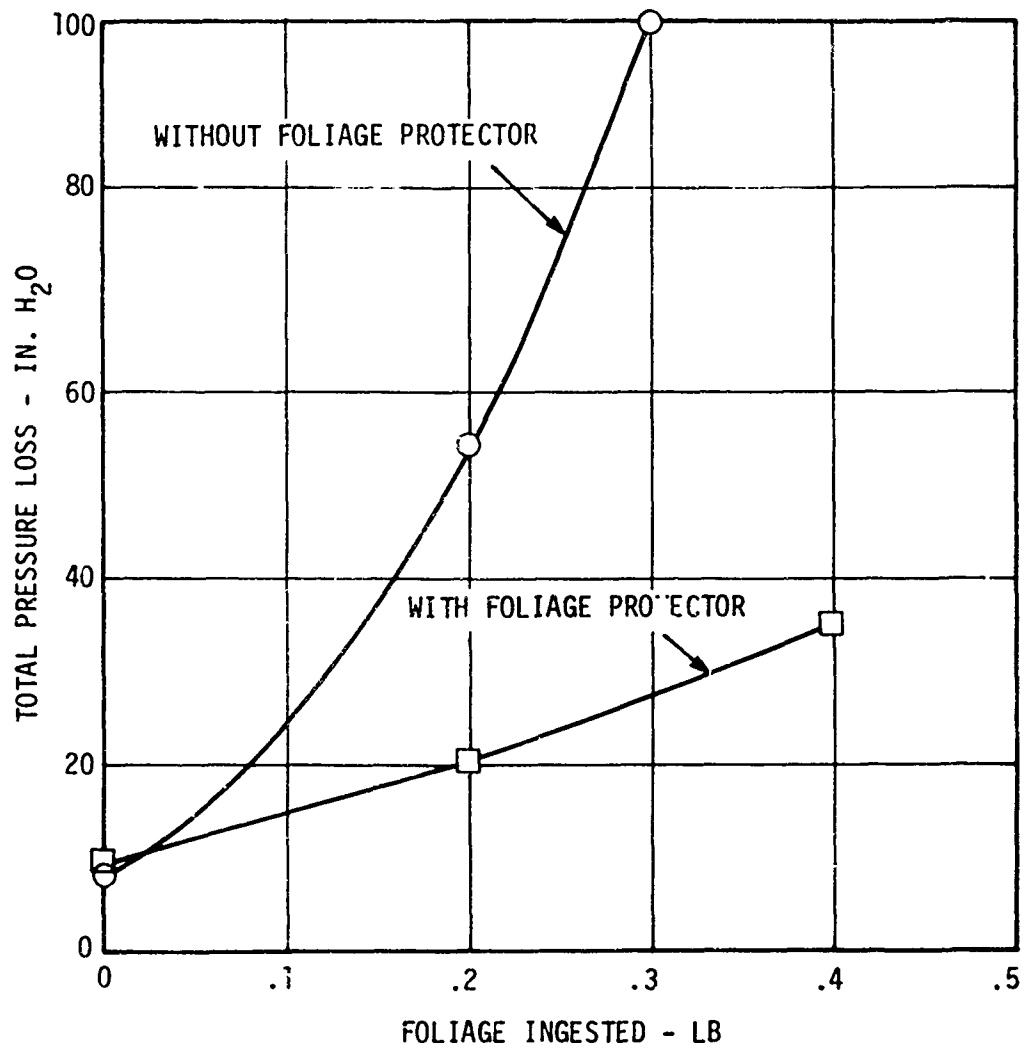


Figure 23. Foliage Collector Capability - Pressure Loss vs Foliage Ingested (Hay).

Reproduced from
best available copy.



Figure 24. Leaves on Foliage Collector.

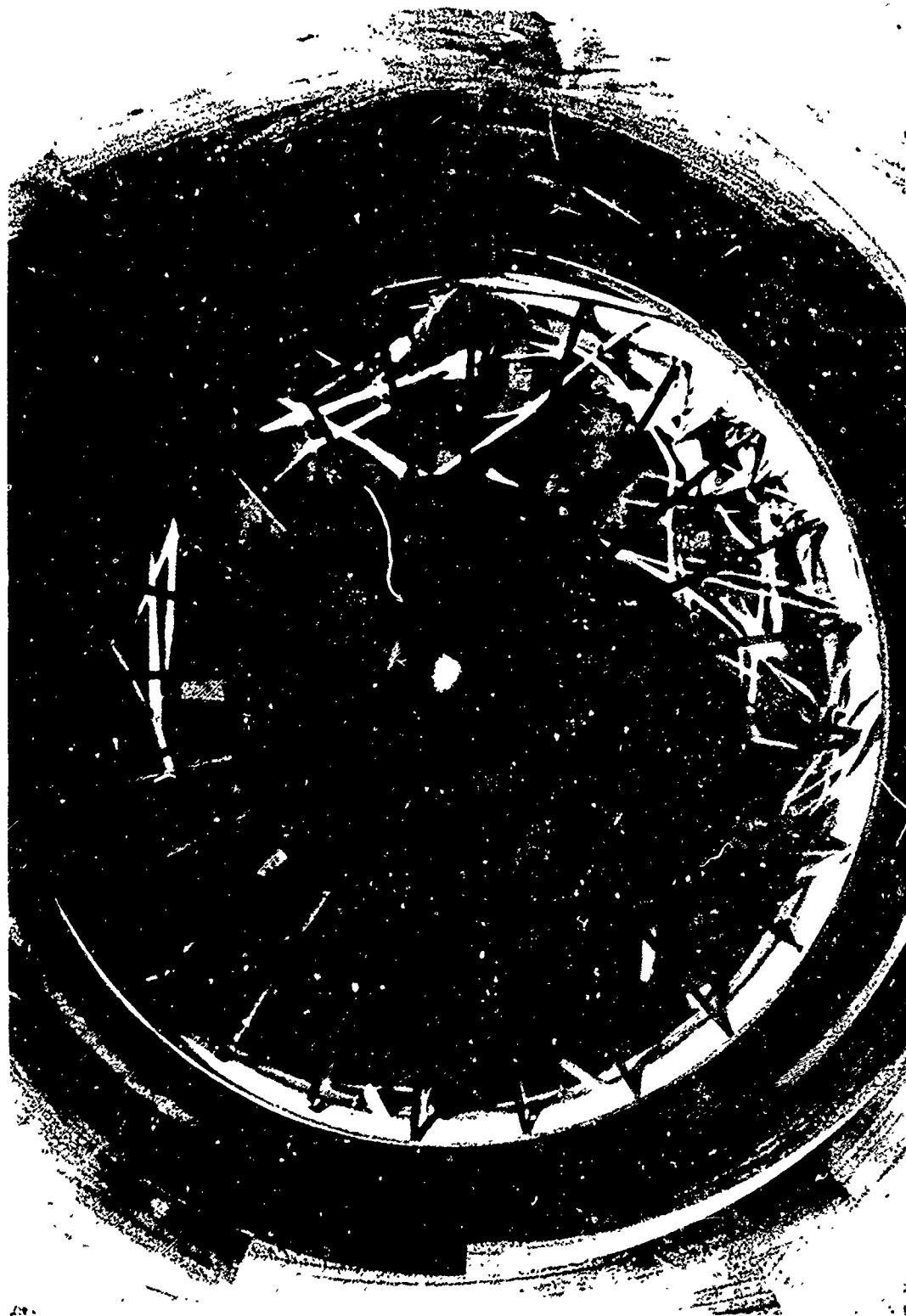


Figure 25. Swamp Grass on Foliage Collector.

SINGLE FOREIGN OBJECTS

Protection from single large foreign objects is an important function of an integral engine inlet separator design. Typical integral axial separator performance in removing foreign objects is presented in Figures 26 and 27 for design point and idle (40%) airflows. Similar performance is expected for intermediate separator sizes.

In designing for single foreign objects, a reasonable design goal is to assure, by design, that whatever can pass through the separator inlet can also pass through the scroll vanes. This requirement influences the choice of the number of vanes in the swirl cascade. Also, it is desirable to have the deswirl vane passages smaller than the scavenge vane passages so that objects trapped on the scavenge vanes cannot come loose and enter the compressor. For both of these criteria, an arbitrary spherical foreign object shape can be assumed. Other shapes could violate the above criteria, but a spherical shape is considered a practical compromise for design purposes.

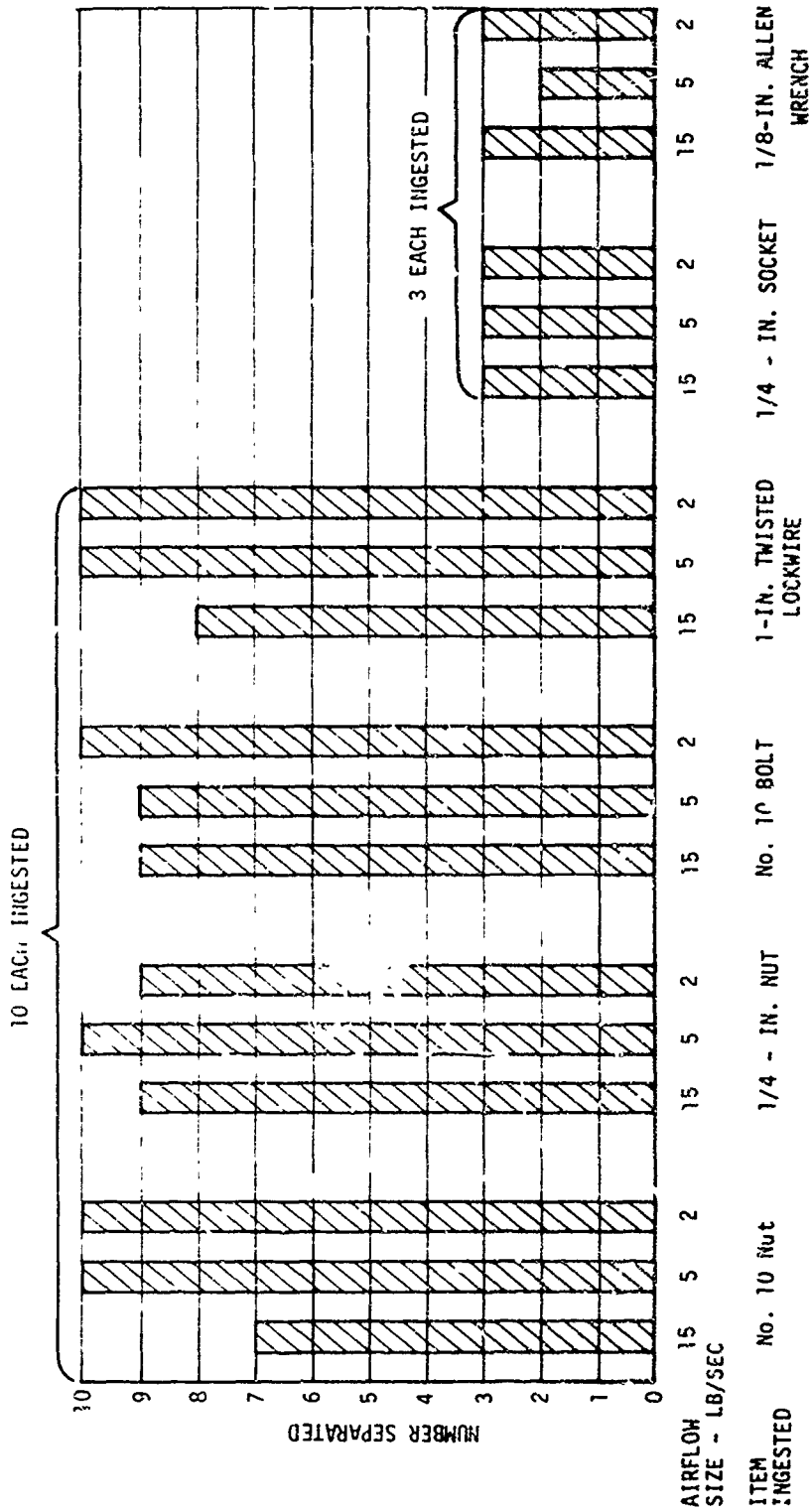
TRADE-OFFS

When the sand ingestion protection desired from the separator is defined, Figures 28 and 29 allow definition of the cost in terms of separator pressure loss. Both figures show test results in the 2, 5 and 15 lb/sec size range. The appropriate size should be used when picking efficiency (η_c) and pressure loss (ΔP_m) combinations from Figures 28 and 29. Choosing a performance goal in the upper left portion of the figures should be considered high risk if outside the experience range and moderate risk if inside the experience range. Choosing a performance goal in the lower right should be considered low risk. For instance, a reasonable, moderate-risk performance goal for a 5 lb/sec separator is 80% efficiency on AC Coarse sand, 95% on C-Spec sand, and 7 in. H_2O pressure loss.

Assessing engine durability in sand ingestion and the separator efficiency defines what protection the separator provides. Cost factors to consider are:

1. Reduced engine removals due to sand erosion.
2. Reduced engine removals due to foreign object damage.
3. Reduced power deterioration with time due to sand ingestion.

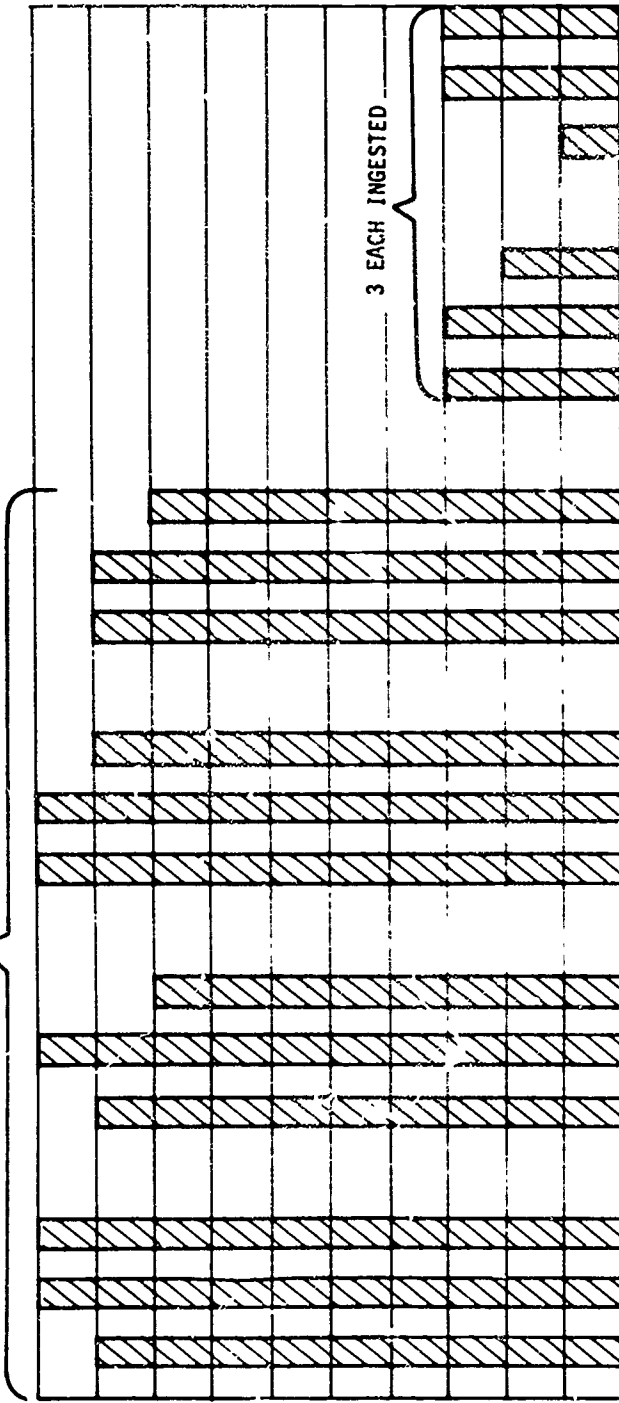
To determine the benefit of reduced FOD events, refer to Figures 26 and 27. The data shown in Figures 26 and 27 can be used to predict the efficiency on foreign objects of the separator design chosen. Then, using field experience from similar engines or installations without integral separators, a cost reduction due to reduced FOD events can be estimated.



CONFIGURATIONS: 15 LB/SEC, XVII; 5 LB/SEC, VI; AND 2 LB/SEC, X

Figure 26. Foreign Object Ingestion Test Results - Airflow at Design Point.

10 EACH INGESTED



NUMBER SEPARATE)

AIRFLOW SIZE - LB/SEC	15	5	2	15	5	2	15	5	2	15	5	2	15	5	2			
ITEM INGESTED	No. 10 NUT	No. 10 NUT	No. 10 NUT	1/4-IN. NUT	1/4-IN. NUT	1/4-IN. NUT	No. 10 BOLT	No. 10 BOLT	No. 10 BOLT	1-IN. TWISTED LOCKWIRE	1-IN. TWISTED LOCKWIRE	1-IN. TWISTED LOCKWIRE	1/4-IN. SOCKET	1/4-IN. SOCKET	1/4-IN. SOCKET	1/8-IN. ALLEN WRENCH	1/8-IN. ALLEN WRENCH	1/8-IN. ALLEN WRENCH

CONFIGURATIONS: 15 LB/SEC, XVII; 5 LB/SEC, VI; AND 2 LB/SEC, X

Figure 27. Foreign Object Ingestion Test Results - Airflow at 40 Percent of Design Point (Idle).

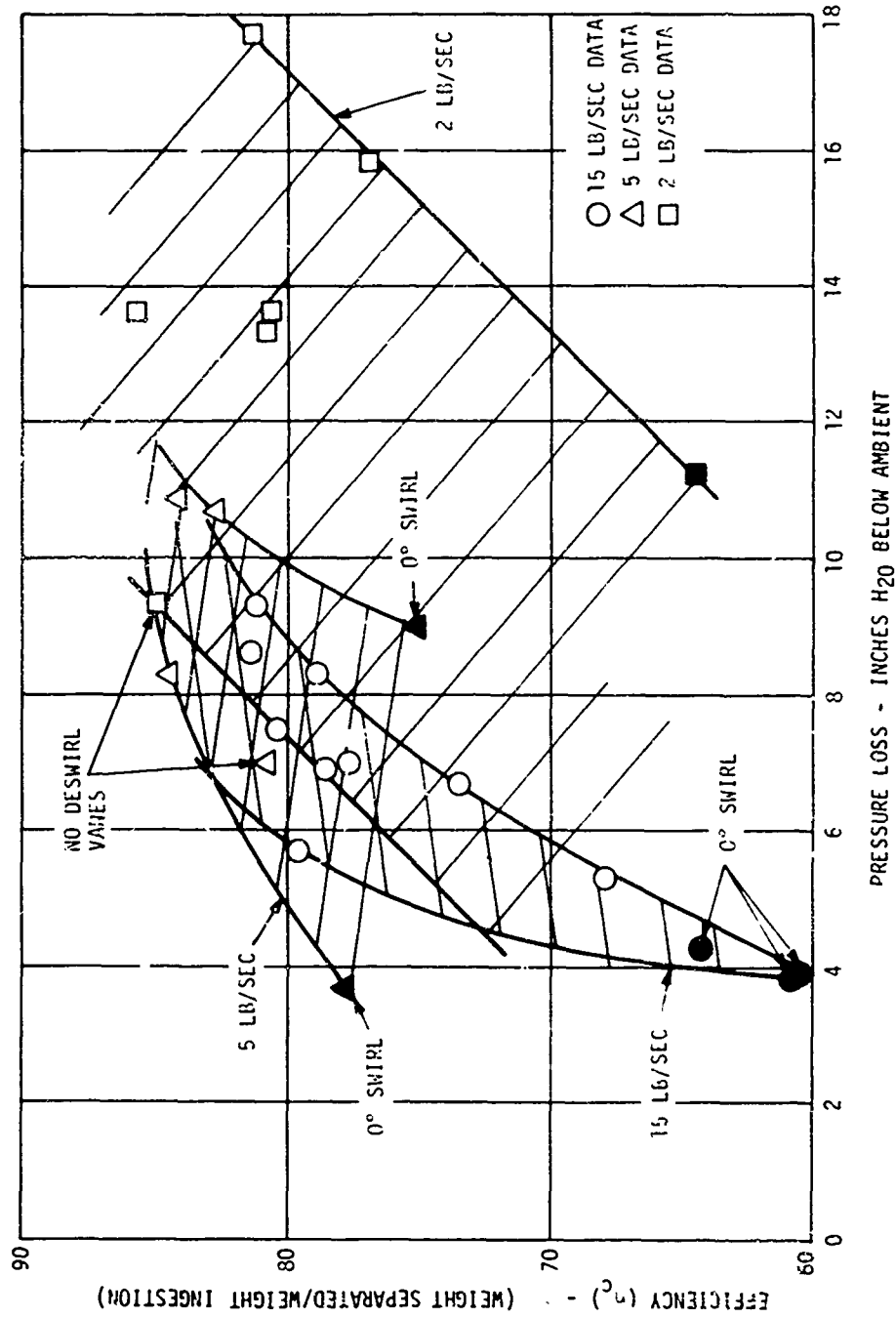


Figure 29. AC Coarse Efficiency vs Pressure Loss.

Cost reduction should be traded off against the engine costs of added:

1. Length.
2. Weight.
3. Diameter.
4. Complexity.
5. Inlet Pressure Loss in terms of power and fuel consumption penalties

The added cost is relative to what would be required to perform all the other functions that an integral separator performs in addition to separation. As shown in Figure 4, numerous necessary functions are performed by the separator in addition to providing a separator air flow path. Also, removing the separator completely does not eliminate all of the inlet pressure loss. A typical turboshaft engine front frame pressure loss at maximum corrected airflow is in the range of 1.0 in. H₂O.

In the preliminary mechanical design of the separator there are several options for material, processes, subsystems and structures. Some of the options in the various mechanical areas are:

1. Type Separator:
 - a. Axial integral separator with swirl vanes.
 - b. Vaneless or swirlless separator.
 - c. Scroll type separator for 2 to 3 lb/sec engines.

2. Vanes Sizes and Locations:

Vane size and location can be varied over a reasonable range without adversely affecting performance. Normally, vane thickness will be in the range of 10-15% of vane length, with exception made for service struts or service vanes.

3. Dual-Purpose IGV's:

Consideration should be given to the use of the IGV to perform the functions of a deswirl vane as well as its normal function as an inlet guide vane. This could be accomplished by using longer and larger IGV's with the front portion as a fixed, hollow structural member and the latter portion variable if required. This may permit the use of a shorter inlet duct (see Figure 13).

4. Anti-Icing Method:

- a. Compressor bleed air.
- b. Hot lube oil.
- c. Heat conduction from hot area.
- d. Hot fuel.
- e. Exhaust gases.
- f. Electricity.
- g. Combinations of above.

Normally the best choices are lube oil and compressor bleed air where conduction from a hot area is inadequate.

5. Oil Storage Tank:

Can be either a separate tank or an integral part of the separator.

6. Accessory Gearbox Location:

For the forward-mounted gearbox, the gearbox can be located on top, bottom, or side of the separator.

7. Structural Load Requirements:

The load can be transmitted through the front frame, the swirl frame, or both.

8. Type Structures:

Evaluations should be made to compare cast structures, fabricated structures, and combination fabricated and cast structures.

9. Front Engine Mounts:

For the front power takeoff turboshaft engine, the main engine mounts are usually at the front of the engine. Choices available are:

- a. Separate pads on the main frame casing.
- b. Separate pads on the swirl frame.
- c. Attachment and support at front flange on inner hub.
- d. Attachment and support at front flange and outer casing of the swirl frame.
- e. Detachable mount supports on the front outer flange of the swirl frame.

10. Materials:

Steel, titanium, aluminum, plastics.

11. Manufacturing Processes:

Fabrication, casting, forging, welding, brazing, EDM, machining.

12. Scavenge Air Exhaust System:

Can be:

- a. Pump or blower driven system.
- b. Ejector driven system.
- c. Combination of pump and ejector driven system.

MATERIALS

The materials used in the inlet separator are subjected to ambient air temperature. Maximum temperatures encountered are from hot anti-icing air or hot lube oil. For a safe design, materials must meet the highest temperature encountered in case of a malfunction, about 300° to 350°F for parts in contact with hot oil, and as high as 500°F for parts exposed to full bleed airflow at rated temperature. Typical materials suitable for use are aluminum, magnesium, titanium, steel, and even plastics, which have been successfully used in the exhaust system. Materials and material processes must meet cost, weight, strength and life requirements.

In general:

1. High-strength, highly-stressed parts are made from steel or from nickel-base or titanium alloys.
2. Low- to medium-strength parts can be made from aluminum, magnesium or plastics.
3. Low- to medium- temperature parts can be made from aluminum, magnesium, or plastics.
4. Magnesium should not be used for any parts exposed to salt water environment.
5. For good heat transfer, aluminum has approximately 10 times the conductivity of steel.
6. 355 cast aluminum may require corrosion protection.
7. Materials processes include casting, forging, fabrication of metals and fabrication or molding of plastics.

SCAVENGE SYSTEM

The scavenge air exhaust system is that part of the separator system that provides the essential function of extracting the scavenge air with its entrained particles before it can enter the engine core inlet. To accomplish this requires a scavenge exhaust system that provides:

1. Sufficient suction capacity with reasonable pressure drop.
2. Sufficient flow capacity.
3. Acceptable operating life including resistance to FOD and erosion.
4. Acceptable weight, size, cost, and complexity.
5. Good reliability, safety and maintainability.
6. Overboard exhaust.
7. Integration with separator and engine configuration.
8. Integration with engine and aircraft systems.

All of the above requirements are vital to the design and operation of a successful scavenge system; however, the key factor is the need to integrate the scavenge system initially into the basic separator and engine design. The method of producing sufficient suction, usually by an impeller, is an engine-aircraft system problem with the size and location of the scavenge system affecting the overall engine rating, physical size, assembly and packaging. The aircraft is affected by the overall size and frontal area of the engine and separator, the horsepower required for the scavenge system, the duct size, and the method of disposing of the scavenge air.

Components that are part of the scavenge air system are:

1. Scavenge inlet including scavenge scroll vanes.
2. Scavenge air collector (scroll) up to its connection to the exhaust duct.
3. Scavenge air suction method.
4. Scavenge exhaust ducting.

Scavenge air should be used to provide other functions beneficial to the engine system. Scavenge air may be used for oil cooling, turbine clearance control, infrared suppression or bay cooling.

No matter how the scavenge air is removed, the design approach is to remove the air in the most efficient manner by use of a system that has maximum durability and reliability. Generally, the system with the simplest geometry and the fewest moving parts is the one most likely to meet this design goal.

Basis for System Selection

After a preliminary design analysis, each scavenge system should be screened to determine whether it meets certain absolute design requirements. Examples of some design requirements:

1. The scavenge system will not diminish the engine capability to meet the durability, reliability and maintainability aspects of the engine Prime Item Development Specification (PIDS).
2. Failure of any part of the scavenge system will not cause an engine failure that results in destruction of the engine, loss of aircraft control, a fire external to the engine, or an in-flight shutdown.

Other factors to be considered are:

1. Durability. Basic durability requirements for the engine apply to the scavenge system, which will be uniquely subject to wear and damage by the material separated from the engine airflow. Durability should be the most important design goal. Any system which will not suffer from deterioration due to sand or damage due to single foreign objects should be considered. Any system which does not have some obvious capability of surviving on FOD experience must be eliminated.
2. Efficiency. A small total engine shaft horsepower (SHP) and specific fuel consumption (SFC) penalty due to the scavenge system is an important design goal. Consider the system efficiency penalties at both design-point and off-design (engine part power) conditions.
3. Reliability. Minimum requirements for reliability of the scavenge system are the engine reliability requirements.
4. Effect of System Failure. Failure of any part of the scavenge system should have minimum performance impact on both the engine and the separator.
5. Size (Volume). System size should be kept to a minimum. Size is considered in terms of its relation to the engine envelope. A system which does not increase the engine envelope is considered best for this design goal.

6. Weight. Weight should be considered as the incremental system weight above that of the engine. Credit should be given if part of the scavenge system performs other necessary engine functions such as providing structure or cooling flow.
7. Cost. System cost should be considered in terms of a real production cost as if the system were to be ultimately produced in quantity.
8. System Integration With the Engine. In assessing each system's capability to meet the design requirements and goals, it is important that each requirement and goal be considered separately to avoid confusion and misleading conclusions. It is also important, however, to credit a system for integration with other engine systems and to consider the scavenge system attributes and penalties in terms of the entire engine. Following are listed some of the benefits to the basic engine that could result from proper integration of the scavenge system:
 - a. Improved rotor clearance by use of the scavenge air to cool the engine casings.
 - b. Reduction of infrared signature due to mixing of the scavenge air with engine exhaust.
 - c. Lower power turbine back pressure if energized scavenge air is introduced downstream of the exhaust diffuser.
 - d. Enhanced engine oil cooling by using scavenge air.
 - e. Reduced engine vulnerability by proper placement of the scavenge system components.
9. Aircraft Mission. By design, some scavenge systems operate continuously throughout the engine envelope. Some advanced systems do not operate under aircraft cruise conditions to reduce the power penalty when scavenge air is not needed. Manually turning scavenge systems ON and OFF introduces human error into inlet protection. A pressure switch could turn the scavenge system ON and OFF if it were sensitive to a parameter like indicated airspeed. An ON-OFF system would have to be considered in terms of its impact on the aircraft mission and the impact of the ON-OFF system on system reliability. Other systems could have a different impact on the aircraft mission than is implied by simply the design point SHP and SFC penalties.
10. Material. Material selections for the scavenge system will be most influenced by resistance to impact and erosive and corrosive environments. Ceramic type materials can be eliminated by impact requirements. Therefore, the pertinent information required for scavenge pumps is the degree of resistance to erosion and reliability offered by the materials and coatings developed for aircraft gas turbines. Careful attention

must be given to system performance deterioration with time due to thermal distortion in the case of systems near engine hot-section parts.

If the scavenge system includes a scavenge blower, materials for the impeller should be steel. Experiences with aluminum impellers coated with nickel plating 0.030 in. thick showed that deplating sometimes occurred, resulting in damage to the system and also to the engine. A steel impeller eliminates the problems and provides durability against erosion.

System Aerodynamic Design

The size of the exhaust system is a function of the amount of scavenge airflow and the efficiency of the exhaust system used. The scavenge exhaust system for the separator is designed for 16.5% w_c air at IRP (intermediate rated power). However, off-design scavenge flow requirements could be an important consideration in the design process. Figure 30 shows percentage of scavenge flow as a function of total engine airflow for the existing T700 integral inlet protection system. Another separator may have a different characteristic than Figure 30.

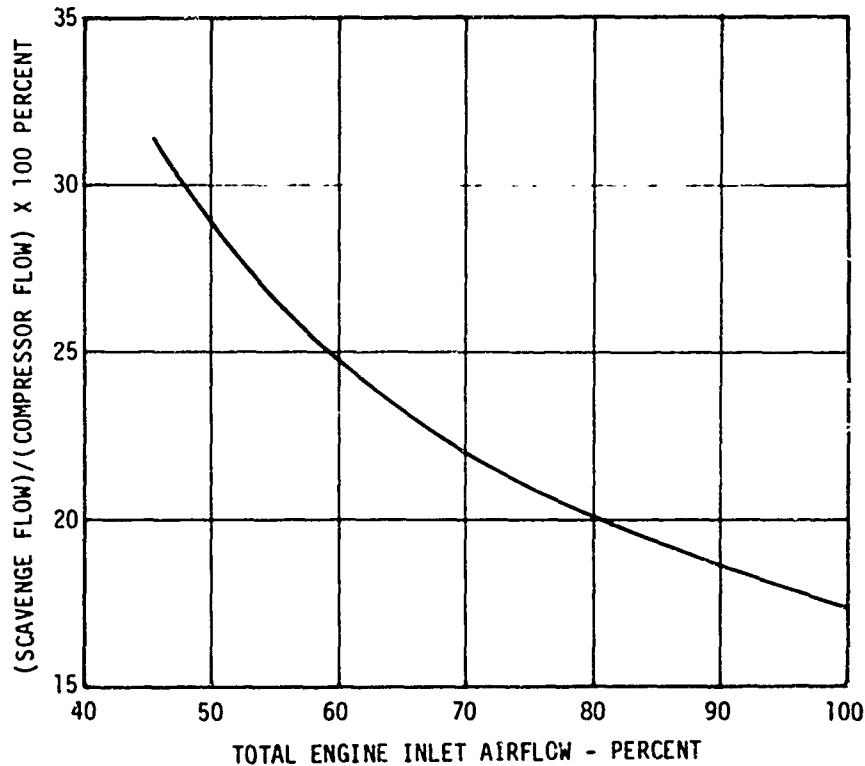


Figure 30. Scavenge Flow Requirements.

Blower Aero Design

The principal factors in the design of a suitable blower are the design flow, RPM, and pressure rise. The parameters are expressed in the specific speed parameter (N_s):

$$N_s = N\sqrt{Q}/\Delta h_{is}^{0.75}$$

where N = speed, rpm

Q = inlet flow, ft³/sec,

h_{is} = isentropic head, ft lb/lb

A typical variation in specific speed with RPM and head rise is shown in Figure 31, where the scavenge blower inlet conditions were:

1. Inlet airflow, 0.9 lb/sec
2. Inlet pressure, 14.0 psia
3. Inlet temperature, 518.7°R.

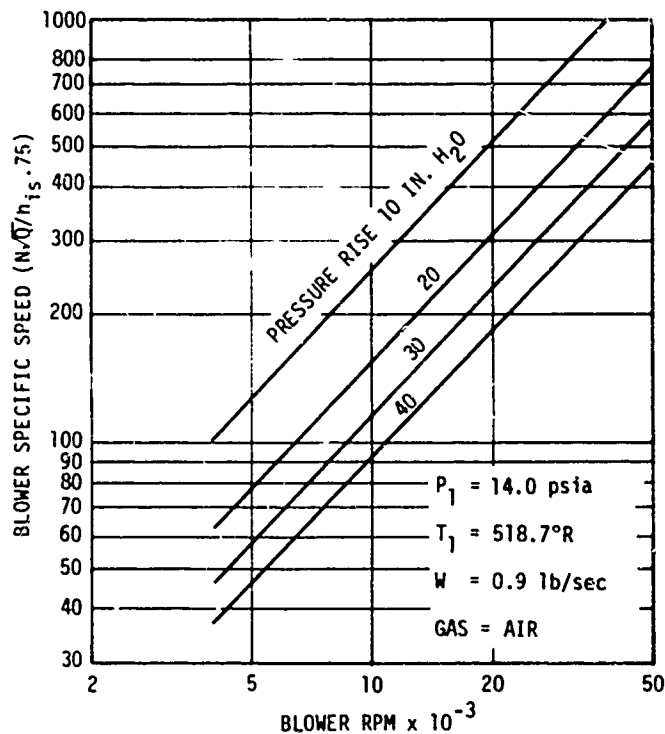


Figure 31. Scavenge Blower Design Parameters.

The general configuration of the blower design changes with specific speed. Radial flow blowers are appropriate at lower specific speeds (N_s approximately 50-120) and axial flow blowers at high specific speeds (N_s approximately 300-400). Between the radial and axial flow designs is the mixed flow blower where the rotor outlet flow is inclined outward from the axial direction (see Figure 32).

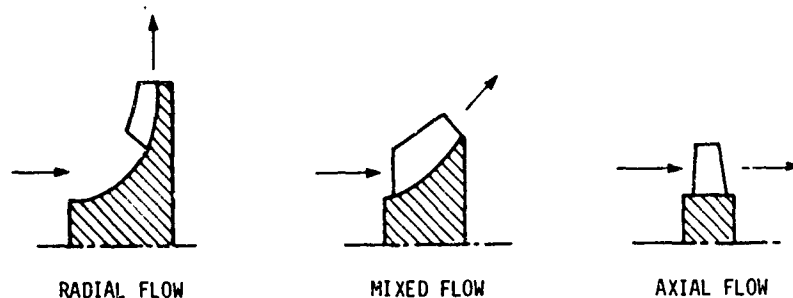


Figure 31. Blower Configurations.

Each configuration has some overlap in the specific speed range, so other design considerations influence the desirability of radial versus mixed flow or mixed flow versus axial flow. Some other design considerations are weight, outlet flow ducting, cost, installation requirements, and drive system. The allowable tip speed of the blower is also a factor in the design since it affects the abrasion life of the blower. In the T700 scavenge blower, the tip speed was held to 475 ft/sec at the inlet and 750 ft/sec at the outlet. These levels of tip speed have demonstrated satisfactory life in the 50-hour sand ingestion test (see Figure 33). In general, as the blower pressure rise requirement is reduced the design outlet tip speeds can be lower. This favors improved life for both the blower rotor and stator.

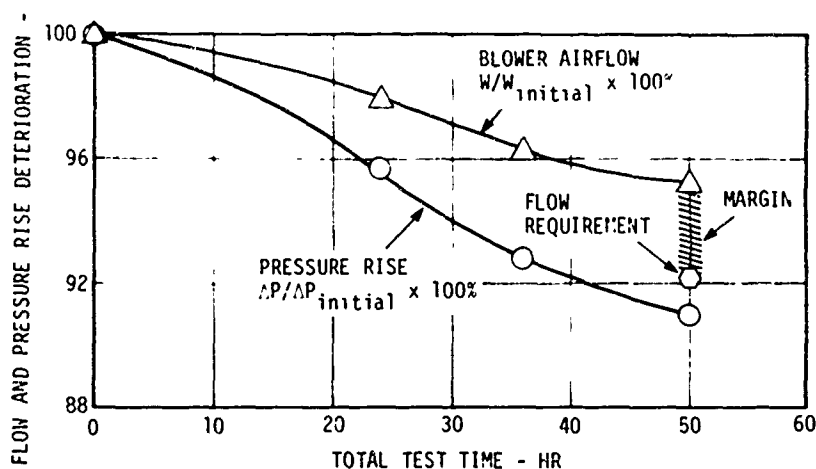


Figure 33. Effect of Sand Ingestion on Scavenge Blower Performance.

An important consideration in the design of the scavenge blower rotor is the use of alternate partial or splitter blades between the full blades. The T700 sand ingestion test demonstrated that the bulk of the abrasion occurs on the full blades (see Figure 34). Any advanced scavenge blower should incorporate full and partial blades to reduce the performance loss from sand ingestion. Figures 34 and 35 show the effect of erosion on the impeller and housing of a scavenge blower. A radial or mixed flow rotor can use the conventional splitter blades, and an axial rotor can use alternate shorter chord blades. The amount of the partial blade cutback can be determined from a particle trajectory analysis.

The aerodynamic design of a scavenge blower is not directed at the state-of-the-art efficiency levels because the blading must be rugged and easy to manufacture. A low number of cast stout vanes is desirable, and an efficiency level of about 60% is reasonable for this type of blower. Since power extraction is relatively small and life, cost, and FOD requirements are important, there is little advantage in designing sophisticated aerodynamic blading for high stage efficiencies.

Scavenge systems with reduced blower pressure rise requirements are desirable because this permits lower rotor tip speeds, hence improved life and FOD resistance. For example, this could be accomplished using a mixed-flow blower like the T700 design at a lower RPM while trimming the annulus area for further flow reductions. If the pressure rise were below about 25 in. H₂O, a simple axial-flow blower could be considered. The basic components could be based on one of the many blowers in production by various suppliers.

Engine Compatibility

Meaningful trade-off studies can be made only with a particular engine and installation in mind. The off-design parameters are of particular importance in determining the acceptability of the design. For that reason, off-design pressure, temperature, and flow information is necessary over the engine power spectrum from idle to peak power. The following four conditions are recommended for this study.

1. Maximum continuous power.
2. 60% of continuous power.
3. 30% of continuous power.
4. Ground idle.

Other integral separator designs are described in References 4 and 5. A nonintegral axial separator design is described in Reference 6.

IMPELLER NO. 13
LONG BLADE NO. 3 AFTER 50 HR SAND TEST



Figure 34. Elower Impeller.



Figure 35. Wear on Blower Aluminum Housing.

AERODYNAMIC DESIGN

FLOW PATH DEFINITION

The separator inner wall which surrounds the engine forward oil sump is fixed by the sump dimensional requirements and the volume provided for the attachment to the engine drive shaft. These mechanical considerations establish the inner boundary of the separator envelope. It is important to make the diameter of the inner wall at the inlet as small as possible in order to obtain large centrifugal acceleration and therefore high efficiency.

An inlet face Mach number of 0.2 was used for all the separator sizes in this guide. Lower face Mach numbers increase separator volume, while higher Mach numbers increase separator losses. Even though the face Mach number of 0.2 is incompressible, the flow in the separator moves very quickly into the compressible range as it traverses the separator. Acceleration across the swirl cascade raises the Mach number to 0.4 - 0.5, while local acceleration around the splitter lip causes Mach numbers of 0.7 and greater. The compressor inlet is located at the core exit. The compressor design therefore establishes the core exit Mach number, which is usually in the neighborhood of 0.5. In computing face Mach number, the design airflow is 1.165 times the engine compressor flow to account for separator scavenge flow.

With the inlet inner wall diameter (ID) and face Mach number fixed, an inlet outer wall diameter (OD) can be established and an area distribution through the separator chosen consistent with Figure 36 and the shape of Figure 37. A summary of performance for various 2 lb/sec, 5 lb/sec, and 15 lb/sec separators is given in Tables 3, 4, and 5. Nonaerodynamic considerations may require a flow path shape which is different from that shown in Figure 37. In that case, it is important for good separation efficiency not to compromise the following:

1. Inlet hub diameter to raiustep hub diameter ratio. A smaller ratio than shown in Figure 37 (also see Table 6) decreases the C-Spec separation efficiency. Figure 38 (also see Table 7) shows a 2 lb/sec separator flow path that was a compromise based on mechanical considerations. Table 3 shows that this flow path (Configuration VIII) did not achieve the vaneless performance of the larger 5 lb/sec separator (Configuration VI, Table 4) or 15 lb/sec separator (Configuration XVII, Table 5) even though all three had hidden splitter lips.
2. Hub flow path shape from $L/R_1 = 1.2$ to $L/R_1 = -0.5$ of Figure 37. This shape was found to be good for separation efficiency both vaneless or with vanes. In Table 5, compare the performance of Configuration III to VI, and VIII to XIV and XV. The design

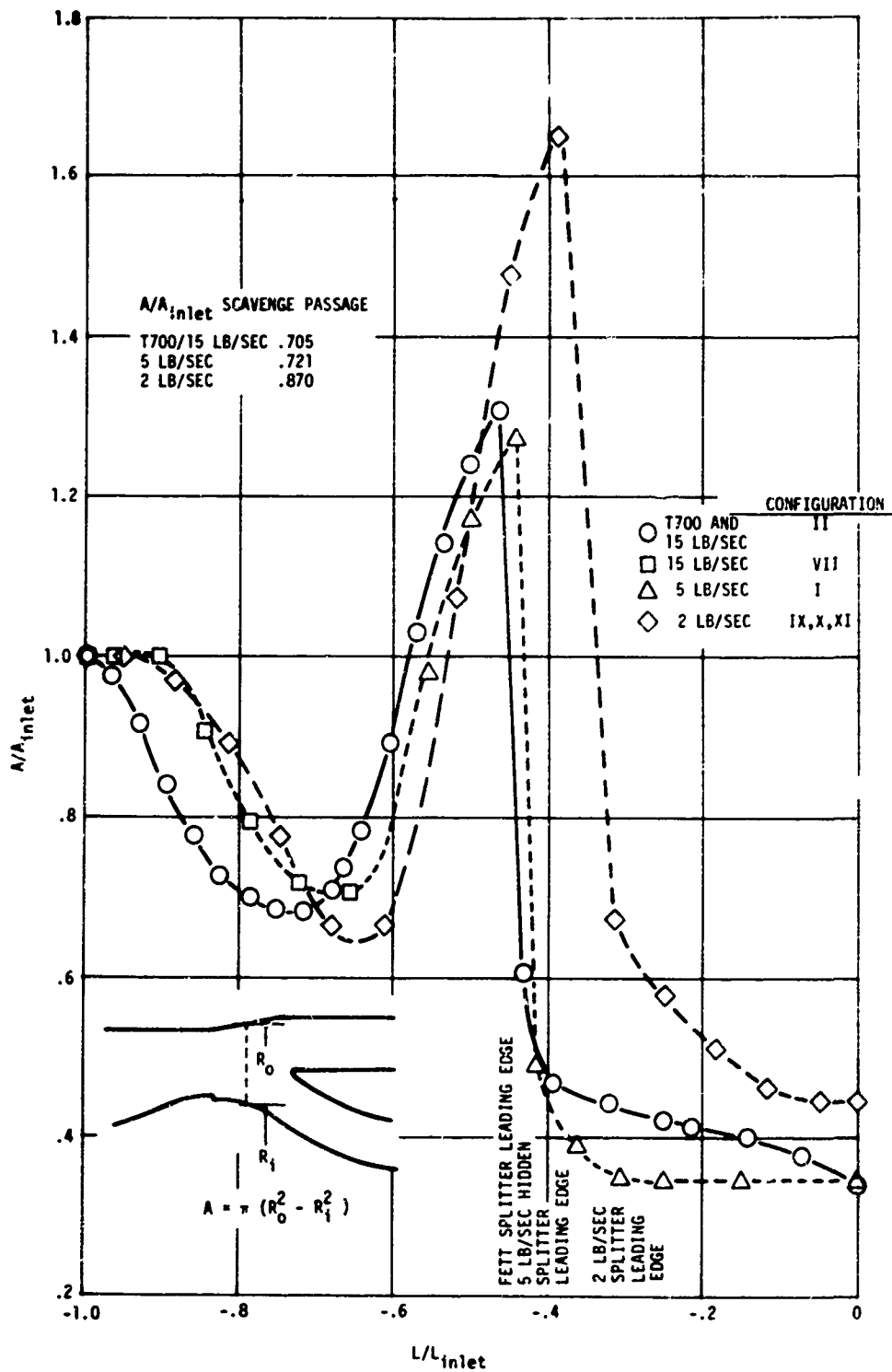


Figure 36. Area Distribution Through Separator Based on Radius.

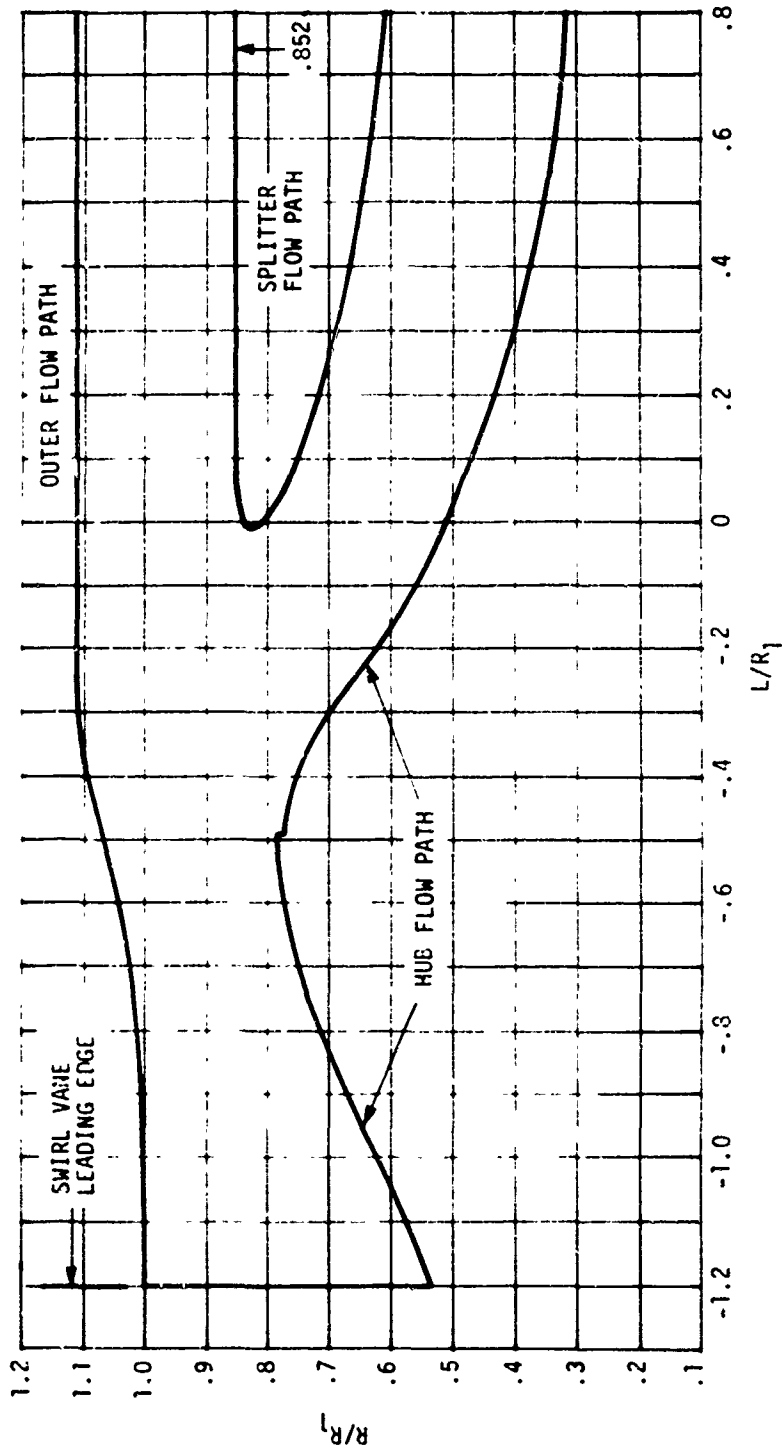


Figure 37. L/R_1 Separator Shape (See Table 6) - T700 Flow Path.

TABLE 3. 2 LB/SEC SEPARATOR TESTING SUMMARY														
No.	Configuration 2 lb/sec Separator Modifications	Swirl Angle (deg)	Pressure Loss		AC Coarse Sand			C-Spec Sand						
			ΔP_T^* (in. Flow H ₂ O) (%)	Core ΔP_T^{**} (in. Flow H ₂ O) (%)	Scav (%)	Flow (lb/sec)	η_V (%)	η_G (%)	Scav (%)	Flow (lb/sec)	η_V (%)	η_G (%)		
	<u>STATUS TEST</u>	32.5	33.3	14.6	15.8	15.2	2.06	14.8	76.7	73.3	2.06	15.0	88.0	86.2
	<u>MODIFICATION TESTS</u>													
I	50% Reduction in Swirl Cascade (13 Vane)	31.5	19.3	17.2	10.1	17.6	--	--	--	--	2.00	16.2	85.0	82.6
I.	13 Vane Swirl at $\pm 5^\circ$	35.5	27.0	16.2	13.6	16.3	2.04	15.2	80.3	77.3	2.03	15.6	86.5	84.5
III	II + Splitter 0.34 in. Forward	35.5	25.0	16.9	17.7	16.9	2.01	16.4	81.0	77.9	2.01	16.4	87.4	85.3
IV	II + Scroll Vanes 0.5 in. θ	35.5	24.8	16.5	--	--	2.06	16.5	81.6	78.6	2.04	16.4	86.2	83.9
V	II + 50% Reduction in. Scroll Vanes	35.5	17.7	17.3	13.3	17.2	2.03	16.7	80.6	77.4	2.04	16.7	82.7	79.8
VI	V + Increased Scavenge	35.5	19.6	26.2	18.4	31.6	2.04	18.6	82.1	78.8	2.02	19.3	86.7	84.1
VII	Basic Flow Path (no vanes)	0	12.8	17.2	5.6	18.0	2.00	17.8	27.9	15.3	2.01	17.4	71.2	66.2
VIII	Vaneless - Reduced Splitter Lip Radius	0	--	--	11.2	18.6	1.97	17.0	64.3	58.2	1.96	17.6	82.1	78.9
	<u>PHASE V TESTS</u>													
IX	VIII + 13 Swirl Vanes, Redesigned Flow Path and No Deswirl Vanes	31.5	--	--	9.3	16.9	1.67	16.8	84.8	82.2	1.66	17.5	93.6	92.5
X	IX + 26 Deswirl Vanes	31.5	--	20.2	13.6	17.3	2.03	16.7	85.5	83.1	2.03	16.7	94.5	93.6
XI	X With 13 Deswirl Vanes	31.5	--	--	11.1	15.6	--	--	--	--	--	--	--	--

* Corrected to 0.33 lb/sec scavenge flow.
 ** Corrected to 2 lb/sec core flow.

TABLE 4. 5 LB/SEC SEPARATOR TESTING SUMMARY

No.	Configuration & lb/sec Separator Modifications	Swirl Angle (deg)	Pressure Loss		AC Coarse Sand				C-Spec Sand				
			ΔP_{TS} (in. H ₂ O)	Core Flow (in. H ₂ O)	Scav (%)	Core Flow (lb/sec)	Scav (%)	η_w (%)	η_c (%)	Core Flow (lb/sec)	Scav (%)	η_w (%)	η_c (%)
<u>MODIFICATION TESTS</u>													
I	Vaneless Flow Path Test	0	-	3.7	17.9	5.02	15.6	77.7	74.2	4.99	16.7	91.4	90.0
II	Design 3A Swirl Vanes and No Deswirl Vanes	30.1	-	7.0	17.4	4.92	16.9	80.7	77.4	5.00	17.8	93.9	92.8
III	II + Deswirl Vanes	30.1	-	10.7	16.3	5.24	16.2	82.6	79.8	5.24	16.2	94.4	93.5
IV	III + Moved Out- er Flow Path	30.1	11.6	16.4	10.9	16.1	4.94	17.8	84.1	81.3	17.8	96.4	95.8
V	IV + 1 Swirl Vanes + Scaled T700 Swirl Hub (i.e., 9 Swirl Vanes + 9 Deswirl)	-	-	-	3.3	17.6	5.03	17.3	84.3	81.6	17.2	96.6	96.0
VI	V With No Swirl and No Deswirl	-	-	8.7	18.1	4.94	17.4	75.0	70.7	4.85	17.5	90.6	89.0
VII	VI + Scroll 4.0 in. Aft	-	-	-	-	4.99	17.6	75.0655	70.7	4.98	17.5	88.7	86.7
VIII	IV & 1 Deswirl Vaness (i.e., 9 Deswirl Vanes)	-	-	9.0	19.2	-	-	-	-	-	-	-	-

* Corrected to 0.33 lb/sec scavange flow.

** Corrected to 2 lb/sec core flow.

TABLE 5. 15 LB/SEC SEPARATOR TESTING SUMMARY

No.	Configuration 1 - 18/700 Separator Modifications	Pressure Loss			AC Coarse Sand			C-Spec Sand					
		AP ₁ [#] (in. H ₂ O)	Core Flow (in. H ₂ O)	AP ₂ ^{##}	Core Flow (lb/sec)	Scav (%)	η _w (%)	η _c (%)	Core Flow (lb/sec)	Scav (%)	η _w (%)	η _c (%)	
	<u>STATUS TESTS</u>												
	<u>MODIFICATION TESTS</u>												
I	50% Reduction in Swirl Cascade Solidity (1. Vane)	19.7	15.6	8.3	15.2	14.9	16.3	78.6	75.1	14.9	16.4	95.2	94.4
II	1 + 6" Increase in Swirl Vane Stagger Angle	--	--	5.7	11.0	15.0	16.4	79.4	76.1	15.1	16.4	92.9	91.8
III	Status Vaneless Flow Path	20.4	16.3	8.3	16.2	15.0	16.2	78.5	75.0	14.9	16.1	93.8	92.8
IV	Status and Design 5 Deswirl Hub (Vaneless)	--	--	4.3	16.1	15.2	16.0	64.2	55.8	14.8	16.6	83.3	80.5
V	IV With .75 in. Reduction in Rainstep-to-Splitter Lip Length (Vaneless)	--	--	3.7	15.1	15.1	15.6	58.1	51.6	15.1	15.4	79.2	76.0
VI	Status Deswirl a Design 5 Swirl (Vaneless)	--	--	3.8	16.6	15.0	16.3	60.8	54.4	14.9	16.5	83.0	80.2
VII	Design 3 Swirl System	--	--	9.3	15.5	15.2	16.0	81.0	78.0	15.2	15.9	95.6	94.9
VIII	Design 3 - 6° Stagger Angle	--	--	7.0	16.5	15.0	16.4	77.5	73.8	15.0	16.6	94.9	94.1
IX	VIII + Filled Outer Flow Path	--	--	6.8	16.2	--	--	--	--	15.1	16.4	87.1	85.0

Corrected to 0.33 lb/sec scavenge flow

Corrected to 2 lb/sec core flow.

TABLE 5. - Continued

No.	Configuration 15 lb/sec Separator Modifications	Swirl Angle (deg)	Pressure Loss			AC Coarse Sand			C-Spec Sand				
			Core Flow (in. H ₂ O) (\$)	Core Flow (in. H ₂ O) (in.)	Scav (%)	Core Flow (lb/sec)	Scav (%)	η_c (%)	Core Flow (lb/sec)	Scav (%)	η_c (%)		
MODIFICATION TESTS - Continued													
X	VIII + Outer Flow Path Step Diffuser	31.7	--	6.8	16.6	15.0	16.2	73.3	69.0	15.0	16.4	87.3	85.2
XI	VII + OD Boundary Layer Trip	31.7	--	7.3	16.0	--	--	--	--	--	--	--	--
XII	VIII + OD and ID Bound- ary Layer Trips	31.7	--	7.3	16.2	--	--	--	--	--	--	--	--
	A. 1/2 Pitch (10°)	31.7	--	6.8	16.4	--	--	--	--	--	--	--	--
	B. 1/2 Pitch (50°)	31.7	--	7.2	16.1	--	--	--	--	--	--	--	--
	C. 3/4 Pitch (150°)	31.7	--	6.8	16.2	--	--	--	--	--	--	--	--
	D. 5/8 Pitch (12.5°)	31.7	--	6.7	16.4	--	--	--	--	--	--	--	--
XIV	Design 3 - 6° Stagger Angle and Status Swirl Hub	38.1	--	8.6	16.0	15.1	16.3	81.2	78.1	15.2	16.0	96.0	95.4
XV	Design 3 - 9° Stagger Angle and Status Swirl Hub	32.1	--	6.9	16.0	15.0	17.0	78.4	74.7	15.0	16.8	95.7	95.0
XVI	XV + Triangular Exten- sion to Trailing Edge of Swirl Vane	32.8	--	7.5	16.6	14.9	17.3	80.2	76.8	14.9	17.3	96.6	96.0
XVII	Scaled 5 lb/sec Hidden Splitter Lip (Same as 5 lb/sec Configuration VI)	--	--	5.3	17.2	15.0	16.4	67.8	62.5	15.6	16.6	90.9	89.4

* Corrected to 0.33 lb/sec scavenge flow.
 ** Corrected to 2 lb/sec scavenge flow.

TABLE 6. TYPICAL SEPARATOR FLOW PATH

Outer Wall		Splitter Wall		Inner Wall	
L/R ₁	R/R ₁	L/R ₁	R/R ₁	L/R ₁	R/R ₁
-1.202	1.000	-.002	.835	-1.202	0.532
-1.126	1.000	0	.814	-1.126	0.560
-1.050	1.000	.022	.798	-1.050	0.595
-.974	1.000	.044	.781	-.974	0.635
-.898	1.002	.071	.767	-.898	0.672
-.822	1.008	.126	.745	-.822	0.705
-.746	1.018	.159	.733	-.746	0.731
-.670	1.030	.197	.720	-.670	0.754
-.594	1.047	.235	.709	-.594	0.772
-.518	1.060	.271	.699	-.518	0.783
-.499	1.064	.311	.689	-.499	0.785
-.488	1.068	.349	.680	-.487	0.777
-.458	1.075	.387	.672	-.449	0.772
-.427	1.082	.425	.664	-.411	0.761
-.397	1.090	.463	.656	-.373	0.745
-.367	1.097	.494	.651	-.335	0.725
-.336	1.104	.596	.635	-.297	0.700
-.306	1.109	.624	.632	-.267	0.678
-.275	1.110	.654	.628	-.236	0.655
-.260	1.110	.708	.621	-.206	0.632
		.761	.615	-.176	0.609
		.814	.608	-.145	0.587
		.867	.602	-.115	0.567
		.881	.599	-.084	0.550
		.895	.597	-.054	0.534
		.909	.594	-.023	0.521
				-.007	0.508
				.037	0.497
				.068	0.485
				.159	0.453
				.190	.443
				.220	.433
				.281	.413
				.324	.395
				.402	.379
				.463	.363
				.524	.351
				.585	.339
				.631	.332
				.654	.329
				.681	.326
				.708	.323
				.708	.321
				.814	.321

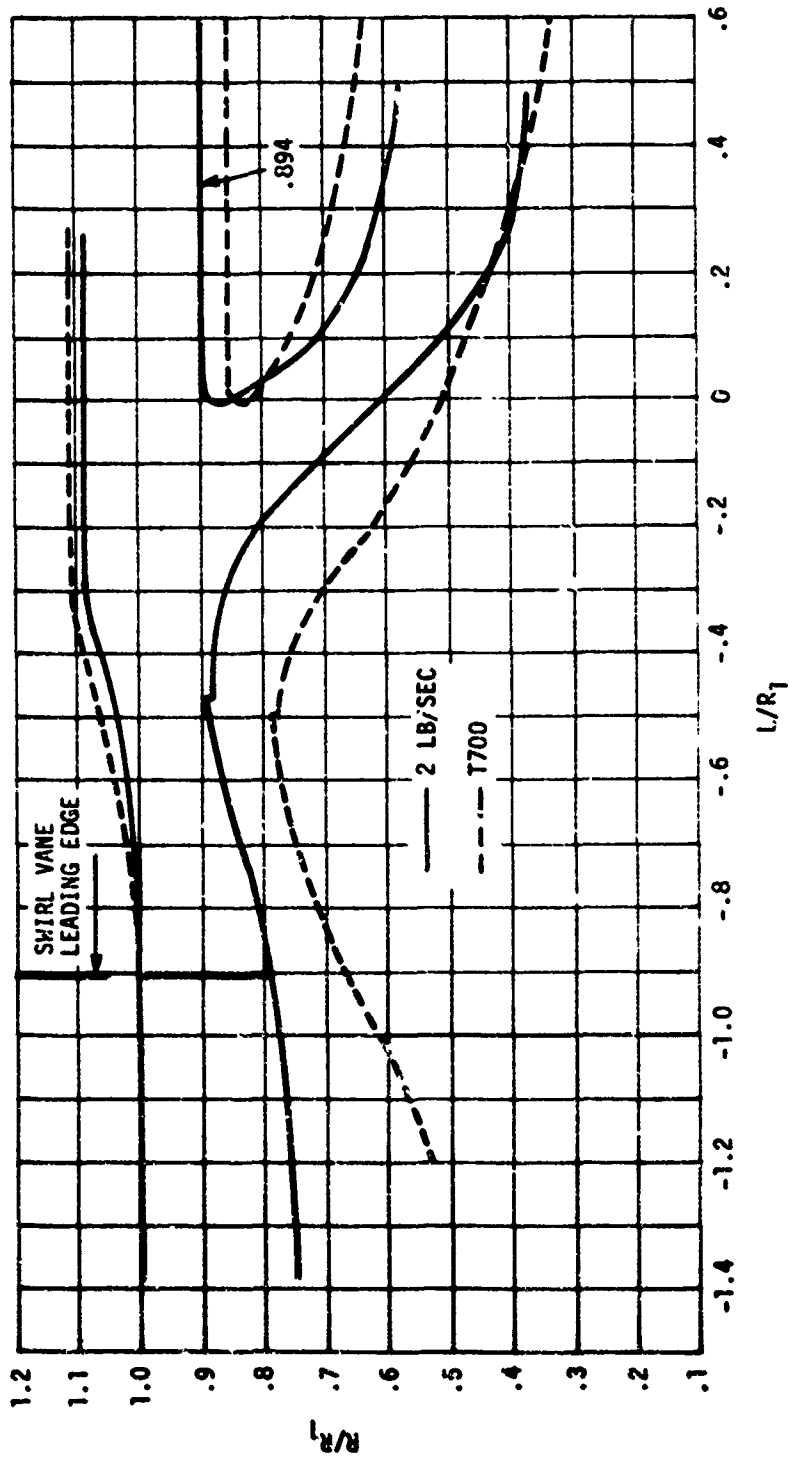


Figure 38. 2 lb/Sec L/R_1 Separator Flow Path,

TABLE 7. 2 LB/SEC SEPARATOR FLOW PATH

Outer Wall		Splitter Wall		Inner Wall	
L/R ₁	R/R ₁	L/R ₁	R/R ₁	L/R ₁	R/R ₁
-.1385	1.0			-1.385	.752
-1.259	1.0			-1.259	.752
-1.132	1.0			-1.132	.761
-1.006	1.0			-1.006	.782
-.879	1.0				-
-.752	1.004			-.752	.819
-.626	1.014			-.626	.859
-.499	1.037			-.499	.886
-.468	1.050			-.468	.894*
-.468	1.050			-.468	.881*
-.373	1.070			-.373	.877
-.297	1.085			-.297	-
-.246	1.085			-.246	.835
-.119	1.085			-.119	.732
-.007	1.085	-.007	0.853	-.007	.628
.068	1.085	+.068	0.762	.068	.537
.134	1.085	+.134	0.682	.134	.462
.260	1.085	+.260	0.627	.260	.410
.387	-	+.387	0.591	.387	.382
.482	-	+.482	0.578	.482	.373

* Rainstep

intent was to provide monotonically decreasing flow area when used with the design 3 vanes. Pressure loss benefited from this approach, but separation efficiency did not.

3. Outer wall shape from $L/R_1 = -0.9$ to -0.3 in Figure 37. This shape causes pressure loss because it causes high rates of local diffusion. However, the purpose of this shape is to deflect sand and other objects into the collection scroll. During sand ingestion, particles bounce off the swirl vanes and hit the OD wall in this area. If the wall is cylindrical, the particles are reflected back toward the ID. Configurations IX and X of Table 5 and Configurations I, II, and III of Table 4 maintained a constant OD radius ratio of 1.06 aft of $L/R_1 = 0.49$ and, as can be seen, caused a significant decrement in separation efficiency.
4. Splitter lip axial location. Moving the lip forward makes it more difficult to turn the air back into the compressor. Moving the lip aft adds length to the separator.

Compromise on flow path shape, if necessary, should be along the lines of previous experience as shown in Figures 38 and 39 (also see Table 8). Whether or not compromise is necessary, the preferred area distribution is the one shown by circular symbols in Figure 36. The large area increase aft of the rainstep results from the large ratio of scavenge passage area to separator inlet area. Even though scavenge flow to core airflow ratio is in the range of only 0.16 at design to 0.35 at engine idle, the scavenge passage area shown is required for good separator efficiency. Note on Figure 36 that the scavenge passage area is larger than the core flow area. A smaller passage would provide a smaller target area for scavenging sand. The area increase shown for the 2 lb/sec separator is undesirable but necessary because of envelope restrictions. The 2 lb/sec distribution in Figure 36 ends at a 0.45 area ratio because of face Mach number requirements of the compressor for which it was designed, not because of separator design considerations. Because of the rapid turning of the air around the rainstep and into the core, the 0.050-in. rainstep on the inner wall is found to be beneficial in keeping the flow attached to the ID aft of the rainstep. Apparently, a trapped vortex is established behind the rainstep as described in Reference 7. Tests on the T700 separator showed a 1.0-in. H_2O pressure drop increase when the area behind the rainstep was faired in. The pressure loss increase resulted because the flow aft of the rainstep did not reattach before it entered the separator deswirl vanes. Rainstep range from 0.04 to 0.07 in. should be sufficient to maintain the trapped vortex.

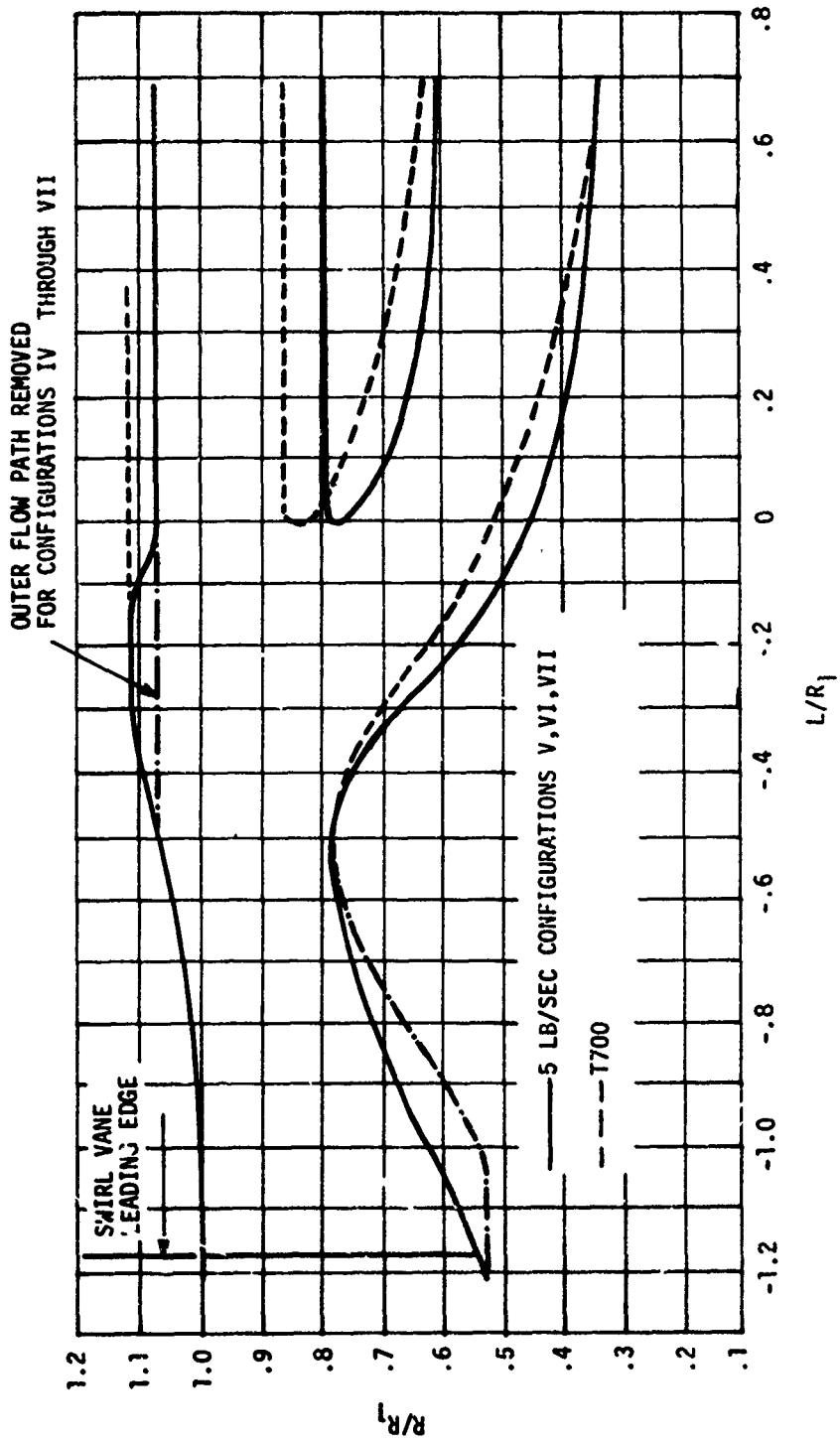


Figure 39. 5 Lb/Sec Swirlless Flow Path With Design 3 Inner Wall.

TABLE 8. 5 LB/SEC SEPARATOR FLOW PATH

Inner Wall		Design 3 Inner Wall Forward of Rainstep		Outer Wall		Splitter Wall		
L/R ₁	R/R ₁	L/R ₁	R/R ₁	L/R ₁	R/R ₁	L/R ₁	R/R ₁	R/R ₁
.861	.322	- .498	.785	-1.200	1.00	0	.594	.785
.801	.325			- .973	1.00	.861	.595	.785
.741	.327	- .524	.781	- .897	1.002	.801	.597	.785
.680	.332	- .562	.773	- .820	1.008	.741	.598	.785
.620	.336	- .690	.763	- .745	1.018	.680	.601	.785
.560	.341	- .638	.748	- .669	1.030	.620	.603	.785
.500	.346	- .676	.731	- .592	1.043	.560	.606	.785
.440	.352	- .714	.712	- .516	1.060	.500	.609	.785
.379	.356	- .752	.691	- .498	1.064	.440	.614	.785
.319	.363	- .828	.643	- .487	1.068	.379	.618	.785
.259	.373	- .866	.618	- .456	1.075	.319	.626	.785
.199	.385	- .903	.593	- .426	1.082	.259	.635	.785
.138	.403	- .942	.570	- .395	1.090	.199	.649	.785
.078	.423	- .980	.550	- .365	1.097	.138	.668	.785
.018	.446	-1.018	.535	- .335	1.104	.078	.697	.785
.042	.470	-1.038	.531	- .304	1.109	.048	.718	.785
-.102	.499			- .274	1.110	.033	-	.785
-.162	.541			- .258	1.110	.018	.743	.782
-.223	.594					.012	.748	.781
-.283	.655			.133	1.110	.006	.754	.778
-.343	.718			- .122	1.109	0	.767	.767
-.403	.760			- .101	1.100			
-.427	-			- .080	1.092			
-.452	-			- .059	1.081			
-.464	.774			- .038	1.072			
-.498*	.774	.785		- .017	1.066			
				0	1.064			

* Flow path forward of rainstep (-.498) identical to Table 6.

Aerodynamic Analysis Tools

The separator flow field is very complicated whether or not swirl and deswirl vanes are part of the design. With swirl and deswirl vanes as part of the design, five analysis tools are required:

1. An axisymmetric compressible potential flow analysis technique that can model:
 - a. Flow splits between core and scavenge airflow.
 - b. Cascades.
 - c. Swirl.
 - d. Pressure and temperature gradients.

A typical basis for such an analysis is described in Reference 8.

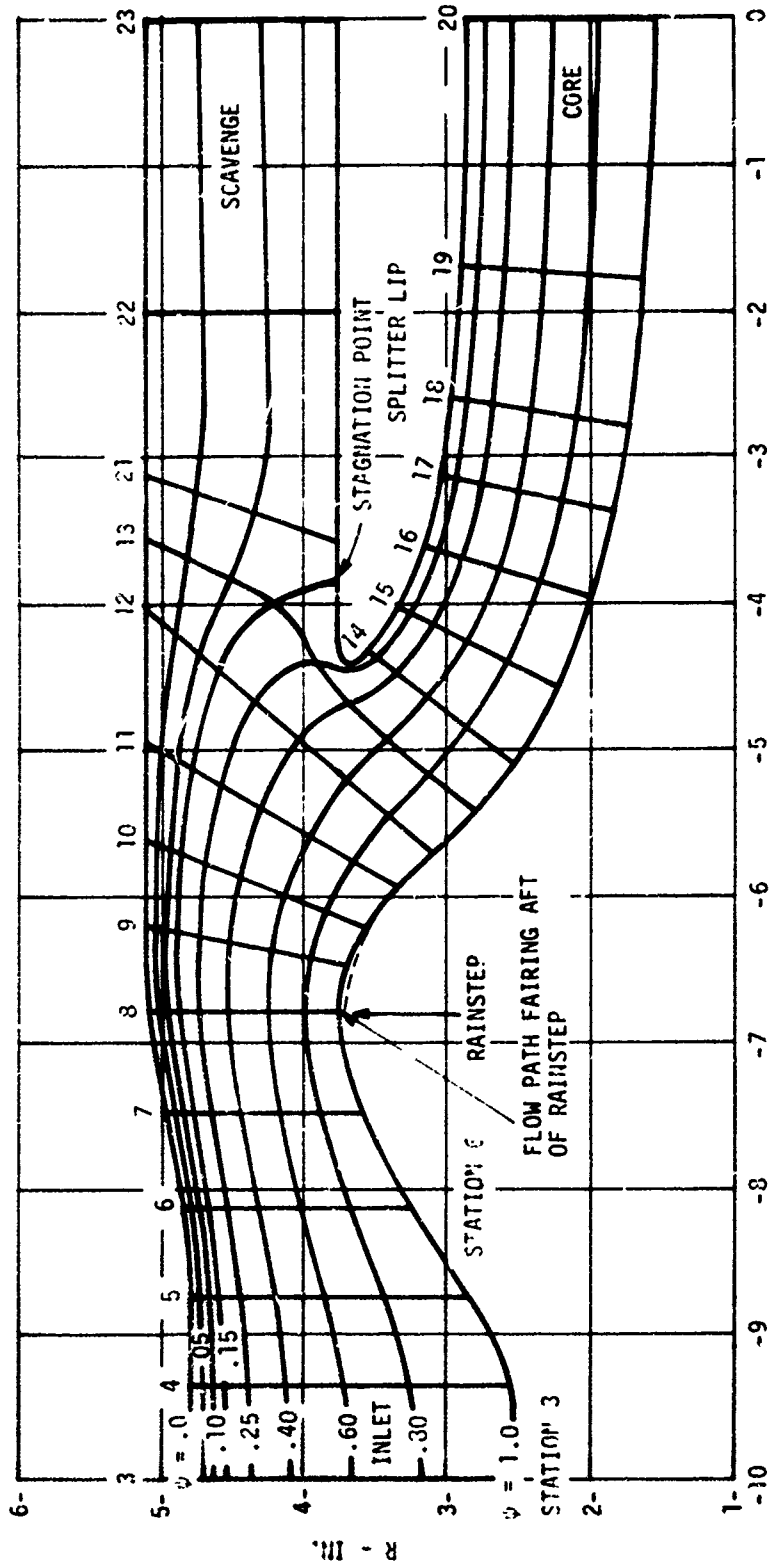
2. Boundary layer growth analysis such as described in Reference 9.
3. Separation criteria analysis such as described in Reference 10.
4. Cascade analysis such as described in Reference 11.
5. Trajectory analysis such as described in Appendix B.

Flow Path Analysis

It is possible to start the aerodynamic analysis with an analytical model of the entire separator including swirl and deswirl vanes. However, it is best to start with a model of the flow path. Progress will be greater if the design is started with a swirlless configuration before the complexity of vanes is added. Also, the flow path analytical model can be easily checked against a model test to give confidence that the analysis technique has been done correctly.

The results of a flow path analysis are shown in Figure 40. The streamlines shown were generated using an axisymmetric flow computer program. When the model is set up, certain steps should be taken to obtain an accurate analysis and to facilitate subsequent steps in the separator design process.

1. An inlet flow path for the separator should be analyzed. Since a component model test will be part of the separator development program, the component test bellmouth should be analyzed with the separator behind it. The separator flow path influences the bellmouth static pressure distribution and could change the bellmouth flow coefficient used in the airflow measurement. Different separator flow paths could influence the bellmouth differently. The bellmouth analysis can also be used to establish the proper component test sand ingestion technique.



Z FROM AERO ZERO - IN.

Figure 40. Aero Analysis of 5 lb/Sec Swirlless Flow Path, Showing Stations.

2. If swirl and deswirl vanes are to be part of the separator design, model calculation stations should be chosen to coincide with vane leading and trailing edges. Stations 3 and 6 are such stations in Figure 40.
3. The rainstep is faired in to simulate what would happen in the real airflow situation. The space behind the rainstep, in the real case, is filled by a trapped vortex that enhances flow reattachment.
4. Calculation stations are chosen to approximate equipotential lines.

The Mach number distribution for the flow field of Figure 40 is shown in Figure 41. Both figures point out the complexity of the separator flow field. Along the outer wall, diffusion starts prior to the rainstep and proceeds at a rate that causes separation. Along the inner wall or hub, the flow decelerates as it approaches the expanding separator hub, accelerates as the flow area is restricted (see Figure 36), decelerates as it expands around the rainstep, then accelerates as it is forced into the core. To decrease pressure losses, an attempt should be made to eliminate areas of local deceleration. The first hub deceleration can be diminished when swirl vanes are added. The second hub deceleration can be lessened by a hub flow path radius increase aft of the rainstep. However, too much of a radius increase raises the average flow Mach number, making deswirl vane losses increase.

The stagnation point on the top of the splitter lip results from the fact that 16.5% of core flow goes through the scavenge system, but the scavenge system flow area is 70% to 87% of the separator inlet area (see Figure 36). This situation is similar to a high-bypass-ratio turbofan engine inlet operating at a high mass-flow ratio. As shown in Figure 41, very large Mach numbers (0.94) followed by rapid diffusion occur at the splitter lip. This is an important pressure loss mechanism, and any reduction in lip local Mach numbers or enhancement of flow reattachment aft of the lip will lessen overall separator pressure loss.

Figure 42 shows wall static pressures calculated for the flow path of Figure 40 compared to data measured in a component model test of the flow path. This type of data is recommended as a check on the analytic model. The data shown agrees with prediction within 10% of the local velocity head everywhere except $Z = -5.4$. This larger deviation at $Z = -5.4$ is probably due to hub separation in the diffusing region aft of the rainstep. Friction losses were not included in the prediction, so the static pressures along the hub are all lower than the predicted levels.

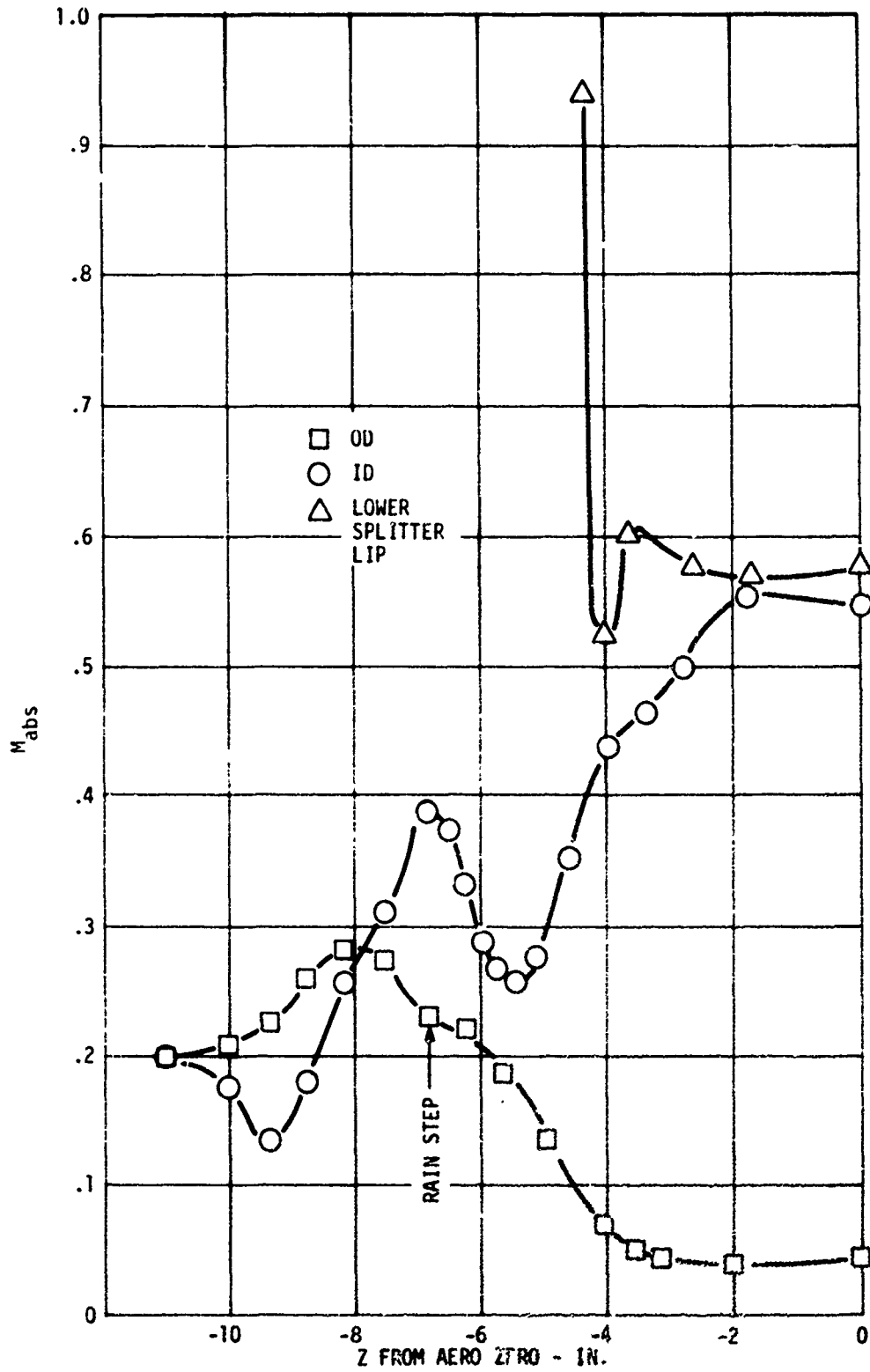


Figure 41. Mach Number Distribution for 5 Lb/Sec Separator Model - Vaneless.

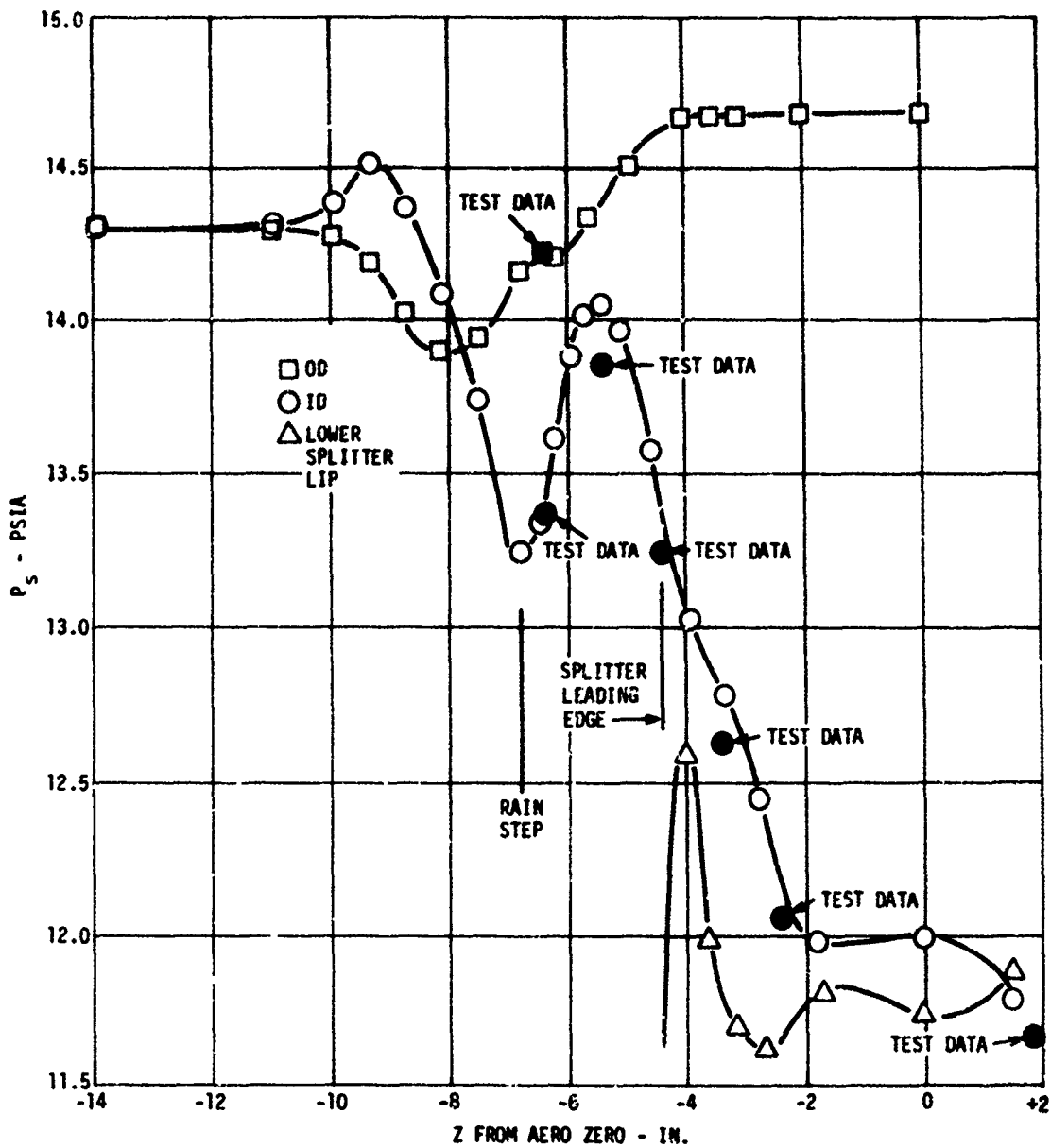


Figure 42. Wall Static Pressures for 5 Lb/Sec Separator Model - Vaneless.

If the separator is to have swirl and deswirl vanes, they should be incorporated into the analytic model at this point. If the separator is to be vaneless, a boundary layer analysis should be carried out to allow prediction of separator losses and to eliminate areas of flow separation where possible. The same techniques described below for a swirling flow boundary layer analysis should be used for the swirlless analysis.

Another output of the swirlless flow path analysis is an area distribution based on flow Mach number as shown in Figure 43. This figure shows that the large diffusion forward of the splitter lip implied by Figure 36 is not experienced by the majority of the airflow. This diffusion always occurs due to the flow path geometry required for separation efficiency. Figure 43 can be used to assess whether a flow path that is different from those of Figures 37, 38, and 39 causes diffusions that are outside the range of previous experience.

SWIRL VANE DESIGN

To achieve above 80% separation efficiency on AC coarse sand and above 91% efficiency on C-Spec sand, swirl vanes are required based on the experience shown in Figures 28 and 29. Figures 44, 45, and 46 can be used to select the swirl level for the desired separator performance. Swirl level is the mass averaged swirl angle measured at the rainstep. The figures show trends such as a 0.4 in. to 0.9 in. $H_2O \Delta P_T$ increase per degree of swirl, 0.2 to 0.4 points of C-Spec efficiency per degree, and 0.6 to 1.1 points of AC coarse efficiency per degree. For separation efficiencies of 80% on AC coarse and 95% on C-Spec, the figures indicate that a swirl level of 33 to 35 deg is reasonable.

Selection of swirl vane design parameters should proceed as follows:

1. Choose a simple shape. A complex shape will not be duplicated in manufacturing.
2. Choose the number of swirl vanes equal to the number of deswirl vanes and equal to the number of compressor inlet guide vanes. Figure 47 shows the data from Configuration XIII of Table 5. The figure shows that 0.5 in. $H_2O \Delta P_T$ difference exists between the best and worst swirl vane positions. Impressing the deswirl vane wakes on the compressor IGV's has been shown to improve IGV losses by an additional 2 in. H_2O . Therefore, the proper choice of swirl and deswirl vane numbers and circumferential location could save 2.5 in. H_2O in pressure loss.
3. Because the separator pressure loss is sensitive to swirl vane losses, plot the area distribution through the cascade passage to the rainstep and make sure it is uniformly decreasing if possible.

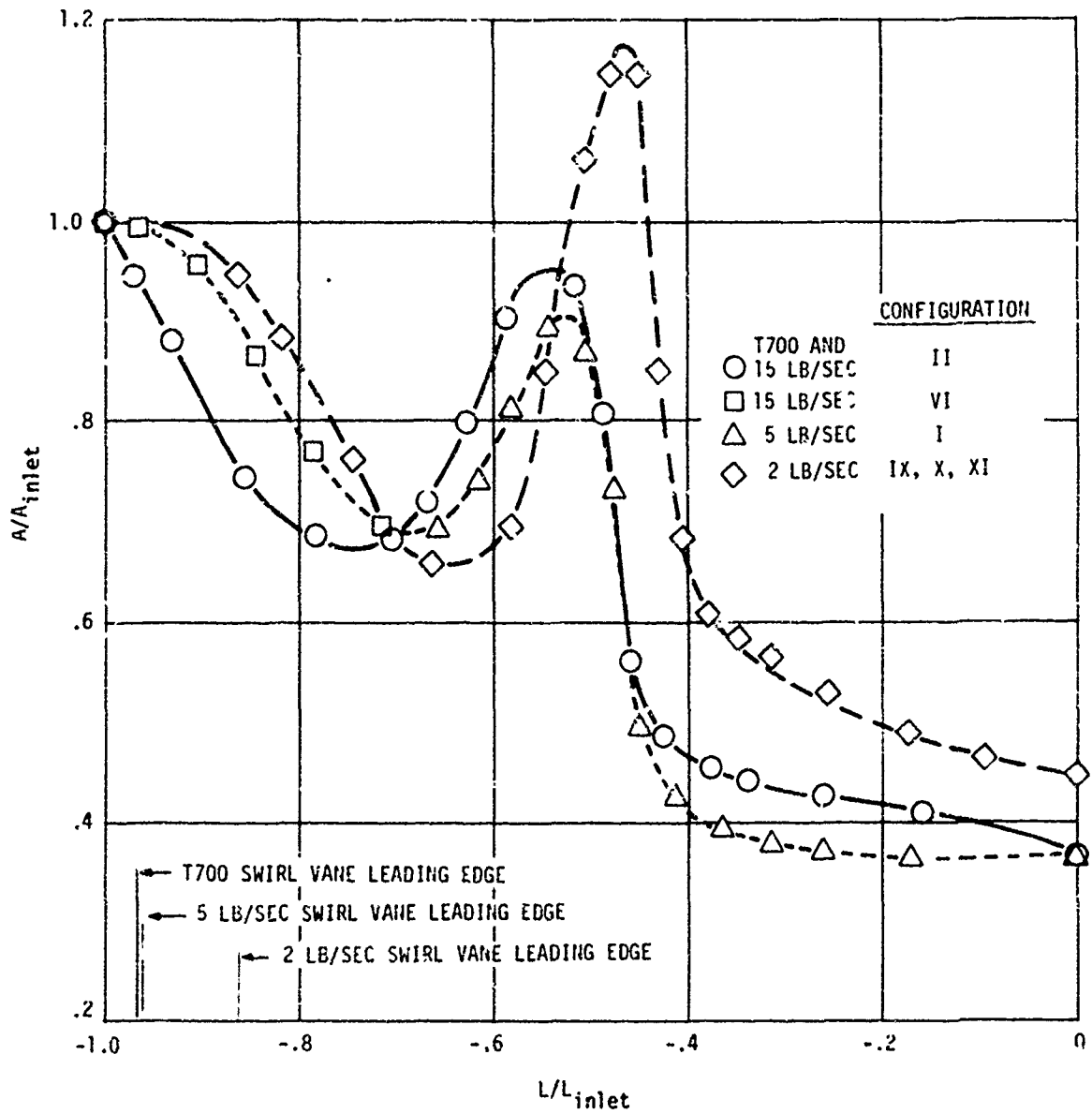


Figure 43. Area Through Vaneless Separator - Based on $\psi = 0.6$ Flow Mach Number.

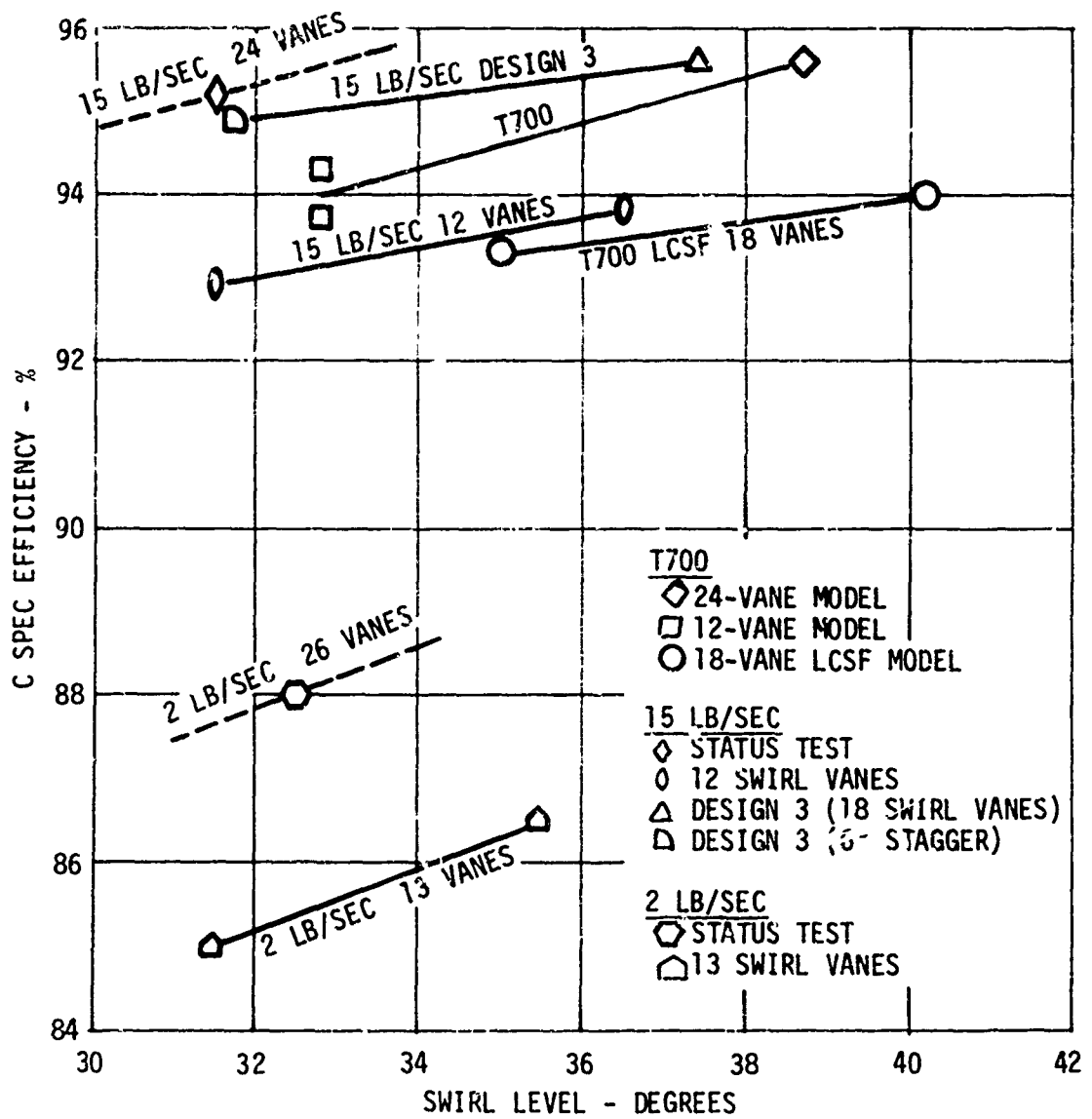


Figure 44. C-Spec Efficiency vs Swirl Level.

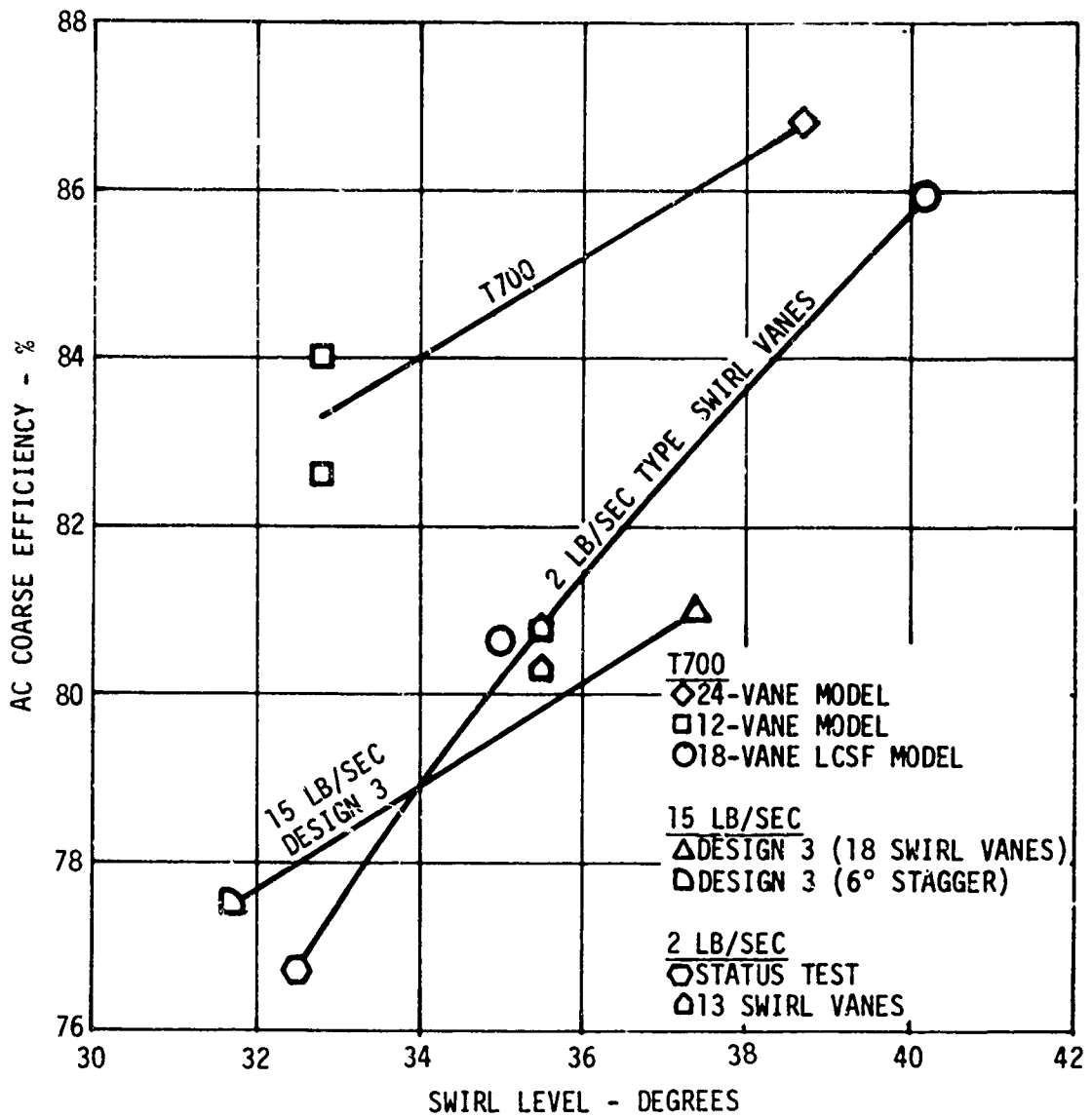


Figure 45. AC Coarse Efficiency vs Swirl Level.

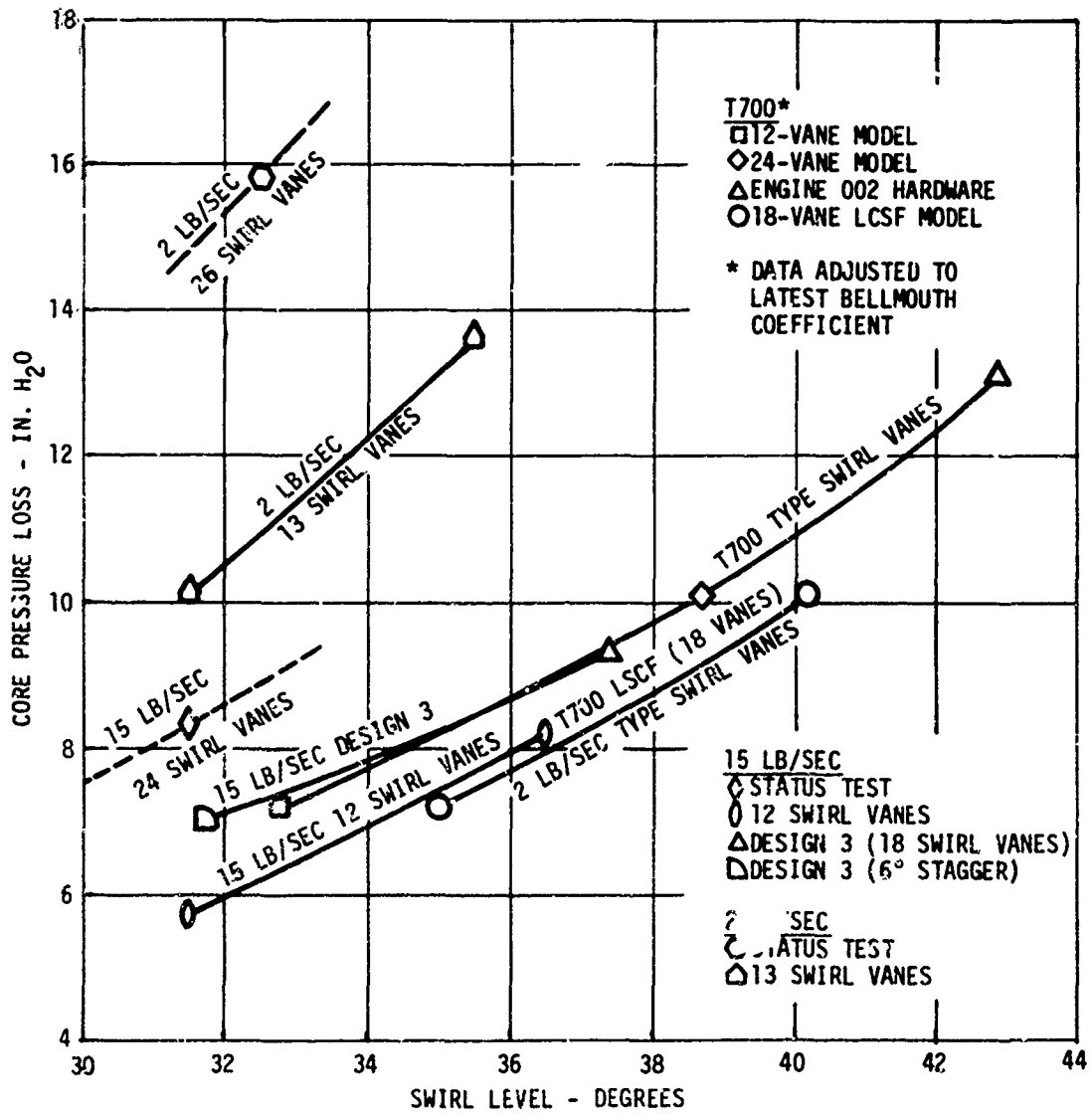


Figure 46. Core Pressure Loss vs Swirl Level.

4. Avoid special "fat" vanes to carry engine services such as oil, electrical leads, or accessory drive shafts. It is desirable to maintain small swirl vane pressure wakes. The presence of unmixed wakes in the diffusing airflow between the rainstep and the splitter lip may amplify the wake loss. During T700 separator development, improvement of swirl vane losses by 0.7 in. H₂O was computed to improve separator losses by 1.8 in. H₂O. Actual loss improvement by component test was 2.5 in. H₂O. The mechanism of diffusion and then mixing causes a total pressure loss that is not measured by a mass averaged survey of the nondiffused unmixed streams.
5. Design short swirl vanes to impart swirl early and to allow wakes to mix before entering the diffusion region aft of the rainstep. Vane spacing will be small, which is desirable for protection from single foreign objects.
6. Desirable solidities are about 1.5 at the inlet ID and 0.8 at the inlet OD. Using the flow path shown in Figure 37, there is not actually a 1.5 solidity at the ID since the expanding ID radius covers most of the hub section. An 0.8 solidity at the OD allows large deviation angles at the OD, but high swirl at the OD is not necessary.

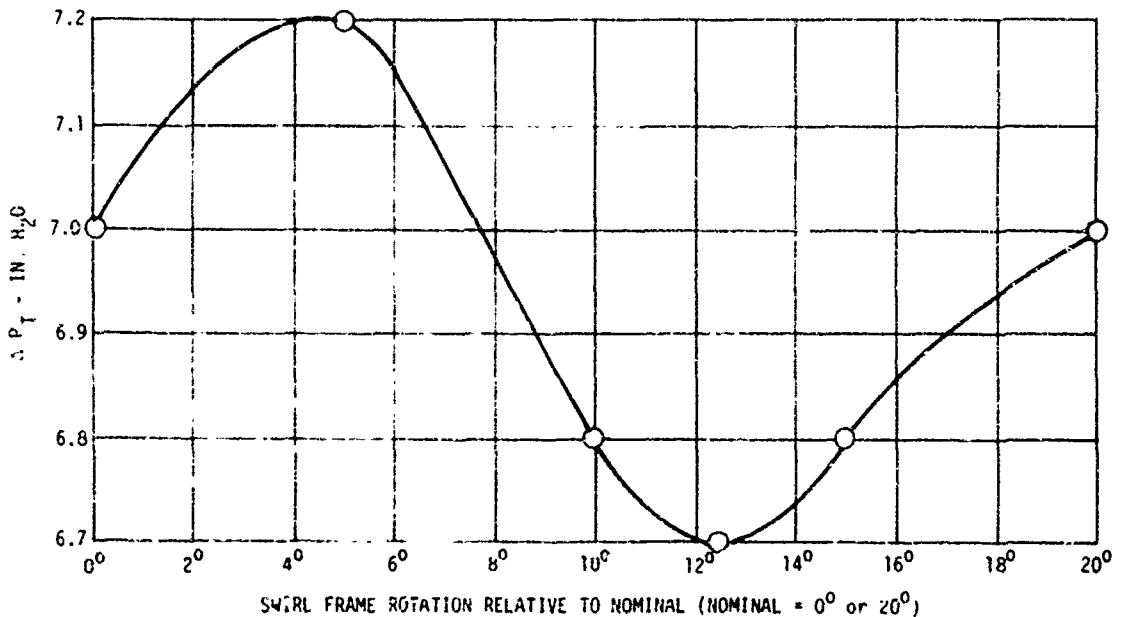


Figure 47. Swirl Vane Clocking Relative to Deswirl Vanes.

Swirl Vane Shapes

For engines in the 2 lb/sec class, the small size requires that a relatively fat vane be used for structural purposes and to supply services. The relatively small annular height (see Figure 38) of this size of separator allows the cascade to be considered as two dimensional. The vane shown in Figure 48 fulfills all these requirements and is the vane used for all testing reported in Table 3. With 26 vanes the pitch-line solidity was 2.2, giving a separator pressure loss of 15.8 in. H₂O. When half the swirl vanes were removed to give a solidity of 1.1, swirl angle dropped 1° and pressure loss dropped 5.7 in. H₂O. As shown, the vane radial stacking axis is close to the leading edge and the design (status) stagger angle is 20.5°. The vane trailing edge was made coplanar with the rainstep axial station. The vane is longer than aerodynamically desirable in order to limit thickness/chord to 0.15 with the vane max. thickness of 0.330 in. Trailing edge thickness of 0.03 in. was as thin as possible. For all swirl cascades, the trailing-edge thickness should be less than 8% of the passage width, as shown in Figure 49. Vane coordinates are given in Table 9. This vane can be scaled to other airflow sizes close to 2 lb/sec.

At 5 lb/sec and above, it is not necessary to use thick vanes to allow space for engine services and anti-icing. The vane shown in Figure 50 as "thinned design 3" was used for both 5 and 9 lb/sec separators simply by scaling the vane coordinates by the square root of the compressor airflow ratio.

The section shown is taken by passing a plane through the vane inclined at 12.35° to the engine axis as shown in Figure 51. The purpose of this plane is to establish a swirl vane section that is approximately coincident with a streamline. The design 3 vane of Figure 50 is a shape that is suitable for casting. The design 3A vane is a shape better for sheet metal fabrication.

Both vane sections shown in Figure 50 were derived by attempting a pressure side slope schedule for early particle deflection. Pressure side slope is defined in Figure 52. The slope schedules shown in Figure 52 yielded the AC coarse collection efficiencies shown in Figure 53, as a function of swirl level. Pressure loss goes up with swirl level, and the slope¹ schedule gives the best efficiency for a given pressure loss. The slopes were computed for the pitch-line radius section of the swirl vane. Using Figure 52 as a guide, designs 3 and 3A were derived by increasing the slope as quickly as possible after the vane leading edge. The coordinates for design 3A are shown in Table 10. Cascade parameters at the design stagger angle are: thickness/chord ratio = 10.6%, pitch-line solidity = 1.5, and trailing-edge mean-line metal angle = 34°.

Note: Designs 3 and 3A vanes have blunt leading edges to allow stagger angle changes during model test without large penalties in swirl cascade pressure losses due to incidence angle. Other aerodynamic and mechanical

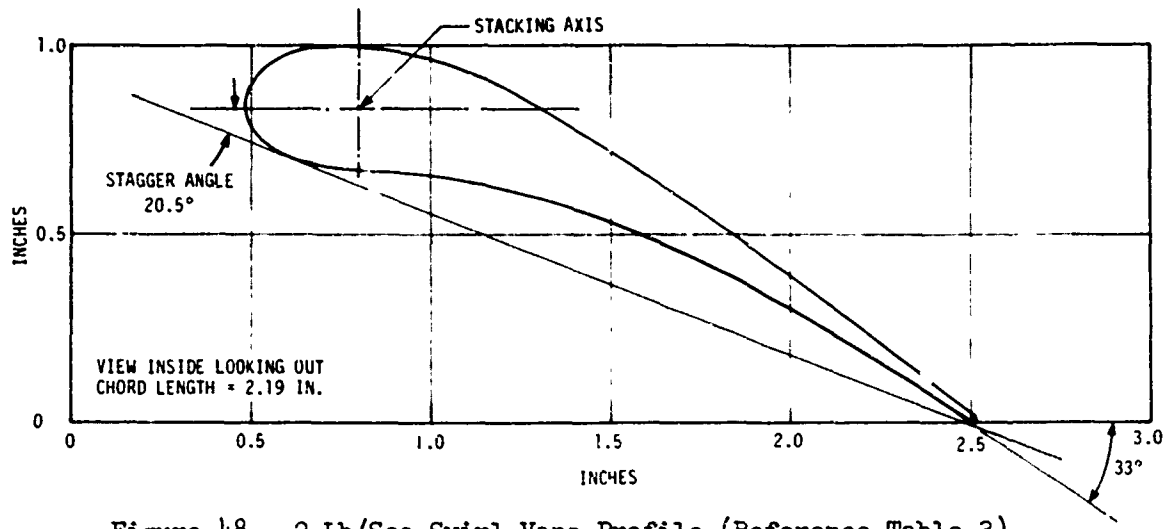


Figure 48. 2 Lb/Sec Swirl Vane Profile (Reference Table 3).

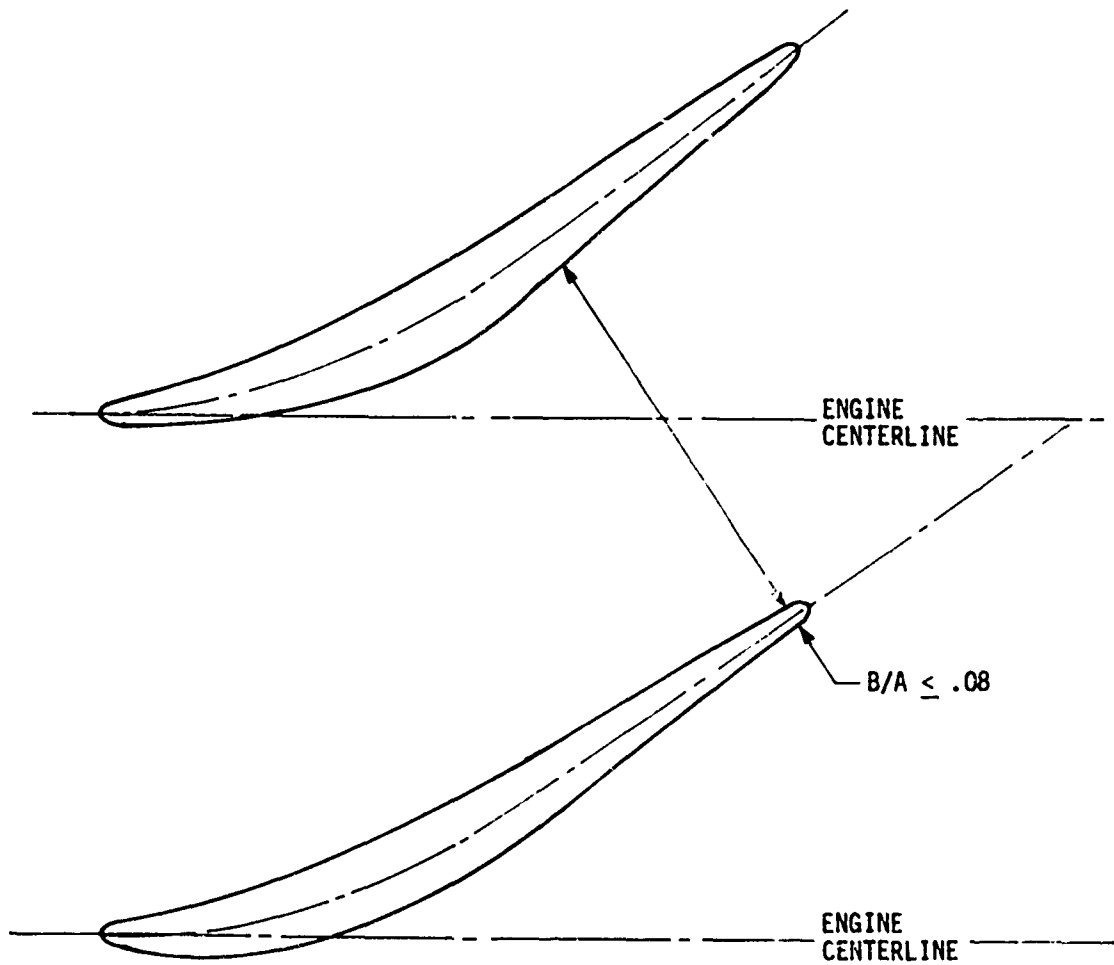
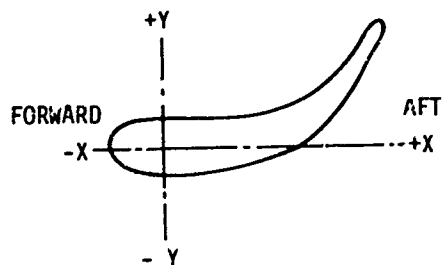


Figure 49. Vane Trailing-Edge Thickness as Part of Passage Width.

TABLE 9. 2 LB/SEC SWIRL VANE



Nose

X	Y
0	$\pm .165$
-.1	$\pm .157$
-.15	$\pm .147$
-.2	$\pm .131$
-.25	$\pm .108$
-.3	$\pm .069$
-.33	± 0

View
(outside looking in)

- NOTE:
1. Section applies to all radii.
 2. Vane is straight and radial.
 3. Trailing edge is coincident with rainstep when installed.
 4. 26 equally spaced vanes.
 5. Chord = 2.205 in.
 $t_m/c = 0.150$
 Solidity = 2.61
 $s = 3.5R$
 Camber = 33°
 Leading-edge thickness = 0.330 in.
 Trailing-edge thickness = 0.030 in.
 Stagger angle = 20.5°

Airfoil

X	Upper Side	Lower Side
	Y	Y
0	+ .165	- .165
.1	+ .168	- .155
.2	+ .176	- .133
.3	+ .192	- .097
.4	+ .209	- .055
.5	+ .235	- .007
.6	+ .269	+ .046
.7	+ .297	+ .106
.8	+ .335	+ .163
.9	+ .378	+ .230
1.0	+ .425	+ .302
1.1	+ .475	+ .3 3
1.2	+ .530	+ .444
1.3	+ .587	+ .515
1.4	+ .647	+ .586
1.5	+ .708	+ .658
1.6	+ .774	+ .732
1.7	+ .835	--)
1.721	--	+ .814) T-E of Airfoil (Note: Add .015R trailing edge radius.)

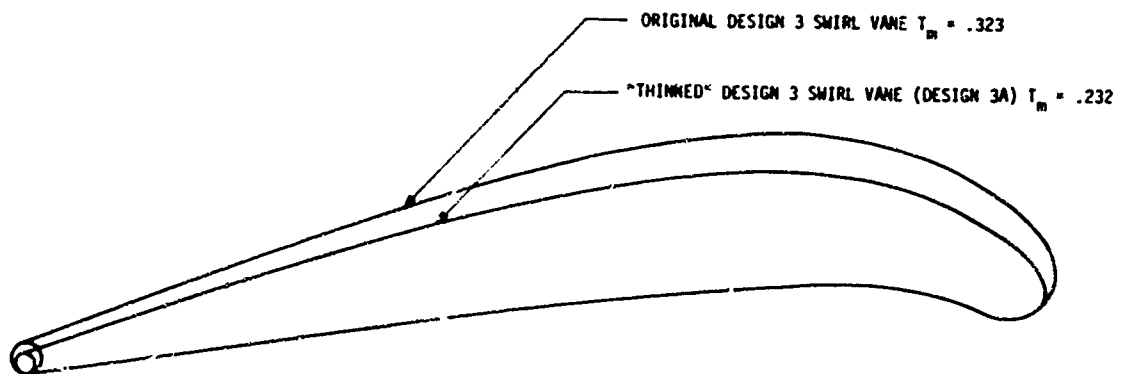


Figure 50. 5 Lb/Sec Thinned Design 3 Vane.

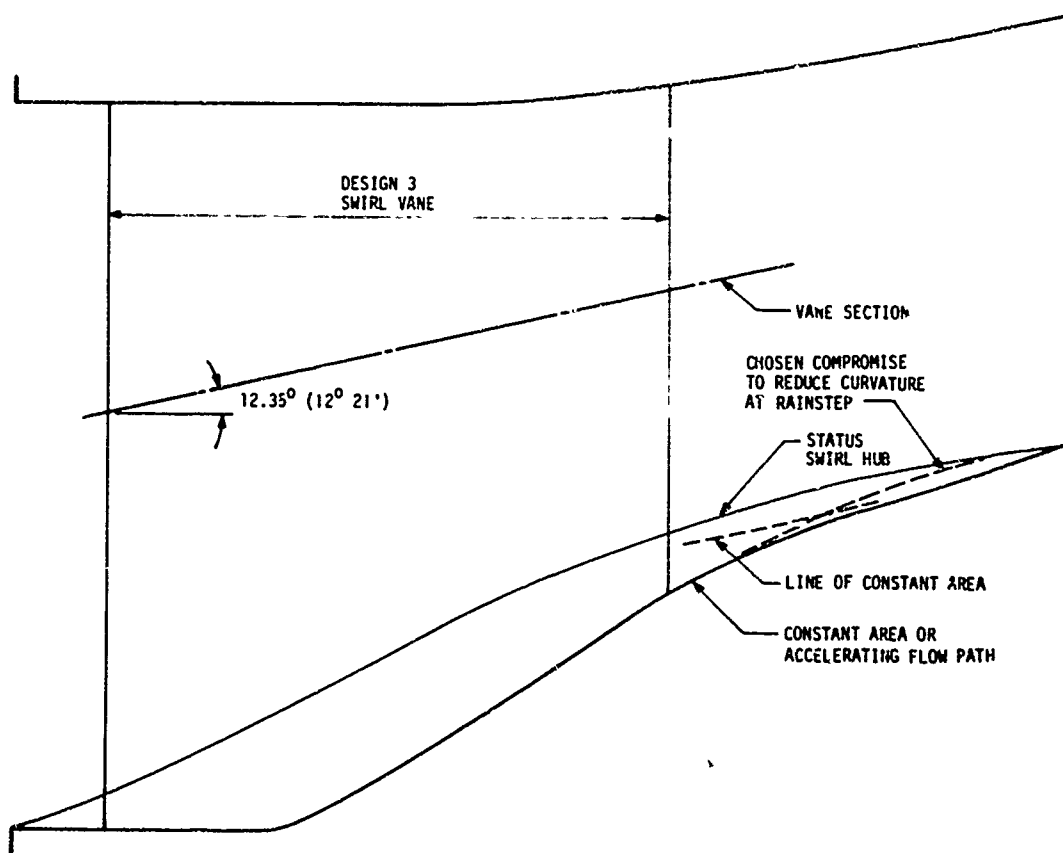


Figure 51. Design 3 Separator Swirl System.

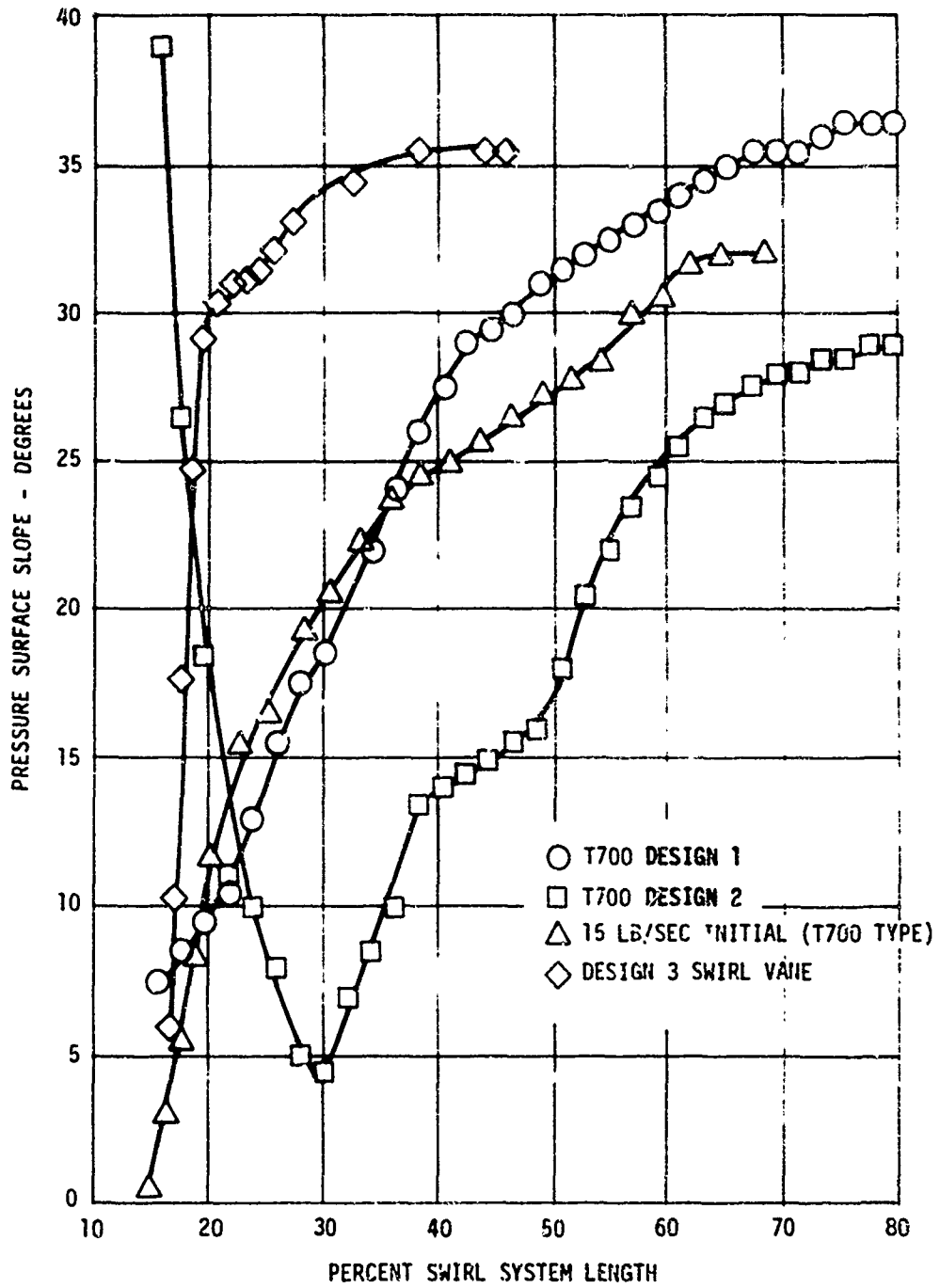


Figure 52. Vane Pressure - Side Slope.

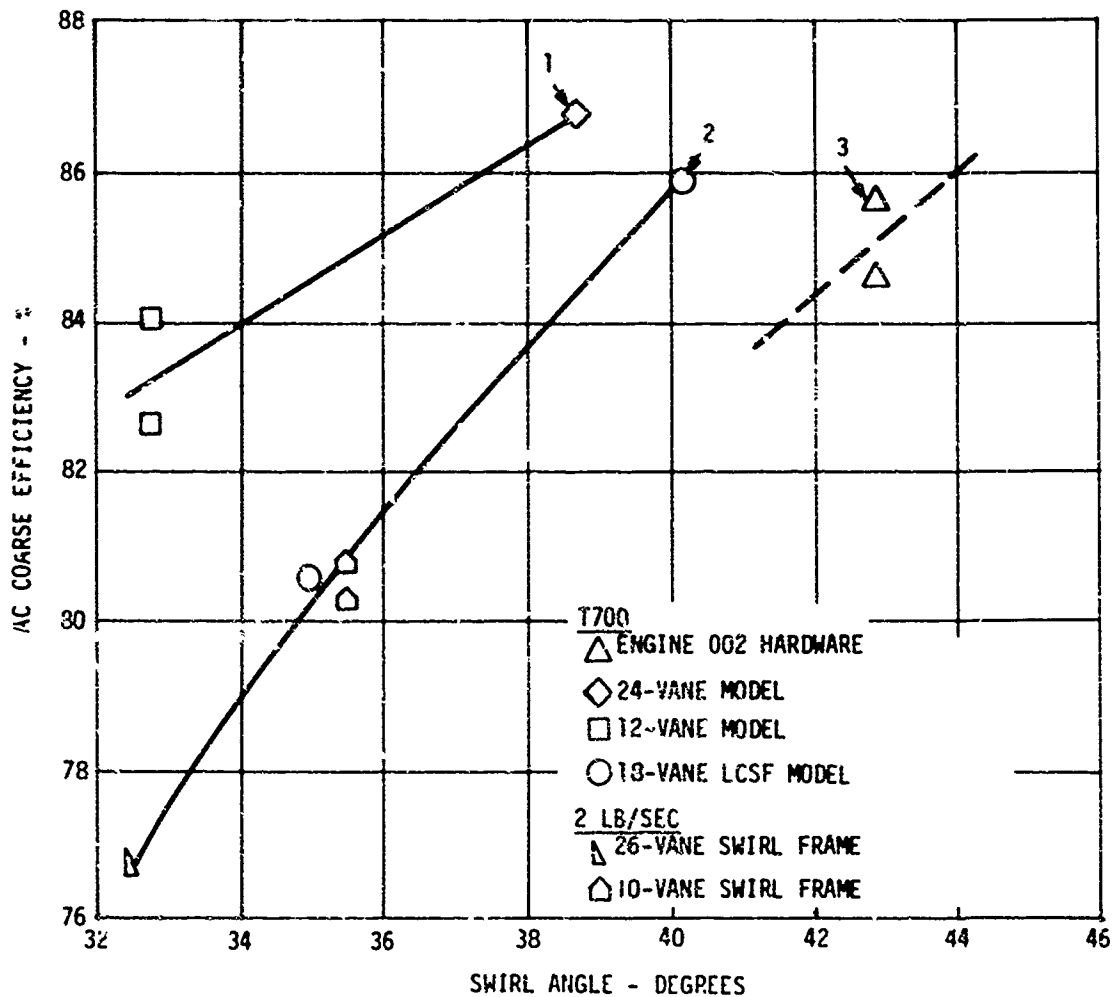


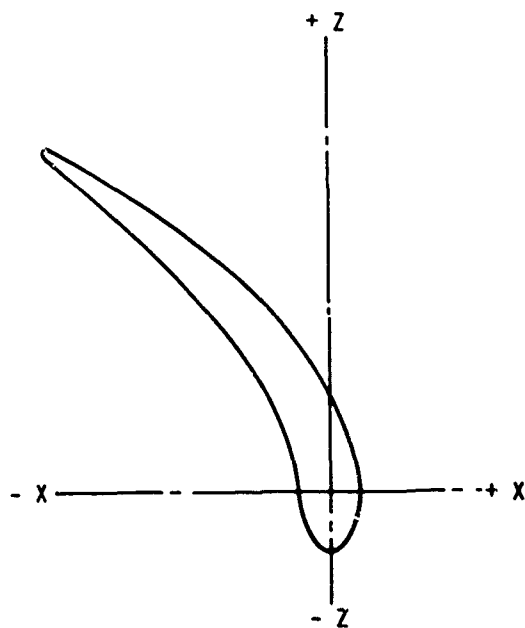
Figure 53. Separation Efficiency With AC Coarse Material vs Swirl Level.

TABLE 10. DESIGN 3A 5 LB/SEC SWIRL VANE

$t_m = .232$

Section No.	Vane Axial Z (in.)	Press. Side X (in.)	Section Side X̄ (in.)
1	-.109	0	0
2	-.073	-.057	.053
3	-.036	-.074	.073
4	0	-.079	.085
5	.073	-.075	.096
6	.146	-.085	.101
7	.214	-.102	.100
8	.282	-1.30	.297
9	.365	-.160	.279
10	.438	-.195	.058
11	.511	-.231	.083
12	.583	-.265	.001
13	.656	-.300	-.034
14	.729	-.339	-.074
15	.875	-.414	-.165
16	1.02	-.892	-.265
17	1.313	-.590	-.374
18	1.313	-.651	-.487
19	1.459	-.734	-.603
20	1.675	-.815	-.719
21	1.750	-.887	-.838
22	1.787	-.917	-
23	1.807	--	-.884

- NOTES: (1) Trailing-edge radius = 0.18
 (2) Vane leading edge at engine L/R = 1.161.
 (3) One section (constant chord and camber) vane.
 (4) Stagger angle = 27.1°.
 (5) 18 vanes equally spaced.



OUTSIDE LOOKING IN

considerations aside, a sharper leading edge at 0° incidence angle would improve swirl vane losses once the appropriate swirl level for separator performance had been set.

The performance of the design 3A vane in the 5 lb/sec separator is listed in Table 4.

The design 3 vane of Figure 50 was used for a 15 lb/sec and 9 lb/sec separator with the vane coordinates scaled by the square root of the core compressor airflow ratio. The coordinates for both the 15 lb/sec and 9.45 lb/sec separators are listed in Table 11. The vane shape was chosen to be suitable for casting, so the thickness/chord ratio was set at 14.6%. Figure 51 shows the relative axial position of the design 3 vanes and also the various flowpath options that are possible. The "chosen compromise" in Figure 51 attempts not to degrade the performance of the rainstep. The compromise gives a constant-area mixing zone aft of the swirl vane to allow wakes to mix before entering the diffusion region aft of the rainstep. Study of Table 5 shows that the "good" aerodynamic hub flow path (design 3) did not give the best combination of collection efficiency and pressure loss. Performance of the design 3 vane improved with installation of the status swirl hub.

If a constant-section vane is judged to be unnecessary for manufacturing ease and tolerance control, the performance of the design 3 cascade can be improved by the addition of triangular extensions as shown in Figure 54. These extensions are constant-thickness flat plates which extend the vane trailing-edge mean-line as shown in Figure 54. The performance improvement between Configurations XV and XVI, shown in Table 5, results from

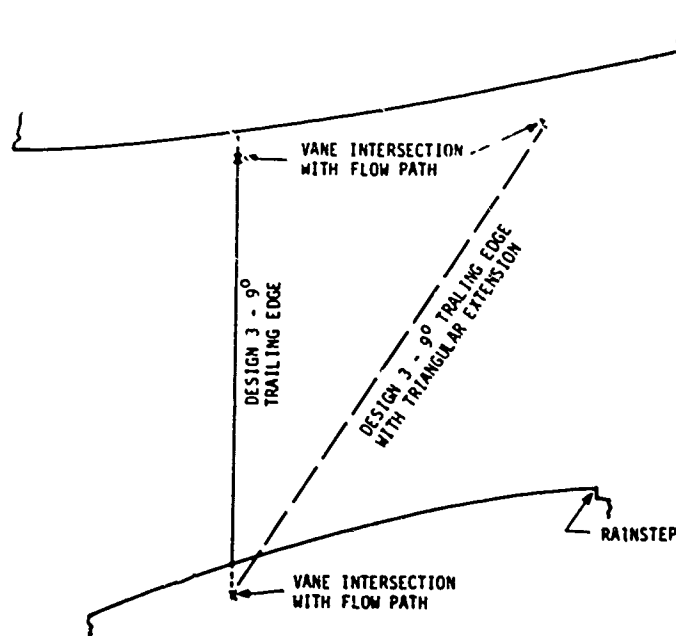


Figure 54. 15 Lb/Sec Design 3 Trailing-Edge Extension.

TABLE 11. DESIGN 3 NEW SWIRL VANE

T700							15 Lb/Sec						
No.	T700			15 Lb/Sec									
	Axial Z	Pressure Side X	Suction Side X	Axial Z	Pressure Side X	Suction Side X							
1	-.15	0	0	-.189	0	0							
2	-.10	-.118	+.084	-.126	-.149	+.106							
3	-.05	-.142	+.113	-.063	-.179	+.143							
4	0	-.155	+.130	0	-.196	+.164							
5	.1	-.168	+.146	.126	-.212	+.184							
6	.2	-.193	+.148	.253	-.244	+.187							
7	.3	-.231	+.143	.379	-.292	+.181							
8	.4	-.283	+.132	.505	-.357	+.167							
9	.5	-.340	+.110	.632	-.429	+.139							
10	.6	-.400	+.080	.758	-.505	+.101							
11	.7	-.460	+.040	.884	-.581	+.051							
12	.8	-.520	-.010	1.010	-.657	-.0126							
13	.9	-.582	-.070	1.137	-.735	-.088							
14	1.0	-.646	-.140	1.263	-.816	-1.763							
15	1.2	-.780	-.299	1.516	-.985	-.378							
16	1.4	-.918	-.432	1.768	-1.159	-.609							
17	1.6	-1.058	-.680	2.021	-1.336	-.859							
18	1.8	-1.200	-.892	2.273	-1.516	-1.127							
19	2.0	-1.344	-1.108	2.526	-1.697	-1.399							
20	2.2	-1.488	-1.328	2.779	-1.879	-1.677							
21	2.307	-1.563	--	2.914	-1.974	-							
22	2.360	--	-1.502	2.981	--	1.897							

LE at $L/R_1 = 1.161$ LE at $L/R_1 = 1.161$

Note:

.040 radius
on trailing
edge tangent
at points 21
and 22

Note:

.050 radius
on trailing
edge tangent
at points 21
and 22

- (1) One section (constant chord & camber) vane.
- (2) *Stagger angle = 33.1°
- (3) 18 vanes equally spaced
- (4) Section & stagger angle defined at $12.35^\circ (12^\circ 21')$ relative to horizontal.

- a. More vane surface to bounce sand to the separator OD.
- b. Filling in of the vane wake in an area where the wake is migrating toward the separator ID, carrying fine sand along with it.

Increased vane surface area for friction losses and "negative" vane loading reduce performance, since the straight extensions cannot be coincident with the natural air streamlines which would result from conservation of angular momentum.

The vane shape shown in Figure 49 has been used in a 9 lb/sec design 12-vane cascade. The section is taken on a $12^{\circ}21'$ plane relative to horizontal (Figure 5i) and was installed in a separator having a 6.575 in. R_1 (Figure 37) with 10° twist. Section stagger angles were 20.2° at $R = 6.6$ in. and 32.7° at $R = 3.35$ in. The radii are measured at the vane leading edge. Stacking axis (0, 0) is located at $L/R_1 = 1.134$.

Engine design constraints require thickness in a swirl vane. Were it not for anti-icing or similar considerations, a swirl vane made from a cambered plate would be acceptable or even desirable. Sharp vane leading edges at 0° angle of attack eliminate sand bouncing off the leading edges and going in undesirable directions.

Swirl Vane Analytical Model

Design 3A (Figure 5C) added to the flow field of Figure 40 with the leading edge at station 3 and the trailing edge at station 6, is a typical swirl vane analytical model. Proceed with the modeling as follows:

1. Compute the appropriate blockages, mean-line metal angles, and deviation angles.⁶ Small deviation angles for the types of swirl cascades described result from the accelerating separator flow path.
2. Include the radial and tangential forces of the swirl vane. A swirl vane with a radial leading edge has a nonradial trailing edge and, therefore, imparts radial forces on the air.
3. In choosing swirl vanes, remember that swirl angle at the rain-step is lower than swirl angle at the vane trailing edge due to conservation of angular momentum.

The computed Mach number through the separator is as shown in Figure 55, which should be compared to the zero swirl case of Figure 41. Predicted versus measured swirl distributions are shown in Figure 56, including the effects of wall boundary layers. The predicted deviation angle was about 1.5° less than was measured.

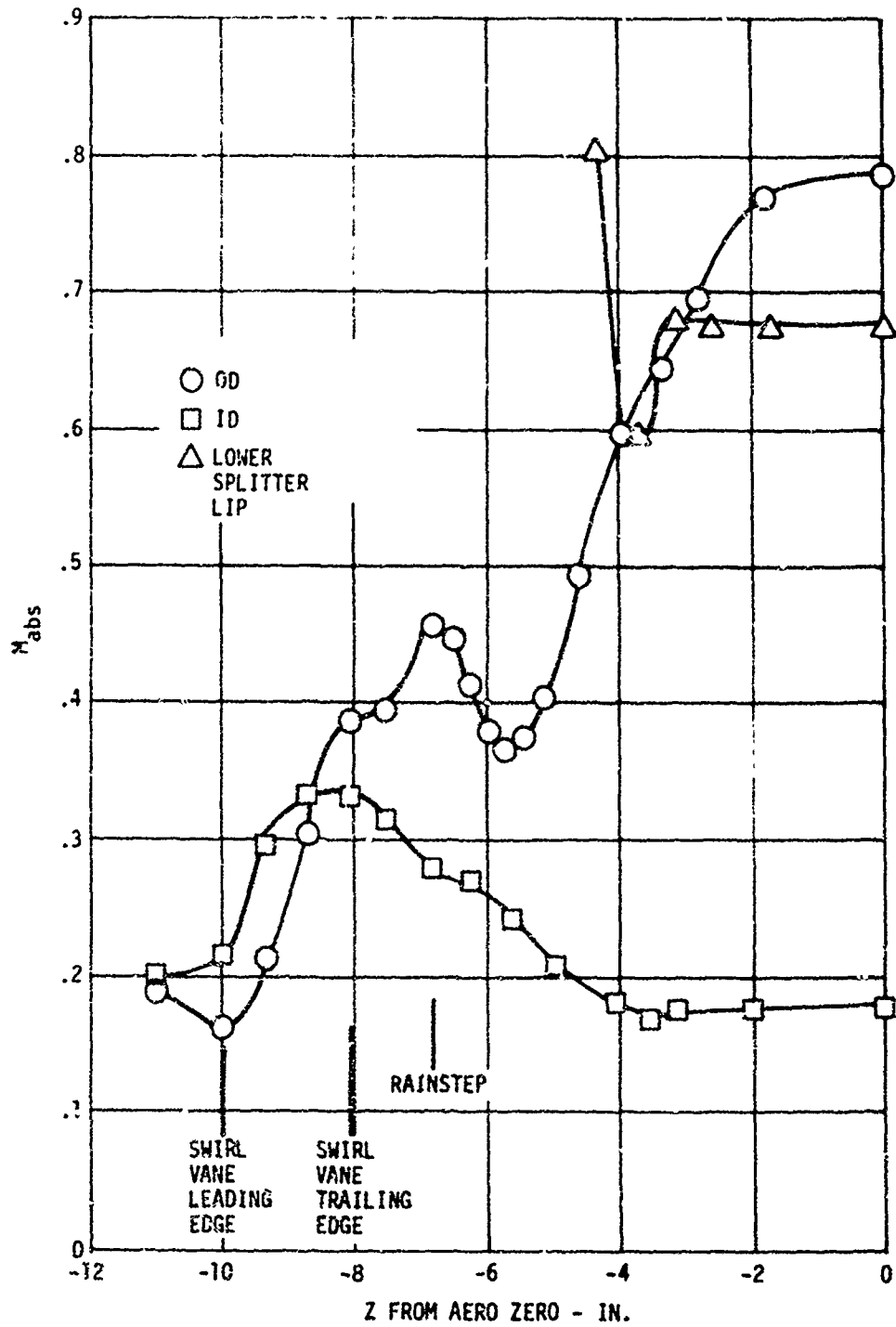


Figure 55. Mach No. Along Wall of 5 Lb/Sec Separator With Swirl Vanes.

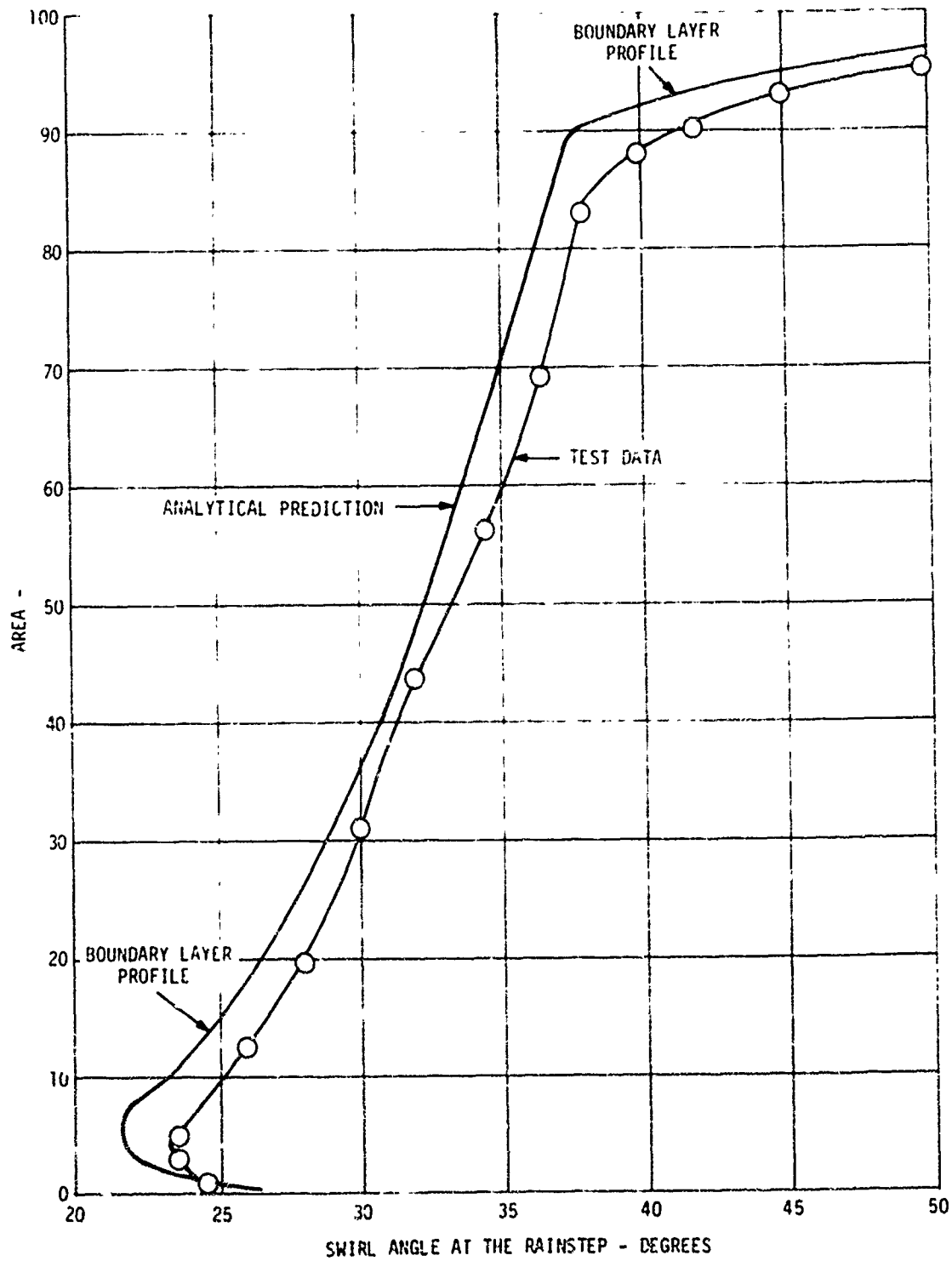


Figure 56. Comparison of Rainstep Swirl Angle Prediction With Test Data.

On the basis of the swirling flow field prediction, a boundary layer analysis can be made of the separator walls. If an analysis that includes the effects of swirl is not available, all lengths should be increased by the cosine of the swirl angle.

1. Use as input to the boundary layer analysis the boundary layers computed for the separator entrance bellmouth.
2. A conservative approach to the boundary layer aft of the rainstep is to use the displacement thickness at the rainstep plus the rainstep height as the starting displacement thickness aft of the rainstep.
3. Use the calculated ID and OD displacement thicknesses to change the wall shapes in the potential flow analysis, and recompute the new wall velocity distributions.
4. Repeat the boundary layer analysis and wall shapes until the same displacement thicknesses and wall static pressures are computed on two successive passes.
5. Using the computed displacement thicknesses at the rainstep and the power law velocity profile from the boundary layer analysis, compute the swirl angles in the boundary layer assuming that angular momentum is conserved through the boundary layer and that the velocity profile applies only to the axial velocity.
6. Apply separation criteria to the regions of adverse pressure gradient which are at the OD just aft of the swirl vanes, and the ID aft of the rainstep and the lower splitter lip. Separated flow on the splitter lip will probably reattach very quickly due to the rapid acceleration downstream as shown in Figure 55. Separation on the ID should be prevented.
7. Separation on the OD occurs just aft of the rainstep due to the very large scavenge area in relation to the amount of scavenge flow. To model this region, it is assumed that a dead air space exists aft of the separation point. A false wall is then constructed such that the static pressure along the wall is equal to the static pressure at the point of separation. Such a false wall is shown in Figure 57. Comparing Figure 57 to Figure 40, it can be seen that the false wall pushes the splitter lip stagnation point forward and diminishes the streamline curvature and diffusion in the area forward of the splitter lip. The Mach number distribution with the false wall is shown in Figure 58. Predicted versus measured static pressures are shown in Figure 59.

Figure 60 shows the predicted versus actual swirl angles of the separator core discharge (Station 0 of Figure 40). Local wall boundary layers at the hub account for the disagreement between predicted and measured results.

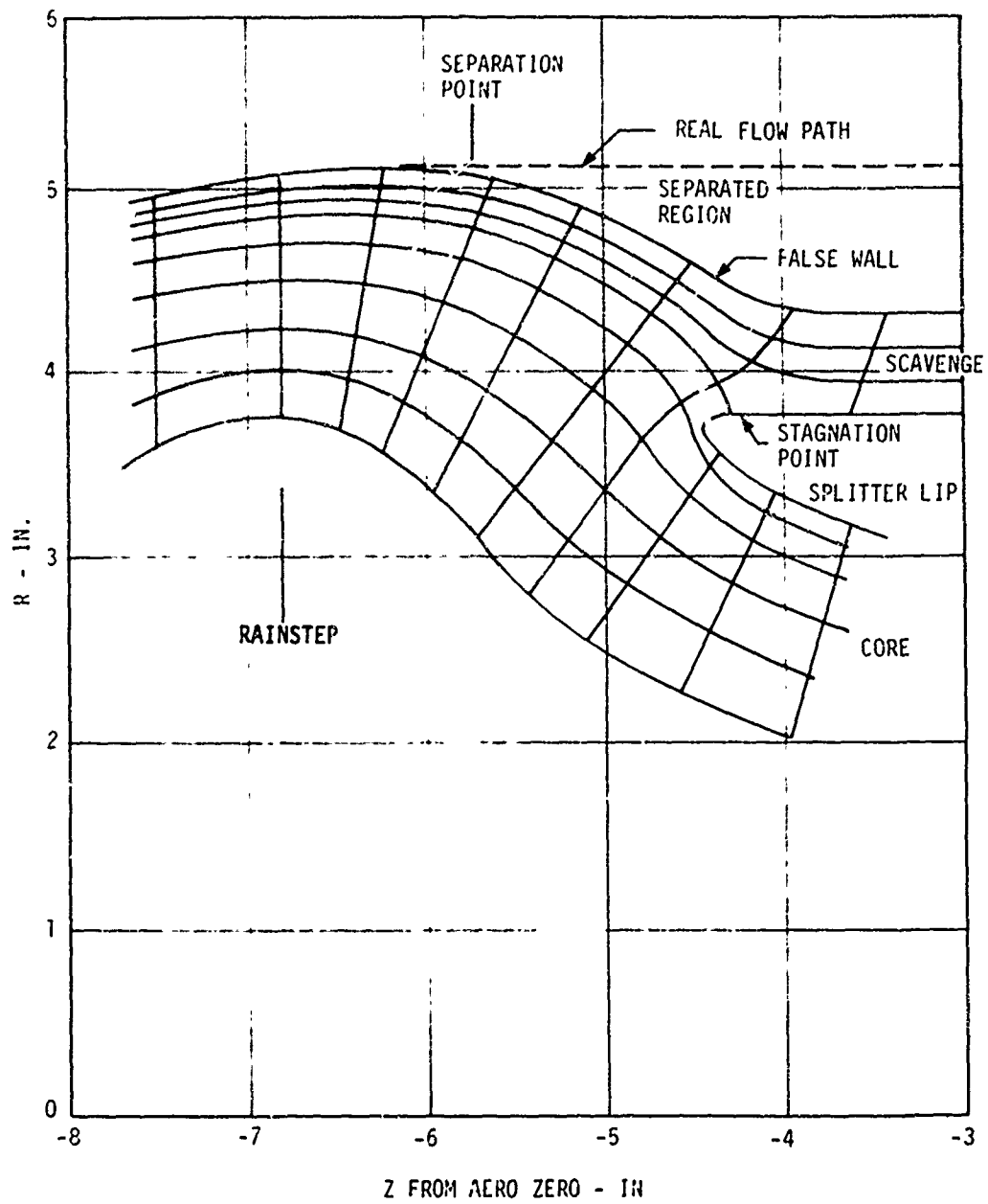


Figure 57. Flow Field With False Wall.

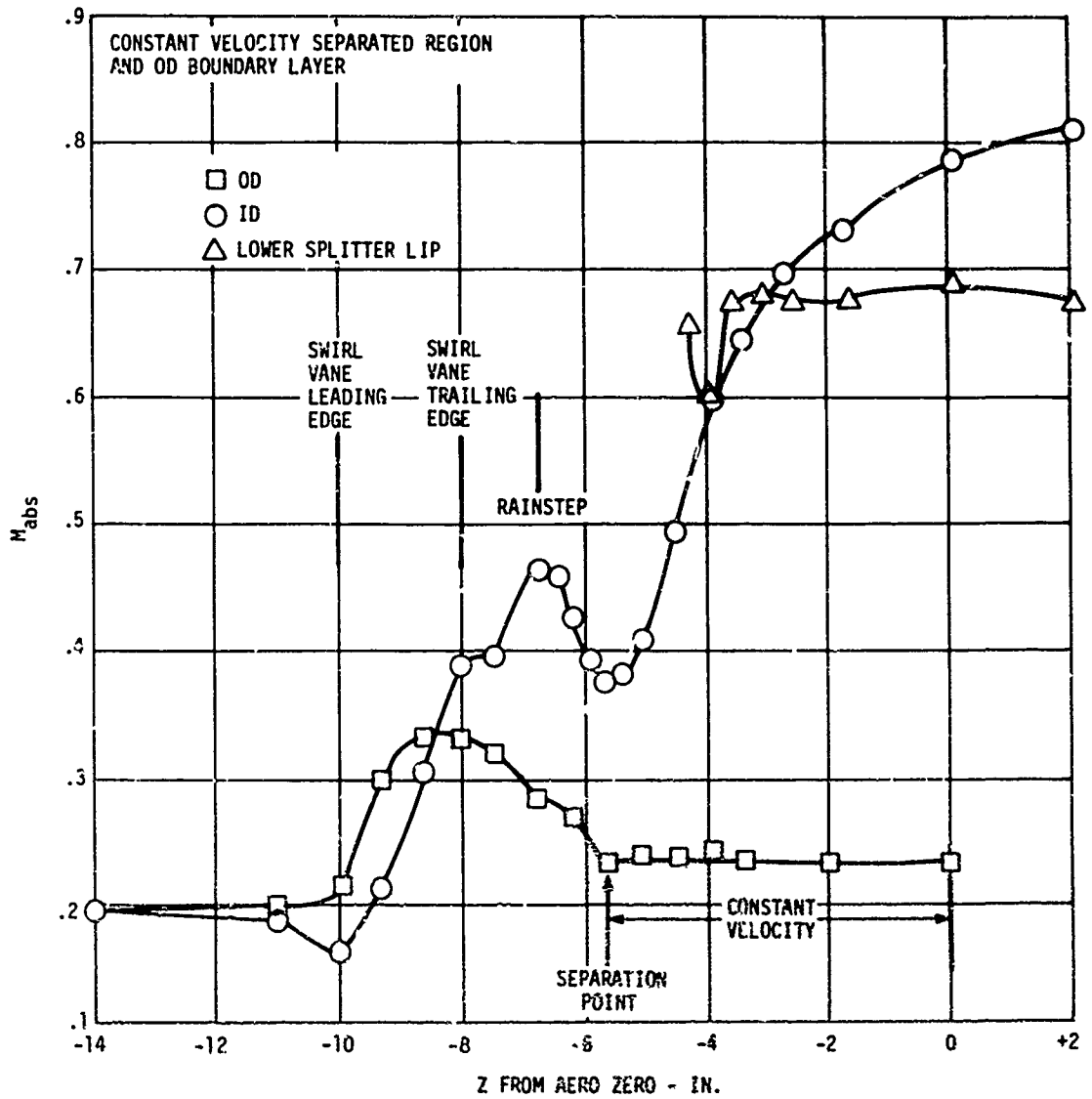


Figure 58. Wall Mach Number Distribution for 5 Lb/Sec Separator With Swirl Vanes.

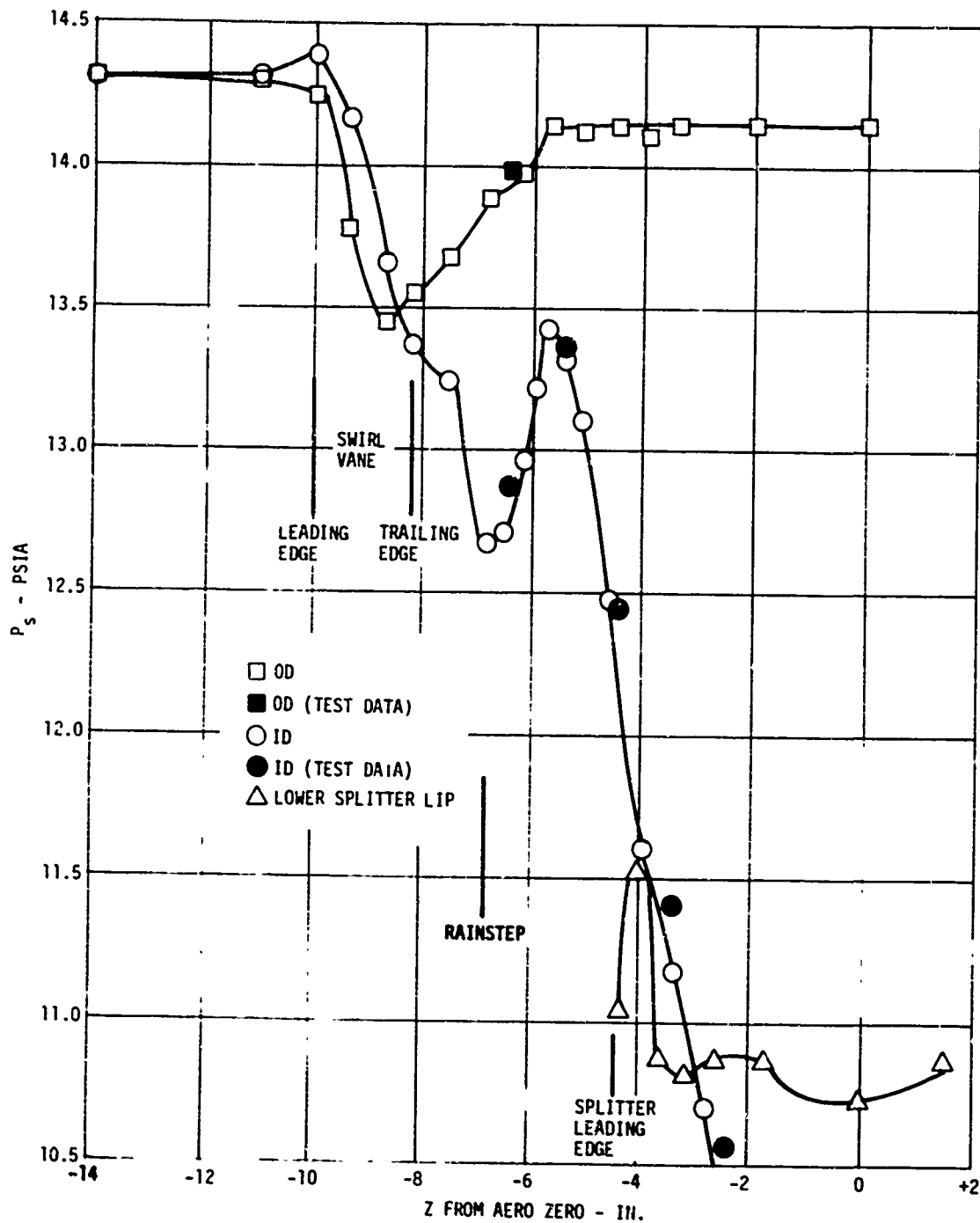


Figure 59. 5 Lb/Sec Separator Model Wall Static Pressure With Swirl Vanes.

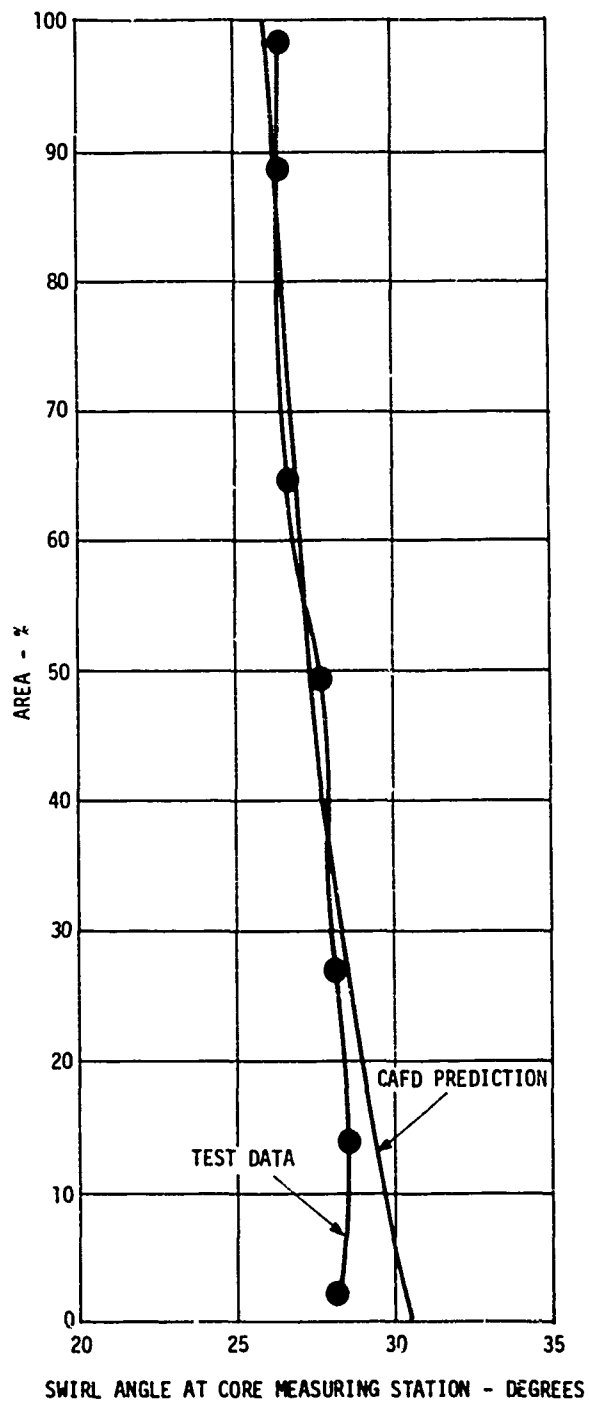


Figure 60. Core Swirl Angle With No Deswirl Vanes - 5 Lb/Sec Separator Model.

DESWIRL VANE DESIGN

Mechanical Constraints

Deswirl vane shapes and cascade parameters are chosen on the basis of aerodynamic and mechanical considerations. The number of deswirl vanes should equal the number of inlet guide vanes and equal the number of swirl vanes for minimum separator plus IGV total pressure loss. Deswirl vanes are circumferentially located or clocked so that their wakes bathe the IGV. Swirl vanes should be clocked (by experiment) so that separator total pressure loss is a minimum.

Mechanical considerations may dictate a deswirl vane shape other than a cambered plate. Anti-icing requirements or structural constraints may indicate a vane with thickness distribution. A biconvex vane cascade having the properties listed in Table 12 has been used with success. This cascade was structural and anti-iced by means of conduction from hot sump oil inside the ID of the flow path and hot air inside the splitter lip at the OD. The vane installed in the separator is shown in Figure 61. The need to carry the PTO shaft out through the deswirl cascade is another barrier to a strictly aerodynamic deswirl cascade design. The section shown in Figure 61 is developed in Figure 62 for the area around the PTO vane. The 18 vane cascade of Table 12 has one of the vanes as shown in Figure 62. Rules for handling the PTO vane area are:

1. Place the PTO vane in the cascade at the required circumferential position and with its maximum thickness at the required axial station.
2. Try to make the PTO position consistent with the need to line up the deswirl vane wakes with the IGV's. If this is impossible, place the other vanes so that their wakes line up with the IGV's (lowest IGV pressure loss clock position of deswirl vanes relative to IGV's may not be exactly inline and is found by component test).
3. Place the leading edge of the PTO vane at the same axial station as the rest of the vane leading edges.
4. Make the area ratio through the passages adjacent to the PTO vane the same as the area ratio through the rest of the cascade passages. Explore changing the PTO vane leading-edge radius and incidence angle to achieve equal area ratios.
5. If the PTO vane is not lined up with an IGV but the other vanes are, it might be necessary to remove the vane closest to the PTO vane to achieve reasonable area ratios. This has been done successfully.

TABLE 12. DESWIRL VANE CASCADE CHARACTERISTICS

R_{LE} (in.)	4.67	5.01	5.26
R_2 TE (in.)	3.48	3.95	4.26
Solidity	1.65	1.58	1.56
t_m/c	.14	.14	.14
t_m (in.)	.23	.23	.22
LE Rad (in.)	.03	.03	.03
TE Rad (in.)	.02	.02	.02
Camber (deg)	51	59	54
Entrance M	.39	.42	.68
No. of Vanes	18	18	18
Chord (in.)	2.74	2.45	2.23
Stagger (deg)	19	16	11.5
<u>PTO VANE</u>			
R_{LE} (in.)	4.67	5.01	5.26
R_{TE} (in.)	2.04	2.97	3.56
Chord (in.)	5.78	4.59	3.81
T_{max} (in.)	.75	.75	.75

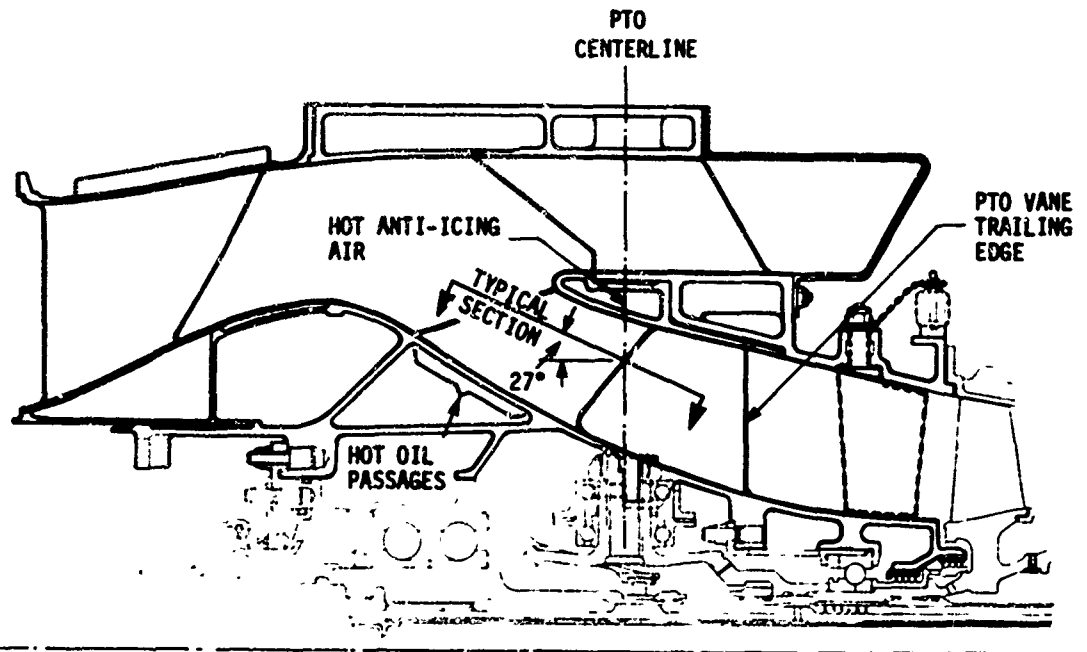


Figure 61. Deswirl Vane in Separator.

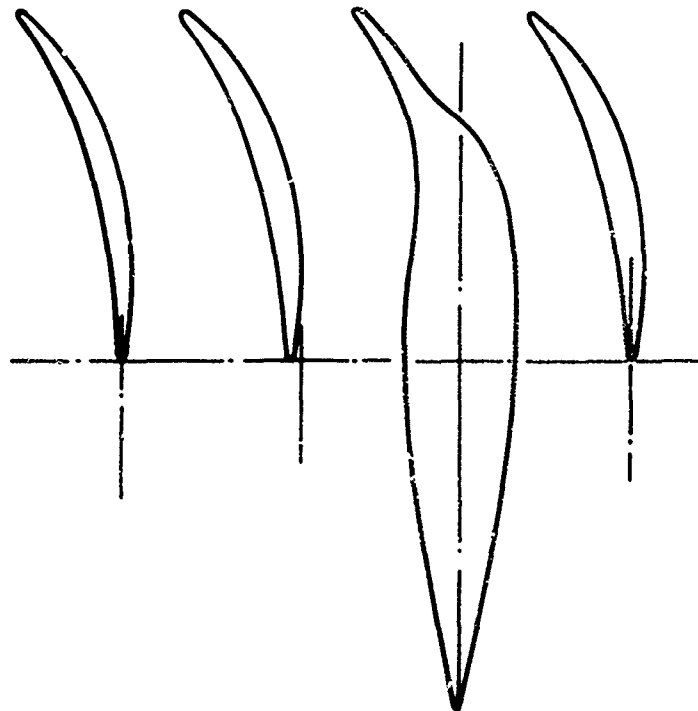


Figure 62. PTO Vane Section.

Deswirl Vanes - Analysis

Removing swirl from an axisymmetric flow field is a diffusing process which may cause very high losses. Calculations on several separator designs have shown that swirl cascades give 30 deg - 40 deg of swirl for approximately 1.0 in. H₂O loss, but deswirl cascades have losses in the order of 2 in. - 4 in. H₂O. Deswirl cascade design should, therefore, be carried out very carefully:

1. Consider the possibility of leaving some residual swirl in the air entering the IGV. There is a trade-off between the added loss due to friction in the duct between the deswirl vanes and IGV, and the reduced loss due to reduced turning in the deswirl cascade. The sense (i.e., clockwise or counter-clockwise) of the swirling flow field may be crucial to this consideration. The compressor must accept in the neighborhood of $\pm 7^\circ$ of swirl.
2. Consider with the compressor entrance swirl conditions the compressor entrance pressure profile. Figures 63, 64, and 65 can be used to estimate separator exit profiles, depending on the separator size and similarity to those designs.
3. Because the air in the deswirl cascade is being turned from flowing radially inward to flowing axially, a hub-to-tip pressure gradient exists, pushing the low-energy air outward. Dye traces and visual observations of a handheld tuft contributed to the schematic representation of secondary flows shown in Figure 66, which is a view looking upstream at the deswirl cascade. It is the aim of good deswirl cascade design to reduce or eliminate this flow migration to the OD.
4. One vane design parameter available to reduce deswirl cascade secondary flows is vane "lean". Lean implies that the vane is nonradial in the manner shown in Figure 67 and therefore applies a force on the air, reducing the amount of secondary flows. Lean, however, may lessen the benefits of lining up the deswirl vanes with the IGV's. Lean can reduce the average radial pressure distortion without affecting total pressure loss. The magnitude of this reduction is illustrated by Figure 68, where the same deswirl cascade was tested first with a radial trailing edge (Table 12), and then with the vane trailing edge leaned 26° from radial with the vane pressure side normal inclined radially outward.
5. Deswirl vane axial location is a trade-off between deswirling at high swirl angles and low Mach numbers or low swirl angle and high Mach numbers. The recommended trade-off, shown in Figure 69, is in the direction of higher swirl angles and lower Mach numbers. Low pressure loss has never been achieved

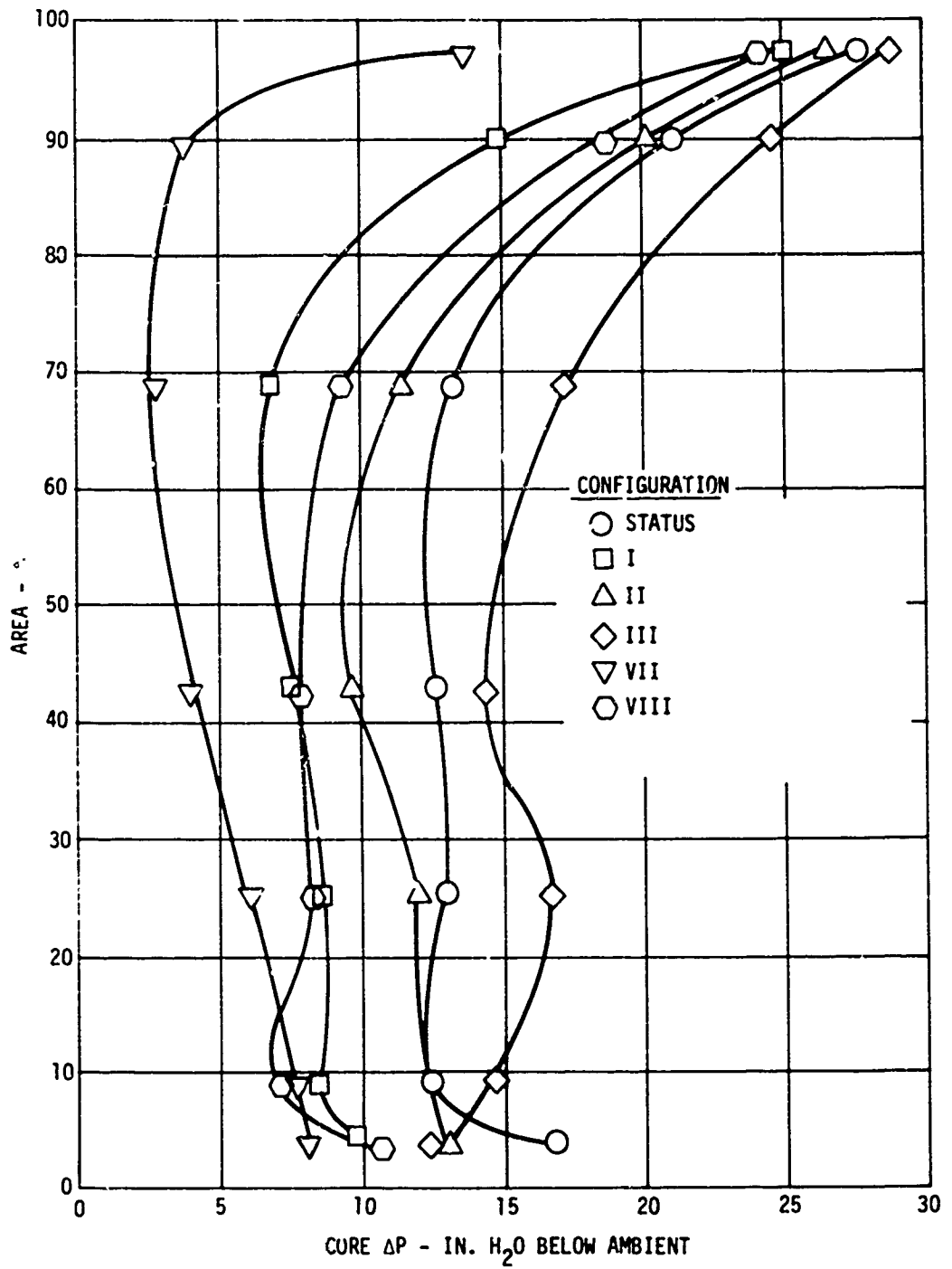


Figure 63. Total Pressure Profiles, 2 Lb/Sec Separator.

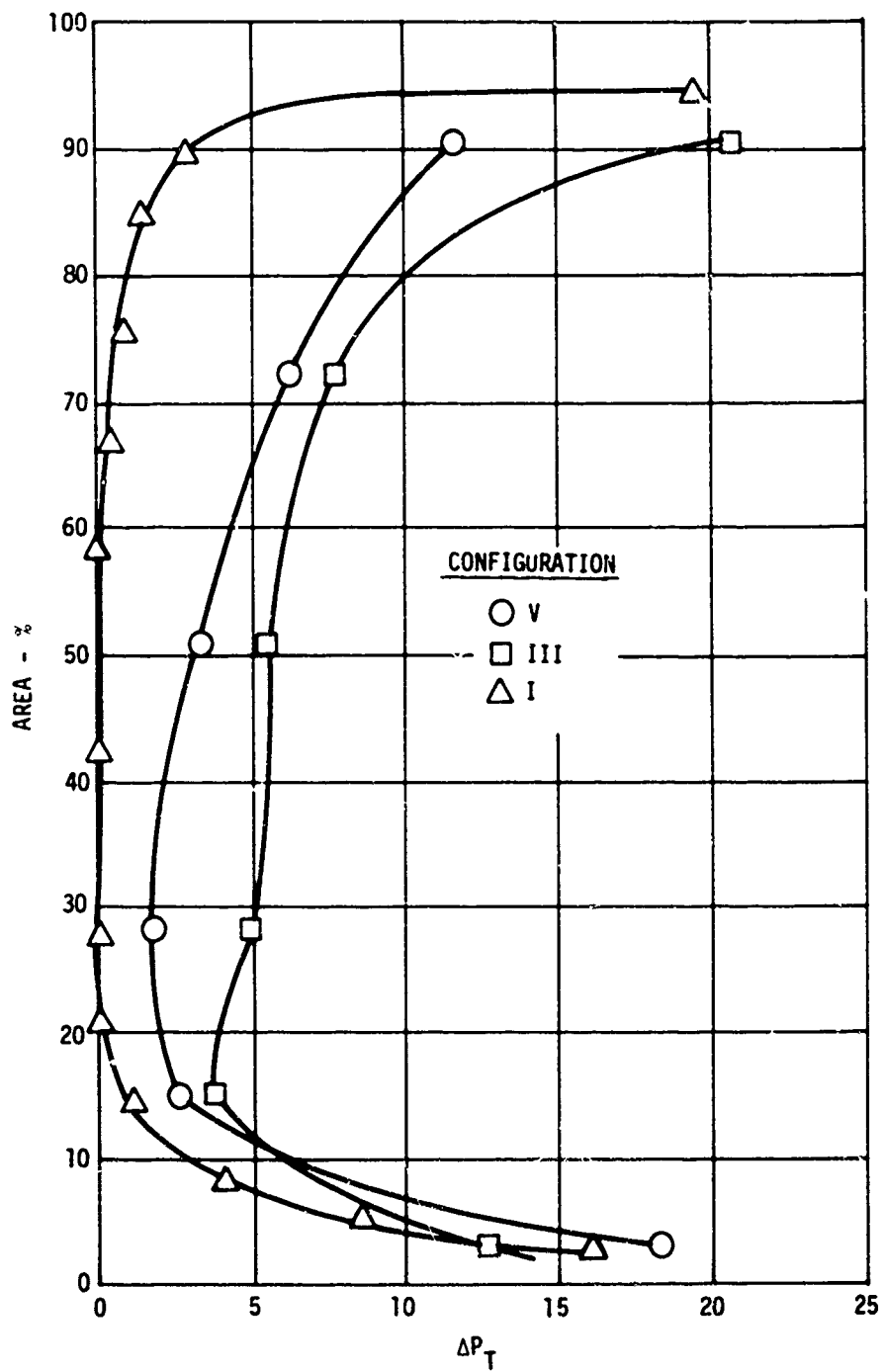


Figure 64. Total Pressure Profiles, 5 Lb/Sec Separator.

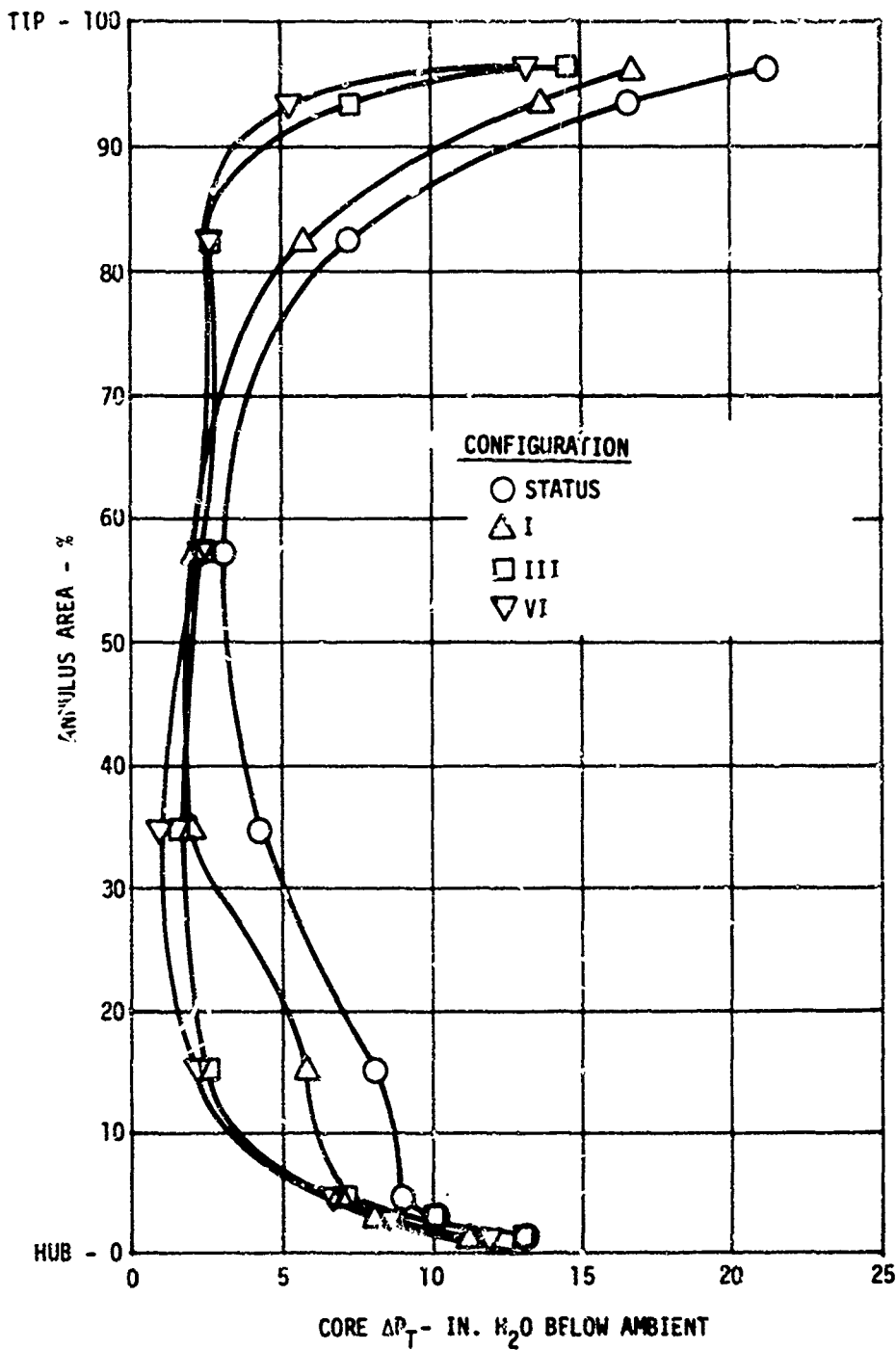


Figure 65. Total Pressure Profiles, 15 Lb/Sec Separator.

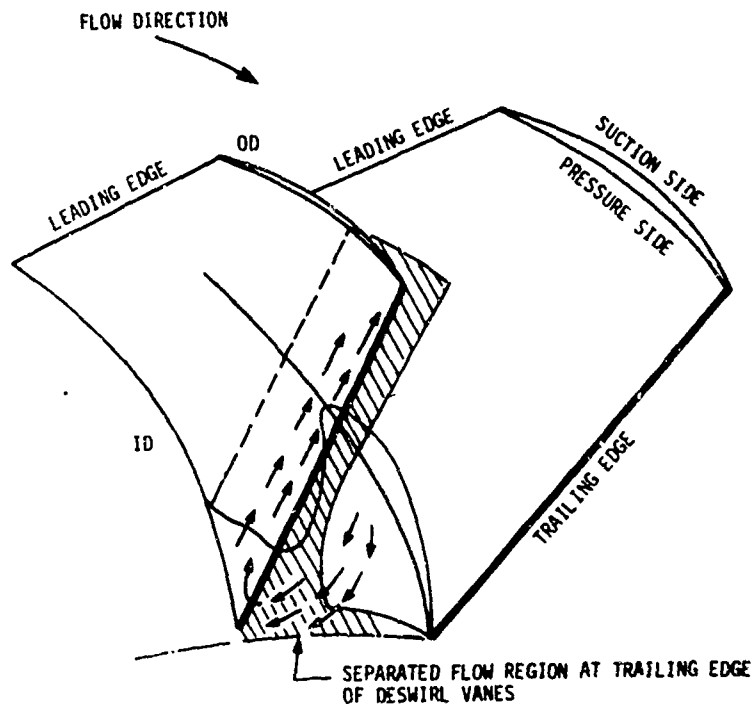


Figure 66. Schematic of Secondary Flows.

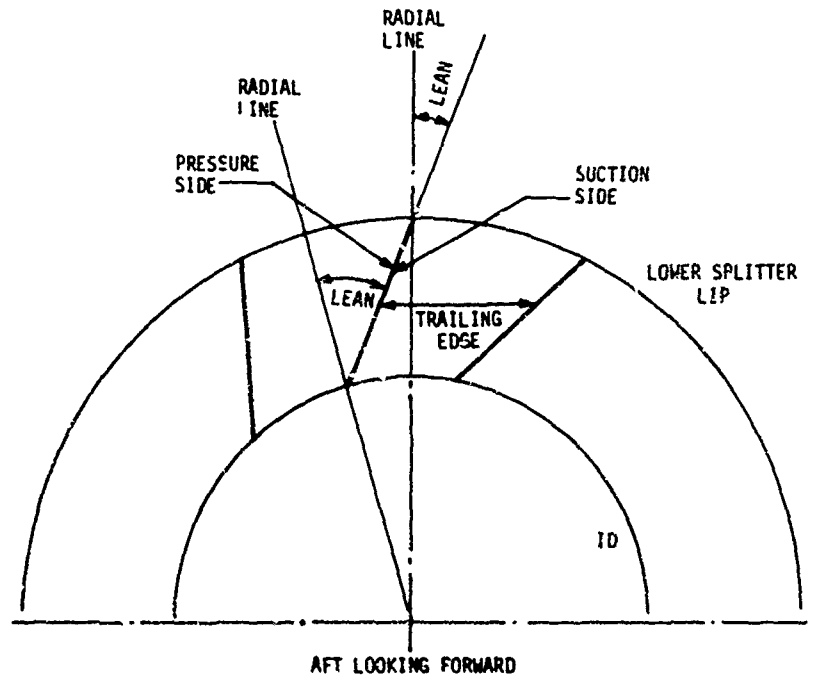


Figure 67. Deswirl Vane Lean.

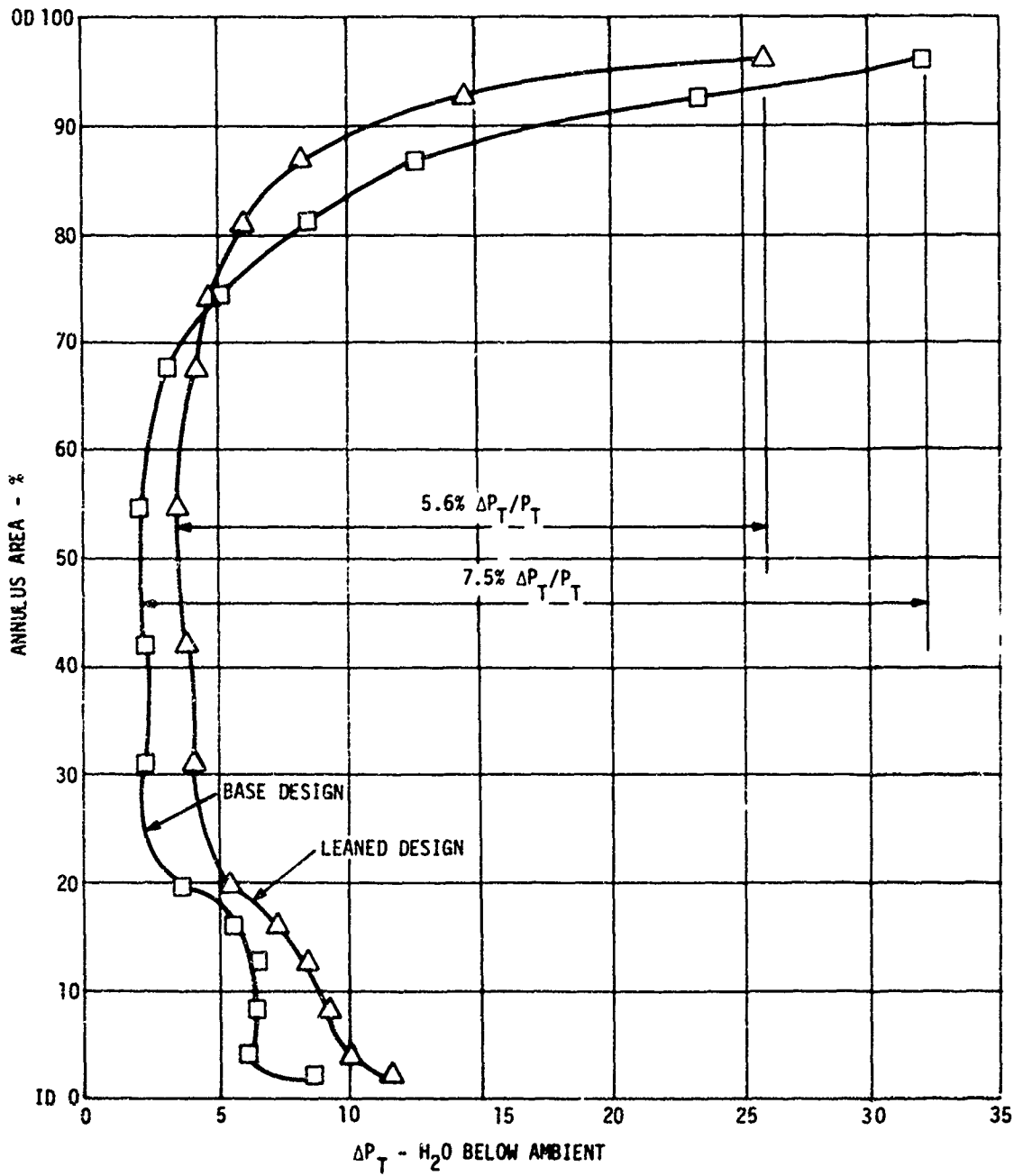


Figure 68. Separator Exit Radial Profiles at Design Airflows.

by placing the swirl vanes down in the compressor inlet passage aft of the splitter lip. An advantage of the location shown in Figure 69 is that the deswirl vane blockage can be used to reduce the hub diffusion aft of the rainstep.

6. With the vane position shown in Figure 69, vane thickness distribution, flow path shape, and lean can be used to vary the pressure gradients through the deswirl cascade. The analytical results of the above three changes on absolute Mach number are plotted in Figures 70, 71, and 72. All three variables influence the wall Mach numbers (static pressures) significantly. A low loss deswirl vane design uses these variables to minimize the hub-to-tip static pressure gradients. The pressure distribution for the deswirl cascade tested is shown in Figure 64. The deswirl cascade used is described by Table 13 and Figure 73. Figure 74 can be compared to Figure 59 to see the influence of the deswirl vanes on the static pressure gradients. The loss profile leaving the separator is shown as Configuration III of Figure 64. Note the high solidity of the cascade in Table 13. When every other deswirl vane was removed, the separator loss was reduced by 1.7 in. H_2O which is half the computed friction loss.

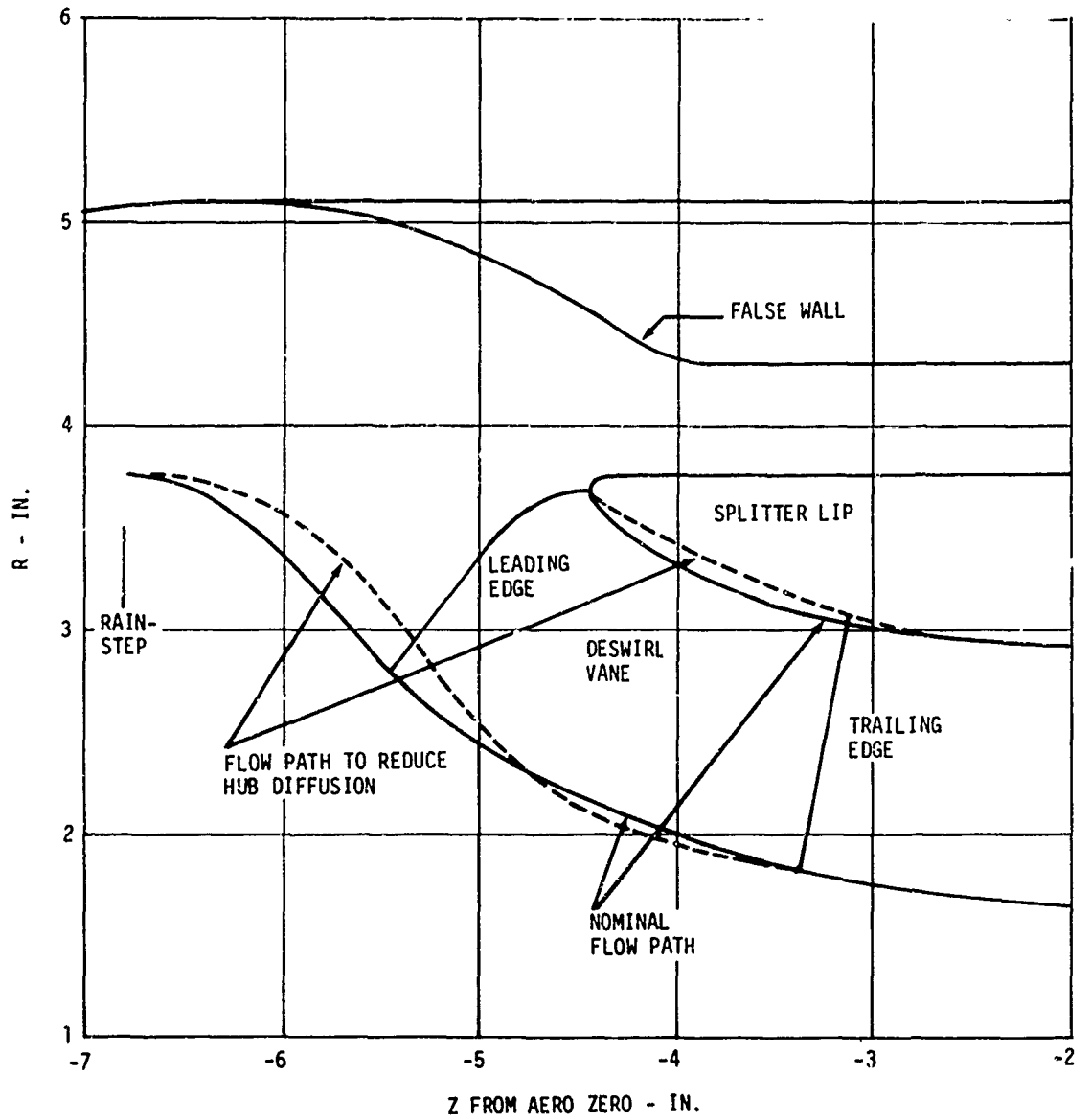


Figure 69. Effect of Changing Flow Path Contour With a Deswirl Vane - 5 Lb/Sec Separator Model With Swirl Vanes.

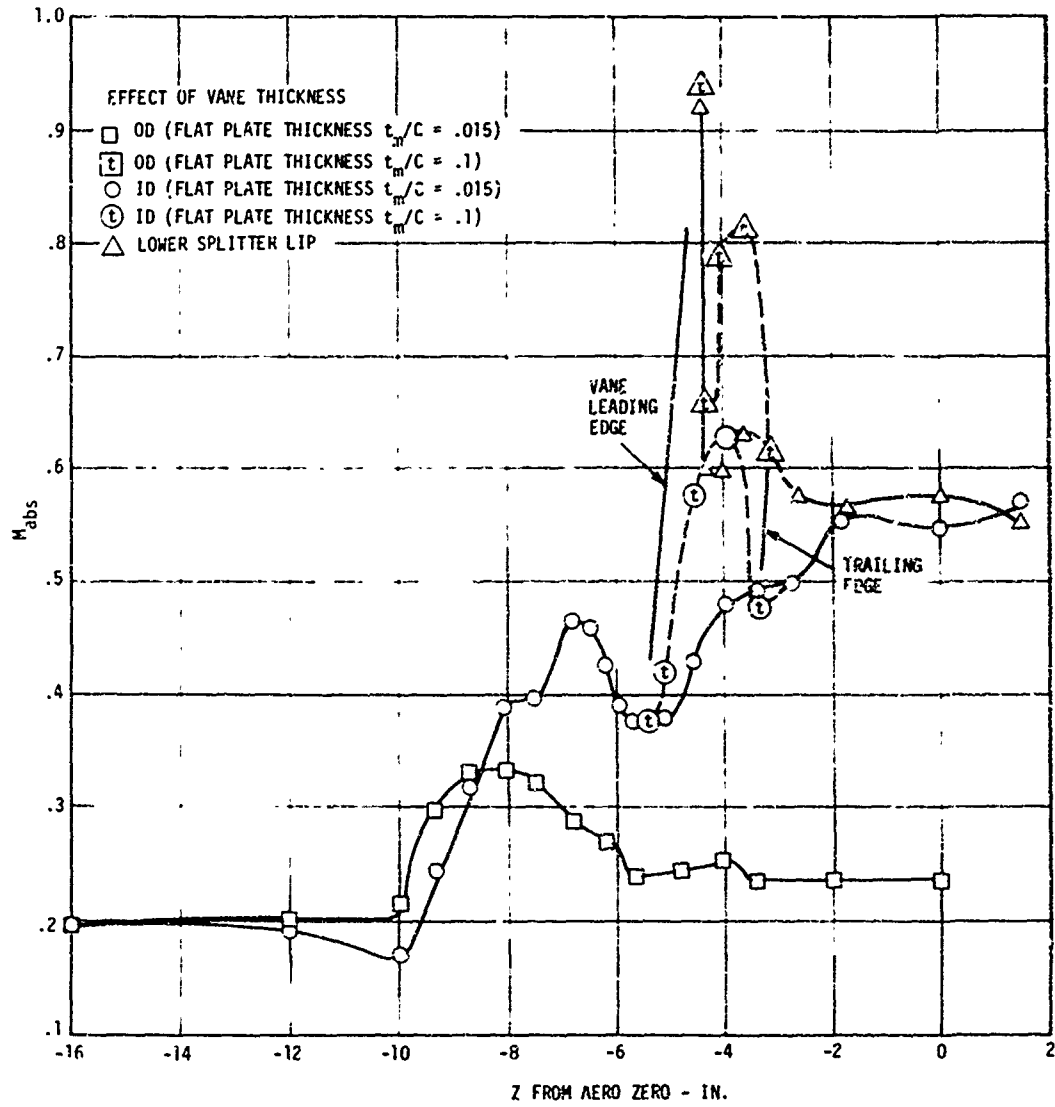


Figure 70. Separated Region and Linear Deswirl Distribution - 5 Lb/Sec Separator Model With Swirl Vanes.

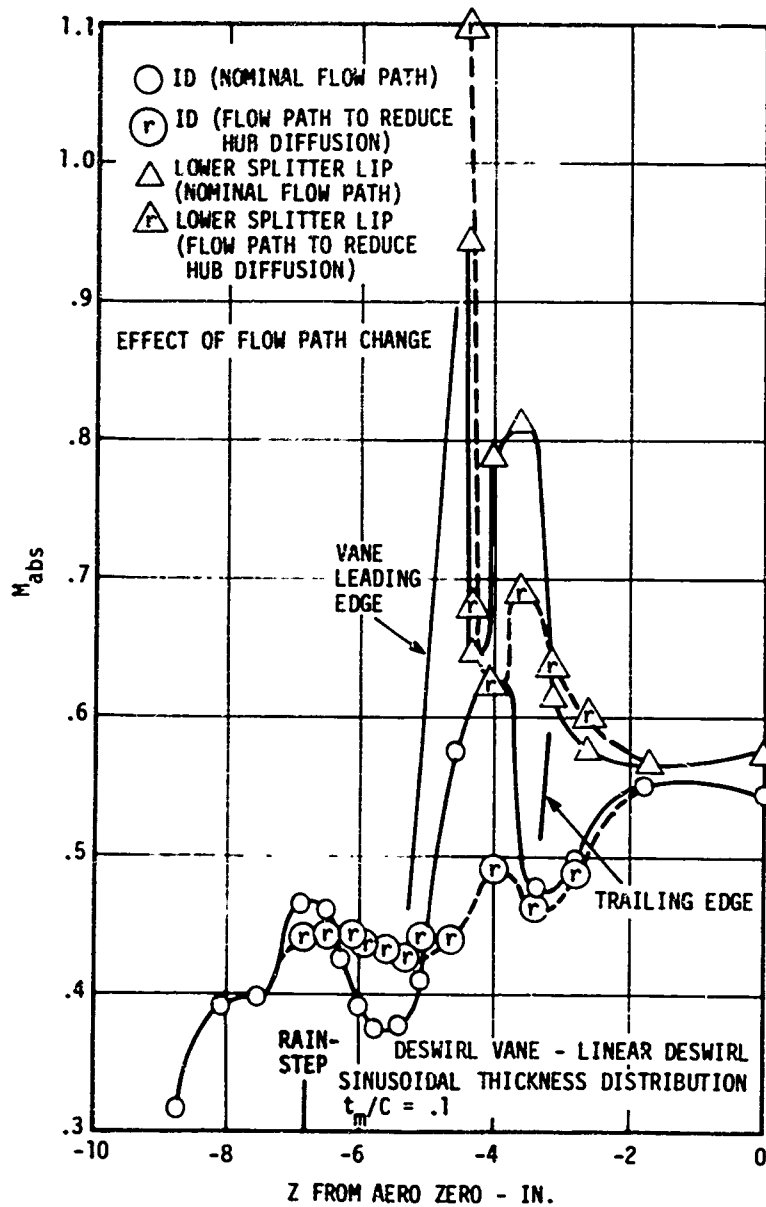


Figure 7. Wall Mach Number Distribution for 5 lb/Sec Separator With Flow Path Changes.

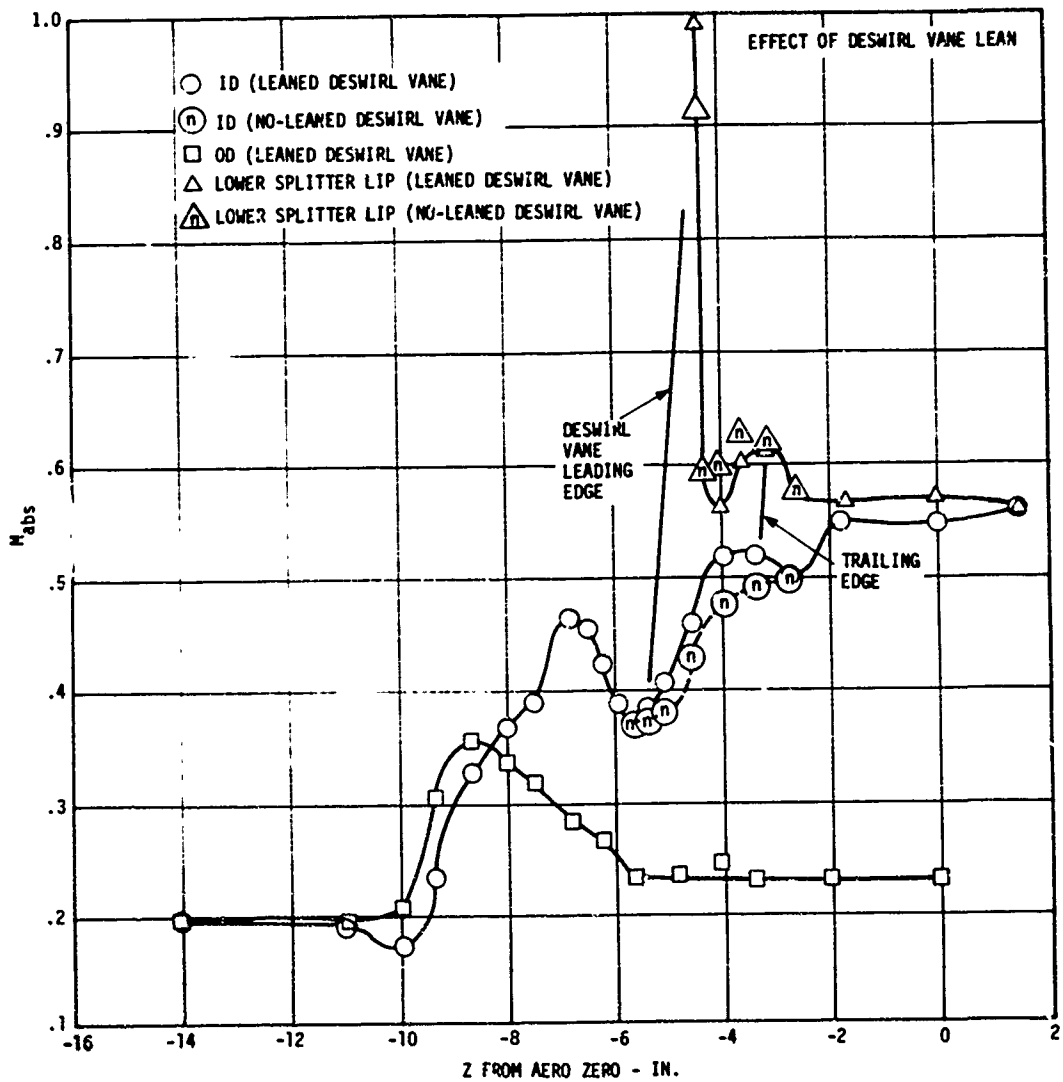


Figure 72. Wall Mach Number Distribution for 5 Lb/Sec Separator With Leaned Deswirl Vanes.

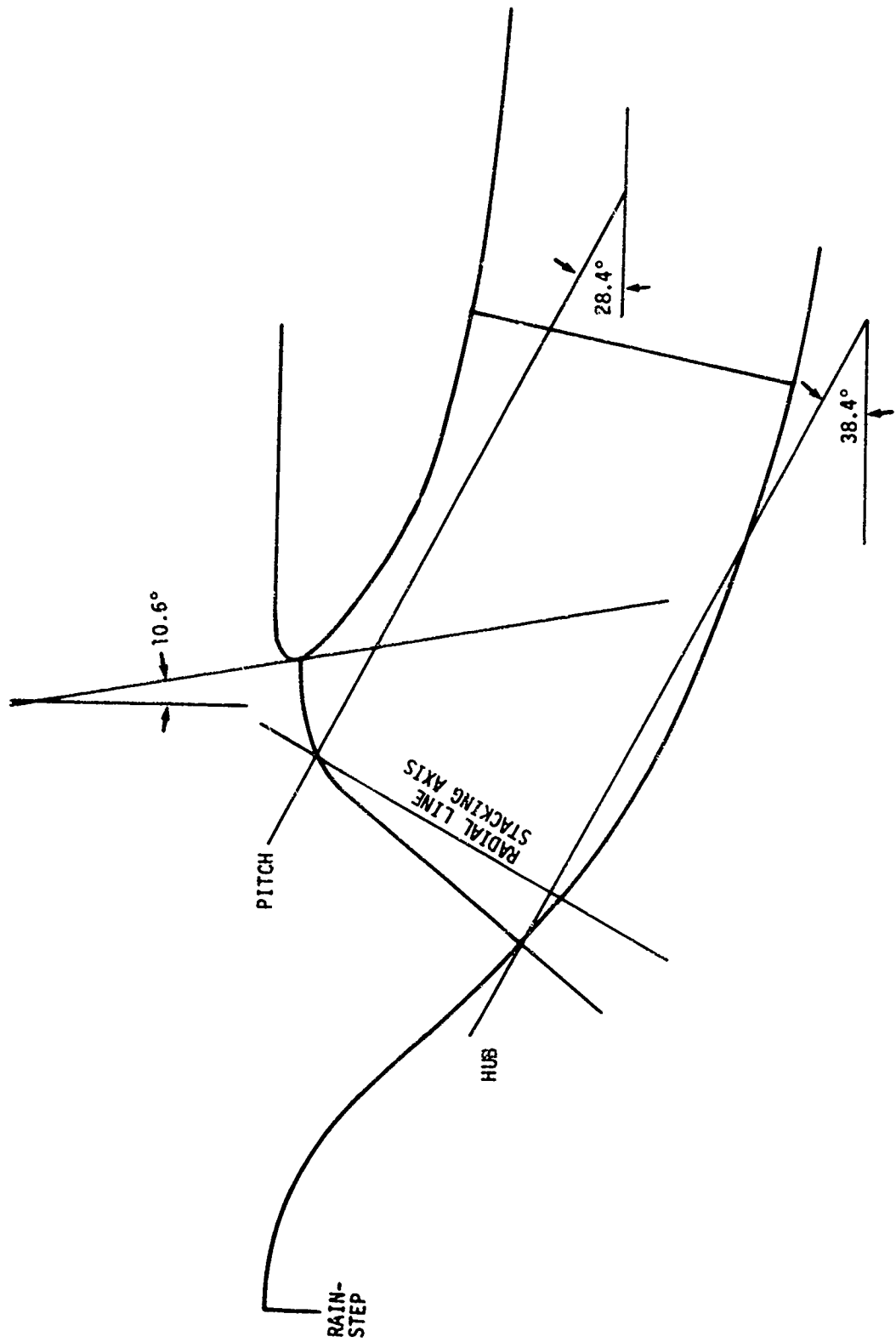


Figure 73. 5 Lb/Sec Separator Cambered Plate Circular Arc Deswirl Vane.

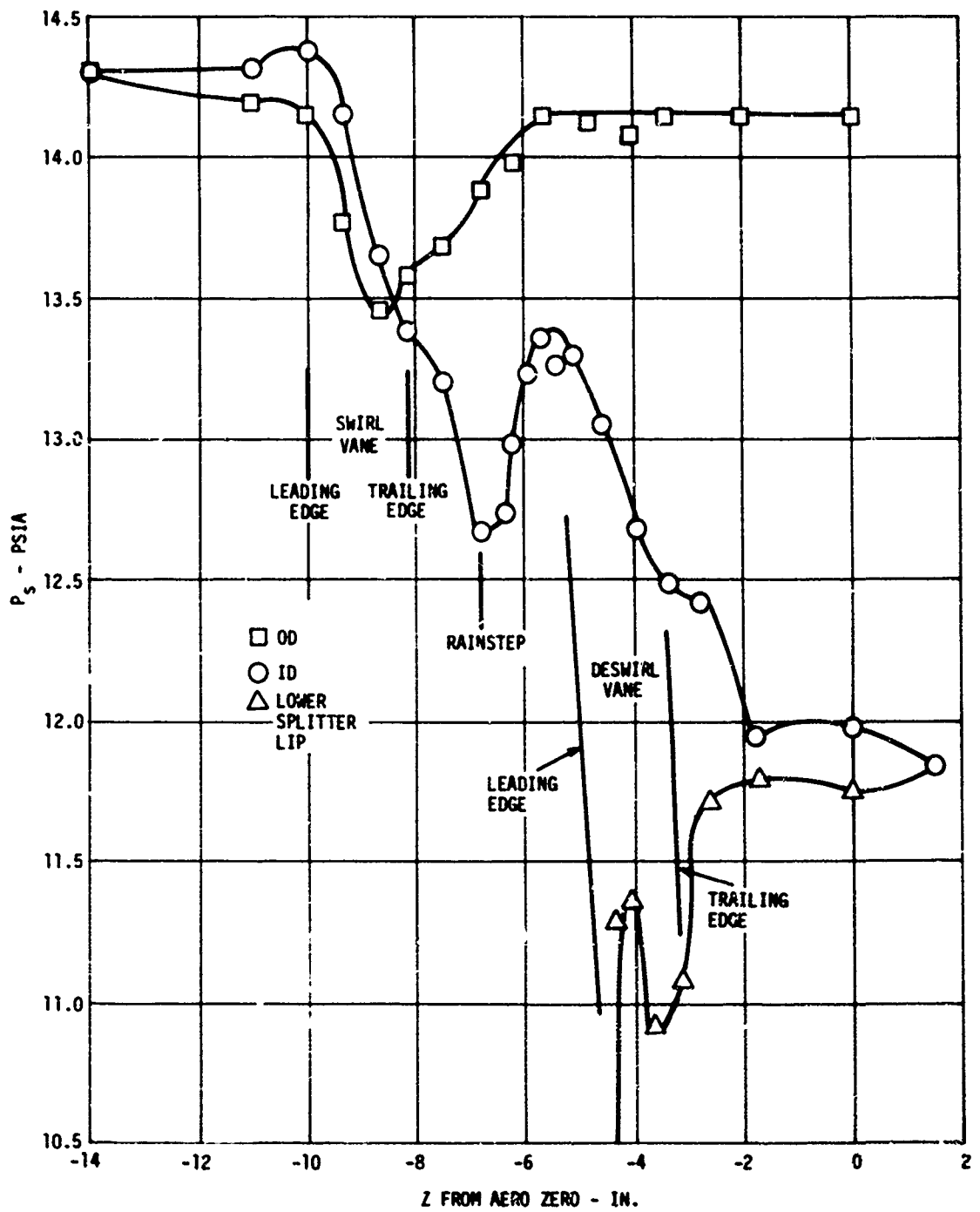
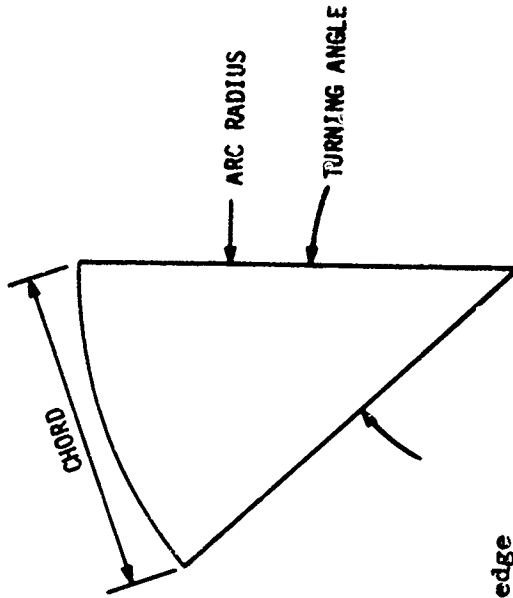


Figure 74. 5 Lb/Sec Separator Model With Vane Wall Static Pressures.

TABLE 13. 5 LB/SEC SEPARATOR MODEL DESWIRL VANE
CIRCULAR ARC FLAT PLATE

	Chord (in.)	Stagger Angle (deg)	Section Slope Relative to Horiz	Arc Radius (in.)	Turning Angle (deg)	Radial Line Co-ordinates R t	Leading Edges Location t (in.)	Solidity at Radial Line	TE Angle	Thick- Ness (in.)	LE Angle of Attack	t_m/c
PITCH	1.868	17.4	28.4	3.124	34.8	3.595 -4.760	-4.760	1.488	0	.040	0	.0214
HUB	2.427	18.1	28.4	3.925	36.0	2.698 -5.242	-5.435	2.577	0	.040	0	.0165

Intersection of radial line with hub
flow path $R = 2.657$ $t = 5.266$



Leading edge coordinates projected to meridional
R 2.80, 3.510, 3.57, 3.62, 3.645, 3.659, 3.66
t -5.435 -4.862 -4.8 -4.7 -4.6 -4.5 -4.42

Hub

Tip angle in 10.6 deg plane at splitter tip lip leading edge
relative to hub and pitch sections = 8 deg

Relative to a meridional plan intersection the 10.6 deg plane = 16 deg clockwise
FWD looking aft

SCAVENGE VANE DESIGN

Scavenge vanes perform a mechanical function in the separation process by trapping the particles that have been separated and directing them to the separator scavenge air discharge. A secondary purpose is to control the scavenge flow in the neighborhood of the splitter lip (see Figure 60). Configurations VI and VII, Table 4, show that moving the scroll vanes aft lowered separation efficiency. From tuft measurements on the two configurations, it is known that the stagnation point moved aft when the scroll vanes were moved aft. The reduction in separation efficiency may have been due to the reverse flow forward of the stagnation point that could sweep into the core airstream sand that had already been separated. Scroll vane designs shown here were developed for swirling separators. However, as the data in Tables 3, 4, and 5 suggest, the scroll vane designs are suitable for 0° swirl separation also. Scavenge vane design procedure and design considerations are as follows:

1. For all designs discussed here, design point scavenge airflow is 14.5% of compressor maximum airflow.
2. Scavenge vane entrance conditions are represented accurately by the large separated region shown in Figure 57. Cobra probe traverse data at the scavenge vane entrance is shown in Figure 75. For the two different clock positions, the total pressure profiles differ by as much as 7 in. H₂O, and the total pressure at the OD is 10 in. H₂O less than the total pressure at the ID. The difference in profile levels of Figure 75 is probably the result of traversing between swirl vane wakes and in a swirl vane wake. Note that for the one profile in Figure 75, total pressure equals wall static pressure for 41% of the annular height consistent with the separated region shown in Figure 57. Swirl angles measured during the survey of Figure 57 are shown in Figure 76 and are considered to be typical for a swirling separator.
3. Because of the flow fields shown in Figures 57, 75, and 76, a large portion of scavenge system loss occurs ahead of the scavenge vanes. Limited measurements have indicated that out of 22 in. H₂O pressure loss at the scavenge blower inlet, 10 in. to 13 in. H₂O loss occurs prior to the scavenge vanes in the diffusion process forward of the vanes, 1 in. to 3 in. H₂O loss occurs in the scroll, and 6 in. to 11 in. H₂O loss occurs in the duct connecting the scroll to the scavenge blower. However, as indicated by Figures 77, 78, and 79, a reasonable target pressure loss for the scavenge system (up to blower inlet) is 13 to 25 in. H₂O. Figures 80, 81, and 82 show that the scavenge system has little impact on the pressure loss of the separator. The scavenge airflow ratio impact on separation efficiency is significant as shown in Figures 83 and 84.

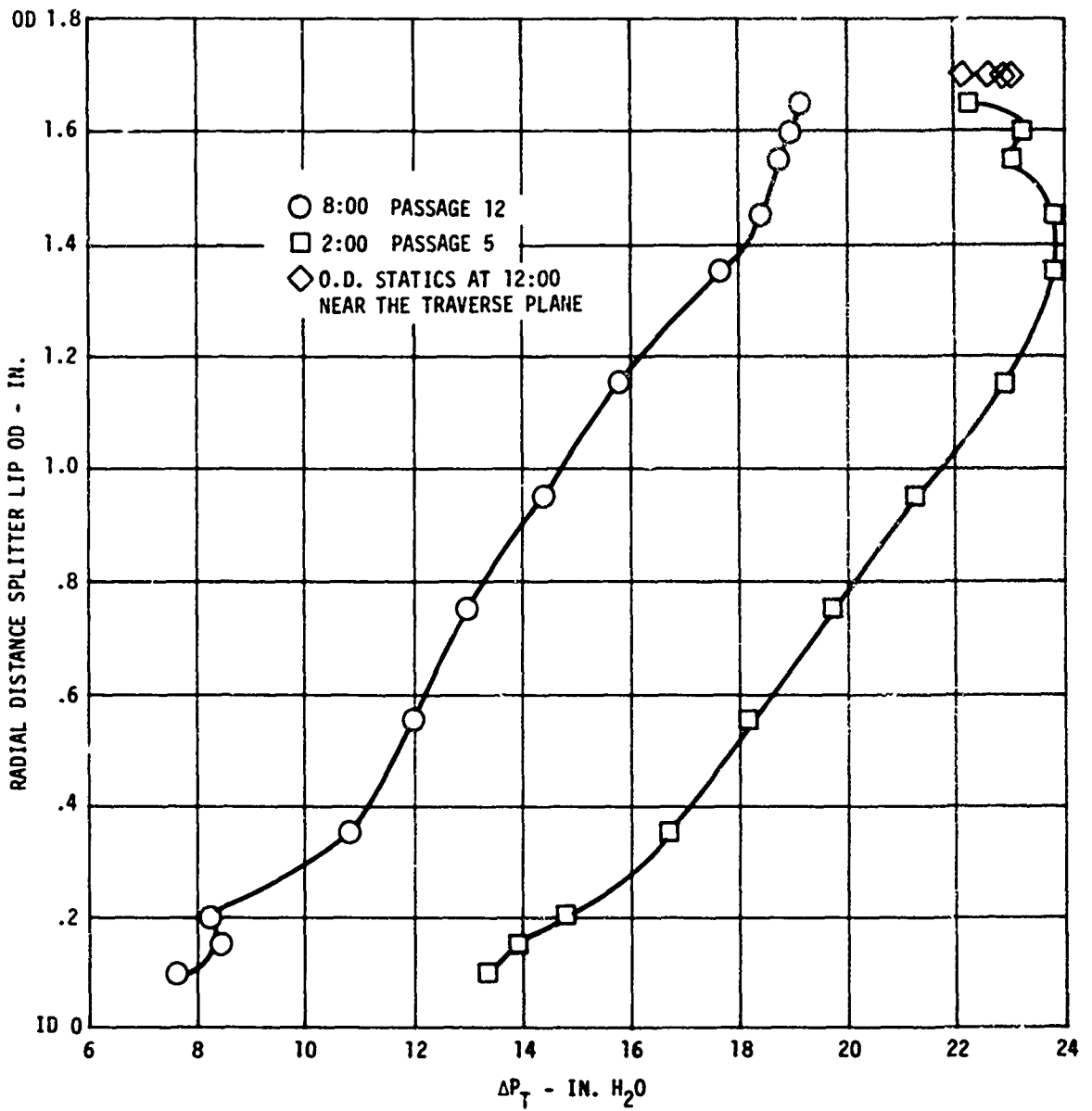


Figure 75. Traverse in Front of the Scavenge Vanes at Design Scavenge Flow.

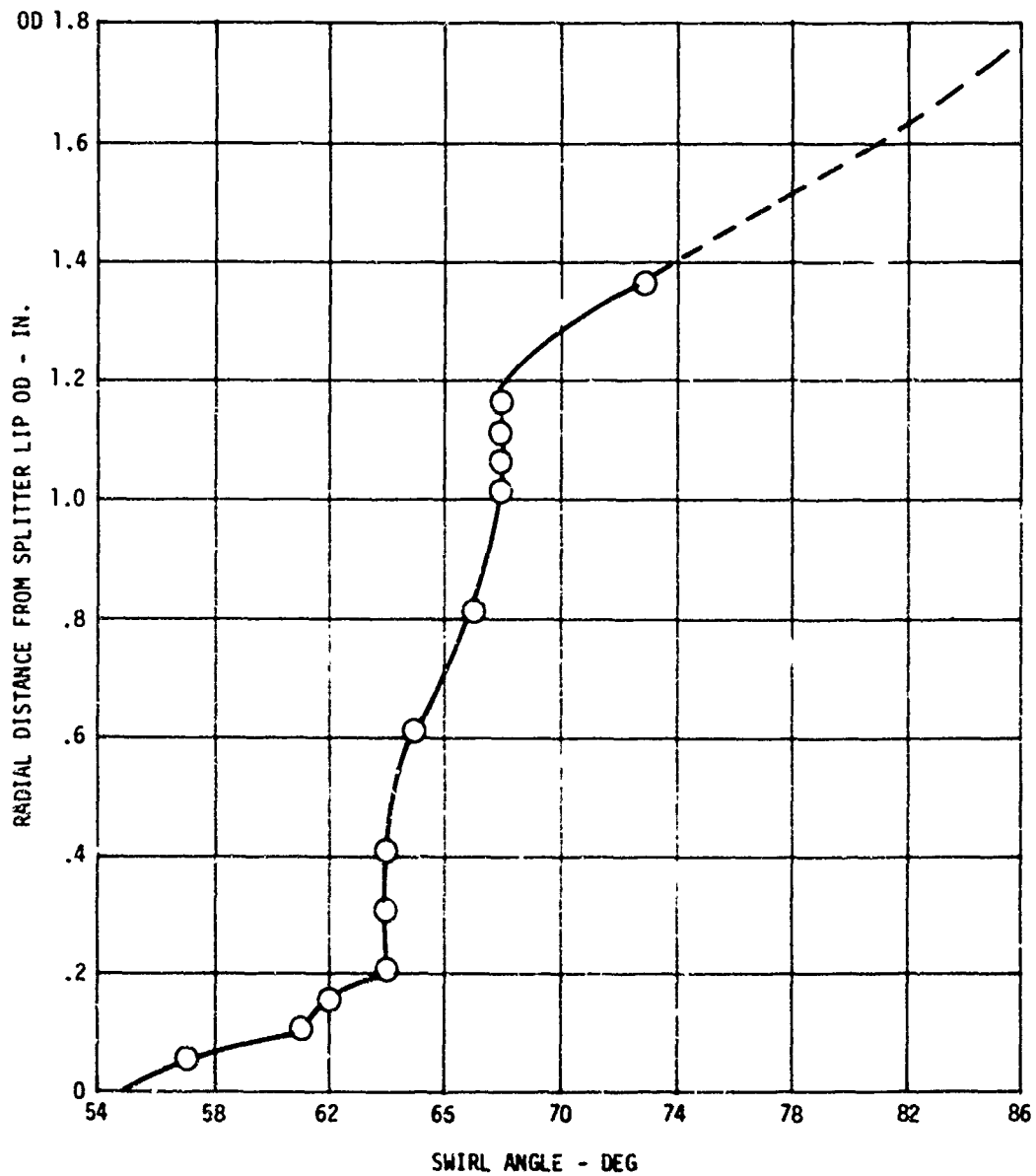


Figure 76. T700 Separator Traverse in Front of the Swirl Vane (Slim Duct)
 - $W_{sa} = 1.32$.

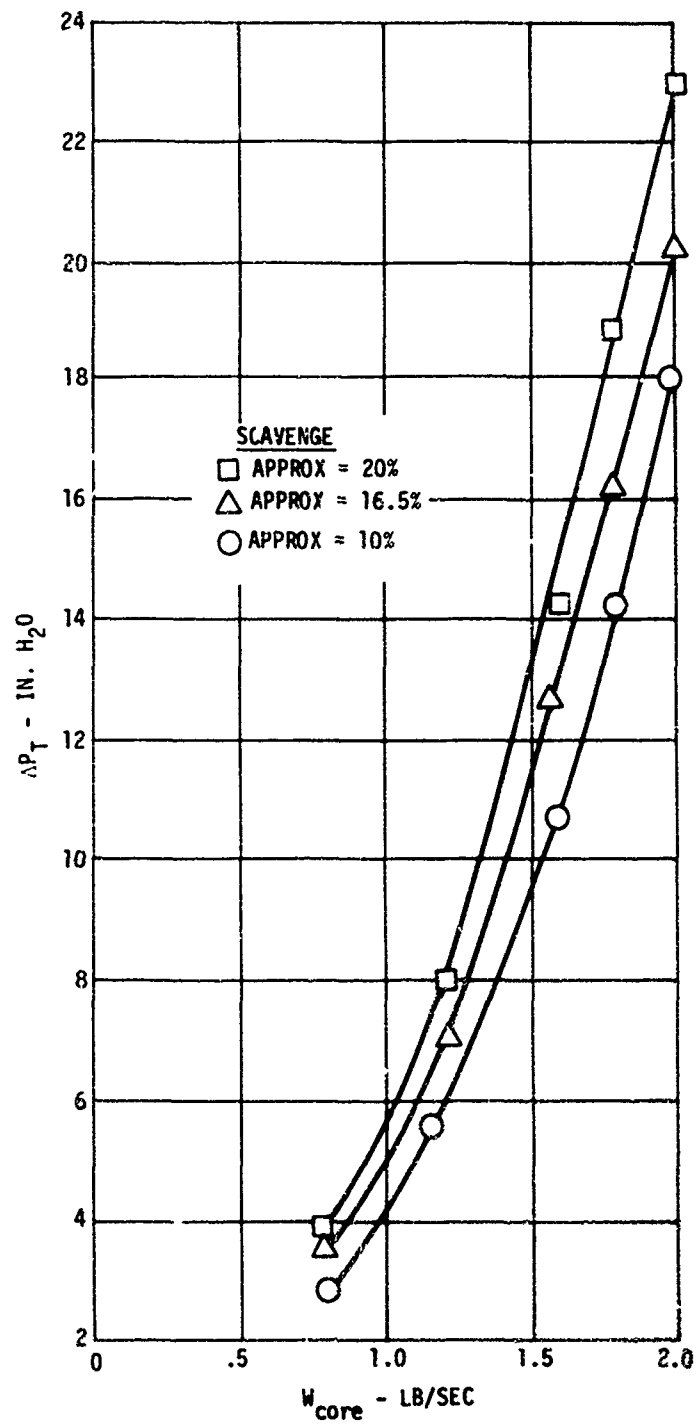


Figure 77. 2 Lb/Sec Scroll Pressure Loss.

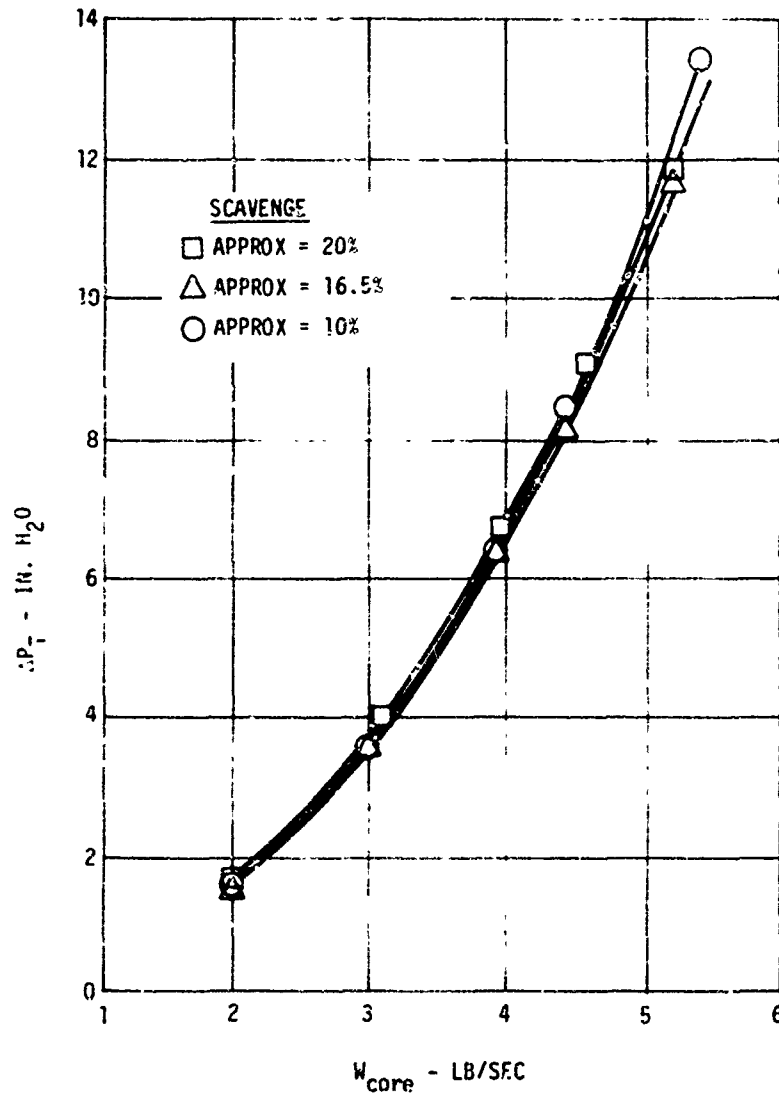


Figure 78. 5 Lb/Sec Scroll Pressure Loss.

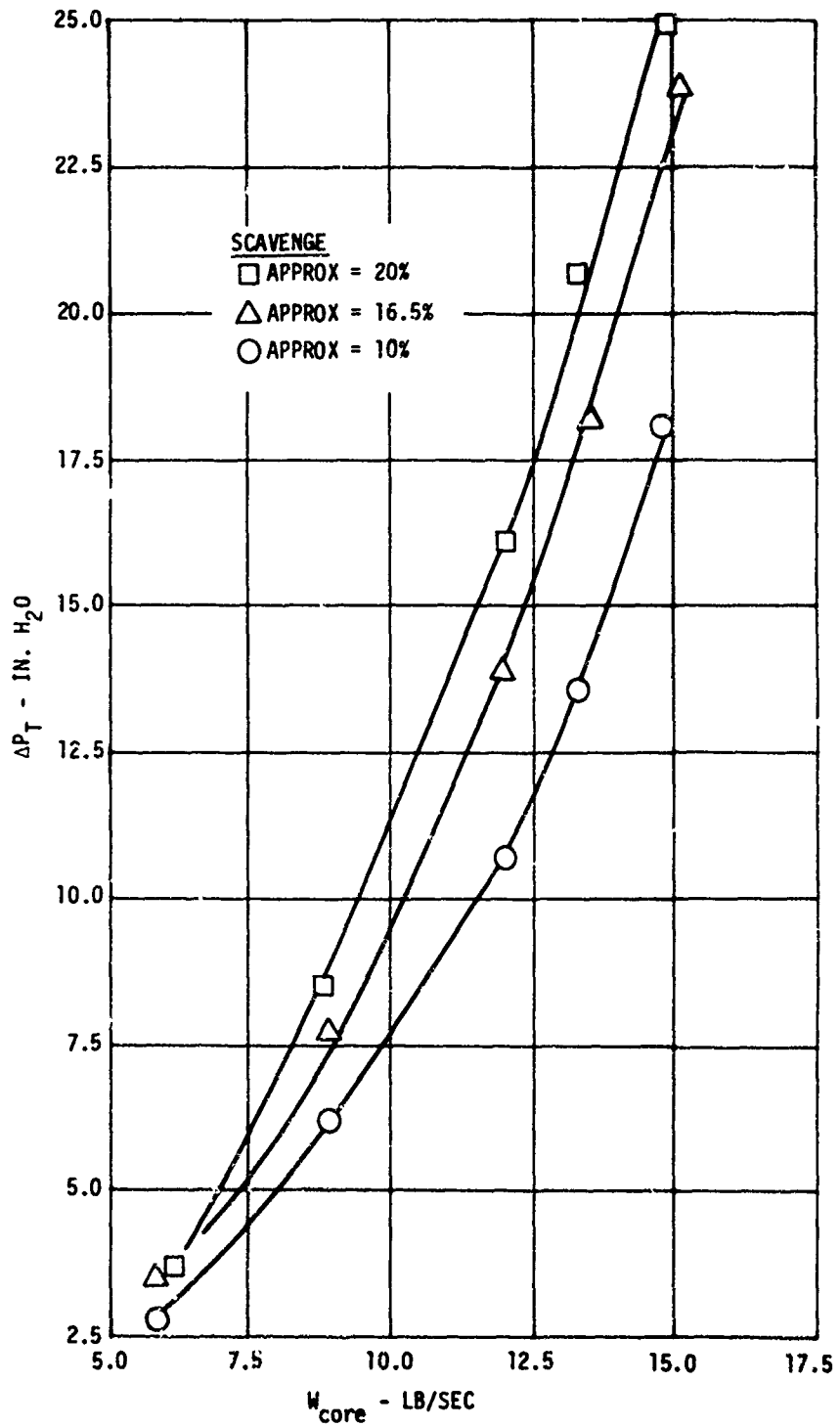


Figure 79. 15 Lb/Sec Scroll Pressure Loss.

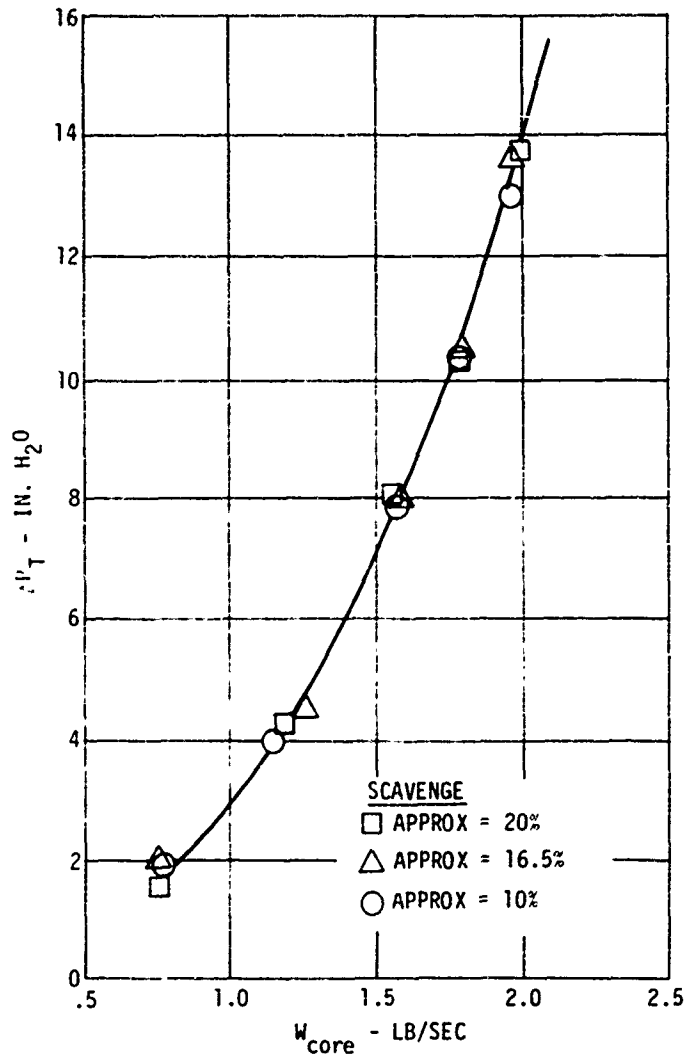


Figure 80. 2 Lb/Sec Separator Off-Design Core Pressure Loss.

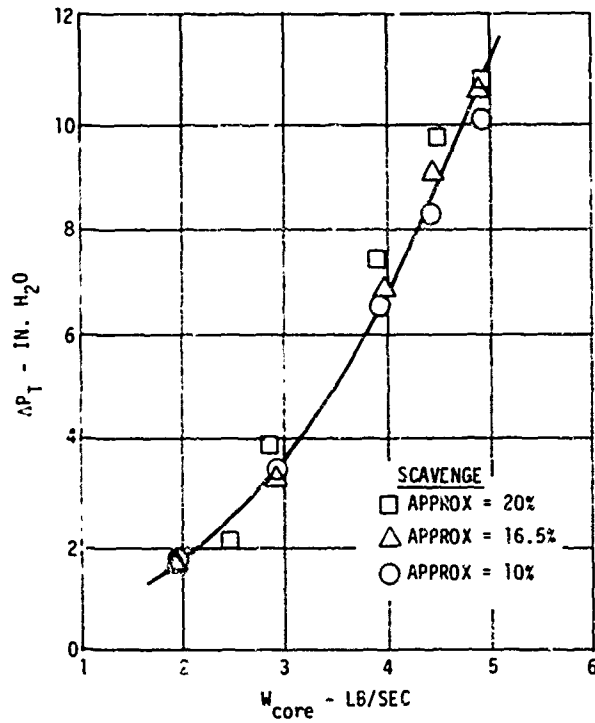


Figure 81. 5 Lb/Sec Separator Off-Design Core Pressure Loss.

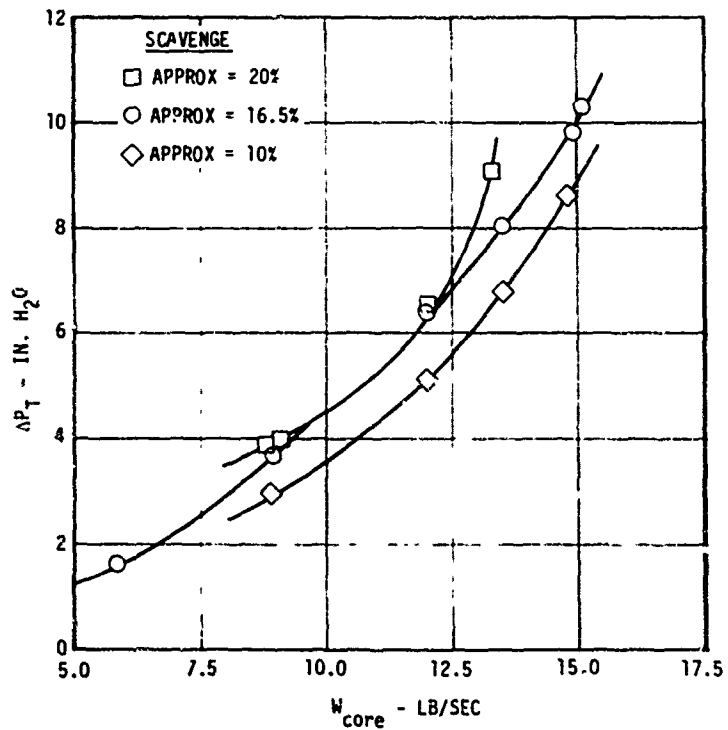


Figure 82. 15 Lb/Sec Separator Off-Design Core Pressure Loss.

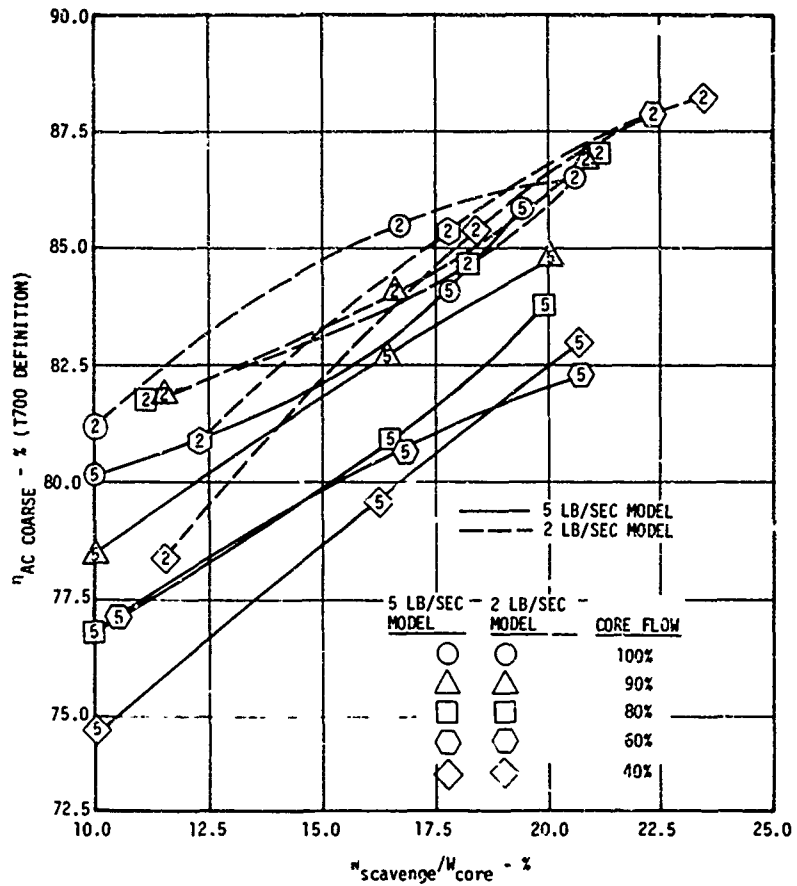


Figure 83. AC Coarse Collection Efficiency vs Scavenge Flow Ratio.

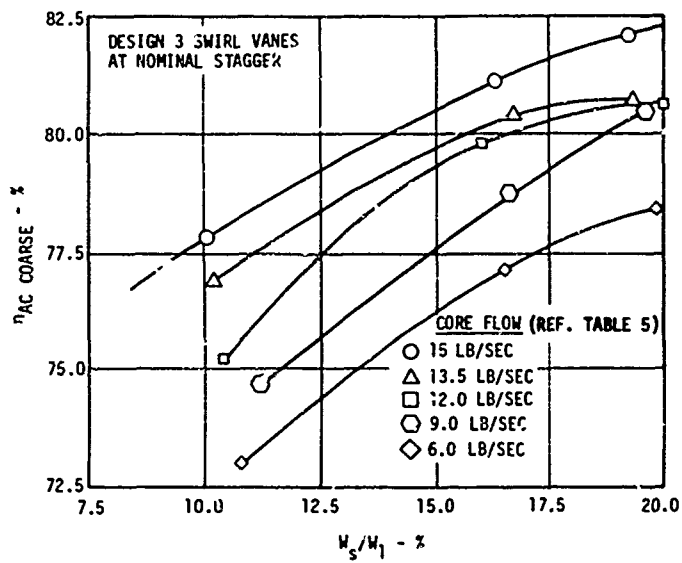


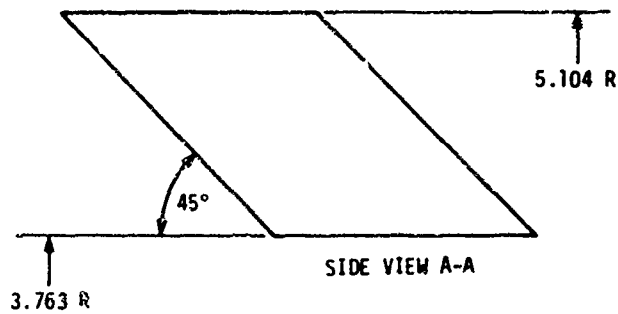
Figure 84. AC Coarse Efficiency vs Scavenge Flow Ratio - 15 Lb/Sec Model.

Table 3 shows that by reducing the number of scroll vanes, level of scroll ΔP_T (25 in. H₂O) can be reduced almost 7 in. H₂O.

4. A smaller number of scavenge vanes is preferred when single foreign object ingestion is considered. It should be a separator design requirement that "whatever can pass into the separator can pass out through the scavenge vanes". Also, "whatever cannot fit through the scavenge vane cascade cannot fit through the deswirl vane cascade". If these requirements are not met, it would be possible to separate foreign objects in the separator but have them trapped on the scavenge vanes, where they could come loose and fall into the compressor at some future date.
5. A typical scavenge vane design is shown in Figures 85 and 86. The important features of the scavenge vane are:
 - a. O.D. leading edge at the same axial station as the splitter lip leading edge.
 - b. Vane leading edge in a radial plane and making a 45-deg line with the engine axis.
 - c. Leading edge pressure surface angle equal to 35 deg.
 - d. Vanes as thin as possible consistent with structural needs and desired throat dimensions to limit sand bouncing off the vanes.
 - e. Vane throats sized so that the cumulative sum of each throat area is no bigger than the net scroll area at any circumferential position.
 - f. The scroll, shown in Figure 87, increased linearly in area from the scroll start to scroll discharge. The shape of the scroll area is not important.
6. For design purposes, the scavenge vane entrance area, A_e , is assumed to be the scavenge annulus height forward of the splitter times the cosine of the average swirl angle projected to the vane leading edge. If the average swirl angle from Figure 76 is assumed to be 65 deg, the entrance area for a scavenge vane passage of the Figure 84 design would be
$$A_e = [3(5.104^2 - 3.763^2)\cos 65 \text{ deg}].9 = 1.754 \text{ in.}^2$$
7. The vane throat area, A_t , for each passage is such that the value of A_e/A_t is the same for all passages. However A_e will probably not be the same for all passages if one of the scavenge vanes houses the PTO shaft.
8. The vane shapes need not all be the same, but the leading edge characteristics should all be as described above. The vane trailing edge should be designed to guide the

air tangentially as much as possible to prevent unguided turning in the scroll.

9. Scroll area at any circumferential position A_s should be such that the area of the scroll is greater than or equal to the sum of the throat areas up to that position in order to maintain constant static pressure in the scroll.
10. The proper A_e/A_t ratio could be accomplished by changing the shape of the annulus walls (compare Figure 37 to Figure 39) as well as by changing the scroll vane cross-sectional shape.



NOTES:

1. ONE SECTION TRANSLATED AXIALLY AT A 45° ANGLE.
2. THE SECTION SHOWN BELOW LIES ON THE CYLINDER - (NOT ON A PLANE)
R = 4.434.
3. THE LEADING EDGE LIES IN AN AXIAL PLANE.
4. SECTION VIEW OUTSIDE LOOKING IN.
5. EIGHT REGULAR VANES.
6. ONE SPLITTER VANE.
7. SPACING ON THE BASIS OF 9 EQUALLY SPACED VANES.
8. MATERIAL ALUMINUM.

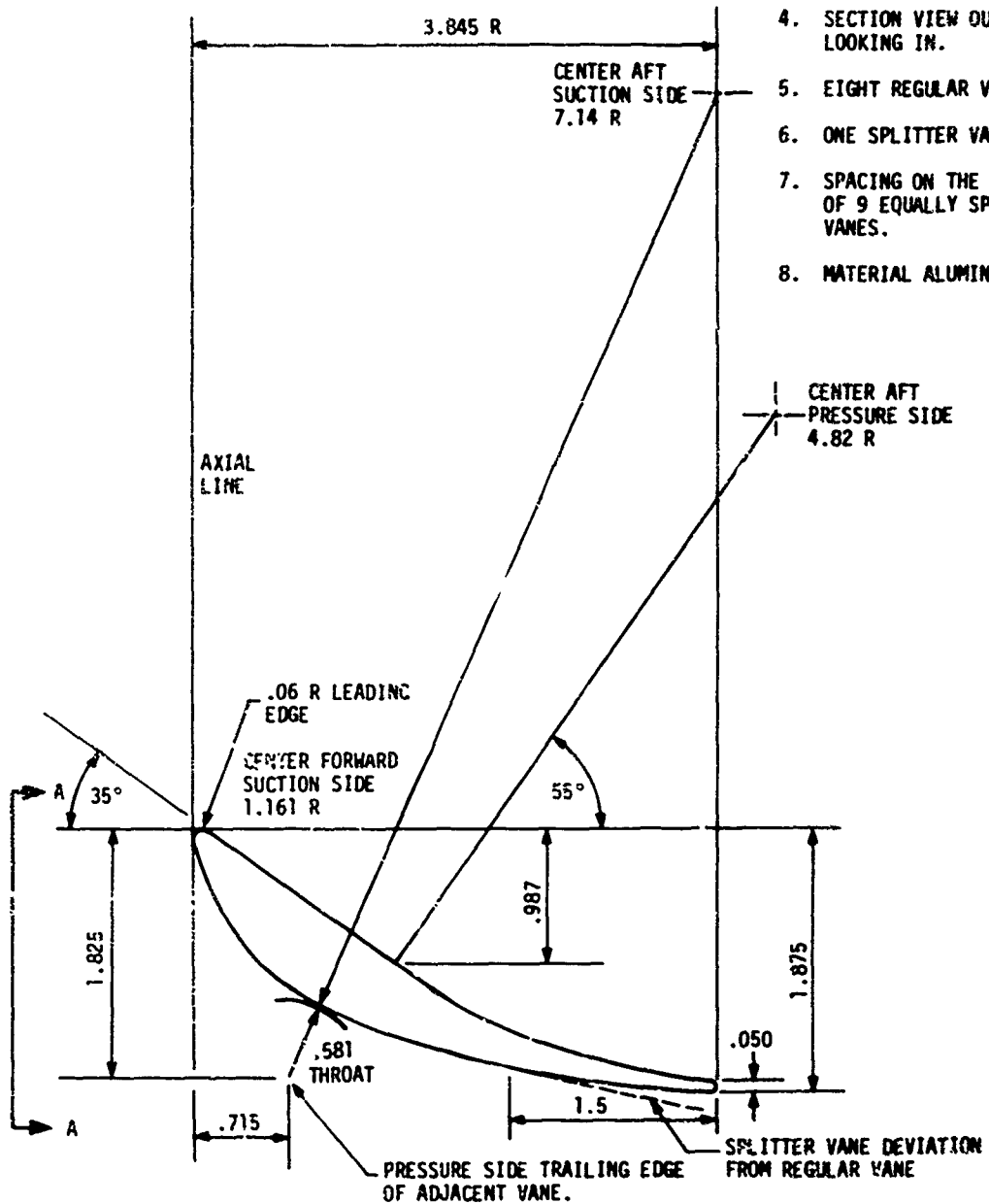


Figure 85. 5 Lb/Sec Scroll Vane.

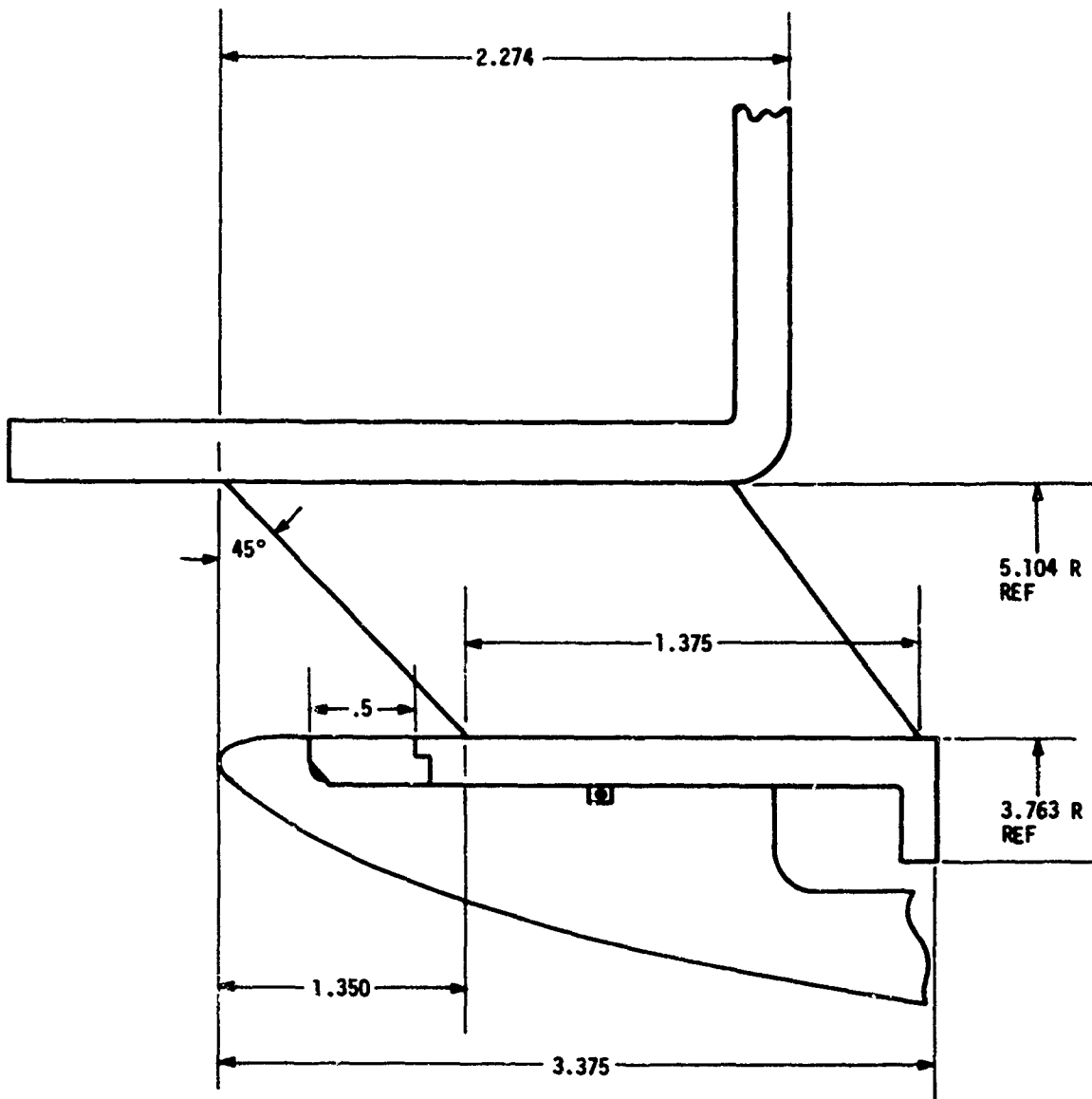
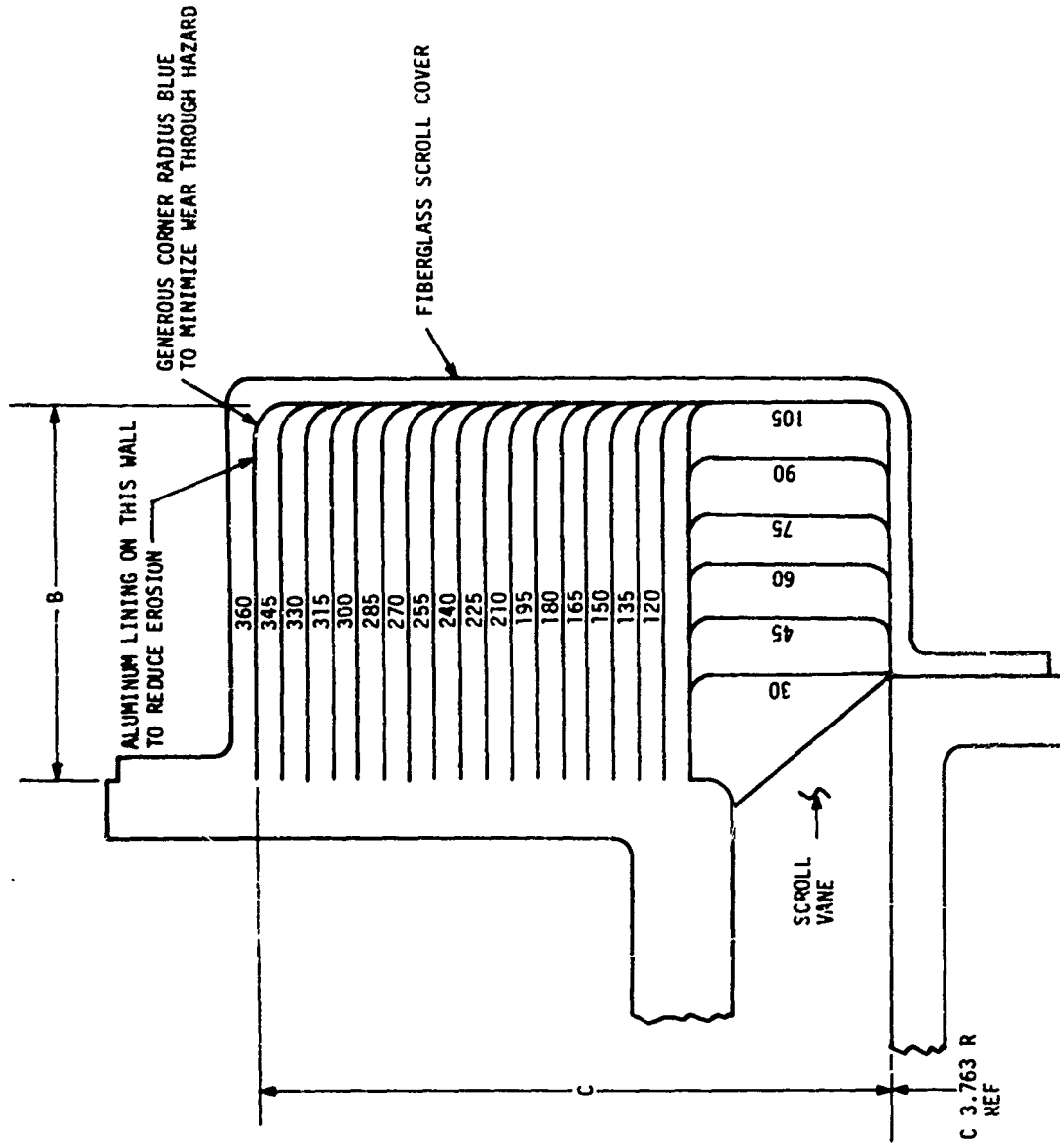


Figure 86. 5 Lb/Sec Model - Scroll Vane Leading Edge Definition.



* BLEND TO FIRST SCROLL VANE

Figure 87. 5 Lb/Sec Inlet Separator Scroll Area Schedule.

MECHANICAL DESIGN

SWIRL FRAME

The swirl frame (Item 3 of Figure 4) is the forward structure of the inlet separator and supplies the attachment interfaces for the aircraft-mounted nose gearbox and inlet duct. The swirl frame can be fabricated or cast depending upon the degree of complexity required for the struts or vanes. For a very complex internal configuration of the vanes, the frame probably is of fabricated, or a combination of fabricated and cast, construction. Swirl frames differ from conventional engine front frames or exhaust frames in that the strut (swirl vane) shapes are more complex than conventional frame struts but are of comparable span. Dimensional tolerances of the swirl vanes are tighter than conventional struts, are more difficult to achieve in manufacturing because of the complex shape, and have a greater impact on engine and separator performance. For a given swirl frame design, separator pressure loss has been found to vary ± 0.6 in. H₂O and AC coarse efficiency varied $\pm 2\%$. Since a 2% efficiency drop at 81% implies that 10.5% more sand enters the engine, the change in separator performance is significant. Therefore, the manufacturing process chosen should be realistically capable of achieving tight swirl frame tolerances.

Customer Connections

A requirement of the swirl frame is to provide easily accessible, quickly attachable connections for customer parts such as the aircraft-mounted nose gearbox and the inlet duct. These are identified on Figure 4 as Items 2 and 15. In the design shown, the front flange on the outer flow path mates with the airframe inlet duct, which is held in position by a V-band clamp. This could be a bolted flange. Connection point 15 on the cross section is the attachment point for the aircraft-mounted nose gearbox housing. It is also possible to support the front of the engine from the separator swirl frame at these same points. A better arrangement is shown in Figure 88.

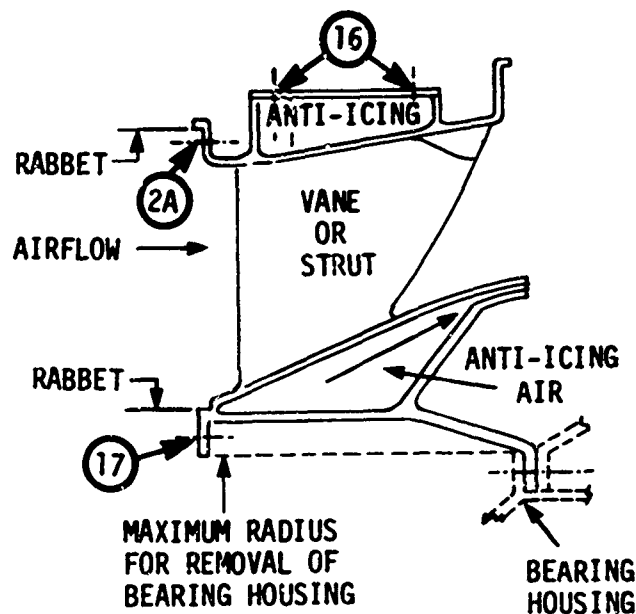


Figure 88. Separator Front Frame Cross Section.

Main mount locations could be:

1. At the forward flange (2A) - outer flow path.
2. At the forward flange (17) - inner flow path.
3. At the outer casing (16).

For attachment at 2A, the flange should be of the bolted type for maximum strength and torque (antirotation). A rabbet on the flange assures good concentricity between the inlet duct and swirl frame, but it can be eliminated if the bolt hold sizes and tolerances are held closely enough to assure good concentricity and alignment of the parts. Dimensioning and tolerancing of the mating parts must ensure that no positive overlap occurs to interfere with the flow of air at the joint; i.e., the swirl frame cannot be larger in diameter than the inlet duct at their interface, nor can the swirl frame be misaligned so that any of its front face projects radially inward beyond the location of its mating inlet duct as shown in Figure 89.

An alternative to the use of the engine flange as a load-carrying member is to add two mounting plates to the flange, as in Figure 90.

Another alternative to the separate pad concept is to add conventional type mounting pads to the outside of the swirl frame casing (Item 16 on Figure 4).

For attachment at 17 of Figure 88 the same fundamentals apply. Care must be taken in applying the negative overlap principle. The flow path may be curved sufficiently that the inlet duct gives a positive overlap dimensionally but, because of the curved flow path, the air acts as though a negative overlap exists (see Figure 91).

FRONT FRAME

The front frame shown in Figure 4, Item 10, houses the A sump, provides support for the number one and two bearings, forms the inner flow path between the swirl frame and the compressor, contains the deswirl vanes (if required) and service struts, and carries structural and torque loads as required. The frame can be fabricated of cast steel or aluminum. Oil from the integral tank of the main frame is conducted through the engine swirl frame struts (or vanes) and then into the front frame. This oil feeds the prime system and the emergency system.

The deswirl vanes are essential to the aerodynamic performance of any separator having swirl vanes. For vaneless frames, deswirl vanes are not required. If vanes are used, aerodynamic considerations require designs that provide minimum blockage to the core air, such as many vanes of thin sheet metal.

If all structural loads can be taken by the swirl frame struts (or vanes), the deswirl vanes in the engine front frame can be reduced in size and made out of very thin material. Exceptions are the "king" strut which is probably needed for service lines or PTO shaft, and the need for vane thickness for anti-icing. It is possible to combine the deswirl vanes and IGV by using fewer but larger IGV's having a fixed front portion but movable trailing edges, with the forward portion carrying anti-icing air, service lines, and structural loads. With this design, separate deswirl vanes or structural vanes can be eliminated and the inlet duct to the core engine shortened (see Figure 13).

MAIN FRAME

In the separator configuration shown in Figure 4, the main frame (Item 5) is a complex structure that performs many functions. The outer periphery contains the oil tank, the air-oil cooler, the accessory gearbox support, the scroll seal and support, a portion of the outer flow path, and the main engine mounts, which can be located on the swirl frame. The inner portion contains the scavenge vanes, the inner box interfacing with the front frame, the inlet guide vane support, the T₂ sensor, the attachment flange that mounts the entire inlet particle separator to the compressor, and part of the flow path. In the integral separator, shown in Figure 1, the main frame is a one-piece sand casting of aluminum with integrally cast lube and

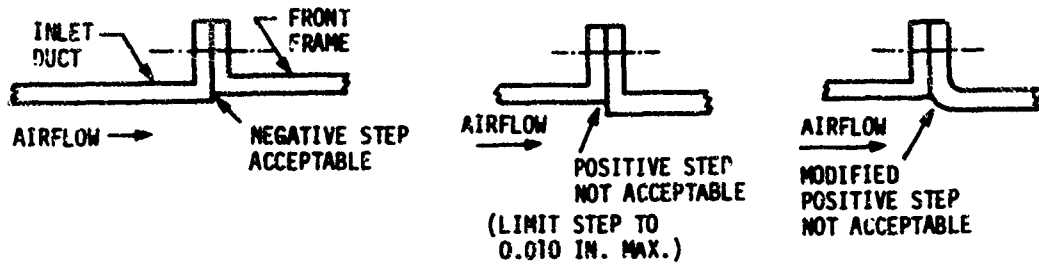
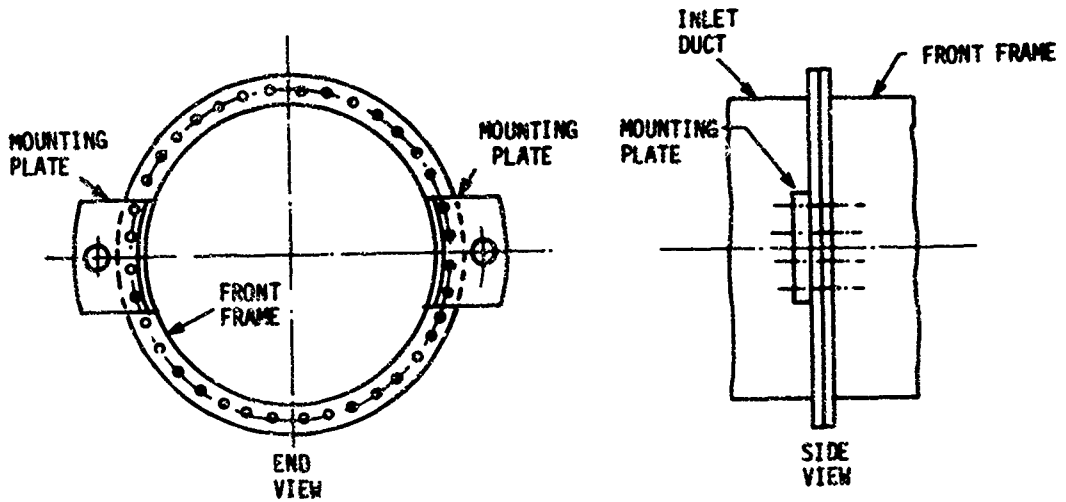


Figure 89. Positive or Negative Overlap at Flange Joints.



NOTE:

MOUNTING PLATES CAN BE ROTATED
CIRCUMFERENTIALLY AROUND CASING TO
NEW MOUNT LOCATIONS, AS REQUIRED

Figure 90. Mount Support Plates on Separator.

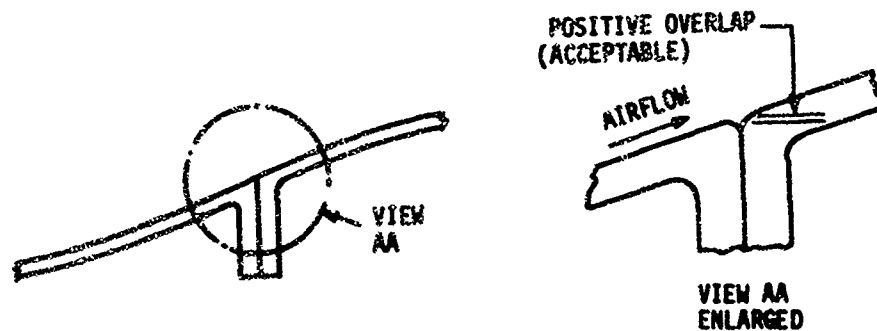


Figure 91. Acceptable Positive Overlap.

scavenge passages that connect to the lube pump. By ducting hot oil through the passageways and the scavenge vanes, excess heat from the oil is transmitted to the scavenge air, providing a good oil-air heat exchanger. As a secondary benefit, the heat exchanger also provides good full-time anti-icing protection for a large part of the separator under most operating conditions.

Scavenge vanes are spaced around the scroll inlet annulus and are used for structural purposes, for service passageways, for cooling of oil, and for directing sand and air into the scroll. Orientation of the vanes is set by collection efficiency considerations. Scavenge vane cross section (length, width) is set by aerodynamics, strength, and service line requirements. Generous scavenge vane leading-edge radii are provided to reduce the pressure loss due to high negative air angle of attack on the vanes. The leading edges of the vanes must be angled 55° in the axial direction to reduce particle deflection into the core inlet. Referring to Figure 4, the outer leading edge of the vanes is furthest forward, and the inner hub leading edge is approximately one passage height aft of the splitter nose.

Scavenge vane discharge area is set to maintain a constant scavenge airflow nominal velocity of approximately 200-270 ft/sec at intermediate rated power (IRP). The scavenge vane exit gaps are also large enough to pass all foreign particles in the collector scroll.

The inlet to the scavenge system is in the aft portion of the main frame and includes the scavenge vanes.

The scroll collector is located directly behind the scavenge vanes and provides a flow path to duct the scavenge air to the impeller inlet duct. The air-sand mixture exiting the scroll vanes is directed into the blower inlet duct, where it is dumped overboard. Attachment to the blower duct can be accomplished by a rubber boot to permit the differential expansion due to mounting the blower on the accessory gearbox and the scroll on the main frame. Since inertial and handling loadings are negligible, the primary design considerations are vibration and relative movement.

The scavenge air collector is not subject to heavy loads and can be made of lightweight materials such as fiberglass or aluminum. It can also be cast integrally with the outer casing and scavenge vanes, or cast as a separate piece. Materials must be able to meet anti-icing air temperatures since anti-icing of the scroll is required for some operating modes. Operating pressures inside the scroll vary from approximately 1 psi below ambient at sea level static maximum power to slightly above ambient at low power settings and ram conditions.

The collector can be utilized for cooling some electrical equipment by mounting this equipment on the collector with heat transfer surfaces in the collector airstream. The collector shape and position are integrated with the engine accessory gearbox and accessories to produce a compact, easily maintained system. The collector generally extends aft and, for ease of

maintenance, allows the removal of one-half of the compressor casing without removing the collector. The collector may have one or more discharge ports depending on the external configuration of the engine.

The scavenge vanes are hollow for anti-icing, and for service lines, oil passageways and oil cooling. The vanes are useful for transferring heat from the hot lube oil to the scavenge air for oil cooling. The hot lube oil also heats the vanes and keeps them from icing at low ambient temperatures. A special oversized "king" strut is required for the PTO and service lines, if they pass through this area.

For the separator configuration shown in Figure 1, the frame contains passages for the lube oil. (See Figure 92.) Oil is carried to the lube pump, from which it is distributed to the front sump (A sump) via the service lines in the swirl frame and cored passages in the engine front frame. The oil then returns directly to the tank during cold operation. The cooling circuit provides a supplementary means of heat rejection where heated engine oil is conducted from the tank through hollow scavenge vanes to the inner box, circulating between the inner and outer boxes and exiting to the tank at the top. The heat is conducted to the scroll vane walls, where it is radiated to the scavenge air and dumped overboard. Circulation of oil through the vanes keeps the temperature difference between the inner and outer frame parts to a minimum (usually less than 10 deg) and thereby produces very low thermal stresses.

Engine Mounts

The engine configuration shown in Figure 1 has its front engine mounts located on the outer walls of the separator mainframe as shown in Figure 93. Axial ribs cast integrally with the tank take the axial and vertical mount loads as shear loads into the sidewalls of the tank. Internal gussets, in the form of toroidal box sections, are used to offset bending loads from the engine mounts. This approach is necessary to carry these loads and should be applied to any similar separator design.

ANTI-ICING

The separator flow path must be heated under certain operating conditions to prevent the formation or buildup of ice on the separator surfaces.

Sources of heat that are available are:

1. Warm compressor bleed air.
2. Hot oil.

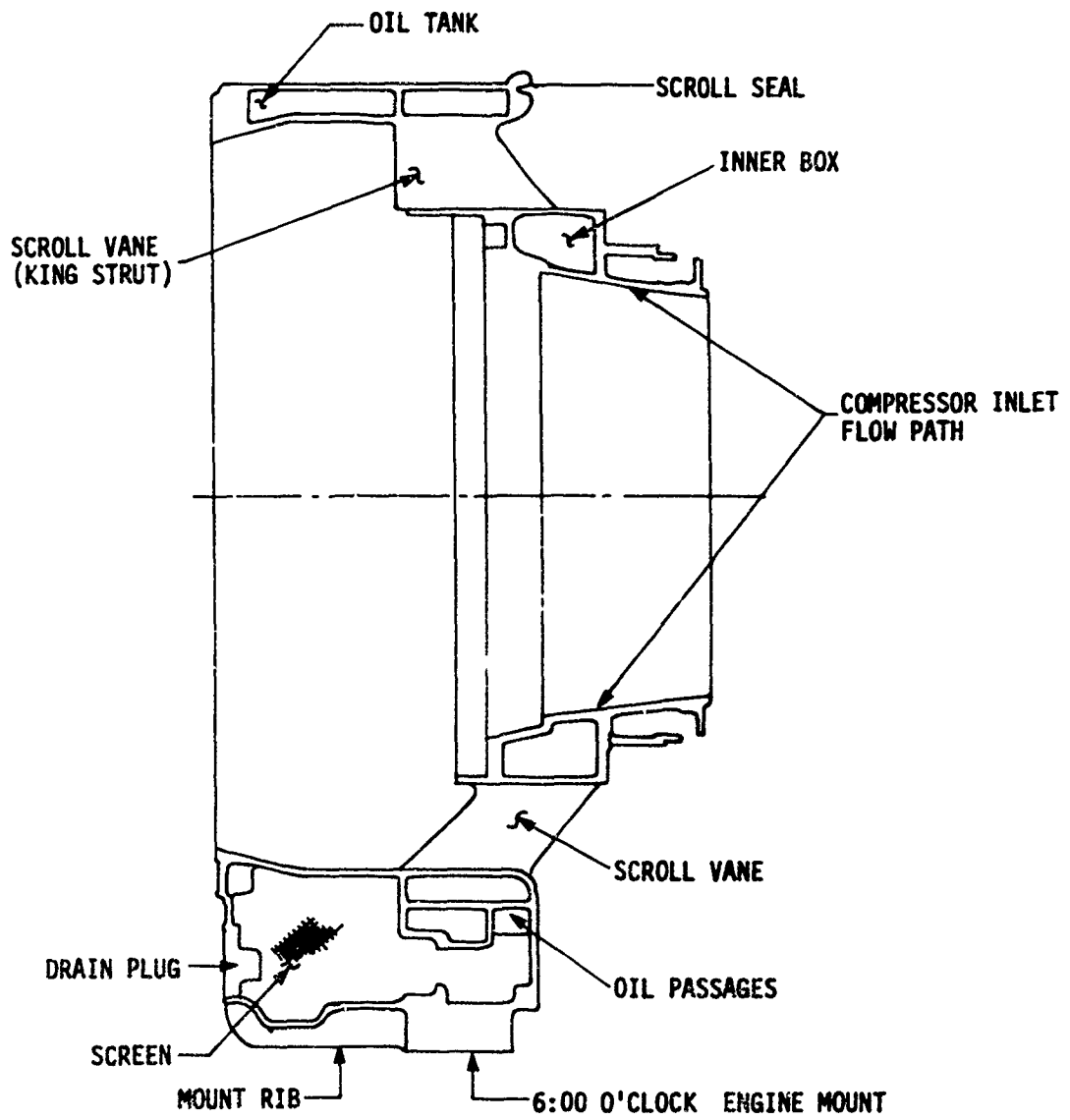


Figure 92. T700 Mainframe Oil System.

3. Electricity.
4. Hot fuel.
5. Exhaust gases.

The most acceptable choices are usually compressor bleed air and hot lube oil. Hot fuel and hot exhaust gases are usually unacceptable due to safety problems, ducting problems, and loss of engine performance. Electrical heaters are possible but difficult to adapt.

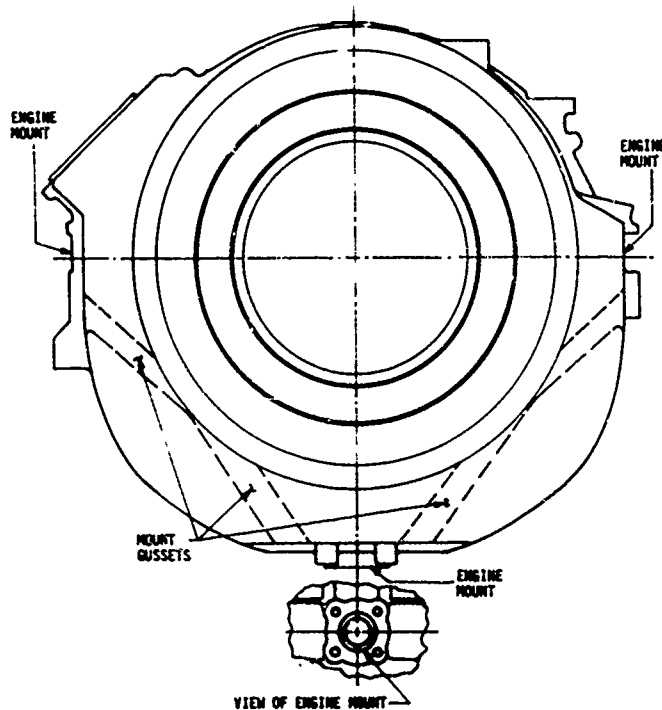


Figure 93. T700 Front Engine Mounts.

Anti-icing of a typical axial type separator (Figure 94) has been successfully accomplished using compressor bleed air for the swirl frame including the swirl vanes, for the splitter nose, and for film heating portions of the inner and outer flow paths aft of the swirl vanes. Hot lube oil provides anti-icing for the major portion of the main frame including the scavenge vanes. Lube oil inside the sump keeps the inner flow path warm, while a combination of heat from the sump and splitter anti-ices the deswirl vanes by conduction. A similar anti-icing system can be applied to a new separator, particularly if it is similar to the axial type separator shown in Figure 94.

The oil tank is integrated into the mainframe structure as shown on Figures 4 and 92. It provides anti-icing of the separator outer wall. If a separate oil tank is used, cored oil passageways or anti-icing air could

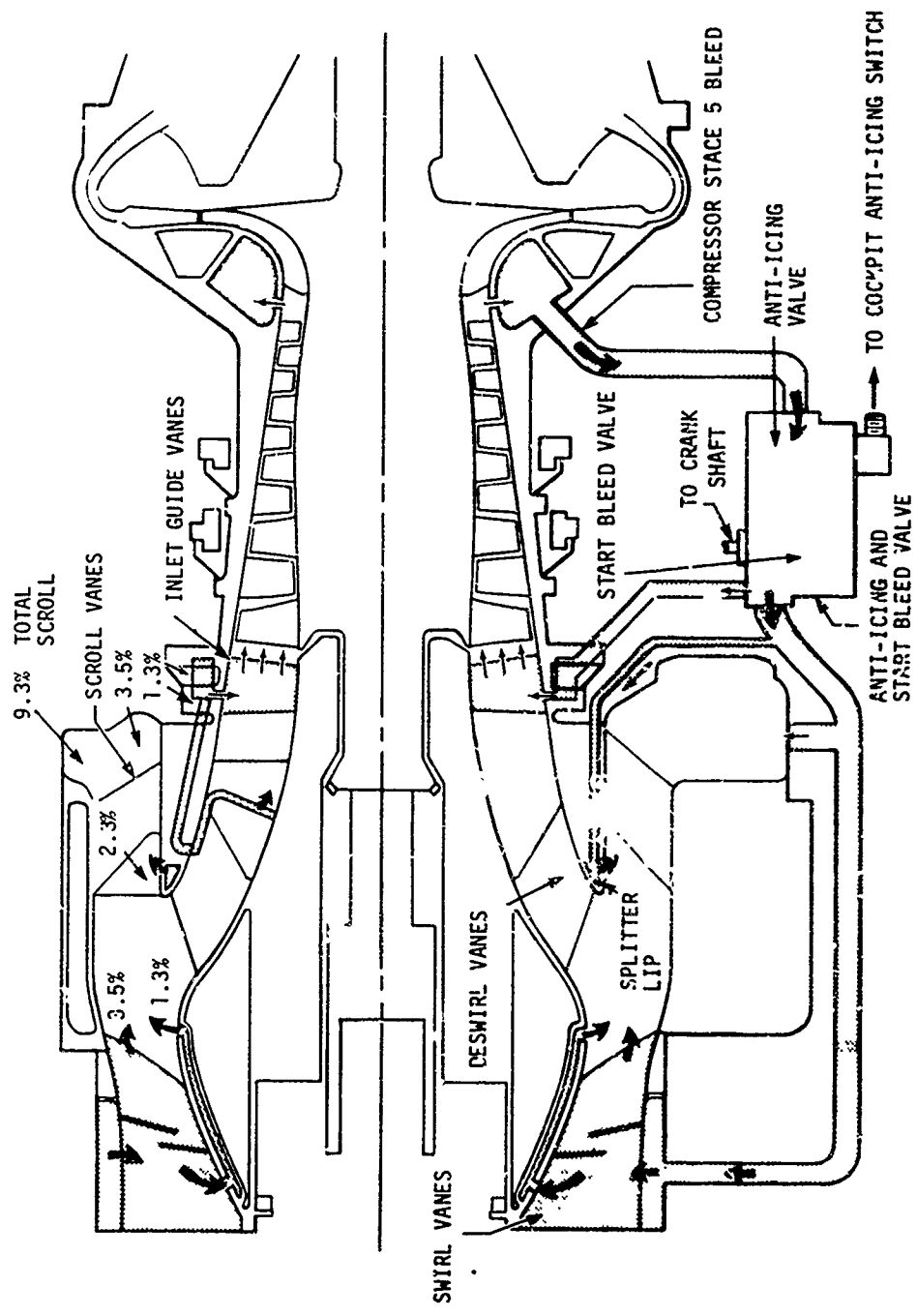


Figure 94. Anti-Icing System of Axial Separator.

be substituted to anti-ice the inner and outer flow path areas. Allowance must be made to have at least 25% extra volume in the tank for deaeration and settling of the oil.

The use of compressor bleed air for anti-icing should be considered for all parts. For example, compressor bleed air can be supplied to a manifold on the outer casing and then ducted through the swirl vanes or struts to an inner manifold. The bleed air is then dumped into the outer flow path at the trailing edge (Item 18, Figure 4) of the vanes or struts and at the inner flow path (Item 17, Figure 4). The amount of air being introduced into the core by the inner flow path should be kept to an absolute minimum since warm air adversely affects the engine's performance. A possible percentage split is 25% anti-icing air at the inner flow path and 75% at the outer flow path.

The exact quantity of bleed air depends upon a number of variables such as:

1. Engine speed.
2. Type of heating system:
 - a. Convection.
 - b. Conduction.
 - c. Impingement.
 - d. Convection with serpentine passages.
 - e. Combination.
 - f. Film.
 - g. Radiation.
3. Amount of pressure drop available.
4. Types of materials.
5. Type of flow control used.

Trade-offs and limitations must be considered in the design. Particularly important design limitations that must be considered are:

1. Low compressor bleed air pressure and temperatures at idle.
2. Pressure drops in passageways, especially if serpentine passages or high-velocity airflows are required.
3. Wide-open flow affects performance and could overheat some materials at maximum operating conditions. A variable schedule of bleed airflow versus engine speed is desirable. Steel is recommended for higher temperature requirements.

For the swirl frame configuration, the leading edges of the swirl vanes are the most critical areas requiring anti-icing. The leading edges are exposed to the direct impingement of inlet air, have the highest local

cooling rates, and are the first place where ice will form if no anti-icing provision is incorporated. Anti-icing of the leading edges is helped by making airfoil leading-edge radii as large as possible. Several different arrangements are available, including vanes or struts with:

1. No baffle.
2. Baffle.
3. Baffle with centerbody.
4. Baffles with serpentine flow path.
5. Film heating with baffle.
6. Impingement heating.
7. Combination film and impingement heating.
8. Other.

Figures 95 through 102 illustrate these configurations. Figure 103 shows how swirl vane trailing edges can be modified to handle large bleed airflows.

All areas subject to icing must be heated to prevent the accumulation of ice; or if ice has already formed, the anti-icing system must be capable of removing the ice over its operating range. Three basic anti-icing requirements are:

1. An anti-icing system must have adequate heat capacity over its operating range.
2. An anti-icing system must remove ice which has already formed. This probably requires a through-flow type system for compressor air. If a strut or vane had film heating through leading-edge holes, compressor bleed air could not remove the ice build-up since there would be no flow of air through the vanes.
3. An anti-icing system must cover all key surface areas. Manifolds must cover inner and outer walls of the separator, and compressor bleed air must be ducted or directed to provide complete coverage of the areas to be anti-iced.

As much anti-icing air as feasible should be dumped into the scroll exhaust system to prevent scroll surfaces from icing. For the example shown in Figure 94, approximately 75% of all separator anti-icing airflow goes through the scroll exhaust system rather than into the engine where it adversely affects performance. Estimates of anti-icing airflows and their locations at engine idle are given in Figure 94 for a typical separator. A comparison of anti-icing airflow requirements at idle and

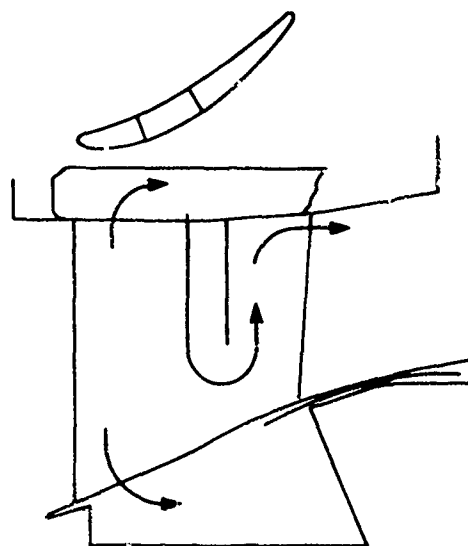
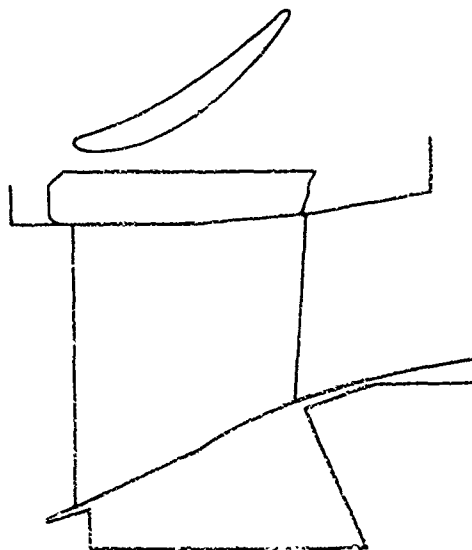


Figure 95. Swirl Vane - No Baffle. Figure 96. Swirl Vane - With Baffle.

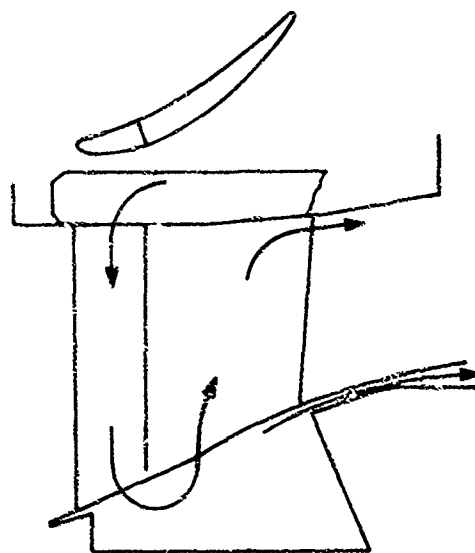
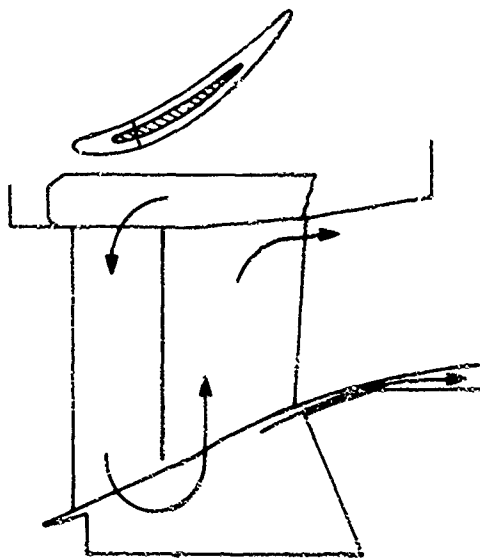


Figure 97. Swirl Vane -
Centerbody Baffle

Figure 98. Swirl Vane -
Partition Baffle.

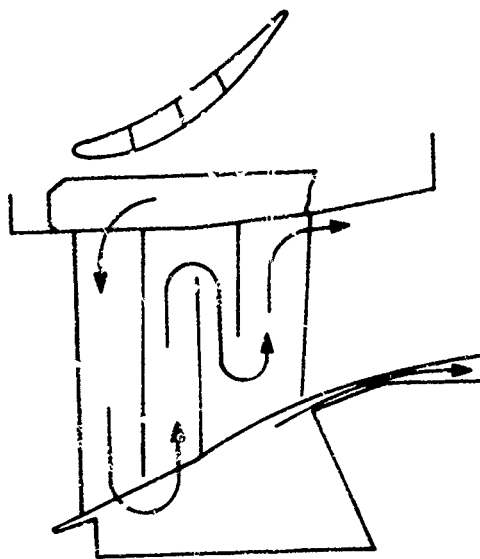


Figure 99. Swirl Vane -
Serpentine Flow Path

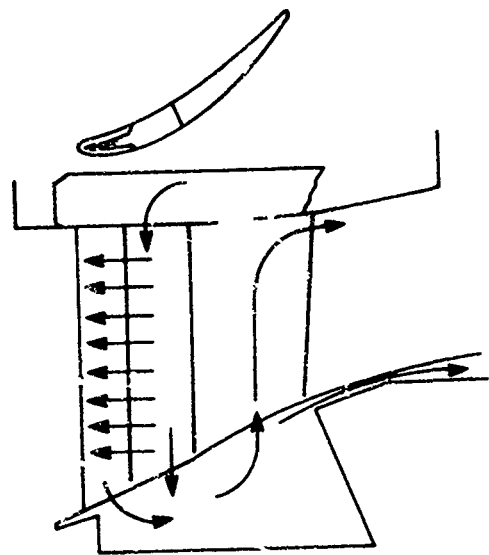


Figure 100. Swirl Vane -
Film Heating With Baffle.

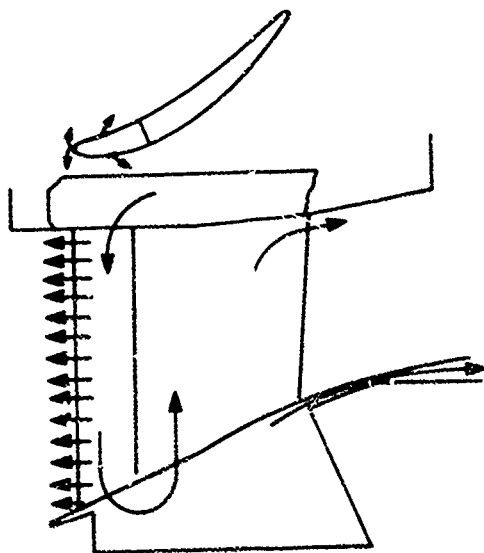


Figure 101. Swirl Vane -
Combination Film and
Impingement Heating.

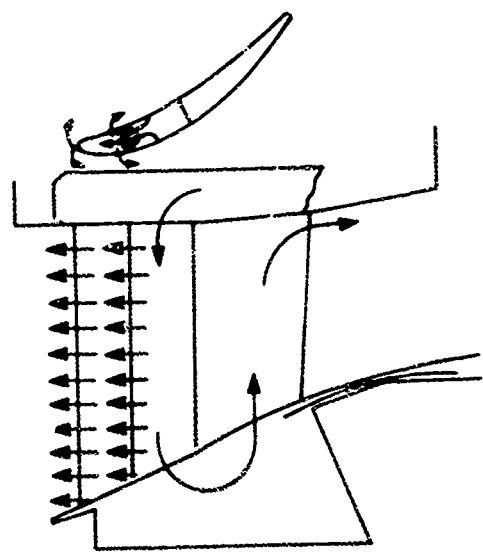


Figure 102. Swirl Vane -
Combination Film and
Impingement Heating.

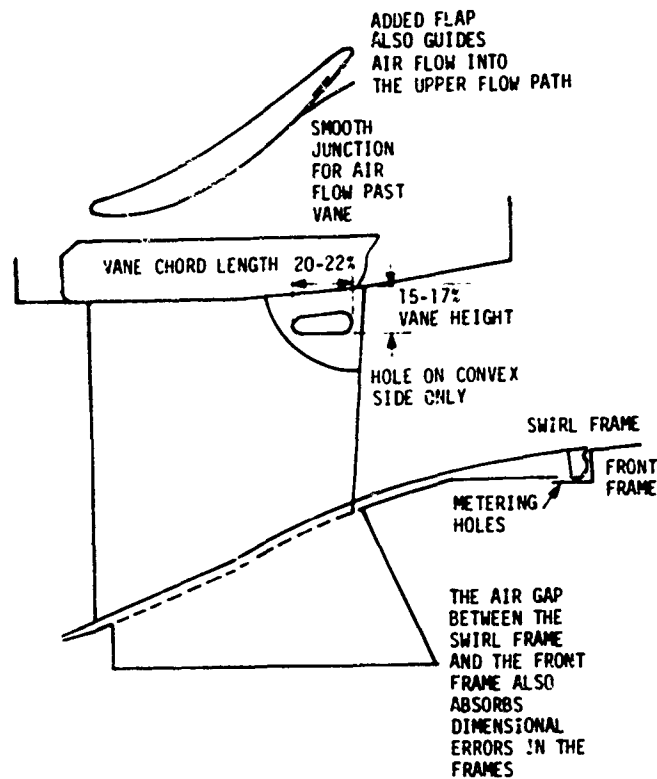


Figure 103. Swirl Vane Anti-Icing Air Discharge Port.

idle is due to the reduced temperature of the bleed air. The large difference in flow requirements for the two conditions emphasizes the need to have bleed flow scheduled as a function of engine speed and shows why a bleed air regulating valve is required for the engine. Air temperature and material temperature capability are important considerations for all anti-iced surfaces.

The separator can be completely and efficiently anti-iced with minimal effect upon engine performance by using a combination of warm bleed air and hot lube oil. Table 14 shows that only about 4% of the compressor air is required for anti-icing the separator and IGV's at intermediate rated power (IRP). Hot lube oil supplies sufficient heat to do the rest. The separator cross section, Figure 94, shows where and how the bleed air is directed for anti-icing. Only about 25% of the separator and IGV anti-icing bleed air is vented back into the engine inlet, and the major portion is carried out through the scavenge exhaust system. This limits the flow into the engine core to only about 0.9% W_2 at IRP and thereby minimizes temperature effects upon engine performance. An ON-OFF bleed air system further limits any harmful performance effects to those situations where anti-icing air is required.

TABLE 14. SCAVENGE EXHAUST SYSTEM, SPLITTER, IGV'S, AND SWIRL FRAME

Anti-Icing Air Location	<u>Idle</u> <u>%W₂</u>	<u>Irp</u> <u>%W₂</u>
Swirl vane outer	3.5	1.17
Swirl vane inner	1.3	.44
Splitter	2.3	.77
Scroll (in)	3.5	1.17
IGV's	1.3	.44
<hr/>		
Total Anti-Icing from Station 2.5	11.9	3.99
<hr/>		
Total through Scroll Collector	9.3	3.1

In contrast to the ON-OFF anti-icing system using regulated compressor bleed air, the lube oil system supplies continuous anti-icing to those areas of the separator which are exposed directly to the lube oil. Specifically, this includes (Refer to Figure 94):

1. Oil tank in the mainframe including aft portion of outer flow path.
2. Scroll scavenge vanes.
3. Inner panel and inner flow path of mainframe.
4. Emergency oil tank and sump wall in engine front frame.
5. Cored passages in engine front frame and mainframe.

Anti-icing tests on a typical axial integral separator have shown that heating of all key areas is necessary to prevent ice build-up in the separator flow path. Increased oil velocities through cored passages are more effective in anti-icing than slow-moving or standing oil. Higher velocity oil flows through cored passages should be used at key areas to be anti-iced. Oil velocities of 150-250 ft/sec assure good heat transfer characteristics between the oil and the metal to be heated.

MANUFACTURING CONSIDERATIONS

Method of manufacture of the separator is determined by:

1. Complexity of the design.
2. Material capabilities and limitations:
 - a. Temperature.
 - b. Manufacturing processes (forming, brazing, etc.).
 - c. Cost.
 - d. Strength.
 - e. Weight.
 - f. Thermal compatibility.
 - g. Life.

Experience shows that fabrication can handle almost any manufacturing and design requirements, castings can handle many requirements, and forgings are more limited in scope.

For a complex part, the choice of method of manufacturing is usually between fabrication and casting. The fabricated structure provides a greater choice of materials, shapes and processes, and it provides greater flexibility for making changes, such as vane settings. This flexibility is particularly useful in the development stages.

Parts can be fabricated from steel, titanium, aluminum or combinations thereof. If the parts are cast, the materials are steel, aluminum, or possibly titanium. Manufacturing processes are usually limited to casting and machining. Some brazing and welding can be done, but on a smaller scale.

Fabricated Structures

Fabricated frames can be made of many small parts and of thin materials. To prevent high bending stress concentrations at intersections, such as those of the swirl vanes with the inner and outer bands, doublers are frequently used. Since welding is difficult on small parts, brazing is used for bonding parts. In that case, small welds are used only to fixture the parts to be brazed. Also, to assure completely brazed joints, special manufacturing processes and inspection procedures are required. The fabricated structure can use thinner vanes than a casting because it does not have the limitations of maximum core size, core shift and core removal. In addition, greater degrees of complexity can be incorporated into the vanes and struts for the fabricated structure.

Some considerations for a fabricated separator frame are:

1. Material thickness must be sufficient that damage will not occur during fabrication or field handling.
2. The fabrication must be designed to transmit major loads in tension, compression, shear and bending. Cast vane ends fabricated into rings should be used whenever possible.
3. The limit loads applied in service must not exceed the material strength. Repeated loads must not exceed the low cycle fatigue strength of the structure.
4. Anti-icing air must not cause low cycle fatigue within the part life requirement.
5. Panels must not resonate (oil can frequencies) with engine or aircraft mechanical stimulus, or be aerodynamically excited.
6. Vanes, particularly service struts, must have sufficient impact resistance to survive foreign object ingestion.
7. The low thermal conductivity of steel and the thin materials required to make a lightweight design dictate that all surfaces subject to icing be "scrubbed" on the inner surface with anti-icing air. Refer to the section on anti-icing for further comments on anti-icing.
8. Selection of materials and brazing must be compatible to assure that subassembly joints and materials do not melt if a subsequent brazing operation is required.
9. Brazed joints must be sufficiently bonded to prevent service line and anti-icing air leakage.
10. In calculating frame weight, allowance must be made for the weight of the braze filler material.

Cast Front Frame

A satisfactory cast frame can be made from steel or aluminum. If the design is particularly complex, such as internal passageways within the vanes, a two-piece frame or a combination cast and fabricated structure may be better than a single cast frame.

A cast aluminum frame results in a lighter weight, lower cost structure than a cast steel frame but has lower temperature capability, which can become a problem if the aluminum is overheated from too much high-temperature, anti-icing compressor bleed air. On the assumption that a reliable flow control system can be achieved, a cast aluminum frame should

be evaluated and compared with a fabricated frame. For minimum weight and minimum wall structures, precision casting methods, such as lost wax and shell molding should be selected. Some considerations are:

1. Precision castings are repeatable within approximately ± 0.005 inch, resulting in small variation in weight between castings and minimum machining.
2. Precision castings give better than 60 RMS surface finish, which exceeds requirements and eliminates hand polishing.
3. Minimum machining is required to finish the cast frame.
4. Wall thickness is a minimum of 0.040 inch.
5. Vane is sufficiently thick to allow coring and core removal for anti-icing air and lubrication services.
6. Core openings are provided in low-stressed areas where welded plugs are not highly stressed.
7. Allowance is made for core shift.
8. Cores are supported on both ends, where possible.
9. Liberal requirements are given for casting quality in low-stressed areas.
10. An easily cast aluminum alloy is selected.
11. Allowance is made for properly feeding all sections of the casting.
12. Anti-icing air with a failed-open anti-icing air valve does not fail or distort the castings.
13. Anti-icing air does not cause low cycle fatigue of the part, within the cycles to meet the design requirements.
14. Limit loads applied in service should not exceed the strength of the material, and the repeated loads should not exceed the low cycle fatigue strength of the casting.
15. Casting is designed to transmit major loads in tension, compression, shear, and not in bending in such regions as vane end attachments.
16. Additional material is allowed in high-stress regions such as at intersection of rings, vanes and flanges.

17. Vane continues into center hub to reduce bending stresses and stress concentrations.
18. Vane is cast into rings on the outer diameter to reduce stress concentrations and bending stresses.
19. Surfaces are "thick cast" to reduce the possibility of "oil canning" fatigue.
20. Aluminum's high thermal conductivity, seven times that of steel, and increased thickness over steel make the anti-icing easier and reduce thermal distortion and stresses.
21. Casting allows considerable freedom in coring the anti-icing circuits to take maximum advantage of the thermal conductivity.
22. Boundary layer trips can be used in the anti-icing cored passages where increased surface heat transfer coefficient is required.
23. Cast frames usually cost less than fabricated frames.

RELIABILITY AND SAFETY

Reliability and system safety objectives can be met by considering the requirements of each application. Some considerations helping to reduce or eliminate potential failure modes or reduce the consequences of a failure are:

1. Frame cracking due to excessive loads imposed by external forces.
2. Low cycle fatigue cracking.
3. Mechanical damage and performance loss due to ingestion of single foreign objects or erosion.
4. Mechanical damage and performance loss due to salt water corrosion and deposits.
5. Fouling with oil and dirt.
6. Containment of fractured rotating elements (e.g., scavenge blower impeller).

The object of a system safety program is to eliminate hazards. If it becomes impossible to completely eliminate hazards by design, hazards may be reduced to a tolerable level by the use of added safety devices. If there is still a hazard, detection and warning devices and, as a last resort, special procedures such as precautionary notices and warning notes may be used.

The inlet particle separator is integrated into aircraft engine designs largely to improve the reliability and safety aspects of engine performance. However, it is important that the separator itself does not contribute potential hazards.

VULNERABILITY

In the design of military engines, it is necessary to reduce as much as possible the possibility of major engine damage as the result of projectile impacts. To accomplish this, it is most important to avoid "hits" by keeping the exposed areas as small as possible. In the event of a hit on the separator, potential effects on the engine are:

1. Ingesting structural material into the engine core.
2. Ingesting combustibles which may result in internal fire, burn-through, or stall.
3. Release of fuel or oil which may result in fuel or oil starvation, or external fire.
4. Vibration caused by unbalance in a damaged scavenge blower.

Barrier filters or tightly packed banks of small separators are usually not desirable for low vulnerability designs. They tend to have large areas which are easily hit and, when hit, release debris directly into the engine inlet. Also, as the result of a hit, relatively brittle castings release more metal than fabricated structures which could be ingested by the engine.

The integral separator system is desirable for low vulnerability because of its capacity for collecting or separating debris caused by hits and detonations upstream of the separator. However, its design must minimize the effects of hits in the separator itself which may release debris and cause major damage to the engine. Therefore, fasteners such as snap rings, tab washers, rivets and lock wire should be eliminated from the separator flow path. They are foreign objects which, during the life of an engine, are certain to be ingested by the engine and cause damage.

SCROLL SEPARATORS

An alternate separator configuration that is particularly promising for the smaller engine sizes (approx 2 lb/sec) is the inlet scroll separator of Figure 104. Investigations have indicated that the scroll design should be competitive in size and performance for small sized engines. Studies have shown that the combined inlet scroll and separator, scroll separator, overall volume is approximately the same as that of the axial type for a 2 lb/sec engine, but it requires a smaller inlet opening. For a 2 lb/sec engine, the inlet air opening is 4.36 in. diameter, giving an inlet area 50% larger than the compressor inlet area to maintain separator pressure losses within acceptable limits.

In the scroll design a plenum chamber is added at the inlet elbow to collect and trap a maximum amount of major size foreign objects, preventing them from going through the separator and scavenge blower. Scavenge air is taken from this collector and from several locations along the scroll. Scavenge air openings are sized so that only small particles can go through the openings. The only exception is the second bleed-off opening, which is at the bottom of the separator. It is large enough to take nuts, bolts, and similar objects if they should get past the collection trap. Cleanout covers to remove trapped objects are located at the inlet elbow (collection trap) and at the second bleed-off opening (see Figure 105 for scroll cross section).

The scroll separator is adaptable to a variety of different installations because of the small inlet opening. Inlet air can be introduced from any direction by designing the inlet so that it can rotate through 360°, or the inlet can be removed so that air can be brought in tangentially. An engine design showing tangential introduction of air is shown in Figure 106.

The scroll separator can be used with an integral oil tank, a separate oil tank in the same relative location and space, or a separate oil tank located elsewhere on the engine. Some additional supplemental cooling of the oil and anti-icing of the scroll are obtained from the integral oil tank arrangement. It is necessary, however, to have other means for cooling the oil since there is not enough air to do the entire job. Methods to be investigated include:

1. Wrapping coils of oil around the inlet scroll.
2. Oil-to-air heat exchanger.
3. Cooling oil by passing it through the scroll struts which are located in front of the compressor.

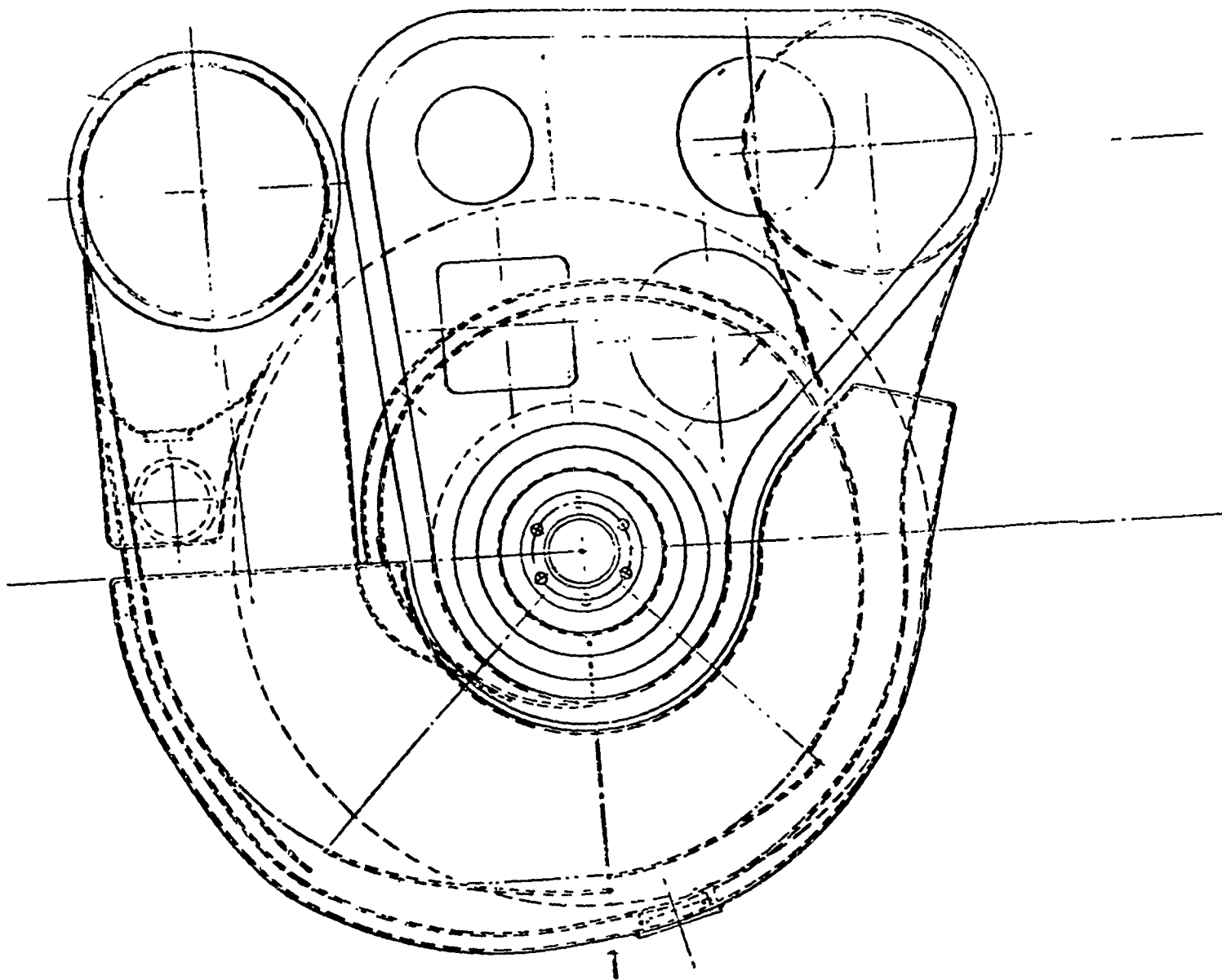
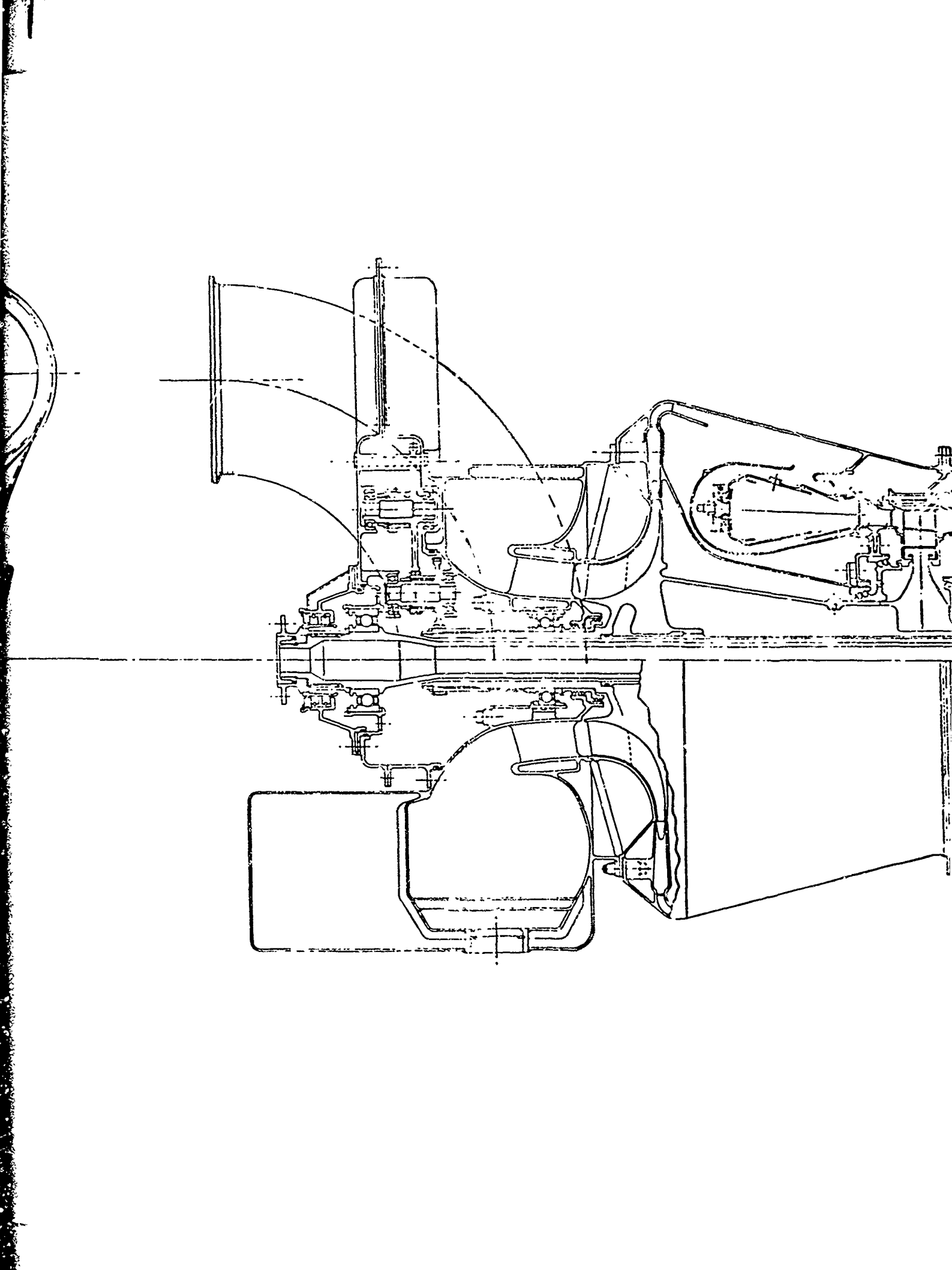
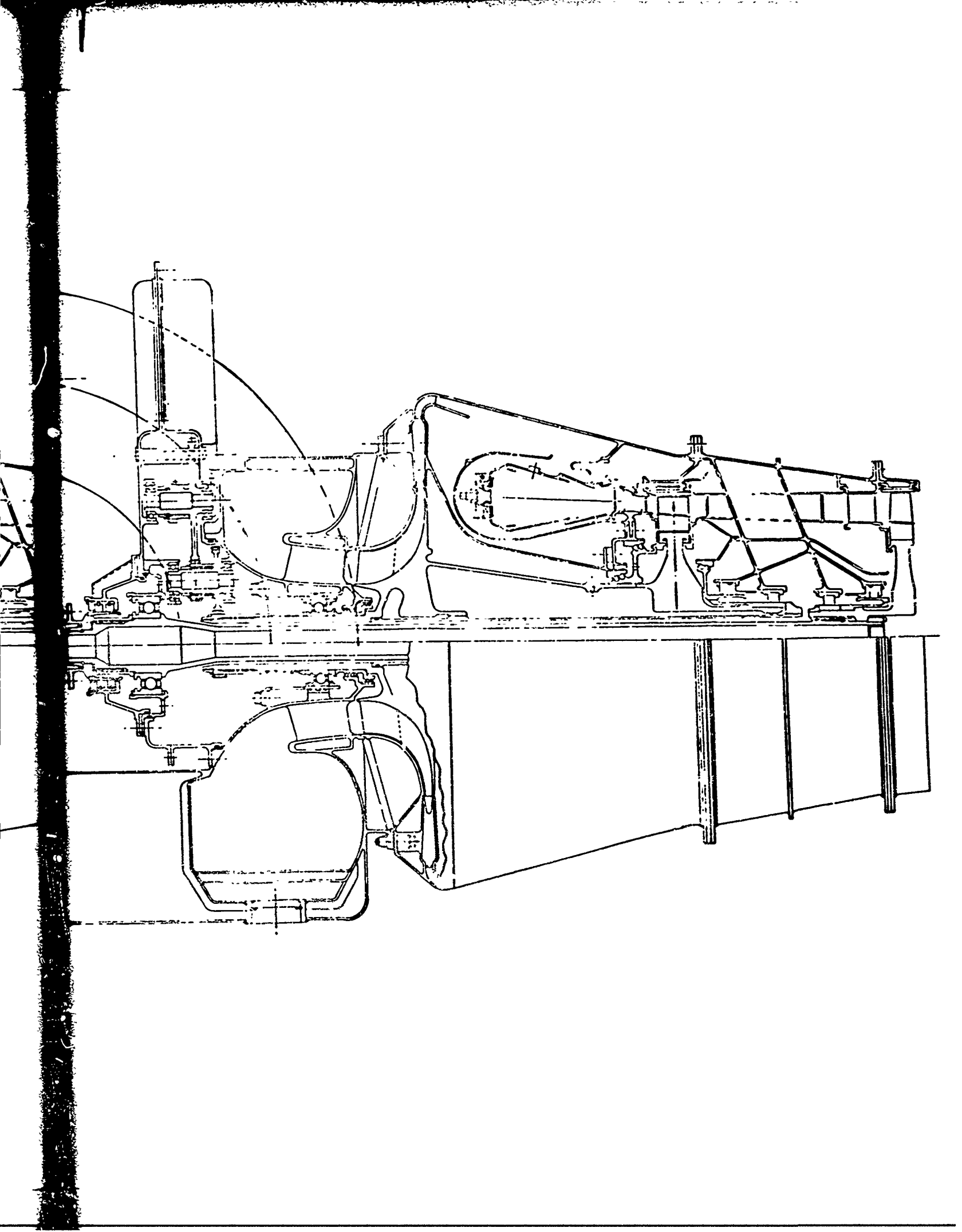


Figure 104. 2 Lb/Sec Turboshaft Engine With Inlet Scroll Separator.





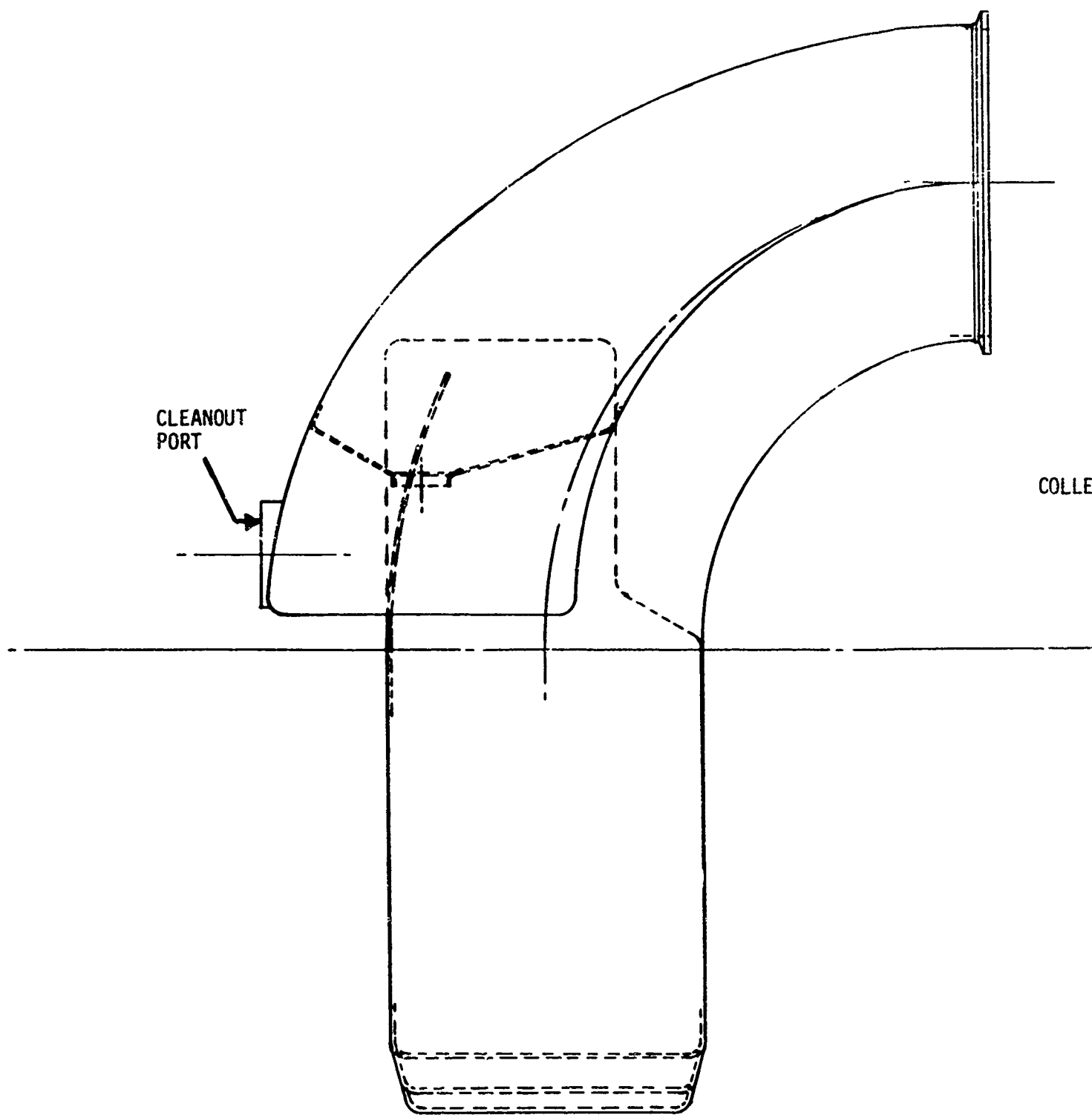
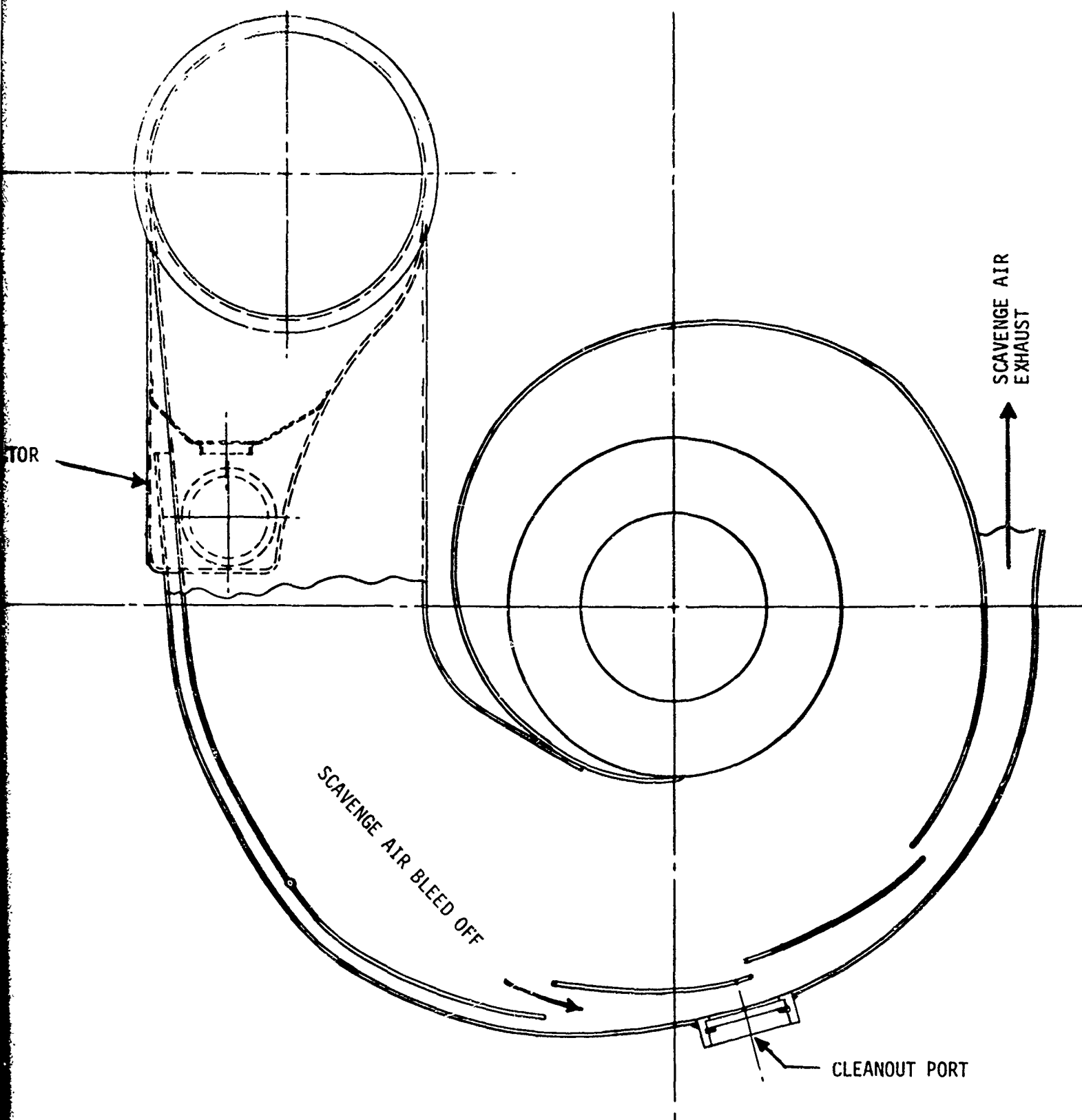
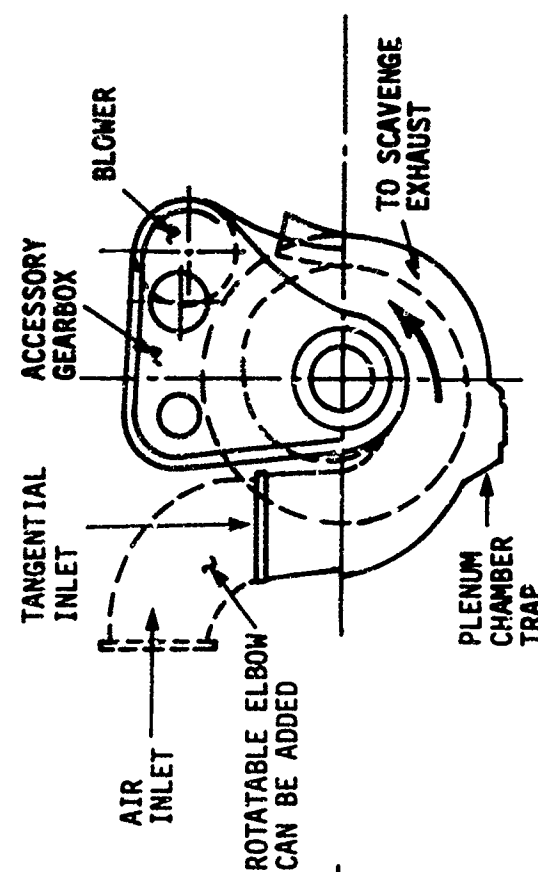


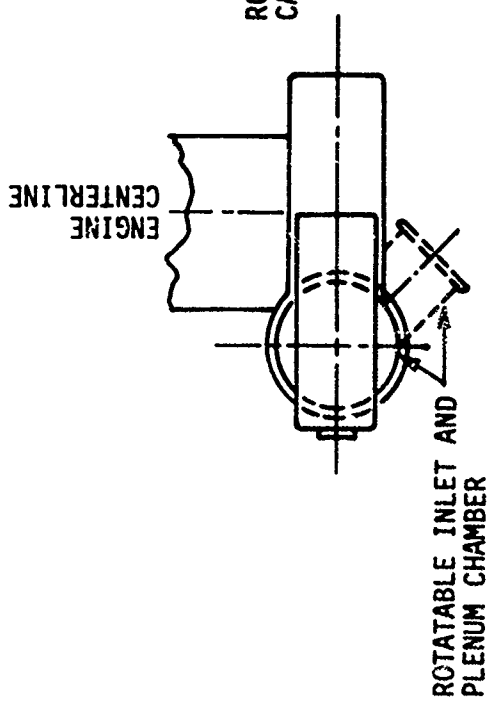
Figure 105. Scroll Separator Cleanout - Cross Section.

Preceding page blank





THIS SCROLL SEPARATOR HAS
A SHORTER SEPARATION LENGTH



A SEPARATE INLET ELBOW
CAN BE ADDED

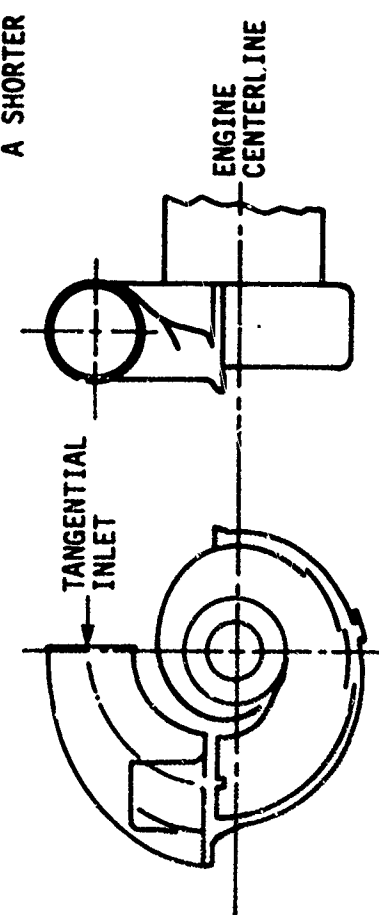


Figure 106. Scroll Separator Tangential Inlet.

Preceding page blank

The scroll separator design also can be adapted to other configurations, such as would result from reversing the locations of the gearbox and oil tank.

Anti-icing is less of a problem with the scroll separator than the axial type since there are no swirl or scavenge vanes and only one set of struts. It is estimated that proper location of oil tubing plus an integral oil tank will provide sufficient anti-icing capability.

Installation requirements are important in prescribing the separator configuration, especially in the 2 lb/sec size. For the scroll separator, the drive shaft is not coaxial with respect to the air inlet as it is in the axial separator. This results in a different installation setup and separate points of attachment for the drive shaft and for the inlet. Although the engines shown are required principally for aircraft installations with air inlet from the front, they could be used for other applications such as tanks, other ground vehicles, and auxiliary power units. The 2 lb/sec scroll separator is especially versatile and flexible for a variety of different installations, because of the small inlet duct. With a rotatable type elbow inlet, air can be introduced at any angular location over a 360-deg arc.

A comparison of the scroll separator and the axial type separator indicates:

1. Advantages for the Scroll Inlet:
 - a. No swirl vanes, no scroll scavenge vanes, and no deswirl vanes are required. There are structural struts in front of compressor inlet.
 - b. Collection of heavy foreign objects at inlet of scroll reduces chances of damaging the scavenge air blower and the engine. Cleanout covers permit removal of foreign objects.
 - c. No PTO shaft is required. This eliminates PTO interference with the flow path and bevel gearing. Only spur gearing is used.
 - d. The aircraft installation can be simpler and more flexible since the inlet is small and not coaxial. It can be easily adapted to accept air from any direction.
 - e. The scroll separator offers potential of good collection efficiency with reduced scavenge airflow. Multiple scavenge ports distributed along the scroll help to assure a good overall collection efficiency.
 - f. Anti-icing is simplified.

- g. Thermal mismatches of structural parts are minimized.
- h. A separate oil tank can be used or an integral oil tank can be built around the scroll. Integral oil tank is susceptible to damage either internally or externally to about the same extent for both separators.

2. Advantages for the Axial Type Inlet:

- a. A compact and efficient oil-to-air heat exchange system has been worked out.
- b. Installation envelope may be slightly smaller.
- c. The gearbox and accessories can be removed as a module without removing the power shaft.

Using trajectory analysis to evaluate scroll separator separation efficiency, it has been shown that all particles 15 microns and larger strike the wall in the initial inlet turn. If all the particles which strike the wall are separated, all particles 15 microns and larger could be separated in the initial turn. On this basis, practically all MIL-E-5007C dust and 70% of AC coarse which is larger than 15 microns would be separated. The importance of the "first turn" efficiency is that most large single foreign objects should be trapped there, eliminating those objects as a source of damage to the engine and scavenge air blower.

A preliminary assessment has been made of the total pressure loss through the scroll separator, which is about 13.5 in. H₂O.

The losses can be assigned to three primary sources:

- 1. Friction throughout the system.
- 2. Turning through the inlet to the scroll.
- 3. Turning through the scroll and into the core.

The latter is both the largest and, due to a lack of directly applicable data, the most uncertain.

The inlet turn into the scroll and the turn through the scroll and into the core can be modeled as offset bends. The bends have R/d ratios which vary from 1.0 to 1.5 and duct Mach numbers which vary from 0.25 to 0.30. Friction losses can be obtained from Prandtl's universal law of friction for smooth pipes, shown in Figure 107. The losses due to turning and friction are shown broken down in Figure 108, which shows the variation of total pressure loss with percentage of flow area change. A scroll separator must be a compromise between frontal area and pressure loss since an increase in duct size tends to increase frontal area, but decreases duct Mach number and, therefore, losses. Since the airflow through the scroll and deswirl vanes is complex, a test program is required to determine reliability and the performance of this configuration.

Table 15 presents the test results for a full-scale model of a 2 lb/sec scroll separator. The configuration tested is shown in Figure 109. Pressure loss for this configuration was greater than design prediction, even though tests were run at 65% of design airflow. Separator efficiency is promising, but all pressure loss improvements in Table 15 were made at the expense of reduced separation efficiency. The loss reported in Table 15 is about 35% high due to the duct loss between the model measuring plane and the probable location of the compressor inlet.

The difference between Configurations I and V of Table 15 is the scroll separator exit/core inlet flow path shown in Figure 110.

Results of this limited scroll separator evaluation indicate that a 2 lb/sec scroll separator is a flexible aerodynamic alternative and should be considered for engines in this size range. An approximate design would be 24% larger in flow area to achieve a 5 to 8 in. H₂O pressure loss with 85-90% C-spec efficiency and 80-85% AC coarse efficiency. Efficiency improvement over the present design (Figures 104 and 109) is accomplished by pointing the inlet elbow in Figure 104 to the left (aft looking forward). Trajectory analysis and collection slot turning should bring further improvements.

TAKEN FROM SCHLICHTING, BOUNDARY LAYER THEORY
 MCGRAW-HILL BOOK COMPANY, 1968, PAGE 562

$$\Delta P/q = \lambda L/d$$

PRANDTL'S UNIVERSAL LAW OF FRICTION FOR SMOOTH PIPES
 $1/\sqrt{\lambda} = 2.0 \text{ LOG (RED } \sqrt{\lambda}) - 0.8$

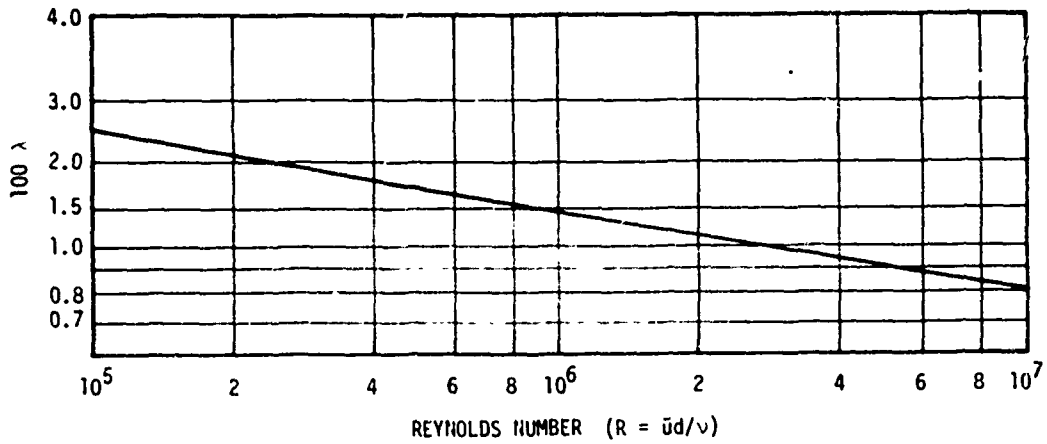


Figure 107. Frictional Resistance in a Smooth Pipe.

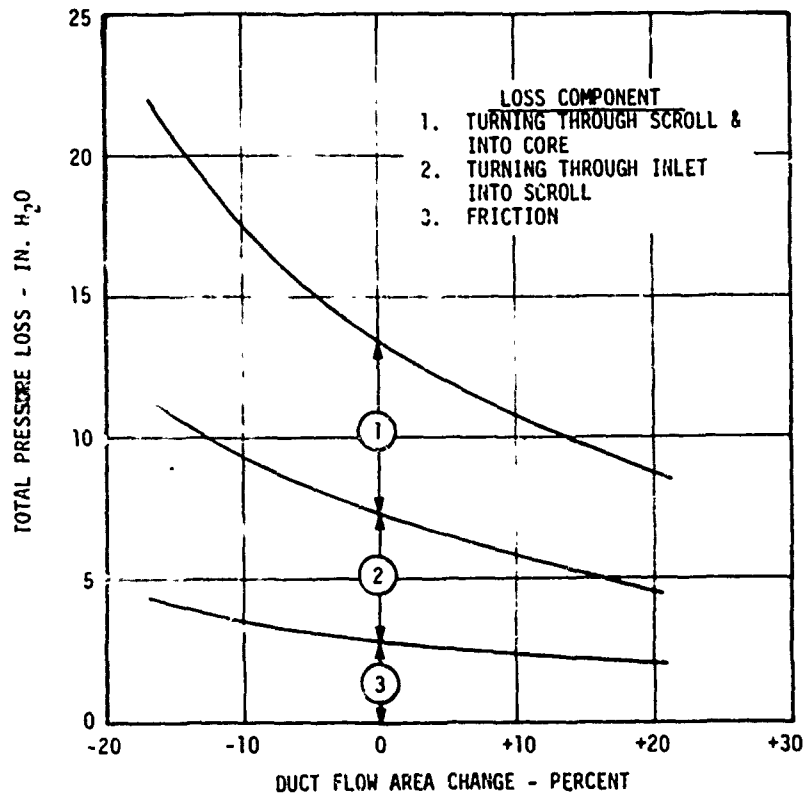


Figure 108. Scroll Separator Pressure Loss Variation With Flow Area.

TABLE 15. 2 LB/SEC SCROLL SEPARATOR TESTING SUMMARY												
Configuration	Test Point				AC Course				C-Spec			
	Core Flow (lb/sec)	Scav (%)	APt (in. H ₂ O)	Residual Swirl (Deg)	APt ¹⁰ (in. H ₂ O)	Core Flow (lb/sec)	Scav (%)	η_{sc} (%)	η_{sc} (%)	Core Flow (lb/sec)	Scav (%)	η_{sc} (%)
No. 2 LB/SEC SCROLL SEPARATOR MODIFICATIONS												
I Basic Scroll + 90° Inlet Elbow	1.31	16.7	18.8	55.0	45.2	1.30	16.5	81.1	78.0	1.29	16.0	87.0
II Basic Scroll Only	1.29	16.3	14.9	55.5	34.2	1.39	15.8	75.4	71.5	1.38	15.7	77.5
III Scroll and Elbow With Large Scavenge Vane Removed	-	-	-	-	-	1.34	16.4	71.1	64.4	1.33	16.6	77.1
IV Scroll and Elbow With Scroll Scavenge Ports Closed	-	-	-	-	-	-	-	-	-	1.32	15.9	63.6
V Configuration I With "Bathub Drain" Removal of Core Inlet	1.33	16.5	10.5	54.5	23.8	1.37	16.1	72.6	61.8	-	-	-
VI V + Cutback Scavenge Slot in Elbow	1.31	16.8	13.1	52.1	30.5	1.33	16.5	74.6	70.4	1.32	16.7	82.8

*Extrapolated to 2 lb/sec.

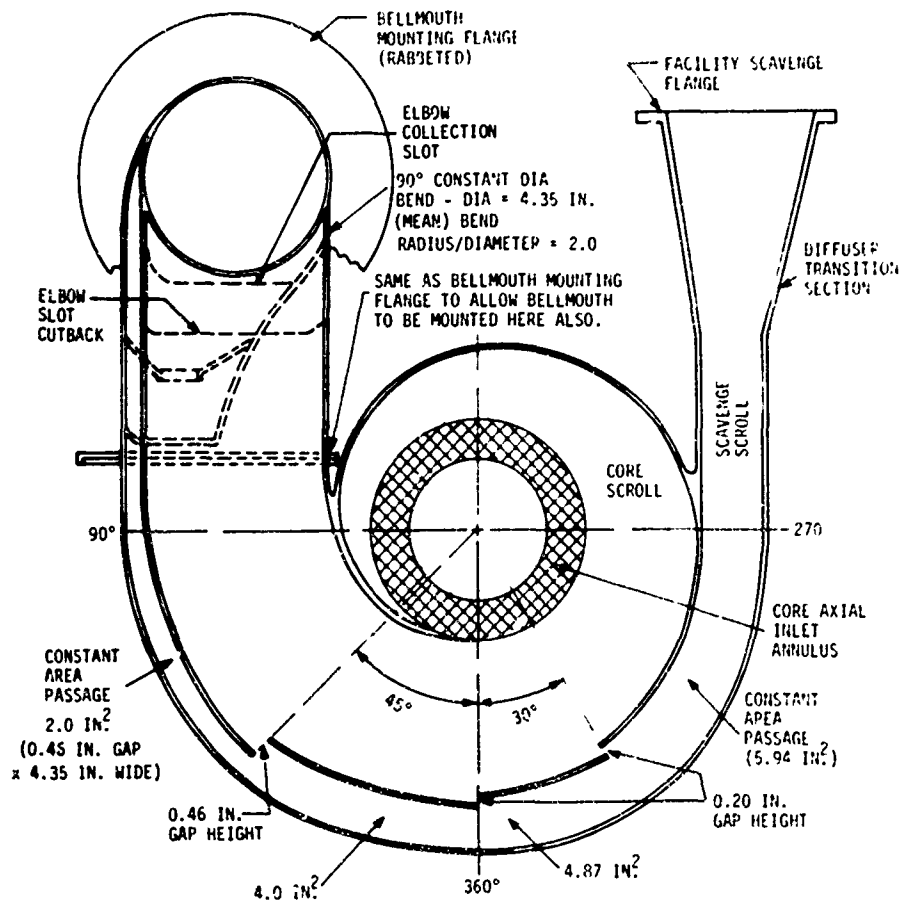


Figure 109. Scroll Separator Tested.

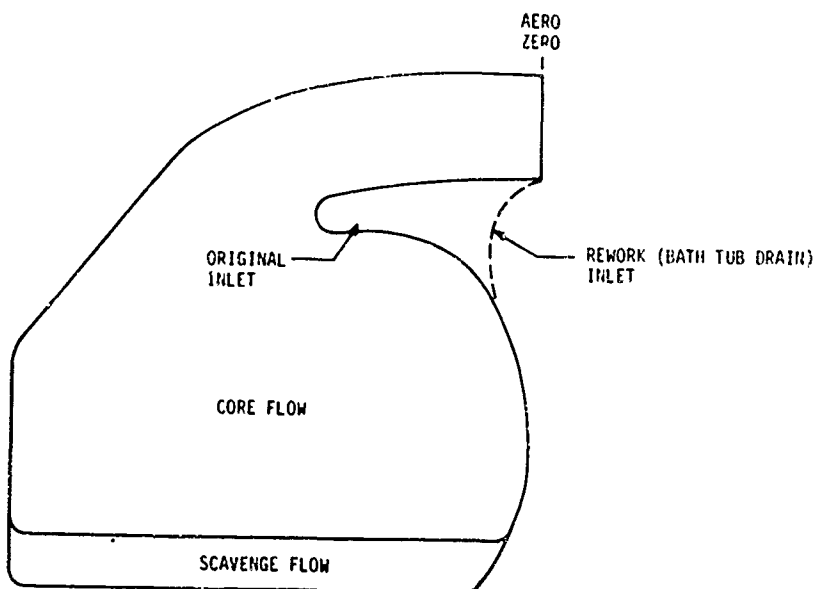


Figure 110. 2 Lb/Sec Scroll Separator Inlet Rework.

DESIGN CHECKLIST

1. Can all ingested foreign material which passes through the swirl frame also pass through the scavenge vanes and scavenge system?
2. Is vane-to-vane spacing of swirl frame small enough to prevent large objects such as birds, large ice balls, flashlights, and wrenches from entering the separator?
3. Is vane-to-vane spacing of deswirl frame smaller than that of swirl frame (to provide insurance against single large foreign objects entering the core)?
4. Can trapped objects be easily removed from swirl frame inlet, deswirl vane inlet, scavenge vane inlet?
5. Can objects be trapped only at locations cited in (4)?
6. If foliage protection is required, is foliage deflected externally, eliminating it from the internal separator-engine flow path?
7. Has a rainstep or other method of removing inner wall surface water been provided?
8. If there are compressor "wash" requirements, has the wash manifold been integrated into the separator in a way that prevents the water from being scavenged?
9. Have all fasteners such as snap rings, tab washers, rivets and lockwire, and all unnecessary obstacles such as overlaps been eliminated from the separator flow path?
10. Are vanes or struts large enough to handle service lines, anti-icing air, oil flow, and other requirements.
11. Is the scavenge blower designed for 25% excess scavenge flow to allow for deterioration in the field?
12. Has the life of the scavenge blower in its operational sandy environment been estimated? (As a minimum, these factors must be included: lubrication, drives, bearings, seals, blade erosion, and rotor blade tip clearances.)
13. Are core and scavenge losses compatible with engine performance requirements.

14. Is the separator discharge core flow field compatible with compressor and IGV entrance requirements?
15. Do calculated separation efficiencies meet engine requirements?
16. Are all engine anti-icing requirements met?
17. Is the major portion of bleed air and anti-icing air dumped into the scavenge exhaust system?
18. Are swirl vanes and inlet anti-iced satisfactorily?
19. Are scavenge vanes and casings anti-iced satisfactorily?
20. If necessary, are the deswirl vanes anti-iced satisfactorily?
21. Can compressor discharge anti-icing air be turned off?
22. Can materials in the system which is anti-iced by compressor bleed air perform adequately when there is a continuous flow of bleed air?
23. Are the oil tank and system integrated with the separator in a way that provides simultaneous oil cooling and anti-icing as much as possible?
24. Is the smallest dimension of discharge openings of all orifices or slots in the separator at least 0.031 in.?
25. Have all installation requirements been met?
26. Has separator installed (in the aircraft) performance been evaluated?
27. Has the effect of inlet distortion on separator losses been evaluated?
28. Has the effect of separator inlet distortion or compressor inlet distortion been evaluated?
29. Is separator design compatible with engine reliability, maintainability, and vulnerability requirements specified in the Prime Item Development Specification?
30. Is the separator designed so that it cannot cause an engine in-flight failure which results in loss of aircraft control, fire external to the engine, or in-flight engine shutdown?
31. Is the scavenge pump fail-safe?

32. Can the scavenge pump be inspected and changed easily?
33. Is the design sealed effectively to reduce or eliminate oil leakage around casing, anti-icing air leakage, and oil leakage at sump?
34. Will oil leaks be scavenged through the separator scavenge system?
35. Is the construction suitable to handle thermal gradients in structural parts, especially due to hot oil passing in and out of vanes?
36. Can the PTO shaft spline be withdrawn through the strut or vane opening? (Is the opening large enough for the spline?)
37. Can half the compressor casing be removed without separator disassembly?
38. Does design permit inspection of compressor first rotor without disassembly?
39. Can the integral separator be removed without interfering with the engine (compressor), particularly in 5 lb/sec or smaller sizes?
40. Can the scavenge scroll cover be easily removed for cleaning or for replacement?
41. Does the structure meet maneuver and maximum load requirements?
42. Can materials meet environment and growth requirements?
43. If the main engine thrust mounts are at the front of the engine, have satisfactory mount support been provided?
44. Can the separator structures carry maximum torque output loads for front drive PTO engines?
45. Has the possibility of overstressing parts due to bearing interferences, vane and structural loading, thermal growth, and gearing interferences been considered and eliminated?
46. Are tolerances acceptable for gearing and bearing components, vane contour, and vane angles?
47. Has the impact of manufacturing tolerances on performance been evaluated?

TEST REQUIREMENTS

TEST SPECIFICATIONS

Dust Test Specification

Test Dust Size and Distribution: Test dusts for component evaluation will be one of those listed below:

1. MIL-E-5007C Specification
2. AC Coarse
3. AC Fine
4. Special

The special dust may be combinations of the first three, or dust from a particular region where there are extensive helicopter operations in dust not adequately represented by the standard dust. Recommended test dusts are AC Coarse and MIL-E-5007C.

Dust Test: Component tests on Specification MIL-E-5007C dust will be conducted with concentrations in air of 1.5 and 15 mg/ft³ at maximum and ground idle airflows. The separation efficiency goal will be 94% based on concentration. Component tests on AC Coarse dust will also be conducted with concentrations of 1.5 and 15 mg/ft³ at maximum and ground idle airflows (and possibly an intermediate point). The separation efficiency goal on AC Coarse will be 80% based on concentration. It is expected that the separation efficiency goals will finally be set by some limiting loss in engine power and SFC over a 50-hour period.

Foliage Specification

Large amounts of foliage or birds larger than 4 ounces will be prevented from entering the separator by some sort of "cowcatcher" (Figure 21) located in front of the inlet. The cowcatcher will shunt these objects overboard. If it is used only under nonicing conditions, it will not be anti-iced. In that case it must be retractable or detachable. It will be actuated or attached to the aircraft on the ground. If the cowcatcher is used under icing conditions, it must be anti-iced. In that case, it can be permanently installed in front of the separator.

In order to verify that the foliage which gets through the cowcatcher and into the separator causes no excessive pressure drop or major damage, tests will be performed with four different types of foliage:

1. Wet swamp grass, random distribution 12-24 inches in length. (Figure 16)
2. Semidry hay, random distribution 4-15 inches in length. (Figure 17)
3. Semidry leaves, random distribution 2 to 10 in² area. (Figure 18)
4. Foliage mixture consisting of equal weights of (1), (2), and (3).

Weight of foliage to be ingested is as follows:

	Separator Size		
	2 lb/sec	5 lb/sec	15 lb/sec
Total foliage weight to be ingested - lb	.080	.080	.25
<u>+ .005 lb</u>			

Separator sizes between 5 lb/sec and 15 lb/sec should ingest an intermediate weight proportional to airflow.

In each test, the foliage will be dumped in front of the cowcatcher in 30 seconds. At the end of the test, the separator pressure drop will have increased no more than 20 in. H₂O and there will be no major damage to the separator.

Foreign Object Specification

Design: The separator will be designed to remove all foreign objects from the compressor airstream before the air enters the compressor. Foreign objects will be either removed completely by the separator or trapped within the separator.

Test: Separator component performance tests will be conducted by randomly hand feeding several single objects into the separator at maximum airflow, at the airflow corresponding to 60% power, and at idle airflow. Measured

separation efficiency will be equal to or greater than listed below:

	<u>Number Ingested</u>	<u>Collection Efficiency (%)</u>
#10 Nut, 9610M50P01 (or P08, P19, P28)	50	90
1/4-in. Nut, 9610M50P02 (or P09, P29)	50	98
#10 Bolt, J643P04 (.438 in. shank)	50	98
.032-in. PIA Lockwire, two shanks twisted together, 1-in. long	20	95
1/4-in. Socket Wrench Head	4	100
1/8-in. Allen Wrench	10	98
12-in. Rag, Cotton, Wool or Linen	4	100
Work Glove	4	100

Similar tests will be conducted by randomly placing a single object in the inlet before air is drawn through the inlet. When airflow is started and increased in the same manner as a normal engine acceleration, to maximum airflow, the object shall be separated with the efficiencies listed below. This specification applies to the following objects:

	<u>Number Ingested</u>	<u>Collection Efficiency (%)</u>
#10 Nut, 9610M50P01 (or P08, P19, P28)	10	90
1/4-in. Nut, 9610M50P02 (or P09, P29)	10	90
#10 Bolt, J643P04 (.438-in. shank)	10	90
.032-in. dia Lockwire (2 strands, 1 in. long, twisted together)	5	80
1/4-in. Socket Wrench Head	4	100
1/8-in. Allen Wrench	5	100
12-x-12-in. Rag, Cotton, Wool, or Linen	4	100
Work Glove	4	100

Similar tests will be conducted at maximum airflow by injecting one 2- to 4- ounce bird per 33 in² of frontal area into the separator. No structurally damaging remains of the birds shall pass out of the separator in the core airflow, and there can be no major damage to the separator. Similar tests will be conducted at maximum airflow by injecting one-half dozen each of 1/2-in.- and 1-in.-diameter ice balls into the separator. Any ice passing through the separator must be disintegrated, and there can be no major damage to the separator.

Rain Ingestion Specification

To determine the performance of a separator in rain, a separator will be subjected to tests in which a uniform spray is directed axially into the inlet. The average particle size will be 1 mm, and the water concentration in air will be 8%. A concentration no greater than 5% can leave the separator in the core airflow. Tests will be run at maximum airflow, ground idle, and two intermediate points. It may also be desirable to determine the water concentration at the separator inlet which results in 5% concentration at the core inlet.

Test Apparatus Specifications

A schematic diagram of a typical facility for testing inlet particle separators is shown on Figure 111. A photograph of a typical test cell is shown in Figure 112. The important elements of the test apparatus are:

1. Core airflow blowers which "pull" the core airflow through the separator.
2. Scavenge airflow blowers which "pull" scavenge airflow through the separator.
3. Orifice to measure scavenge airflow.
4. Sand feeder system including scales to weigh sand fed to separator.
5. Scavenge system including sand filter and scales to weigh scavenged sand.
6. Separator inlet airflow measuring instrumentation located in bellmouth inlet.
7. Pressure drop instrumentation behind swirl vanes, deswirl vanes, and scavenge vanes.
8. Swirl angle instrumentation behind swirl and deswirl vanes.

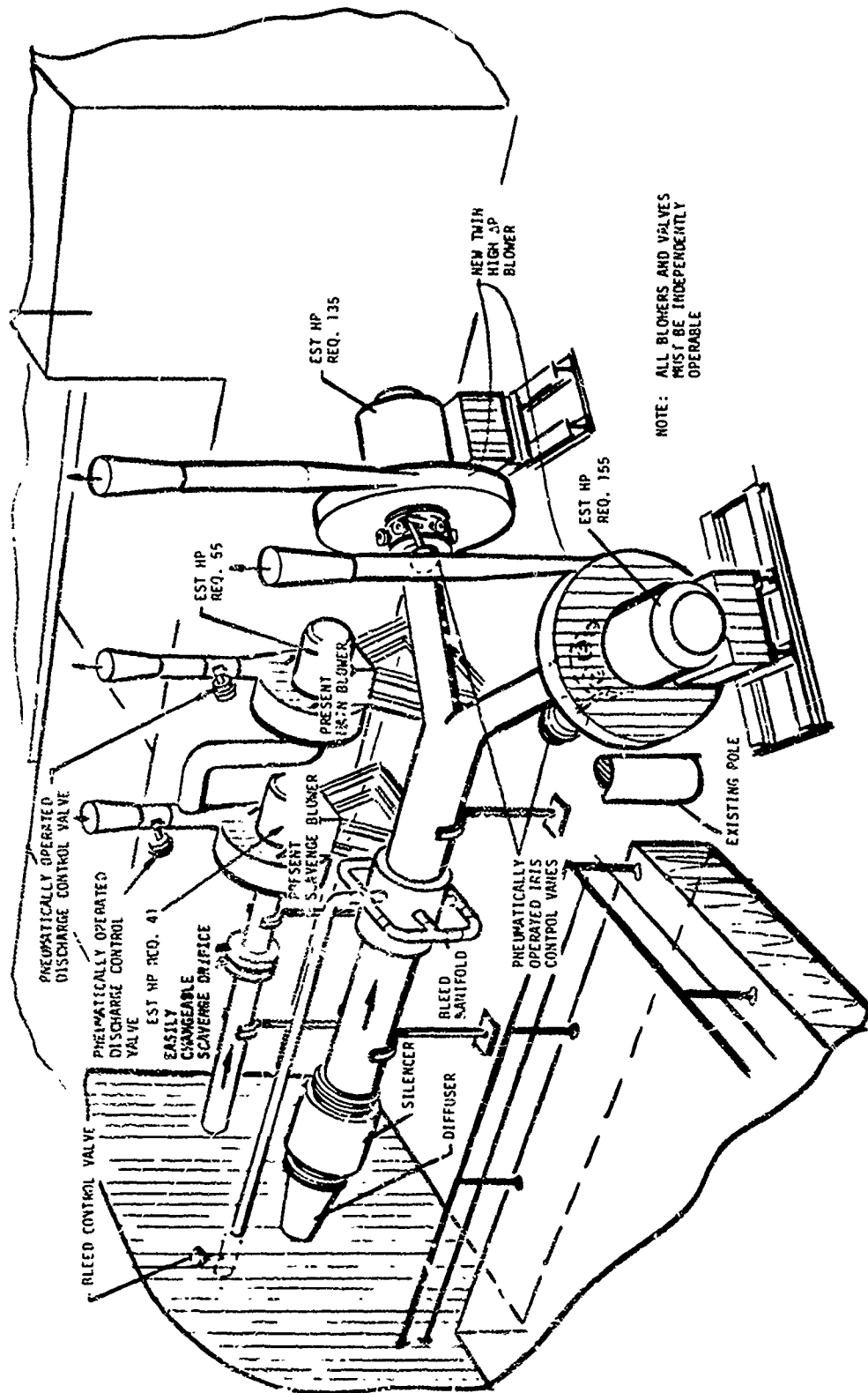


Figure 111. Schematic of Separator Facility.

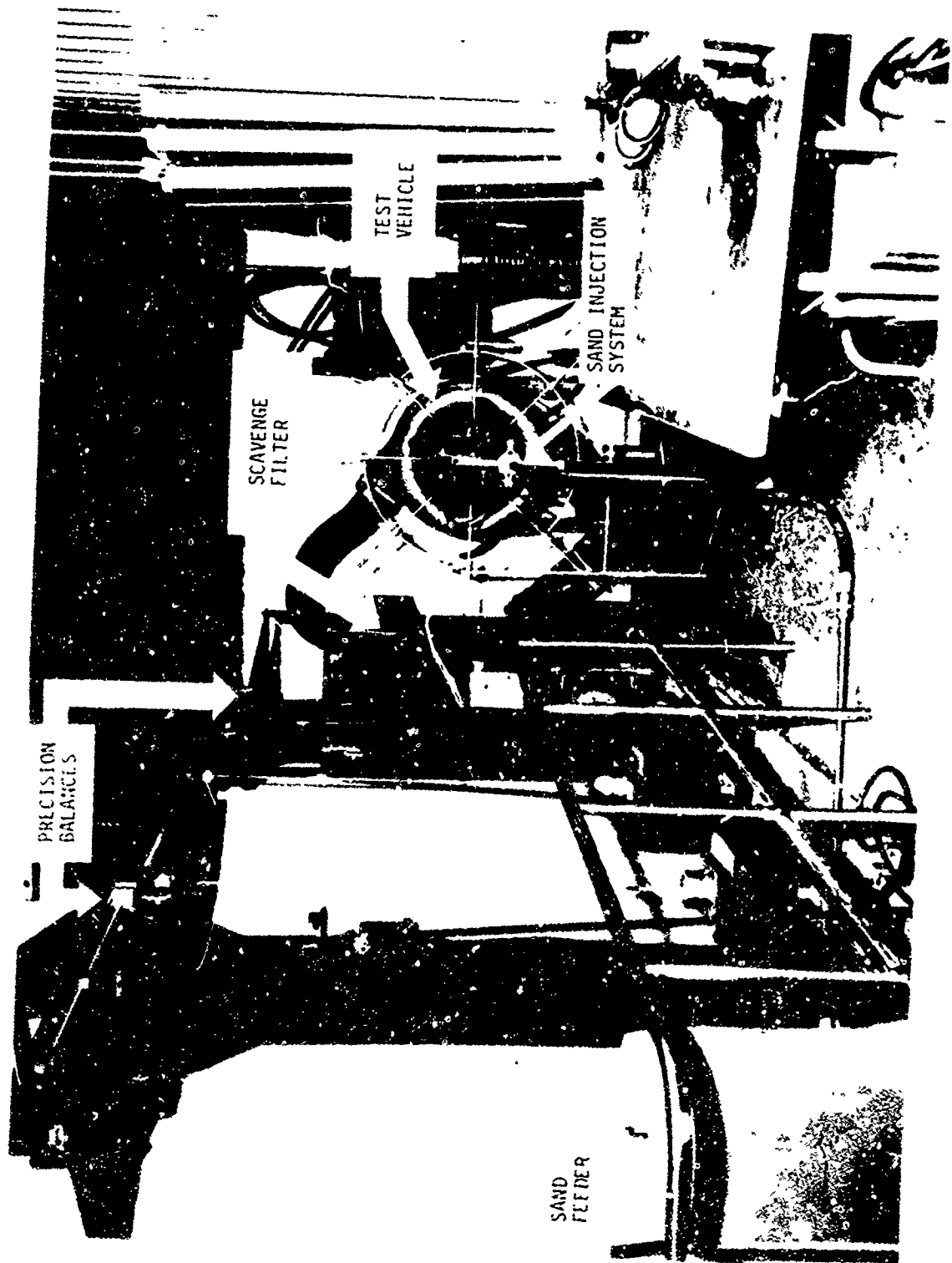


Figure 112. Inlet Separator Test Cell.

The core and scavenge airflow blowers should be capable of 20% more airflow and 50% more pressure rise than required for the separator design to assure adequate capacity at maximum and emergency power conditions. The system should permit setting any combination of core and scavenge airflow within the capability of the blowers.

The sand feeder system should be capable of delivering sand at the rate of 0.43×10^{-3} x (airflow) in order to achieve 15 mg/ft³ concentration. It should be able to deliver sand at any rate below its maximum. For a 1-hour run at 15 mg/ft³ concentration, the capacity of the feeder in pounds must be at least 1.6 x (airflow in lb/sec). In order to accurately determine the weight of sand ingested during a test, the sand feeder is weighed before and after the test. Also, the scavenge tank, which includes a filter to collect scavenged sand, is weighed before and after the test. In order to achieve $\pm 1/2\%$ accuracy in collection efficiency, it is necessary to obtain about a 1/4% accuracy in both ingested and scavenged sand weight. It is also necessary to eliminate the effect of humidity from the weight. To accomplish that, the ingested sand must be as dry as possible, and the entire test setup should be stabilized by running at test conditions without sand flow for at least a half hour before sand flow is started.

Pressure drop across the separator is important since it decreases power output and increases SFC. The integrated pressure drop can be measured with an accuracy of about ± 0.5 in. H₂O, which corresponds to about $\pm 5\%$ for 10 in. H₂O pressure drop. The pressure drop is roughly proportional to the airflow squared. Since airflow can be measured with an accuracy of about $\pm 1\%$, pressure drop accuracy is affected $\pm 2\%$ by the accuracy of setting airflow. It is also affected by inlet density, which is determined by ambient pressure (the barometer) and temperature. However, the effect of these is negligible compared to the errors incurred by integrated pressure drop measurement.

Pressure drop and collection efficiency both depend on the swirl introduced into the flow by swirl vanes. Because of its importance, angle measuring instrumentation capable of $\pm 1^\circ$ is desirable. It should be capable of radial traverse at different circumferential locations.

COMPONENT TEST

Development of a successful integral inlet separator requires that the design process be coupled with a flexible component model test program followed by an evaluation of the real engine separator hardware. A full-scale aerodynamic model of the separator should be tested before the design is frozen for manufacture into engine hardware. Component model test allows the design to be tuned to the required performance level quickly and cheaply. Model test also allows evaluation of the design details that are not amenable to analysis, such as flow path protuberances for anti-icing air, PTO assembly, and corner fillets.

Model Design

A typical separator model is shown in Figure 113. Rules for model design are:

1. The separator model should be full scale to avoid any doubt that the performance of the model represents the performance of the engine.
2. The model should be durable. Even though the model test program may be conceived as short term, the model will be used in an abrasive sand environment through many hours of testing. All separator surfaces that will experience sand impingement are preferably of the same metal as will be used in the engine design. However, aluminum is an acceptable substitute since no performance differences have been proven to be due to the sand reflection differences between aluminum and other metals. Wood is not acceptable. Because aluminum is easily cast and machined, aluminum models are very flexible for development programs. Recommended bellmouth and bulletnose materials are either hardwood or epoxy-fiberglass, both with hard, erosion-resistant coatings.
3. Separator model subassembly interfaces should be identical to engine subassembly interfaces. This allows freezing and releasing of some subassembly designs while others are still being worked on. It also allows isolation of any performance decrement in the engine hardware by interchanging engine and model subassemblies for component tests. Flexibility should be built into model subassemblies. This is the reason for the removable rings and sliding overlapping cylinders in the model of Figure 113. The rings allow the scroll vanes to be repositioned axially and circumferentially, and flow path changes can be made without extensive remachining of model interfaces.
4. The model should be aerodynamically scaled like the engine hardware. Leaks affect both separator efficiency and pressure loss.
5. Aerodynamic instrumentation provisions similar to those shown in Figure 114 are desirable. Static taps can be used to verify the aerodynamic analysis, locate flow separation points, locate the splitter lip stagnation point, and identify scroll and scavenge vane flow nonuniformities. Because of the large amount of sand that is ingested by a model, the static taps will erode and cause measurement errors. They should be checked frequently so that they can be replaced if necessary. Since the vane wakes do not mix quickly, pressure and flow angle surveys behind the vanes should cover enough representative passages with sufficient measurement density to define the vane wakes.

Reproduced from
best available copy.

INLET INNER FLOWPATH	
Z FROM HEAD"	R ₁
0.00	2.668
0.10	2.668
0.20	2.668
0.30	2.668
0.40	2.668
0.50	2.668
0.60	2.668
0.70	2.668
0.80	2.668
0.90	2.668
1.00	2.668
1.10	2.668
1.20	2.668
1.30	2.668
1.40	2.668
1.50	2.668
1.60	2.668
1.70	2.668
1.80	2.668
1.90	2.668
2.00	2.668
2.10	2.668
2.20	2.668
2.30	2.668
2.40	2.668
2.50	2.668
2.60	2.668
2.70	2.668
2.80	2.668
2.90	2.668
3.00	2.668
3.10	2.668
3.20	2.668
3.30	2.668
3.40	2.668
3.50	2.668
3.60	2.668
3.70	2.668
3.80	2.668
3.90	2.668
4.00	2.668
4.10	2.668
4.20	2.668
4.30	2.668
4.40	2.668
4.50	2.668
4.60	2.668
4.70	2.668
4.80	2.668
4.90	2.668
5.00	2.668
5.10	2.668
5.20	2.668
5.30	2.668
5.40	2.668
5.50	2.668
5.60	2.668
5.70	2.668
5.80	2.668
5.90	2.668
6.00	2.668
6.10	2.668
6.20	2.668
6.30	2.668
6.40	2.668
6.50	2.668
6.60	2.668
6.70	2.668
6.80	2.668
6.90	2.668
7.00	2.668
7.10	2.668
7.20	2.668
7.30	2.668
7.40	2.668
7.50	2.668
7.60	2.668
7.70	2.668
7.80	2.668
7.90	2.668
8.00	2.668
8.10	2.668
8.20	2.668
8.30	2.668
8.40	2.668
8.50	2.668
8.60	2.668
8.70	2.668
8.80	2.668
8.90	2.668
9.00	2.668
9.10	2.668
9.20	2.668
9.30	2.668
9.40	2.668
9.50	2.668
9.60	2.668
9.70	2.668
9.80	2.668
9.90	2.668
10.00	2.668

INLET SWIRL FLOWPATH	
Z FROM HEAD"	R ₁
0.00	2.955
0.10	2.955
0.20	2.955
0.30	2.955
0.40	2.955
0.50	2.955
0.60	2.955
0.70	2.955
0.80	2.955
0.90	2.955
1.00	2.955
1.10	2.955
1.20	2.955
1.30	2.955
1.40	2.955
1.50	2.955
1.60	2.955
1.70	2.955
1.80	2.955
1.90	2.955
2.00	2.955
2.10	2.955
2.20	2.955
2.30	2.955
2.40	2.955
2.50	2.955
2.60	2.955
2.70	2.955
2.80	2.955
2.90	2.955
3.00	2.955
3.10	2.955
3.20	2.955
3.30	2.955
3.40	2.955
3.50	2.955
3.60	2.955
3.70	2.955
3.80	2.955
3.90	2.955
4.00	2.955
4.10	2.955
4.20	2.955
4.30	2.955
4.40	2.955
4.50	2.955
4.60	2.955
4.70	2.955
4.80	2.955
4.90	2.955
5.00	2.955
5.10	2.955
5.20	2.955
5.30	2.955
5.40	2.955
5.50	2.955
5.60	2.955
5.70	2.955
5.80	2.955
5.90	2.955
6.00	2.955
6.10	2.955
6.20	2.955
6.30	2.955
6.40	2.955
6.50	2.955
6.60	2.955
6.70	2.955
6.80	2.955
6.90	2.955
7.00	2.955
7.10	2.955
7.20	2.955
7.30	2.955
7.40	2.955
7.50	2.955
7.60	2.955
7.70	2.955
7.80	2.955
7.90	2.955
8.00	2.955
8.10	2.955
8.20	2.955
8.30	2.955
8.40	2.955
8.50	2.955
8.60	2.955
8.70	2.955
8.80	2.955
8.90	2.955
9.00	2.955
9.10	2.955
9.20	2.955
9.30	2.955
9.40	2.955
9.50	2.955
9.60	2.955
9.70	2.955
9.80	2.955
9.90	2.955
10.00	2.955

INLET OUTER FLOWPATH	
Z FROM HEAD"	R ₁
0.00	3.227
0.10	3.227
0.20	3.227
0.30	3.227
0.40	3.227
0.50	3.227
0.60	3.227
0.70	3.227
0.80	3.227
0.90	3.227
1.00	3.227
1.10	3.227
1.20	3.227
1.30	3.227
1.40	3.227
1.50	3.227
1.60	3.227
1.70	3.227
1.80	3.227
1.90	3.227
2.00	3.227
2.10	3.227
2.20	3.227
2.30	3.227
2.40	3.227
2.50	3.227
2.60	3.227
2.70	3.227
2.80	3.227
2.90	3.227
3.00	3.227
3.10	3.227
3.20	3.227
3.30	3.227
3.40	3.227
3.50	3.227
3.60	3.227
3.70	3.227
3.80	3.227
3.90	3.227
4.00	3.227
4.10	3.227
4.20	3.227
4.30	3.227
4.40	3.227
4.50	3.227
4.60	3.227
4.70	3.227
4.80	3.227
4.90	3.227
5.00	3.227
5.10	3.227
5.20	3.227
5.30	3.227
5.40	3.227
5.50	3.227
5.60	3.227
5.70	3.227
5.80	3.227
5.90	3.227
6.00	3.227
6.10	3.227
6.20	3.227
6.30	3.227
6.40	3.227
6.50	3.227
6.60	3.227
6.70	3.227
6.80	3.227
6.90	3.227
7.00	3.227
7.10	3.227
7.20	3.227
7.30	3.227
7.40	3.227
7.50	3.227
7.60	3.227
7.70	3.227
7.80	3.227
7.90	3.227
8.00	3.227
8.10	3.227
8.20	3.227
8.30	3.227
8.40	3.227
8.50	3.227
8.60	3.227
8.70	3.227
8.80	3.227
8.90	3.227
9.00	3.227
9.10	3.227
9.20	3.227
9.30	3.227
9.40	3.227
9.50	3.227
9.60	3.227
9.70	3.227
9.80	3.227
9.90	3.227
10.00	3.227

INLET (R ₂) EXIT (R ₃)		
Z FROM HEAD"	R ₂	R ₃
0.00	4.44	6.56
0.10	4.44	6.56
0.20	4.44	6.56
0.30	4.44	6.56
0.40	4.44	6.56
0.50	4.44	6.56
0.60	4.44	6.56
0.70	4.44	6.56
0.80	4.44	6.56
0.90	4.44	6.56
1.00	4.44	6.56
1.10	4.44	6.56
1.20	4.44	6.56
1.30	4.44	6.56
1.40	4.44	6.56
1.50	4.44	6.56
1.60	4.44	6.56
1.70	4.44	6.56
1.80	4.44	6.56
1.90	4.44	6.56
2.00	4.44	6.56
2.10	4.44	6.56
2.20	4.44	6.56
2.30	4.44	6.56
2.40	4.44	6.56
2.50	4.44	6.56
2.60	4.44	6.56
2.70	4.44	6.56
2.80	4.44	6.56
2.90	4.44	6.56
3.00	4.44	6.56
3.10	4.44	6.56
3.20	4.44	6.56
3.30	4.44	6.56
3.40	4.44	6.56
3.50	4.44	6.56
3.60	4.44	6.56
3.70	4.44	6.56
3.80	4.44	6.56
3.90	4.44	6.56
4.00	4.44	6.56
4.10	4.44	6.56
4.20	4.44	6.56
4.30	4.44	6.56
4.40	4.44	6.56
4.50	4.44	6.56
4.60	4.44	6.56
4.70	4.44	6.56
4.80	4.44	6.56
4.90	4.44	6.56
5.00	4.44	6.56
5.10	4.44	6.56
5.20	4.44	6.56
5.30	4.44	6.56
5.40	4.44	6.56
5.50	4.44	6.56
5.60	4.44	6.56
5.70	4.44	6.56
5.80	4.44	6.56
5.90	4.44	6.56
6.00	4.44	6.56
6.10	4.44	6.56
6.20	4.44	6.56
6.30	4.44	6.56
6.40	4.44	6.56
6.50	4.44	6.56
6.60	4.44	6.56
6.70	4.44	6.56
6.80	4.44	6.56
6.90	4.44	6.56
7.00	4.44	6.56
7.10	4.44	6.56
7.20	4.44	6.56
7.30	4.44	6.56
7.40	4.44	6.56
7.50	4.44	6.56
7.60	4.44	6.56
7.70	4.44	6.56
7.80	4.44	6.56
7.90	4.44	6.56
8.00	4.44	6.56
8.10	4.44	6.56
8.20	4.44	6.56
8.30	4.44	6.56
8.40	4.44	6.56
8.50	4.44	6.56
8.60	4.44	6.56
8.70	4.44	6.56
8.80	4.44	6.56
8.90	4.44	6.56
9.00	4.44	6.56
9.10	4.44	6.56
9.20	4.44	6.56
9.30	4.44	6.56
9.40	4.44	6.56
9.50	4.44	6.56
9.60	4.44	6.56
9.70	4.44	6.56
9.80	4.44	6.56
9.90	4.44	6.56
10.00	4.44	6.56

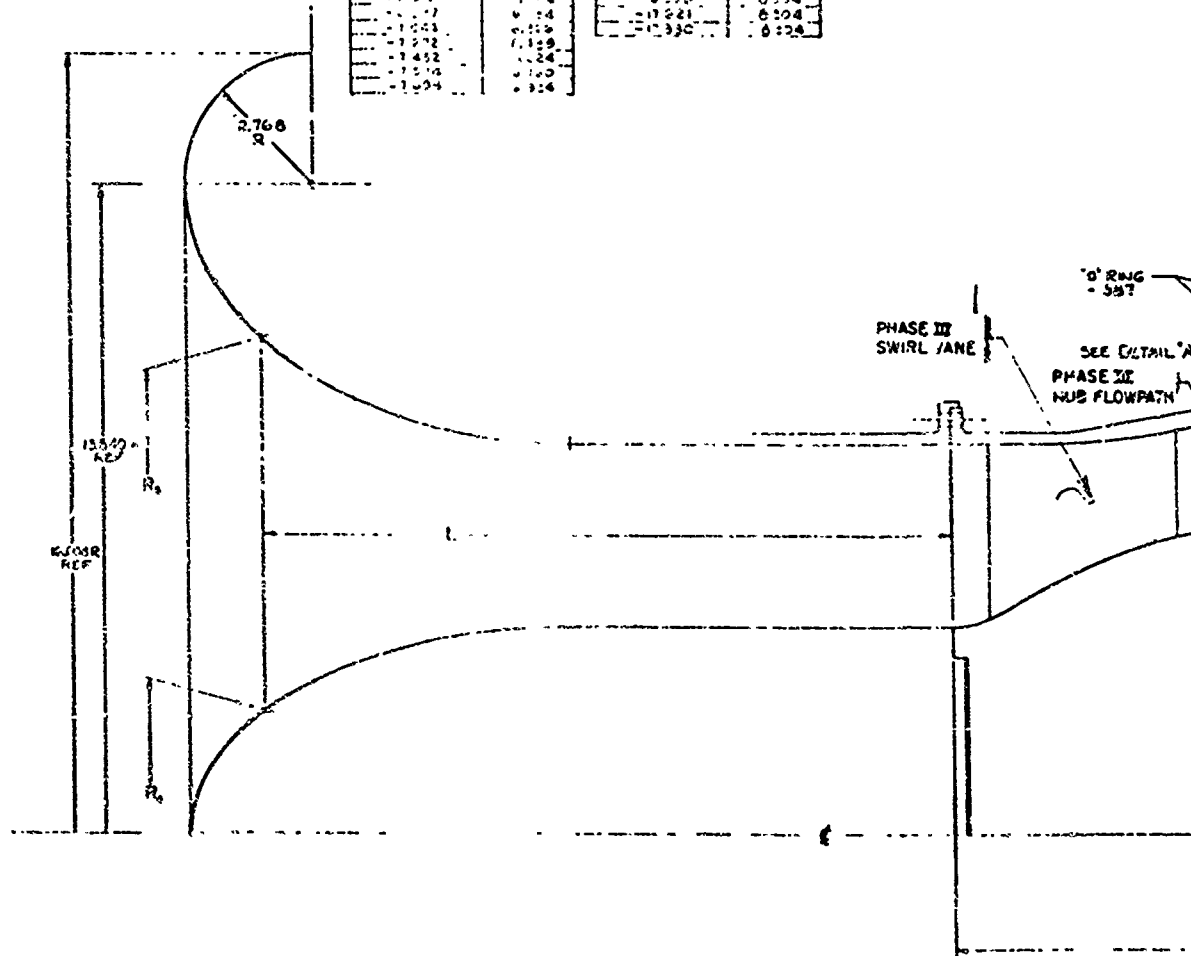
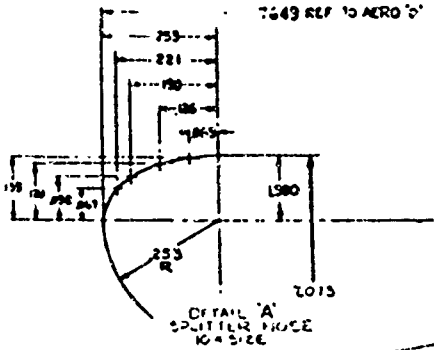


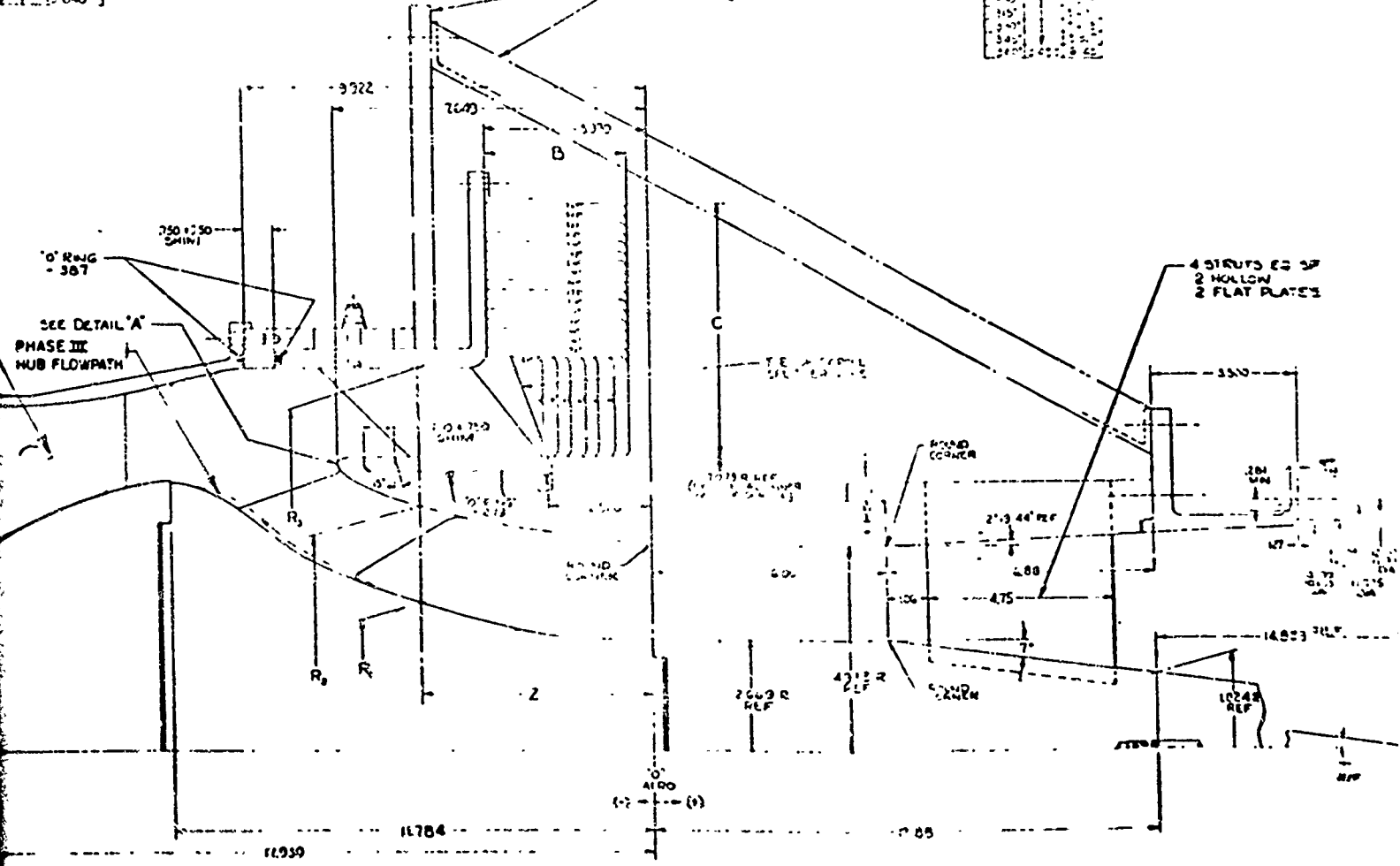
Figure 113. Cross Section of Typical Sept Model.

INCH	MILLIMETER
0.000	0.000
0.001	0.025
0.002	0.051
0.003	0.076
0.004	0.102
0.005	0.127
0.006	0.152
0.007	0.178
0.008	0.203
0.009	0.229
0.010	0.254
0.012	0.305
0.015	0.381
0.020	0.508
0.025	0.635
0.030	0.762
0.040	1.016
0.050	1.270
0.060	1.524
0.070	1.778
0.080	2.032
0.100	2.540

ANGLE	B	C
30°	1.500	2.000
45°	1.000	1.000
60°	0.500	0.866
75°	0.250	0.966
90°	0.000	1.000
105°	-0.250	0.966
120°	-0.500	0.866
135°	-0.707	0.707
150°	-0.866	0.500
165°	-0.966	0.250
180°	-1.000	0.000
195°	-0.966	-0.250
210°	-0.866	-0.500
225°	-0.707	-0.707
240°	-0.500	-0.866
255°	-0.250	-0.966
270°	0.000	-1.000
285°	0.250	-0.966
300°	0.500	-0.866
315°	0.707	-0.707
330°	0.866	-0.500
345°	0.966	-0.250
360°	1.000	0.000



ALTERNATE STRUCTURE
CIRCULAR PLATE
4 CHANNEL (OR EQUIV) 25



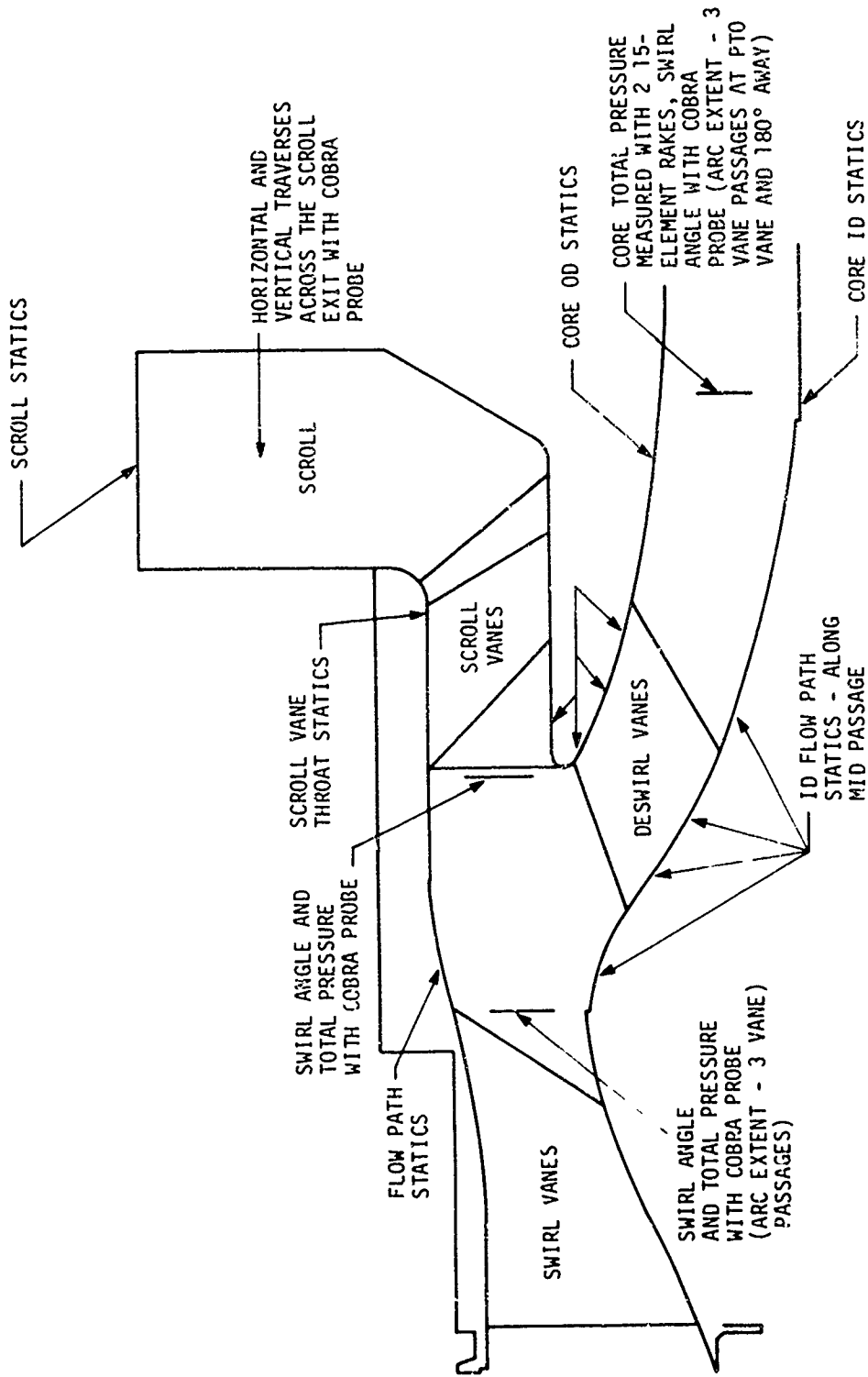


Figure 114. Separator Model Instrumentation.

Preceding page blank

One or two rakes which extend into the boundary layers and can rotate about the engine axis are recommended for the core total pressure loss measurement.

6. Glass or transparent plastic windows in the model are of limited usefulness. Both materials "frost over" almost immediately due to sand erosion. However, some qualitative understanding of the sand behavior in the separator can be gained from the use of windows if the sand is ingested preferentially so as not to impact on the windows.
7. If all sand impingement surfaces of the model are painted with 2 to 3 layers of different color paint, the paint erosion patterns can be studied to gain some understanding of the sand behavior in the separator.

Facility Design

Three different methods of generating separator airflow which have been used are blowing air into the separator, drawing air through the separator with steam ejectors, and drawing air through the separator with electrically driven blowers. It is usually preferable to draw air through the separator with electric blowers. Steam ejectors are noisy, inefficient, and expensive and require test schedule coordination with other steam users. Blowing through the separator limits test flexibility by limiting access to the separator inlet and causes the separator model to operate at unrealistic temperatures and pressures. However, blowing through the separator can be beneficial if access to the deswirl vanes during operation is desired for detailed aerodynamic probing or tuft surveys. The separator test facility should have the electrical load capability of starting all blowers simultaneously with the flow control valves set at design point airflow.

It is desirable to be able to stand next to the separator during test. For this reason, sound attenuation and personnel protection should be part of the facility design. Standing next to the separator allows probing of the flow field with tufts, and watching sand ingestion and paint erosion. Also, manual angle and pressure surveys, which are cheaper and easier to set up than automatic surveys, can be made.

Electronic data acquisition is desirable but not mandatory. Reasonable success has been achieved in operating a separator cell with a water manometer bank of forty 100-in. tubes. However, separator core flow pressure loss measured with the two 15-element rakes of Figure 114, requires that readings be taken every 2 degrees over two 60-degree annulus sectors. This means that one pressure loss test requires more than 900 total pressures. For these tests an automatic data acquisition system is desirable.

Aerodynamic Testing

Since an essentially 100% efficient filter must be included in the scavenge flow system, scavenge airflow can be measured with a standard flow meter downstream of the filter without danger of sand causing damage to the flow meter. A filter in the core airflow system, however, is usually impractical, and bellmouth rakes during sand ingestion are also impractical. For this reason, the initial aerodynamic test should be a separator inlet bellmouth calibration. This can be a bellmouth flow survey from which airflow can be calculated. The airflow can be plotted against bellmouth (including boundary layer measurement) static pressure to provide a calibration to be used in the ingestion tests. The separator flow path can influence the bellmouth flow field. A calibration should be made to account for this effect.

All flow surveys should be made at some design point that should not be varied from survey to survey. For angle and pressure surveys inside the separator, a bellmouth flow at a fixed scavenge flow ratio at the maximum power condition is convenient for data reduction. Core pressure loss data generated this way can then be corrected to a fixed core corrected airflow. Core pressure loss should also be corrected to a fixed axial reference plane like the IGV inlet plane.

Some techniques which can be used to aid in understanding separator aerodynamics are:

1. Dye traces using glycerine and coloring. Drops of the mixture are placed on the vanes and flow path; then the blowers are turned on simultaneously at design point settings. Photographs of the traces are taken after the test.
2. Handheld tuft. A wool tuft attached to a rod can be inserted into the separator while it is running. Areas of local separation and turbulence can be identified.
3. Observation of dust accumulation on the separator. Fine dust (AC Coarse or AC Fine) accumulates on surfaces adjacent to highly turbulent or separated flow regions. Photographs after the test and review of the dust patterns can point out model-to-model flow differences and problem areas.
4. Observation of ingestion tests. Dust, water and even No. 10 nuts have been observed to dwell in the separator for several seconds at the separator outer wall forward of the scroll vanes. This phenomenon is felt to be undesirable and should be closely studied if it arises. Normal particle traverse time through the separator is well under one second.

Ingestion Testing

Measurement of the separator's sand separation efficiency sounds simple and straightforward. It is not.

If the separator is to be designed for one specific aircraft installation, it is suggested that a model of the inlet area of the aircraft replace the bellmouth for sand ingestion testing. Realistic introduction of the sand to the inlet should also be used. If the separator is to be used in several different installations, a bellmouth with ingestion nozzles should be used as the "referee" ingestion test setup. This arrangement is shown in Figure 112.

For the initial ingestion tests, the swirl vanes should be painted so that sand distribution at the separator inlet can be verified. If the separator is vaneless, a coarse mesh painted screen at the separator inlet face can be used for this purpose. Do not leave the screen in for actual separation efficiency tests. It is feasible to use isokinetic sampling to verify that the sand is uniformly spread over the separator face. However, isokinetic sampling has inherent system errors when particle velocity vectors are not aligned with air velocity vectors. Another approach is to establish a standard ingestion test setup that appears to give uniformity.

The setup is not varied in any way as separator configurations are changed. Using ingestion setups similar to that pictured in Figure 112, $\pm 3.5\%$ variation in AC Coarse efficiency has been measured due to variation in nozzle radial position. A test setup similar to Figure 112, but with the nozzles in the bellmouth and pointing upstream, was found to give results different from those with the Figure 112 setup by as much as -10% on AC Coarse and $+2\%$ on C-Spec dust. Sand nozzle radial location, axial location, and nozzle-aspirator air pressure should be held the same for every ingestion test.

Sand used for ingestion tests should be analyzed to make sure it meets the particle distribution specification. For back-to-back tests to demonstrate collection efficiency improvements, the same "batch" of sand should be used. A 1.3% AC Coarse efficiency difference has been measured on the same separator using different batches of AC Coarse dust. Sand used in ingestion tests should never be reused.

A synopsis of a representative separator test procedure is:

1. Inspect the model to note the painted areas and to verify that the model meets design intent and that previous sand tests have not eroded away key areas. Eliminate any forward-facing steps in the model.

2. Set all flows including sand nozzle flow, and run the test setup for 30 - 45 minutes to stabilize the system. Note filter pressure drops and air relative humidity and temperature at the bellmouth during the test.
3. After stabilization, measure filter and sand feeder initial weights. Run the ingestion test measuring filter pressure drop, scavenge and core flows, and air relative humidity and temperature at the bellmouth during the test. Witness the test.
4. Weigh the filter and feeder immediately after shutdown and inspect the model for erosion.

Water Ingestion

Separator designs presented in this design guide are not as effective in removing water as they are in removing sand. The designs reduce the amount of water reaching the compressor, but no quantitative measure of separator efficiency on water has been made. Water removal mechanisms are:

1. Aircraft inlets accumulate water by impingement in forward flight. Without an integral separator, this water flows back along the inlet skin and eventually flows into the compressor. With the separator, the run-back water which is on the outer wall flows out the scavenge system.
2. Water impinging on the inlet and separator inner wall also flows naturally into the compressor. Even in the swirling separator field, water surface tension helps it adhere to the flow path skin as it runs through the separator. To diminish this runback, a rainstep is included on the separator inner wall. This forward-facing step, whose height is 0.040-0.070 in., breaks the water adherence to the skin. Droplets are then formed and are centrifuged to the scavenge system by the swirling flow field.
3. Some airborne water droplets are centrifuged out in the same manner as sand particles.
4. Some airborne water droplets impinge on the swirl vanes, coalesce into larger drops and peel off the swirl vane trailing edge into the scavenge system.
5. Turboshaft engines may ingest "slugs" of water similar in nature to a cup or bucket full of water. The separator swirl vanes and the flow velocity variation across the annulus tend to break up the slug of water, and part of the water slug is separated. These effects lessen the shock to the compressor of ingesting a large slug of water. However, all of the water cannot be separated. If conditions

leading to the ingestion of large slugs of water are expected, engine tests should be conducted to verify that the engine can recover satisfactorily from a representative slug of water.

REFERENCES

1. Bianchini, G. V., T63 ENGINE SAND AND DUST TOLERANCE, Proceedings of the Sixth Annual National Conference on Environmental Effects on Aircraft and Propulsion Systems, D. A. Wysaki, Ed (1966).
2. Bergman, P.A., EROSION TESTS OF COMPRESSOR ALLOYS AND COATINGS FOR AIRCRAFT GAS TURBINE APPLICATIONS, General Electric Report, R67FPD34 (1967).
3. Goodwin, J.E., RIG DEVELOPMENT AND INVESTIGATION OF VELOCITY EFFECT ON SAND EROSION, National Gas Turbine Establishment Note No. NT698, Ministry of Technology, London, England, May 1968.
4. McAnally, W.J., III, and Schilling, M.T., INVESTIGATION OF FEASIBILITY OF INTEGRAL GAS TURBINE ENGINE SOLID PARTICLE INLET SEPARATORS, PHASE I, FEASIBILITY STUDY AND DESIGN, Pratt and Whitney Aircraft; USAAVLABS Technical Report 70-44, U.S. Army Aviation Materiel Laboratories, Fort Eustis, Virginia, August 1970, AD 875 953.
5. McAnally, W.J., III, and Schilling, M.T., INVESTIGATION OF FEASIBILITY OF INTEGRAL GAS TURBINE ENGINE SOLID PARTICLE INLET SEPARATORS, PHASE II, FEASIBILITY DEMONSTRATION, Pratt and Whitney Aircraft; USAAVLABS Technical Report 71-13, Eustis Directorate, U.S. Army Air Mobility R&D Laboratory, Fort Eustis, Virginia, April 1971, AD 725 593.
6. Duffy, R.J., DESIGN AND COMPONENT TEST OF ENGINE AIR INLET PARTICLE SEPARATOR FOR THE CV-7A AIRCRAFT, General Electric Company; Laboratories, Fort Eustis, Virginia, August 1968, AD 678 493.
7. Lachmann, G.V., Editor, BOUNDARY LAYER AND FLOW CONTROL - ITS PRINCIPLES AND APPLICATION, Vol. 1. Pergamon Press, 1961, pp 265 - 294.
8. Smith, L.H., Jr., THE RADIAL EQUILIBRIUM EQUATION OF TURBOMACHINERY ASME Paper No. 65-WA/GTP-1, American Society of Mechanical Engineers, 1965.
9. COMPUTATION OF TURBULENT BOUNDARY LAYERS, Vol I and II, Conference on Computation of Turbulent Boundary Layers, Stanford University, 1968.
10. Stratford, B.S., THE PREDICTION OF SEPARATION OF THE TURBULENT BOUNDARY LAYER, Journal of Fluid Mechanics, Vol 5, Para 1, January 1959.

REFERENCES -- Continued

11. AERODYNAMIC DESIGN OF AXIAL-FLOW COMPRESSORS, Revised, NASA N65-23345-362, 1965.
12. Smiltzer, C.E., Gulden, M.E., McElmury, S.S., and Compton, W.A., MECHANISMS OF SAND AND DUST EROSION IN GAS TURBINE ENGINES, Solar Division of International Harvester Company; USAAVLABS Technical Report 70-36, U.S. Army Aviation Materiel Laboratories, Fort Eustis, Virginia, August 1970 AD 876 584.
13. ENGINES, AIRCRAFT, TURBOJET AND TURBOFAN, GENERAL SPECIFICATION FOR; Military Specification MIL-E-5007C, October 1966.
14. Montgomery, J.E., and Clark, J.M., Jr., DUST EROSION PARAMETERS FOR A GAS TURBINE, SAE Paper 538A, June 1962.
15. Bianchini, G.E., and Koschmann, R.B., T63 ENGINE SAND AND DUST TOLERANCE, Allison Division of General Motors; September 1966.
16. Page, D.M., CH-3C/T58-1 YUMA SAND SAMPLING EVALUATION, General Electric Company, Report No. TM64SE1395, November 1964.
17. Colussy, B.A., CH-46A/T58 SAND EROSION TESTS AT PATUXENT RIVER NATC - SAND SAMPLING TESTS (PHASE IV), General Electric Company, Report No. TM64SE210, September 1964.
18. Watjen, E.A., AMOUNT OF DUST RE-CIRCULATED BY A HOVERING HELICOPTER The Kaman Aircraft Corporation, Report No. R-169, December 1956.
19. Grimston, R.A., Preliminary Sand Sampling Information for Issue at Meeting to be held at Ministry of Aviation on 14th December 1964, Company Affiliation unknown, Report Number unknown, December 1964.
20. Rodgers, S.J., EVALUATION OF THE DUST CLOUD GENERATED BY HELICOPTER ROTOR DOWNWASH, MSA Research Corporation; USAAVLABS Technical Report 67-81, U.S. Army Aviation Materiel Laboratories, Fort Eustis, Virginia, March 1968, AD669 676.
21. Pauly, J., THE DUST ENVIRONMENT AND ITS EFFECT ON DUST PENETRATION, Southwest Research Institute; WADC Technical Report 56-556, Wright Air Development Center, Wright-Patterson Air Force Base, Ohio, September 1956, AS 110 472.
22. Authors Unknown, Title Unknown, Report No. CPL-70-1063, Bell Helicopter Company, Fort Worth, Texas, July 1970.

REFERENCES - Continued

23. Proceedings of the Seventh Annual National Conference on Environmental Effects on Aircraft and Propulsion Systems, September 1967.
24. Nye, J.L., SAND SAMPLE COMPARISON, Report No. TM66SE2702, General Electric Company, Lynn, Massachusetts, July 1966.
25. Engelhardt, R.E., and Knebel, G.W., CHARACTERISTICS OF THE DUST ENVIRONMENT IN THE VICINITY OF MILITARY ACTIVITIES, Southwest Research Institute, Report No. AR-642, U.S. Army Mobility Equipment Research and Development Center, Fort Belvoir, Virginia, January 1968, AD 665 439.
26. Proceedings of the Ninth Annual National Conference on Environmental Effects on Aircraft and Propulsion Systems, 1969.
27. Hafer, C.A., and Skinner, D.J., DEFINITION OF THE DUST ENVIRONMENT FOR PURPOSES OF GAS TURBINE INGESTION STUDIES - PHASE I, SWRI Report No. EE-387, Southwest Research Institute, San Antonio, Texas, October 1960, AD 472 676.
28. Hanlon, J.P., T58 RELIABILITY AND MAINTAINABILITY - SUMMARY REPORT, General Electric Company, TIS Report No. R71AEG2, December 1970.
29. Brown, L.J., and Cohen, D.T., T64 RELIABILITY AND MAINTAINABILITY - SUMMARY REPORT, General Electric Company, TIS Report No. R70AEG17, July 1970.
30. SUMMARY OF JET ENGINES REPORTED DAMAGED BY FOREIGN OBJECTS FOR PERIOD JUNE THROUGH NOVEMBER 1963, Report Number Unknown, Naval Air Technical Services Facility, Philadelphia, Pennsylvania, Date Unknown.
31. Letter from Commanding Officer, Naval Air Technical Services Facility to Commander, Naval Air Systems Command (AIR-4113), dated 21 March 1968, Subject: "Information Concerning Foreign Object Damaged Jet Engines; forwarding of".
32. Letter from Commanding Officer, Naval Air Technical Services Facility to Commander, Naval Air Systems Command (AIR-4113), dated 16 August 1968, Subject: "Information Concerning Foreign Object Damaged Jet Engines; forwarding of."
33. Letter from Commanding Officer, Naval Air Technical Services Facility to Commander, Naval Air Systems Command (AIR-4113), dated 26 March 1969, Subject: "Information Concerning Foreign Object Damaged Gas Turbine Engines: forwarding of."

REFERENCES - Continued

34. Letter from Commanding Officer, Naval Air Technical Services Facility to Commander, Naval Air Systems Command (AIR-4113), dated 2 July 1969, Subject: "Information Concerning Foreign Object Damaged Gas Turbine Engines: forwarding of."
35. Letter from Commanding Officer, Naval Air Technical Services Facility to Chief of Naval Operations (OP-514), Department of the Navy, Washington D.C. 20350, dated 13 April 1970, Subject: "Information Concerning Foreign Object Damaged Gas Turbine Engines, January 1969 through June 1969: forwarding of."
36. Letter from Commanding Officer, Naval Air Technical Services Facility to Chief of Naval Operations (OP-514), Department of the Navy, Washington, D.C. 20350, dated 10 November 1970. Subject: "Information Concerning Foreign Object Damaged Gas Turbine Engines, July 1969 through December 1969: forwarding of."
37. Letter from Commanding Officer, Naval Air Technical Services Facility to Chief of Naval Operations (OP-514), Department of the Navy, Washington, D.C. 20350, dated 14 January 1972. Subject: "Foreign Object Damaged (FOD) Gas Turbine Engines, Information Concerning; forwarding of."
38. Petach, A., A SUMMARY OF AIRCRAFT ICING CRITERIA, The Boeing Company, Vertol Division, NATTS-ATL-SP-4, U.S. Naval Air Turbine Test Station, Trenton, New Jersey, September 1963.
39. Binckley, E.T., SOME EXPERIENCES IN ARTIFICIAL ICING, Wright-Patterson AFB, NATTS-ATL-SP-4, U.S. Naval Air Turbine Test Station, Trenton, New Jersey, September 1963.
40. Mueller, E.A., and Sims, A.L., LIQUID WATER CONTENT OF RAIN, Illinois State Water Survey, Paper 64-ENV-9 published in the Proceedings of the Fourth Annual National Conference on Environmental Effects on Aircraft and Propulsion Systems, 1964.
41. Schumacher, P.W.J., FREE WATER AT HIGH ALTITUDES, Wright-Patterson, AFB, NATTS-ATL-SP-4, U.S. Naval Air Turbine Test Station, Trenton, New Jersey, September 1963.
42. Doubleday, L.C., A PROPOSED STANDARD FOR ALL WEATHER TESTING, Naval Air Engineering Center, Paper 64-ENV-8 published in the Proceedings of the Fourth Annual National Conference on Environmental Effects on Aircraft and Propulsion Systems, 1964.

REFERENCES - Continued

43. Shirck, L.C., T58-8 COMPRESSOR INLET RAIN INVESTIGATION TEST, General Electric Company, Technical Memorandum TM65S2-1829, August 1965.
44. Warwick, W.R., EFFECT OF WATER INGESTION ON J79-GE-8 ALTITUDE PERFORMANCE, U.S. Naval Air Turbine Test Station, NATTS-ATL-SP-4, U.S. Naval Air Turbine Test Station, Trenton, New Jersey, September 1963.
45. Connors, H.D., WATER INGESTION CAPABILITIES OF LYCOMING T53 AND T55 GAS TURBINE ENGINES, Avco Corporation, Lycoming Division, NATTS-ATL-SP-4 U.S. Naval Air Turbine Test Station, Trenton, New Jersey, September 1963.
46. Zenz, F.A., and Othmer, D.F., FLUIDIZATION AND FLUID PARTICLE SYSTEMS, Reinhold Publishing Corp., New York, 1960.
47. Schlichting, H., BOUNDARY LAYER THEORY, McGraw-Hill, New York, 1968.
48. Carlson, D.J., and Hoglund, R.F., PARTICLE DRAG AND HEAT TRANSFER IN ROCKET NOZZLES, AIAA Journal, Vol. 2, No. 11, p 1980, 1964.
49. Hoerner, S.F., FLUID DYNAMIC DRAG, published by the Author, 1958.
50. Tabakoff, W., Grant, G., and Ball, R., AN EXPERIMENTAL STUDY OF THE EROSION REBOUND CHARACTERISTICS OF HIGH SPEED PARTICLES IMPACTING A STATIONARY SPECIMEN, Department of Aerospace Engineering, University of Cincinnati, Report No. 73-36 May 1973

APPENDIX A

IMPORTANT ELEMENTS OF THE HELICOPTER ENGINE ENVIRONMENT

ENGINE DAMAGE MECHANISMS

Impact

The damage caused to an engine by the ingestion of single foreign objects or distribute material such as sand or water depends primarily on the change in kinetic energy of the individual impacting objects, the number of impacts, material properties, and the ability of the impacting particle to maintain its "shape" during the collision.

A large single foreign object such as a wrench, bolt, or stone ingested by an engine compressor is extremely damaging because it is heavy, has very high kinetic energy with respect to the rotor, and is not easily deformed. Ingestion of these kinds of objects almost always causes engine failure and premature engine overhaul. Birds and chunks of ice are somewhat less harmful because they are more easily deformed. However, their large mass may also lead to massive engine damage. Therefore, it is most important, when designing an engine inlet protective device, to provide for complete protection from large single foreign objects.

Erosion

When a distribution of particles such as dust or rain is ingested by an engine, each impact of a particle, with kinetic energy greater than a "threshold" value, removes a small bit of the target. The way that this erosion takes place depends on the material characteristics of the target and on the kinetic energy, impingement angle, and material characteristics of the particle. A brittle target material like glass develops increasing internal stresses as it is bombarded by great numbers of particles, until the stress reaches the critical value at which the target starts to break up. Ductile metallic targets also develop internal stresses as the result of continual bombardment by small particles. It is generally accepted that high-velocity water droplets (developed by cavitation or by rain on high-speed aircraft) work-harden metals, developing high internal stresses which make them brittle and then gradually break them up. The erosion of metal by hard particles is much greater than by nonrigid particles like water because more of their kinetic energy is transferred to the target. It appears¹² that heat is generated in the target, as the result of impacts by hard particles, which melt a small bit of the target. Then part of the melted metal escapes ("erodes") into the airstream. If the particle impacts the target at an angle, the shearing effect of the particle also contributes

to erosion of the target. The removal of sand and dust from engine airflow is very important for aircraft operating in a sandy environment. Engine life and performance are both affected detrimentally by their presence in the engine airflow.

Flow Path Blockage

If foliage, rags, birds or similar objects are ingested by an engine, the entire inlet or a portion of it is usually blocked. If the engine airflow is cut off by blockage, the engine shuts down probably by a stall, and is not operable until the debris is removed. If the inlet is partially blocked, the distortion level at the compressor inlet increases, probably causing stalls which also lead to engine shutdown. Flow path blockage by foliage, rags or other ground debris is undesirable but does not normally cause appreciable engine damage, and the engine shutdown which it causes is likely to occur on or near the ground.

Birds, on the other hand, may cause mechanical damage and also block the engine airflow. They are a serious problem for aircraft engines, since they are normally ingested in flight and can be expected to at least shut down an engine. Therefore, it is doubly important to provide complete protection from bird ingestion in the design of engine inlet protection devices. Complete protection against foliage is more difficult and less important, so there is more room for a trade-off between foliage separation efficiency, cost, and the resulting mechanical complexity.

Water Damage

Excessive water ingestion can cause loss of engine power, compressor stalls, or flameouts. It can also cause mechanical damage because it tends to collect on the compressor and turbine casings, causing them to shrink with respect to the rotor and resulting in tip rubs. When the engine later operates under normal conditions, tip clearances are increased and performance has deteriorated. However, clear water is not damaging unless it is ingested in large quantities. Military Specification MIL-E-5007C¹³ requires engines to operate throughout the flight envelope at water levels up to 5% of the engine airflow. An engine inlet protection device should be designed to collect all water in excess of 5%.

Salt water is damaging because of corrosion. The engines of aircraft operating in salt water environment should be protected against corrosion by choice of materials (metallurgy), by cleaning or washing the engine, and by removing as much water as possible. A particle separator should not be expected to solve the corrosion problem, but attention paid to water removal in its design will result in reduced corrosion.

SAND AND DUST EROSION

Concentration

The mass eroded from a target is proportional to particle concentration, and engine life¹⁴ and power¹⁵ decrease as mass is eroded from the engine flow path. Because of the importance of sand and dust concentration, representative values of this factor are presented in Figures A-1 through A-6. The concentration data were obtained from various helicopters at different altitudes by isokinetic sampling at the engine inlet^{16, 17} near the blade root and on the cabin roof^{18, 19} and over the right rear wheel.^{18, 20} Also included on each plot is the current concentration test specification from Military Specification MIL-E-5007C. In these figures the data are erratic from one flight test to another and show essentially no consistency with respect to sampling location. However, in spite of this data scatter, results exhibit a tendency toward reduced concentration at higher altitudes. Also, in nearly all cases, the concentration encountered exceeds the current test specification value by a considerable margin, regardless of where measured on the vehicle or of the operational altitude of the aircraft up to 75 feet. As a basis for comparison, Figure A-6 shows the concentration measured in a dust storm.²¹ The yield data shown in Figures A-1 through A-5 indicate that sand concentration is adequately bracketed by the MIL-E-5007C test specification concentration and a concentration of about 15 mg/ft³.

Size Distribution

Particle size distributions for several dust samples are shown on Figures A-7 through A-14. Figures A-7, A-8, and A-9 are terrain samples. Figures A-10 through A-13 are distributions under various operating conditions. Figure A-14 shows the standard distributions.

Figure A-7 shows soil size data for the Near East.^{21, 22} Figure A-8 shows the same type of data for various locations in the United States.^{23, 24, 25} Figure A-9 shows similar information from Southeast Asia.^{22, 23, 24, 26} These three figures indicate that there is a striking similarity in the particle size distribution of soils from widely separated areas of the globe. The majority of terrain particles are sized between 100 and 2000 microns.

When the terrain particles are disturbed or stirred up, the distributions shown on Figures A-7 through A-9 are no longer representative of the aircraft's environment. Figures A-10 through A-12 illustrate this phenomenon for a helicopter hovering at three different heights over three different locales.²⁰ These figures indicate that as altitude increases, the composition of the dust becomes finer. These differences can be significant. For example, Figures A-10 and A-12 show that 10 percent of the surface soil is smaller than 100 microns, but 75 feet from the ground, 70-80 percent of the dust is smaller than 100 microns.

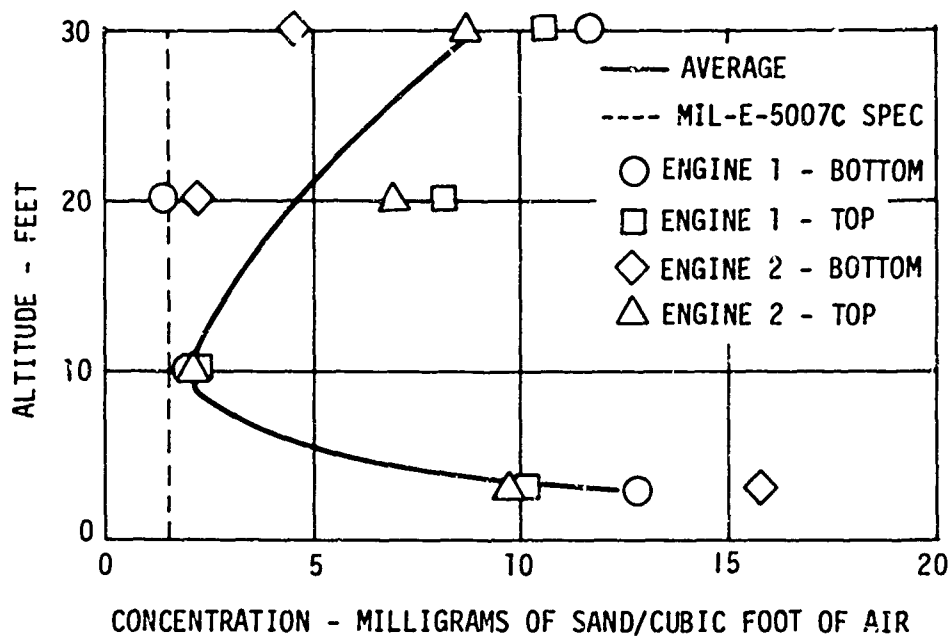


Figure A-1. Engine Inlet Sand Concentration CH-3C (Single Rotor) - MCAS, Yuma, Arizona.

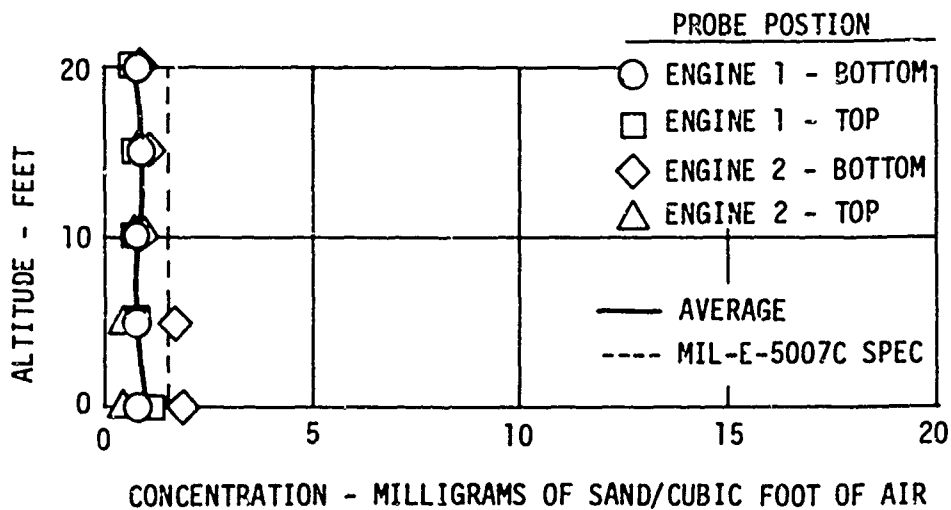


Figure A-2. Engine Inlet Sand Concentration - CH46A (Tandem Rotor) - Patuxent River NATC.

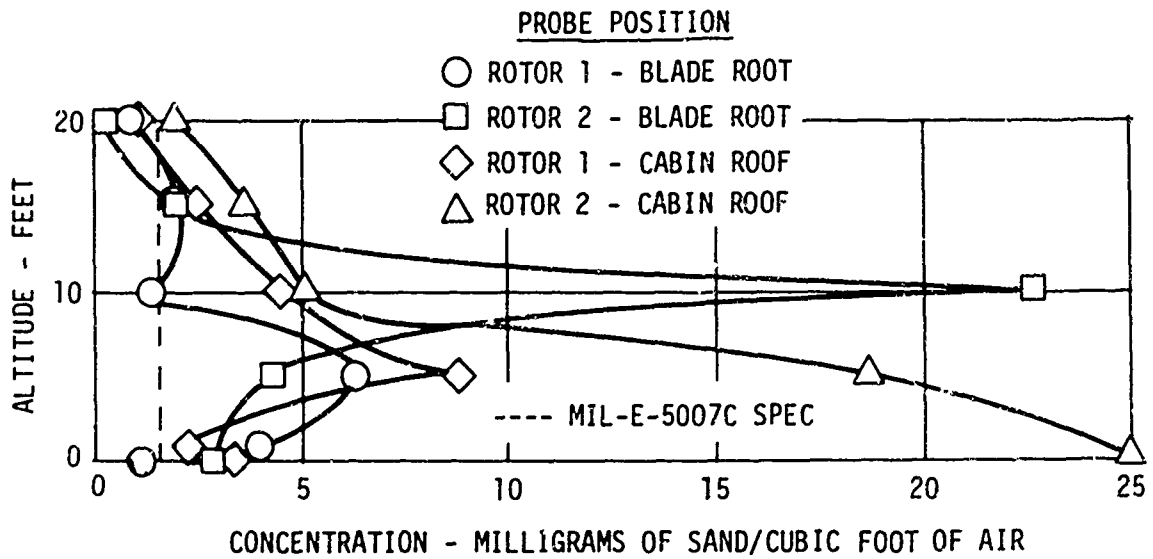


Figure A-3. Aircraft Cabin Roof Sand Concentration - HTK (Dual Rotor) - Test Site Unknown.

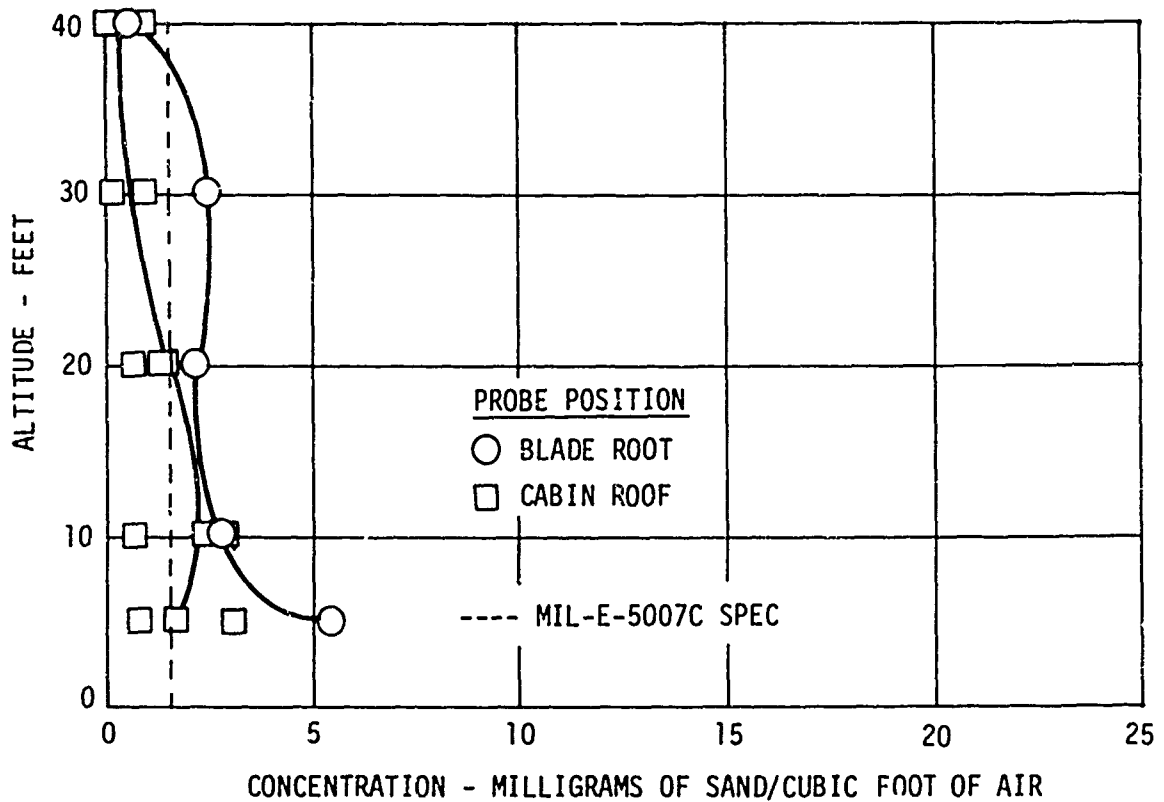


Figure A-4. Aircraft Cabin Roof Sand Concentration - Wesser (Single Rotor) - Ghibli, North Africa.

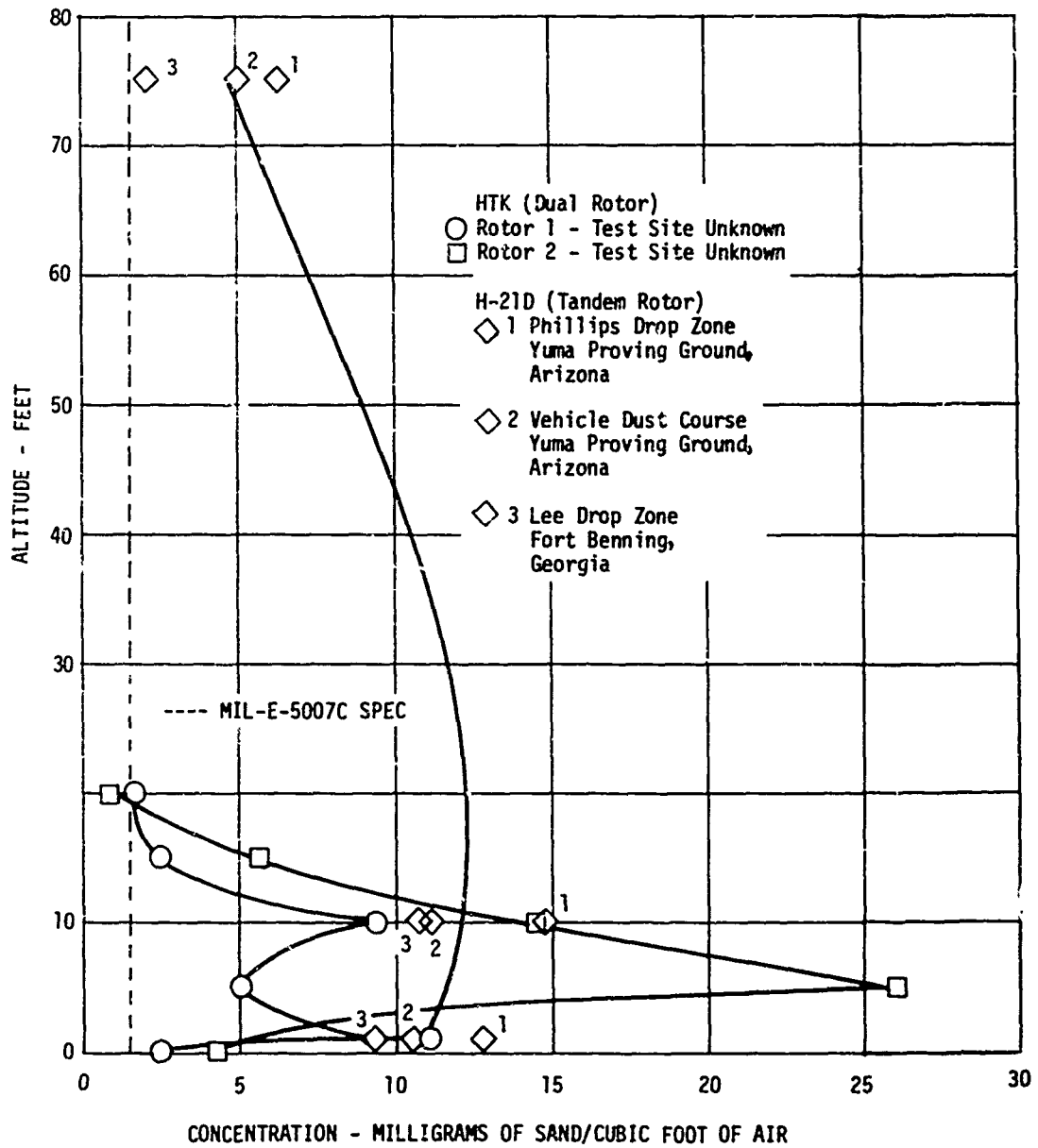


Figure A-5. Aircraft Right Rear Wheel Sand Concentration.

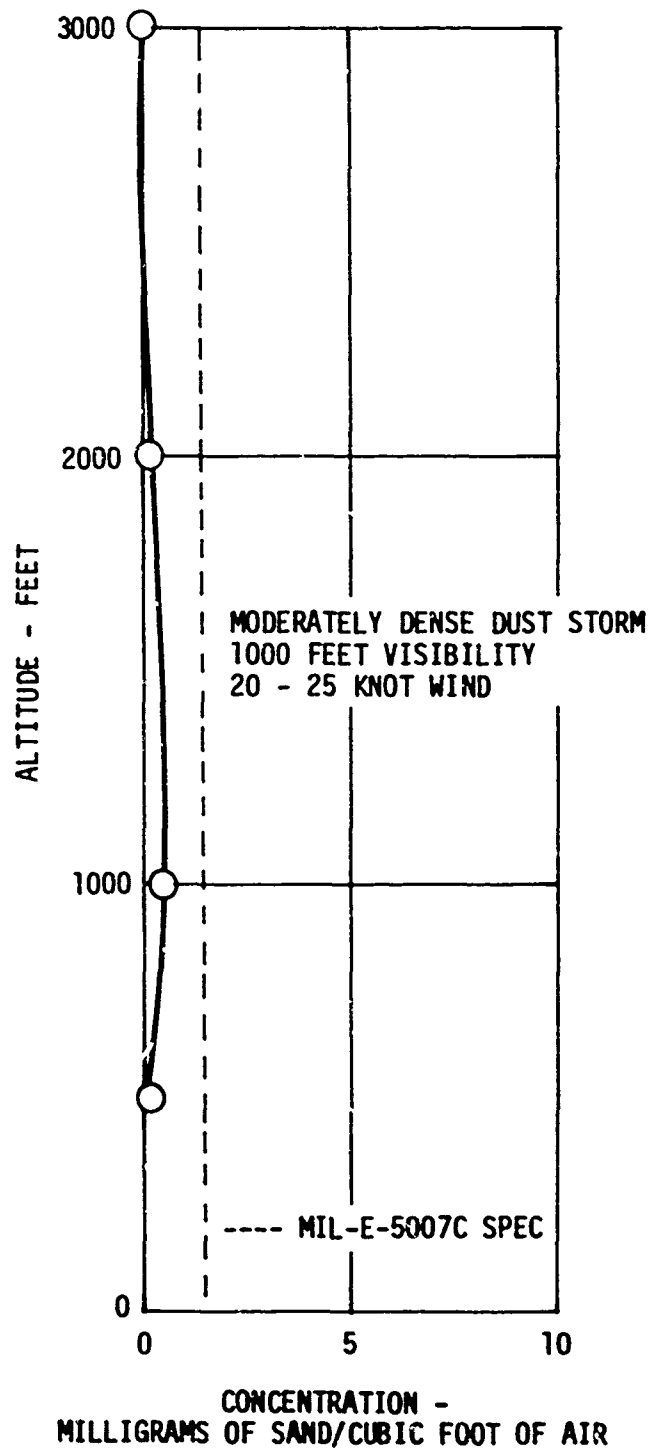


Figure A-6. Sand Concentration - Australia.

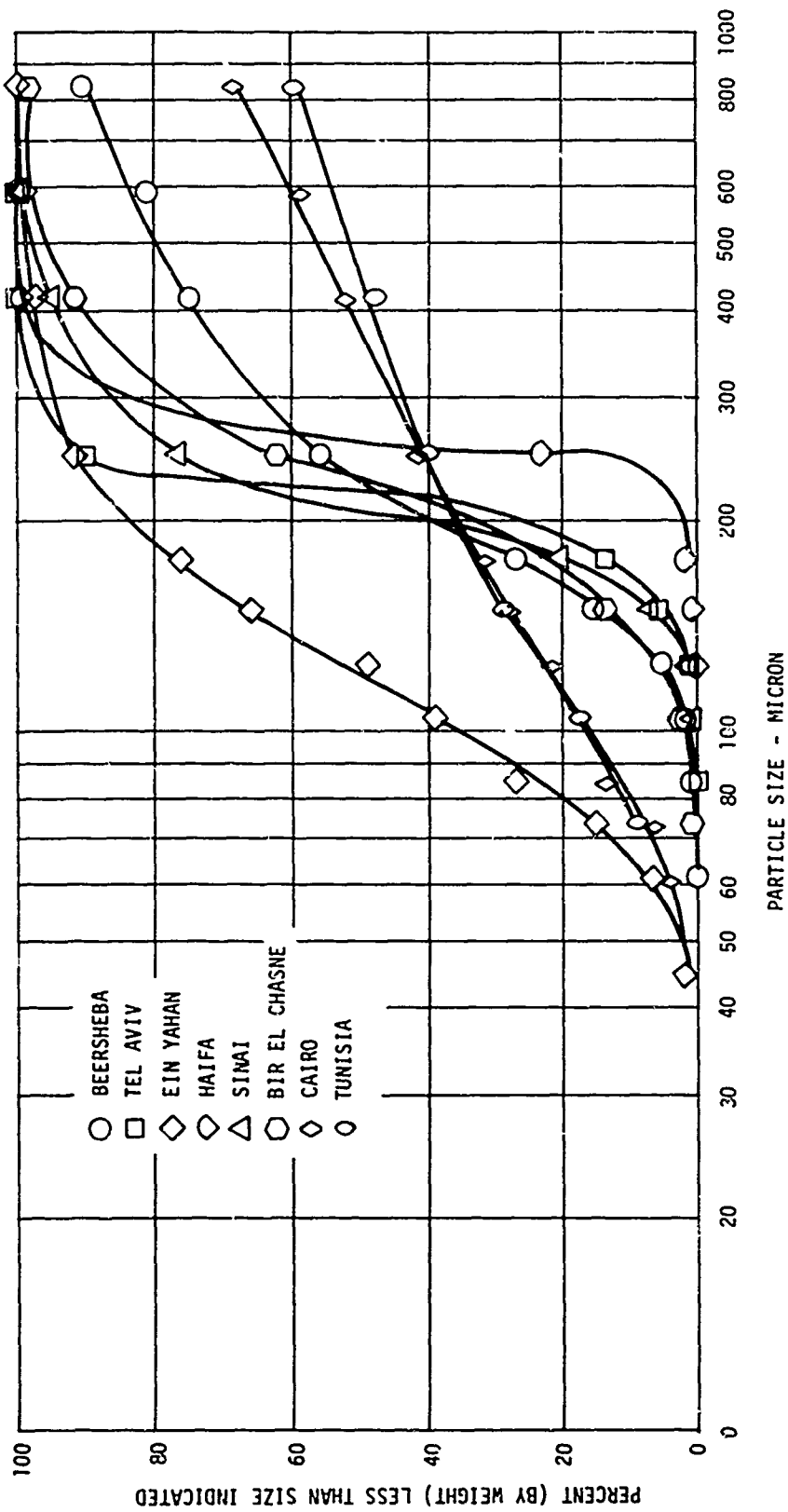


Figure A-7. Terrain Particle Size Distribution - Far East.

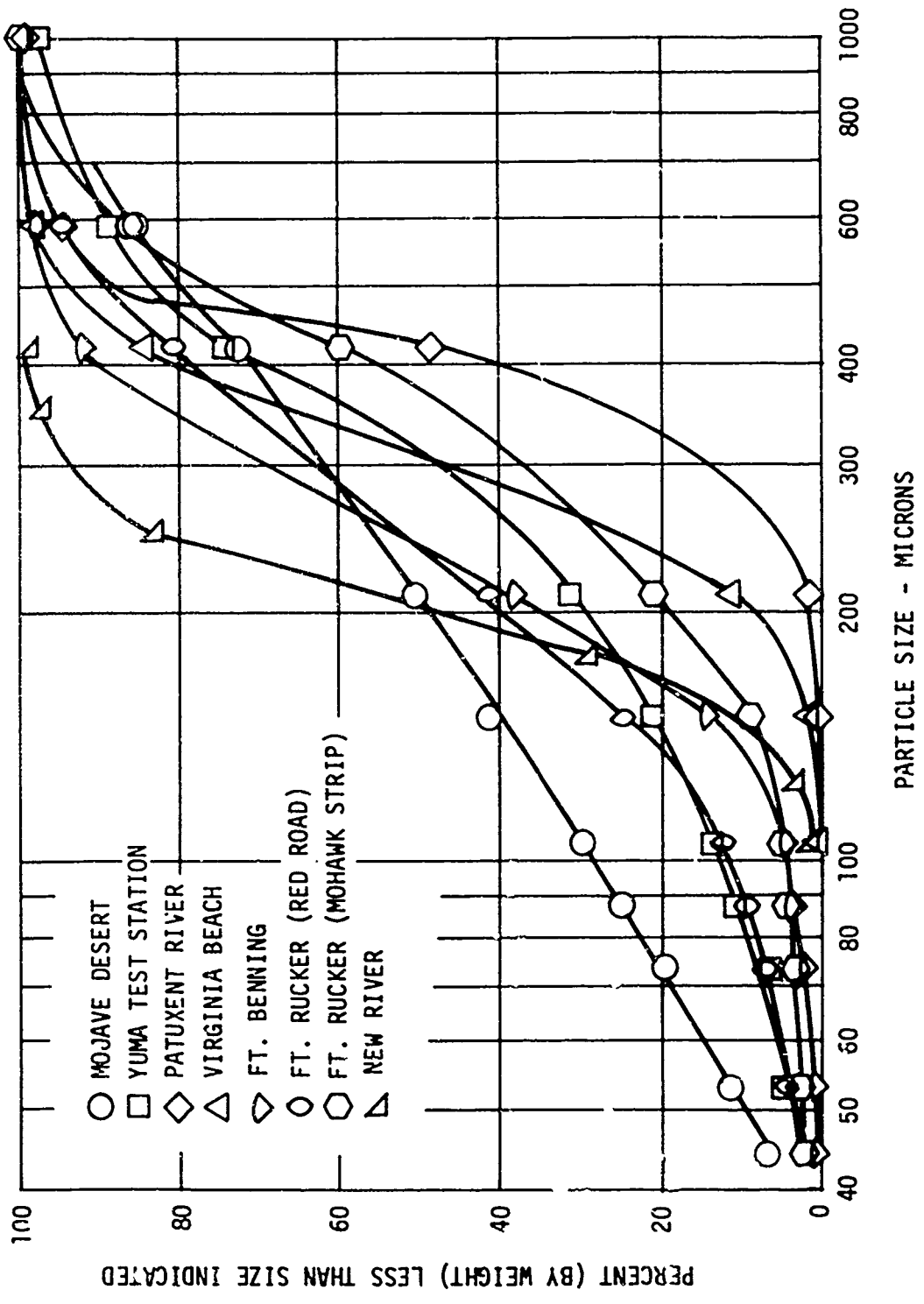


Figure A-8. Terrain Particle Size Distribution - United States.

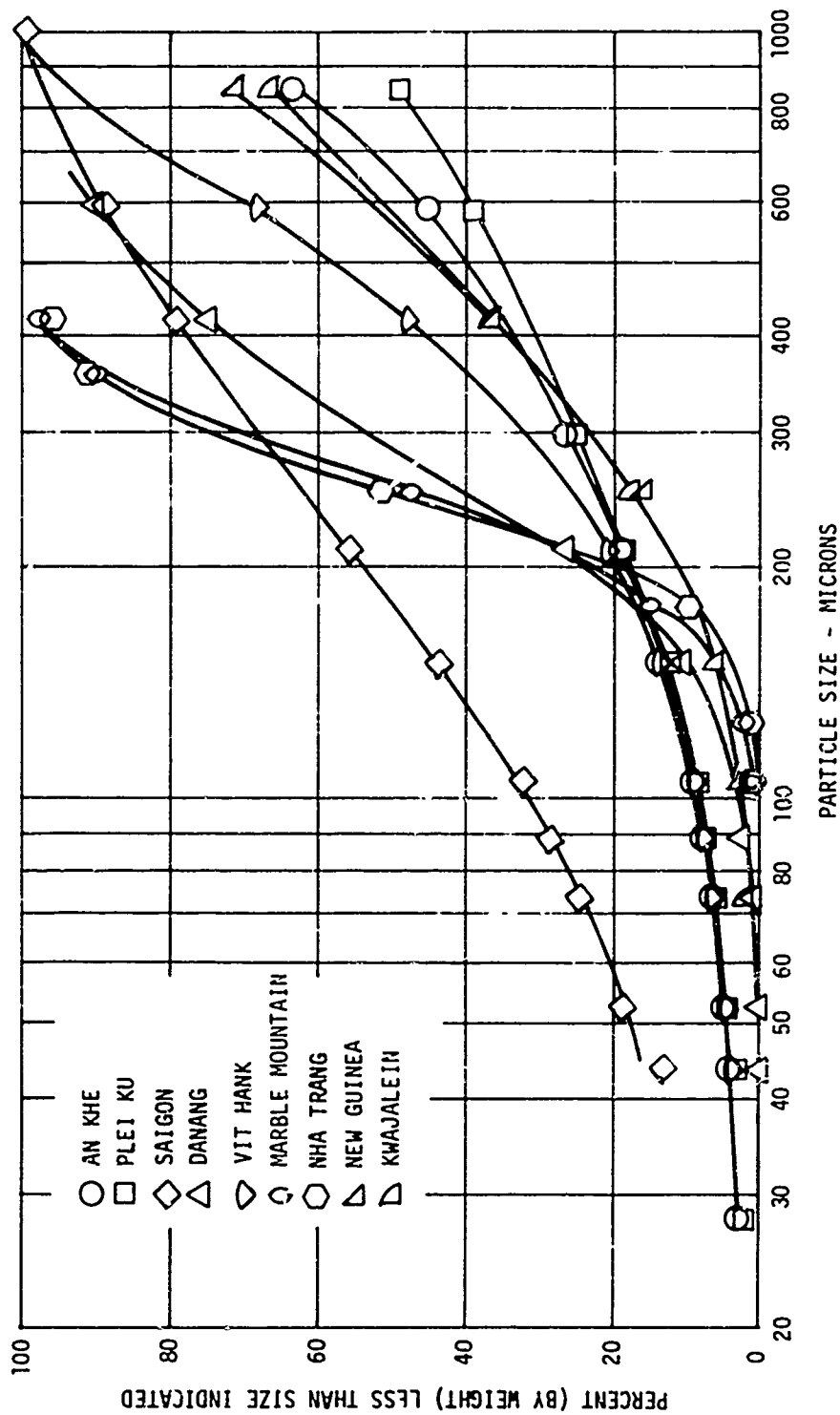


Figure A-9. Terrain Particle Size Distribution - Southeast Asia.

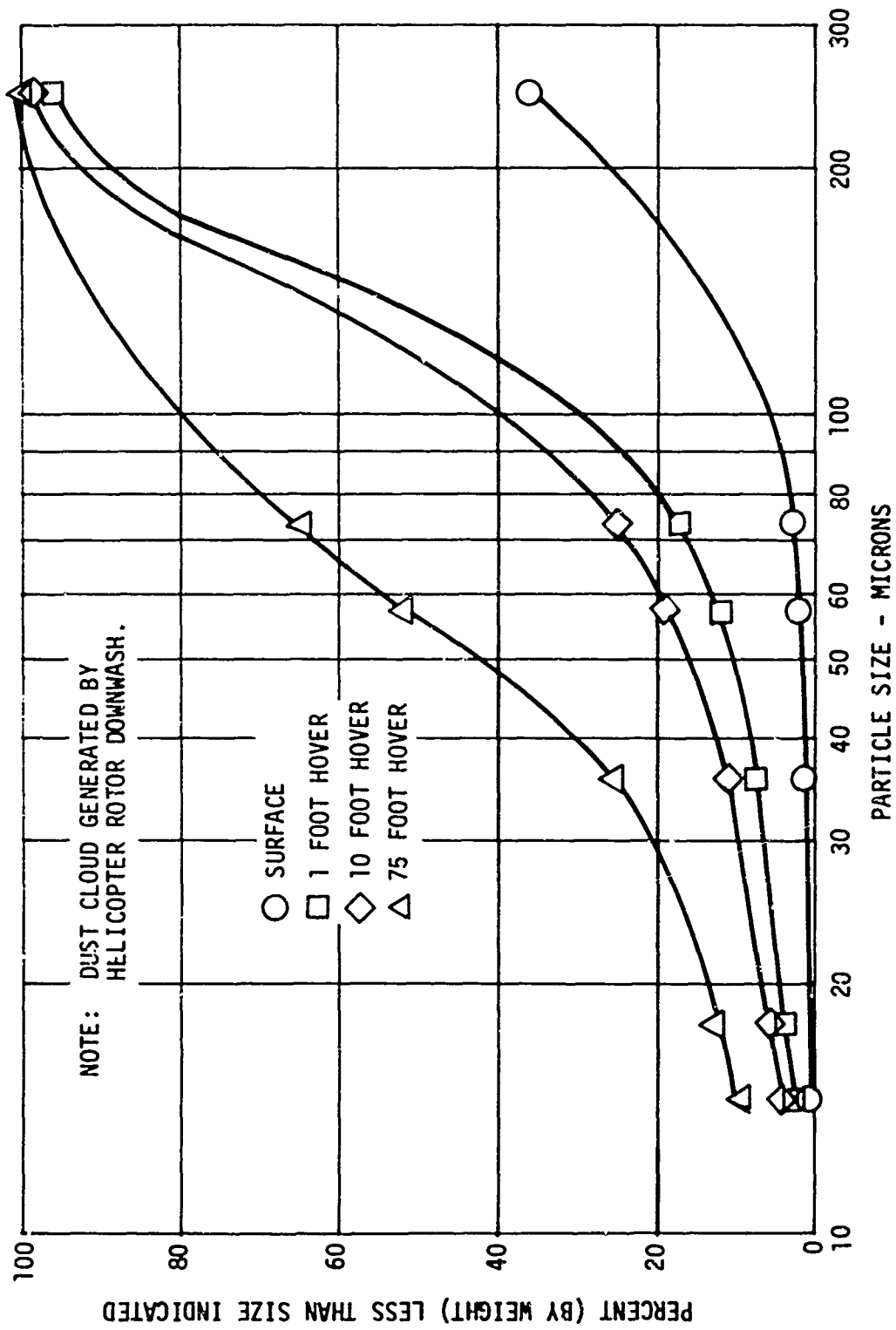


Figure A-10. Particle Size Distribution - Phillips Drop Zone, Yuma, Arizona.

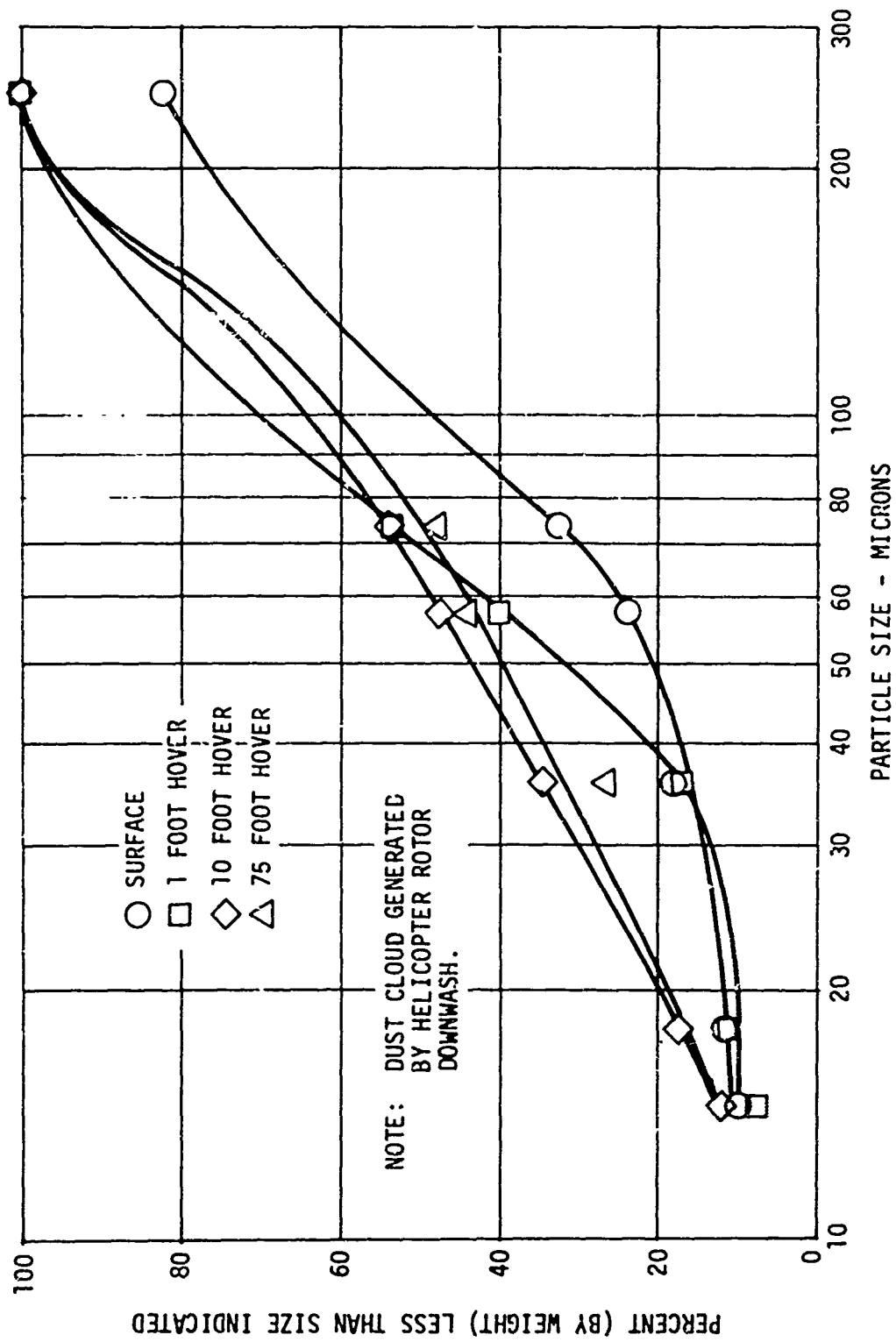


Figure A-11. Particle Size Distribution - Vehicle Dust Course, Yuma, Arizona.

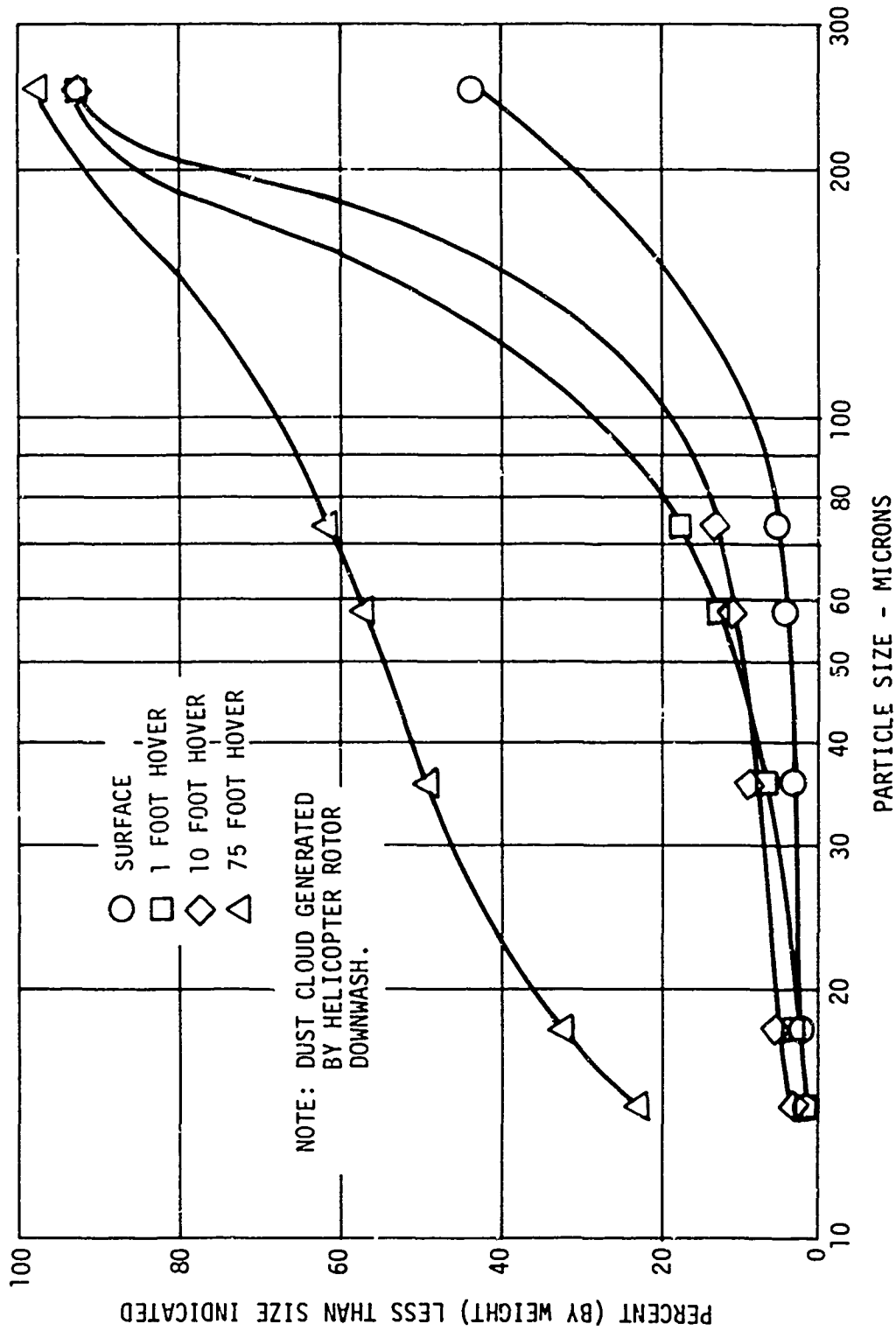


Figure A-12. Particle Size Distribution - Lee Drop Zone, Ft. Benning, Georgia.

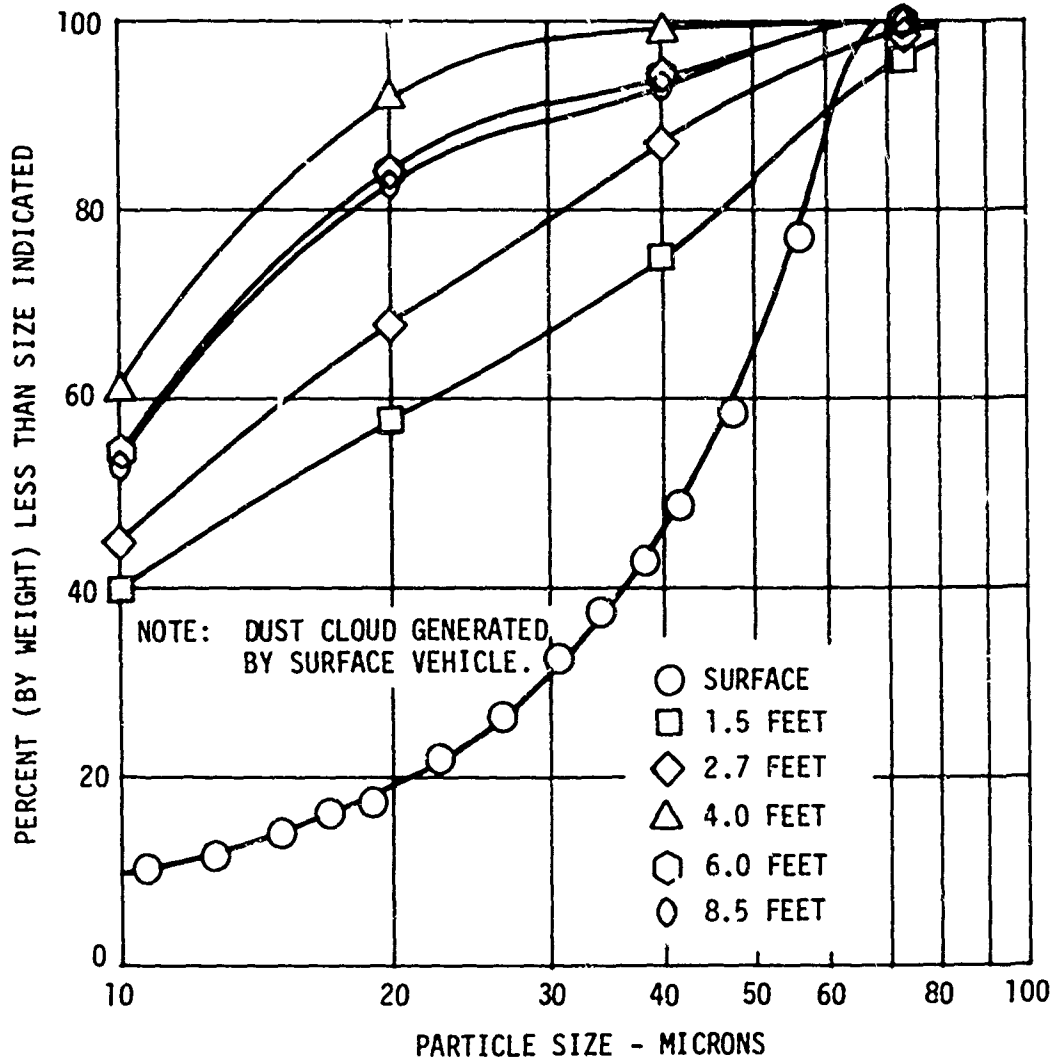


Figure A-13. Particle Size Distribution - Southwest Research Institute Dust Course, San Antonio, Texas.

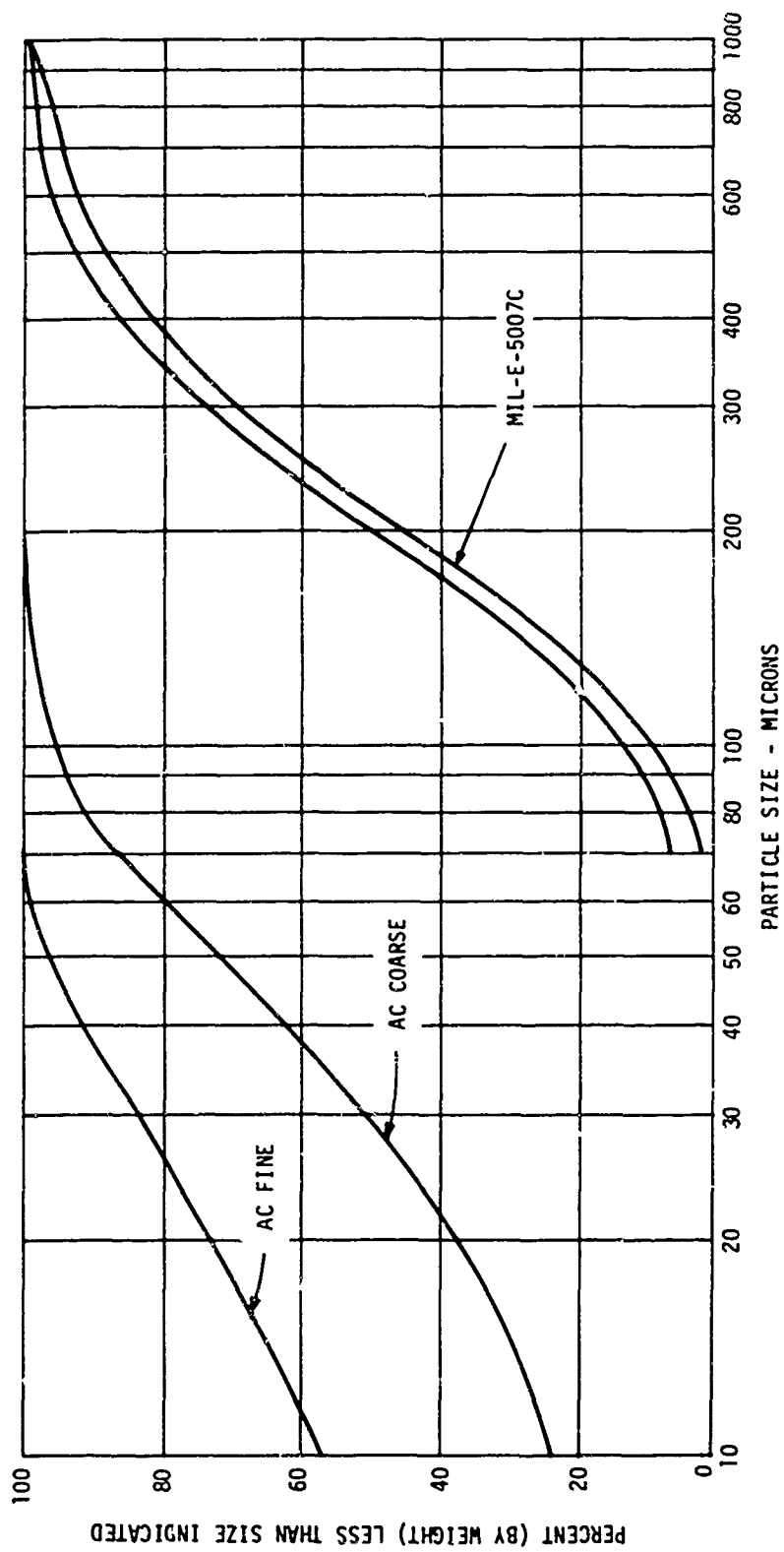


Figure A-14. Particle Size Distribution - Standard United States Test Dusts.

The same trend is observed when the terrain is disturbed by a vehicle traversing the surface rather than by helicopter blade downwash. Figure A-13 illustrates results from a vehicle dust course in south Texas.²⁷ Here the terrain sample is much finer, the surface disturbance is of a different nature, and the smaller particles are found at an intermediate height (4 feet). But, as with a helicopter, the airborne particle size distribution is generally finer than that on the surface.

Illustrated on Figure A-14 are the particle size compositions of the three standard test dusts commonly in use in the United States. When Figure A-14 is compared to Figures A-7, A-8, and A-9, the result shows that MIL-E-5007C test dust is fairly representative, though a little on the fine side, of all terrain particle size distributions found in the world. Figures A-10 through A-13 show that a test dust with a particle size distribution curve about midway between those for AC coarse and MIL-E-5007C would be appropriate for most airborne particles. Note that AC fine would best fit the data on Figure A-13. However, a comparison of Figure A-13 with Figures A-7, A-8, and A-9 shows that the terrain sample on the dust course is of much finer composition than generally encountered.

Three approaches, which can be used to define dust for inlet separator evaluation, are:

1. A new test dust more closely simulating dusts encountered by operational aircraft might be developed.
2. Since AC coarse and MIL-E-5007C Specification (C-Spec) dusts bracket most size distributions for aircraft operating at various geographical locations and altitudes, tests could be run with both. This would test a separator's ability to collect heavier components in the dust represented by C-Spec dust which are more likely to "bounce". It would also test the separator's ability to collect finer AC coarse dust which has more of a tendency to follow the streamlines.
3. Since the damage caused by foreign matter which is ingested in an engine increases with the size of the particles, it is more important to collect the larger components starting with birds, nuts, bolts, and ice and going down to coarse and fine dust. Therefore, tests may be concentrated on the coarser C-Spec dust which must be removed to a high degree since it is more erosive than the finer dusts. "Proof tests" would be required to show adequate performance on AC coarse dust.

Each of these approaches has its place. Under special operational conditions for an aircraft, the first approach may be necessary. For instance, an engine to be run in a helicopter on the ground or at low altitude over the Sahara Desert should be tested with Sahara sand probably at its temperature. Except for such a special case, this approach seems impractical. The differences between dust samples are too great to try to trim the dust

to a universally applicable size or distribution of size. The second approach is practical since it provides check points on fine and coarse dust. It seems probable that interpolations could be made to correct the results to other dust sizes which will be encountered under changing operational conditions.

The third approach is similar to the second, but it places emphasis on C-Spec performance. Figures A-7, A-8, and A-9 show that at the ground level, dust is generally similar to C-Spec in distribution and size. Figures A-10, A-11, and A-12 show that, in general, increasing altitude is accompanied by finer dust. At the same time, Figures A-1 through A-5 indicate that concentration is less at altitude than on the ground.

Since dust which is smaller than 40 microns in diameter is less erosive to an engine¹² and is less concentrated under operational conditions than coarse dust, it appears that AC coarse dust is less a problem than C-Spec. On this basis, the collection efficiency of a separator on dust coarser than 40 microns should be emphasized. When an engine runs in coarse dust, all of the dust possible must be collected. When it runs in fine dust, the coarse end of the size distribution must be collected. The third approach to the definition of dust for separator evaluation puts emphasis on the coarser dust.

FOLIAGE INGESTION

There is very little information on the incidence of engine malfunctions because of foliage ingestion. The lack of information indicates that foliage has not been a serious cause of premature engine overhauls or serious aircraft accidents. However, there have been incidents in which aircraft engines lost compressor blades due to stalls caused by foliage blockage of an inlet. The reasons for the few reported incidents are probably that they occur on or near enough to the ground to prevent serious accidents and that the problem is easily solved by cleaning the debris from the inlet. The engine normally is not mechanically damaged and requires no overhaul work as a result of foliage ingestion. While foliage data are scarce, protection from "foliage and the like" is needed to prevent incidents such as:

CH-53A New River 8/69

"Aircraft landed in hayfield...during take-off, No. 1 engine accel to 118% N_f and 680° CT...Engine intakes were choked with grass.."

SH-3A NAS-Lakehurst 6/67

"Engine ingested a rag while hovering over the fan tail of the USS Jenkins...Aircraft landed hard in the water, inverted and sank.

Because foliage may occur in large quantities, it should be separated from the engine airflow ahead of the inlet system and shunted overboard. Otherwise, it should be expected to clog the inlet particle separator and engine inlet.

FOREIGN OBJECT DAMAGE (FOD)

Engine manufacturers' records^{28, 29} usually register the frequency of FOD and sum up the number of incidents but do not explain the causes or describe the extent of engine damage. United States Army and Air Force records are similar. The Navy maintains more detailed FOD records for selected events.³⁰ For example, 193 were covered by reports which contained sufficient detail to identify the cause.

References 31 through 37 summarize U.S. Navy engine experience with FOD from 1967 through 1970. Reports of the seven most common objects are shown in Figure A-15 as a percentage of all useful FOD reports. Leading the lists of objects ingested are nuts, screws, and bolts. Birds are second, while safety pins and flags are probably third. The commonly ingested items make up about one-half of the incidents. The other half is made up of objects such as flashlights, ice and other unique items. Essentially all engines ingesting these objects were damaged and required repair or removal, but no data is available to indicate any correlation between the objects ingested and the degree of damage.

Since an unscheduled engine removal is caused by almost every large object ingested by an engine, an inlet protection device must be designed to collect all such objects. This is the most important requirement for a separator.

WEATHER ENVIRONMENT

An important element in the environment of aircraft engines is the weather, which may cause the ingestion into engines of unacceptable quantities of rain, snow, or ice. Of these, ice is the most destructive. Its formation is governed by weather conditions^{38, 39} and anti-icing provisions of the aircraft. Its effects are foreign object damage (FOD) to the engine and inlet blockage or flow reduction. The most serious effect is FOD which results when ice chunks or slivers break away from the fuselage or inlet and enter the compressor. Therefore, ice is a problem to be solved by anti-icing vulnerable areas of the engine inlet system, especially the separator itself. If ice is ingested, it should be removed with other single foreign objects such as nuts, bolts and stones.

Because excessive water ingestion deteriorates engine aero-thermo and mechanical performance, rain is an environmental problem for aircraft engines. Studies⁴⁰ of sea level water concentration (pounds of water per pound of air) at several locations gave results which ranged from 0.1 percent at Corvallis, Oregon, to 2.4 percent at Miami, Florida. Airborne sampling⁴¹ in heavy rainfall during aircraft penetration into severe thunderstorm cells showed that water concentration under these conditions varies from 0.3 percent to 3.1 percent, an increase of almost 30 percent from that encountered at sea level. In general, more water than this enters the engine because the combination of density, drag and surface tension of a raindrop encourages the collection of rain on aircraft and inlet surfaces.

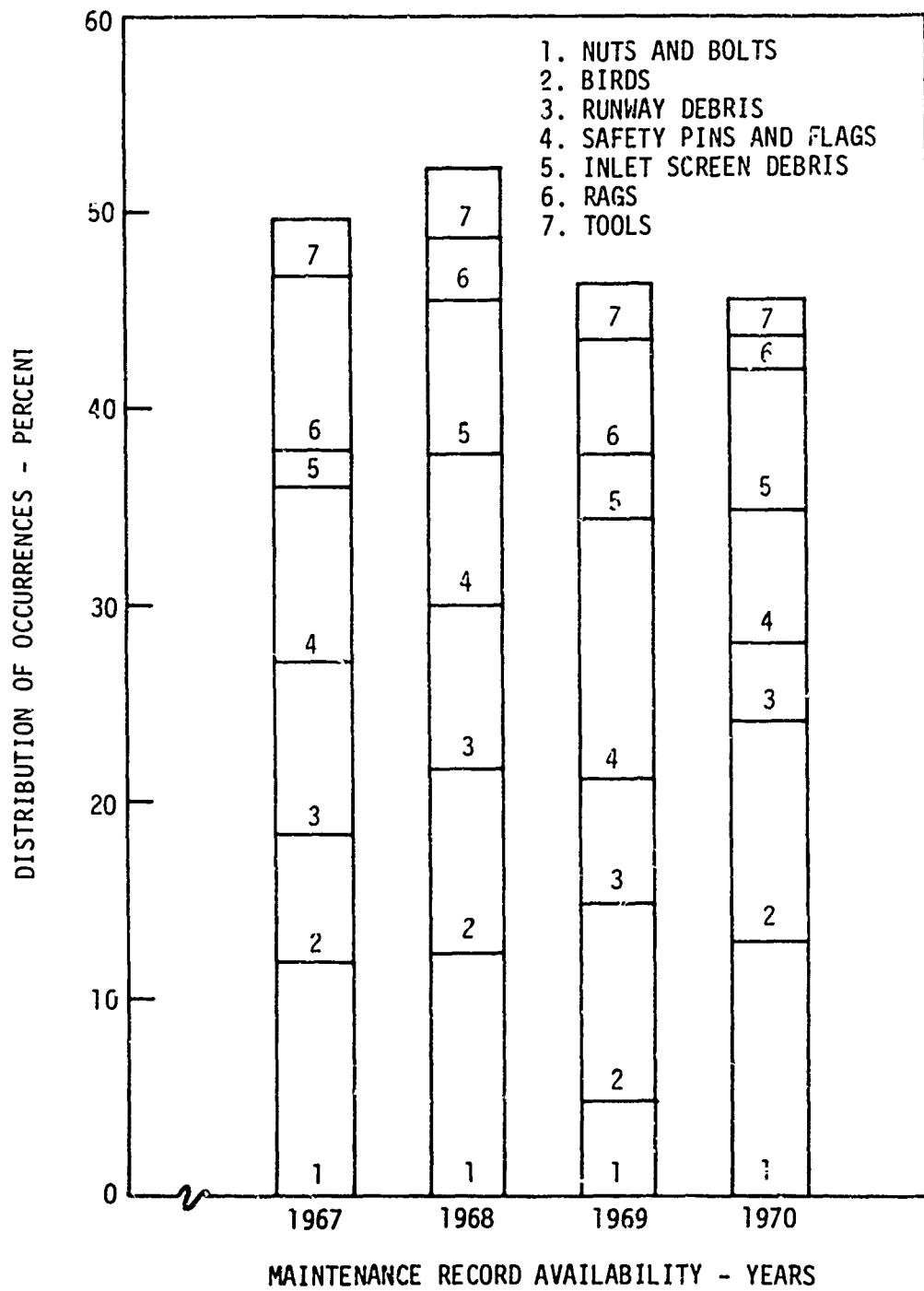


Figure A-15. Foreign Object Damage - Commonly Ingested Items.

A portion of this water enters the engine along with the water which is entrained in the air. Unsubstantiated reports ⁴² from investigations conducted at the U.S. Naval Air Turbine Test Station and the Patuxent River Naval Air Station with the F3H aircraft noted that "...fuselage runoff water ingested into the engine was up to 8 percent of the engine airflow."

Excessive water ingestion affects engine operation in a variety of ways: gradual loss of power, ⁴³ compressor stall, ⁴⁴ flameout, ⁴⁴ and compressor and turbine tip rubs. ³⁵ While the amount of water that an engine can safely ingest depends on the design, extensive testing ^{43, 44, 45} has shown that most jet engines can operate satisfactorily with inlet water/air ratios equivalent to those associated with moderate thunderstorm activity. Military Specification MIL-E-5007C¹³ requires that jet engines "...shall operate satisfactorily throughout the flight operating envelope... at all levels up to 5.0 percent of the total airflow weight in the form of water...". Since this percentage is somewhat in excess of that reported in active thunderstorm cells and is acceptable to the average jet engine, any integral inlet protection device is acceptable if it can reduce the concentration of water at the compressor inlet to the 5 percent level. Since concentrations of 8 percent can occur, ⁴² an inlet separator must remove at least 37.5 percent of the water which enters it. In the design of an inlet particle separator, rain is treated as a distributed entrained material like dust or sand and as boundary flow over the flow path walls from which it must be separated and forced to flow into the main airstream.

Snow is not considered to be destructive to aircraft engines. The combination of density and drag of a snowflake ensures that most snow will remain entrained in the airflow and not build up a flow path walls. On the assumption that the greatest concentration of snow is no greater than that of water, it is less than about 3 percent. Since aircraft engines must be able to ingest 5 percent, snow is not considered an environmental problem. Care should be taken, however, to assure that no "pockets" exist in the inlet/fuselage system where large amounts of snow can build up and eventually be dislodged to be ingested by the engine as a single large mass of snow.

COMBINED ELEMENTS OF THE ENVIRONMENT

It is possible that combinations of undesirable material, such as wet hay or ice-covered sand, could be ingested by an engine. Most combinations, however, are not important since one element of the environment completely dominates the other or since they are unlikely to occur at the same time.

The most destructive element in the engine inlet's environment is a single large foreign object, whether or not it is combined with foliage, dust, or rain. Therefore, any combination of that kind is treated as a foreign object. Combinations of foliage with dust or weather are likely to occur rarely and for short periods of time. Therefore, any time that foliage or a rag is ingested, there is a foliage type problem which overwhelms other

considerations except large single foreign objects. Because of the differences in texture between wet and dry foliage, foliage tests which include ingestion of wet swamp grass and semidry hay and leaves are recommended.

It is very unlikely that any large amounts of wet or icy sand and dust could be ingested since they would be difficult to stir up on the ground. If such an unlikely combination occurred, it is probable that it would make the much more destructive sand less erosive. The small, hard particle erodes a target by generating high temperature or stresses in it. The water or ice is expected to provide a sink for the heat and a cushion for the impact which would reduce the sand's erosiveness.

Combinations of ice and rain may occur. The major adverse effect of such a combination is the buildup of ice in the inlet system. The separator is expected to separate water and ice particles entrained in the air just as though they did not occur together. Vulnerable areas in the inlet system, especially the separator itself, must be anti-iced to prevent the formation of ice. If ice chunks are ingested, they will be the predominant factor like any other large single foreign object.

The design of an inlet protection device should satisfy the requirements of each applicable element of the environment separately. Foliage requirements should apply to both wet and dry foliage.

APPENDIX B
TRAJECTORY ANALYSIS

DERIVATION

Analytical prediction of collection efficiency is the ultimate goal of individual sand particle trajectory analysis.

The analysis method requires a definition of the air velocity and flow direction from engine inlet to separator exit, as well as specification of all flow path geometry including vanes. These data are obtained from the separator aerodynamic design process. For swirl vanes, the resultant potential flow field within the vanes is a two-dimensional axisymmetric approximation.

Assumptions used in the particle trajectory analysis are:

1. The effect of sand particles on the fluid flow field is neglected.
2. Only the viscous drag force on the particle is considered. Forces due to the pressure gradient in the surrounding fluid, and that required to accelerate the mass of fluid which surrounds the particle and moves with it (apparent mass), are neglected.
3. Gravity is neglected.
4. Viscous effects in the fluid are neglected.

The trajectory of a particle is calculated from the equation of motion for a particle, which is

$$m\bar{a} = C_d \times 1/2 \rho V^2 A \bar{e}_v \quad (B-1)$$

in which m is mass of a particle, \bar{a} its acceleration, C_d its drag coefficient, V its relative velocity $\sqrt{(u_r - v_r)^2 + (u_\theta - v_\theta)^2 + (u_z - v_z)^2}$, A its frontal area, and ρ is the gas density. The air velocity is \bar{u} and the absolute particle velocity is \bar{v} . In cylindrical coordinates the acceleration of the particle is

$$\bar{a} = d\bar{v} = \bar{e}_r (dv_r/dt - v_\theta^2/r) + \bar{e}_\theta (dv_\theta/dt + v_r v_\theta/r) + \bar{e}_z dv_z/dt \quad (B-2)$$

The term v_{θ}^2/r is centrifugal acceleration and $v_r v_{\theta}/r$ is the Coriolis acceleration. The symbol \bar{e} means unit vector in the direction of the subscript. Equation (B-1) can also be written

$$\bar{a} = (C_d \rho V A / Z m) (\bar{u} - \bar{v}) \quad (B-3)$$

In scalar form Equation (B-3) becomes

$$dv_r/dt = C(u_r - v_r) + v^2/r \quad (B-4)$$

$$dv_{\theta}/dt = C(u_{\theta} - v_{\theta}) - v_r v_{\theta}/r \quad (B-5)$$

$$dv_z/dt = C(u_z - v_z) \quad (B-6)$$

in which

$$C = C_d \rho A V / 2m \quad (B-7)$$

The mass and frontal area of the particle are

$$m = \rho_p D^3 Z, \quad A = \frac{\pi}{4} D^2 \quad (B-8)$$

The parameter Z in Equation (B-8) is the "shape factor" of the particle. For a sphere it is $\pi/6$. For sand it is in the neighborhood of .26 to .28. Equation (B-7) now becomes

$$C = \pi C_d \rho V / 8 D Z \rho_p \quad (B-9)$$

Expressions for the drag coefficient 47, 48, 49 are

$$C_d = [24/Re] \{1 + .15 Re^{.687}\} [(1 + e^{-.487/M \cdot 463 - 3/Re^{.88}}) / (1 + (M/Re)(3.82 + 1.28 e^{-1.25 Re/M})] \quad (B-10)$$

for $0 < Re \leq 2000$

$$C_d = .44 \quad (B-11)$$

for

$$Re < 2000$$

where $Re = D_p V_{\rho} / \mu$ and

M = Mach No. based on relative velocity

Particle rebound characteristics⁵⁰ can be expressed

$$v_2/v_1 = 1 - 2.03 \beta_1 + 3.32 \beta_1^2 - 2.24 \beta_1^3 + .472 \beta_1^4 \quad (\text{B-12})$$

$$\beta_2/\beta_1 = 1 + .409 \beta_1 - 2.52 \beta_1^2 + 2.19 \beta_1^3 - 531 \beta_1^4 \quad (\text{B-13})$$

$$v_{n2}/v_{n1} = .993 - 1.76 \beta_1 + 1.56 \beta_1^2 - .49 \beta_1^3 \quad (\text{B-14})$$

$$v_{t2}/v_{t1} = .988 - 1.66 \beta_1 + 2.11 \beta_1^2 - .67 \beta_1^3 \quad (\text{B-15})$$

where β_1 = incidence angle

β_2 = rebound angle

Note: Subscripts 1 and 2 apply to Equations (B-12) through (B-15).

v = particle velocity

v_n = particle velocity normal to impacted surface

v_t = particle velocity tangent to impacted surface

Efficiency Determination - Vaneless Separators

Figure B-1 is a flux plot of a typical separator flow path. The streamline function, Ψ , defines airflow direction and mass distribution, information required in order to calculate sand particle trajectories. Inlet sand concentration can be defined as

$$c_s/c_o = f(\psi) \quad (\text{B-16})$$

where C_o = average sand concentration = W_s/W

C_s = local sand concentration at separator inlet

Specification of initial sand concentration as well as initial velocity has a strong influence on final collection efficiency estimates. For the case of uniform sand concentrations,

$$c_s/c_o = 1.0$$

Total sand mass flow is then

$$W_s = W \int_0^1 C_s d\psi \quad (\text{B-17})$$

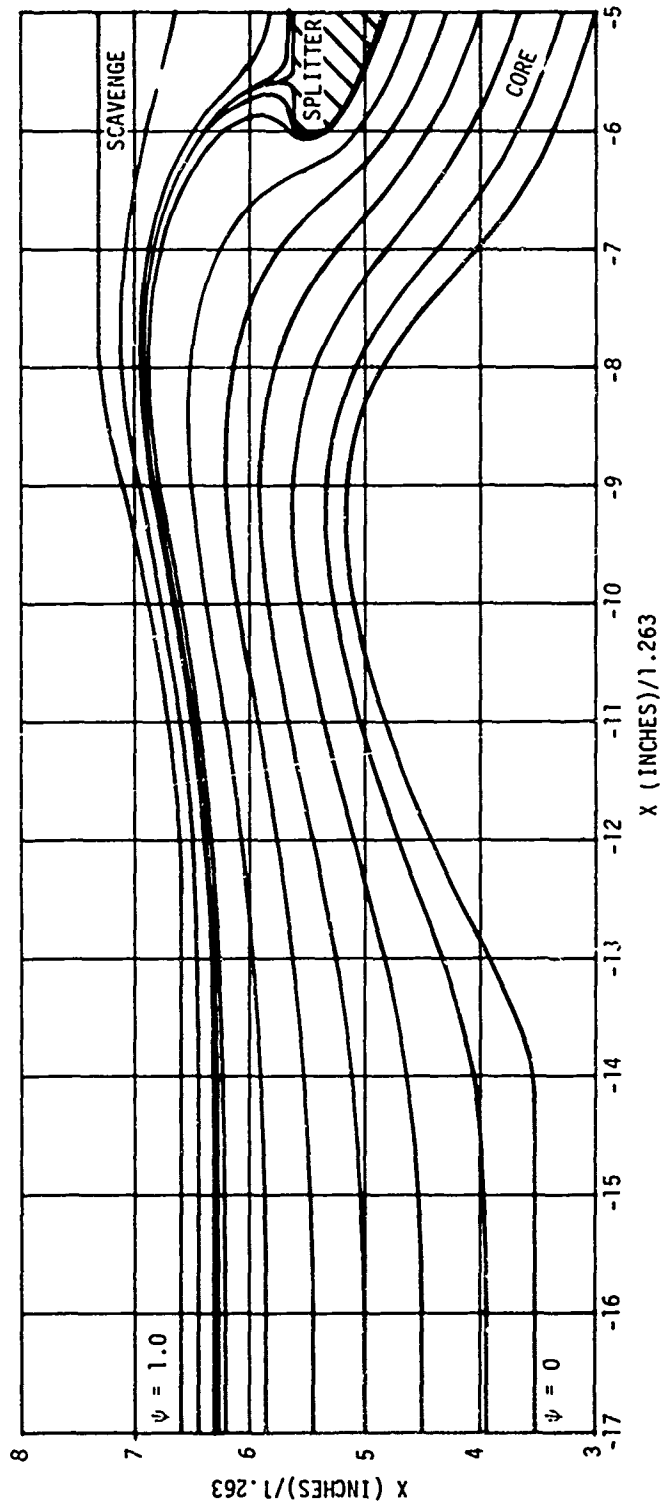


Figure B-1. Typical Separator Flux Plot.

Figure B-2 shows typical test sand particle size distributions for AC coarse, AC fine, and C-Spec sands, where $\% (D_p)$ = weight fraction of sand with particle diameter less than D_p .

Figure B-3 is a particle trajectory plot of various sized particles injected (at the same location) into the separator shown in Figure B-1. As can be seen from the plot, for $D_p > 21$ microns, all particles are separated. With the definition that critical particle diameter, D_c , defines the maximum size particle separated for a given particle injection point and initial velocity, the quantity $1.0 - \% (D_c)$, for a given sand distribution, defines a local separation efficiency, i.e.,

$$\eta_e = 1.0 - \% (D_c)$$

The results for a complete trajectory analysis on the separator shown in Figure B-1 are plotted in Figure B-4, as D_c versus injection streamline. The corresponding local efficiency plots for AC coarse and C-spec sands are shown in Figure B-5.

Overall separation efficiency is then calculated by

$$\eta_o = \int_0^1 C_s/C_o \eta_e d\psi \quad (B-18)$$

where $C_s = f(\psi)$

$$\eta_e = f(D_c)$$

The large efficiency drop shown in Figure B-5 is due to radial placement of the splitter lip with respect to the upstream flow path. By contrast, analysis of the flow path shown in Figure B-6 results in much higher efficiencies, and elimination of the line-of-sight "hole" as can be seen from Figures B-7 and B-8.

With the assumption of uniform inlet sand density, the bellmouth inlets of the two separators described above were replaced by cylindrical walled inlets, with the individual particles started from rest; the first is a 15 lb/sec size separator, while the hidden splitter version is of 5 lb/sec size. Eight equally spaced sand nozzles were used in testing each of the separators, and they were placed in the same scaled position relative to the bellmouth.

Results of an analysis performed on a 9 lb/sec size vane separator are discussed below. Figure B-9 is a flux plot of the separator, with several particle trajectories (with vane impact) superimposed.

Critical particle diameter versus injection streamline is plotted in Figure B-10, with no vane impact phenomena taken into account. (The swirl field only is simulated.) Also included are boundaries representing centerbody impact and combination centerbody impact with outer wall impact

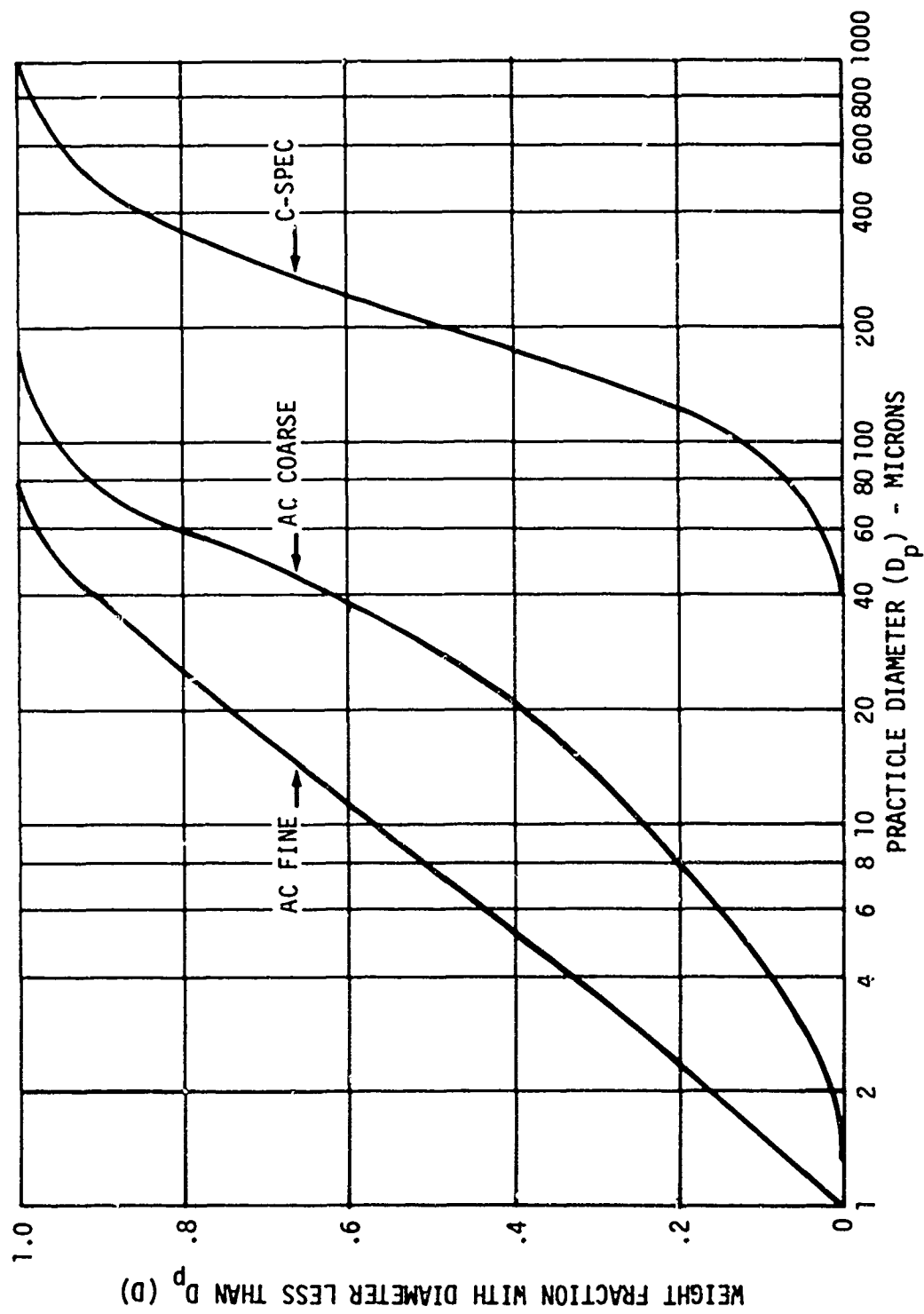


Figure B-2. Typical Test Sand Particle Size Distribution.

SAMPLE TRAJECTORIES $\psi = .122$
 $Z = .28$
 $V_{init} = 0.0$

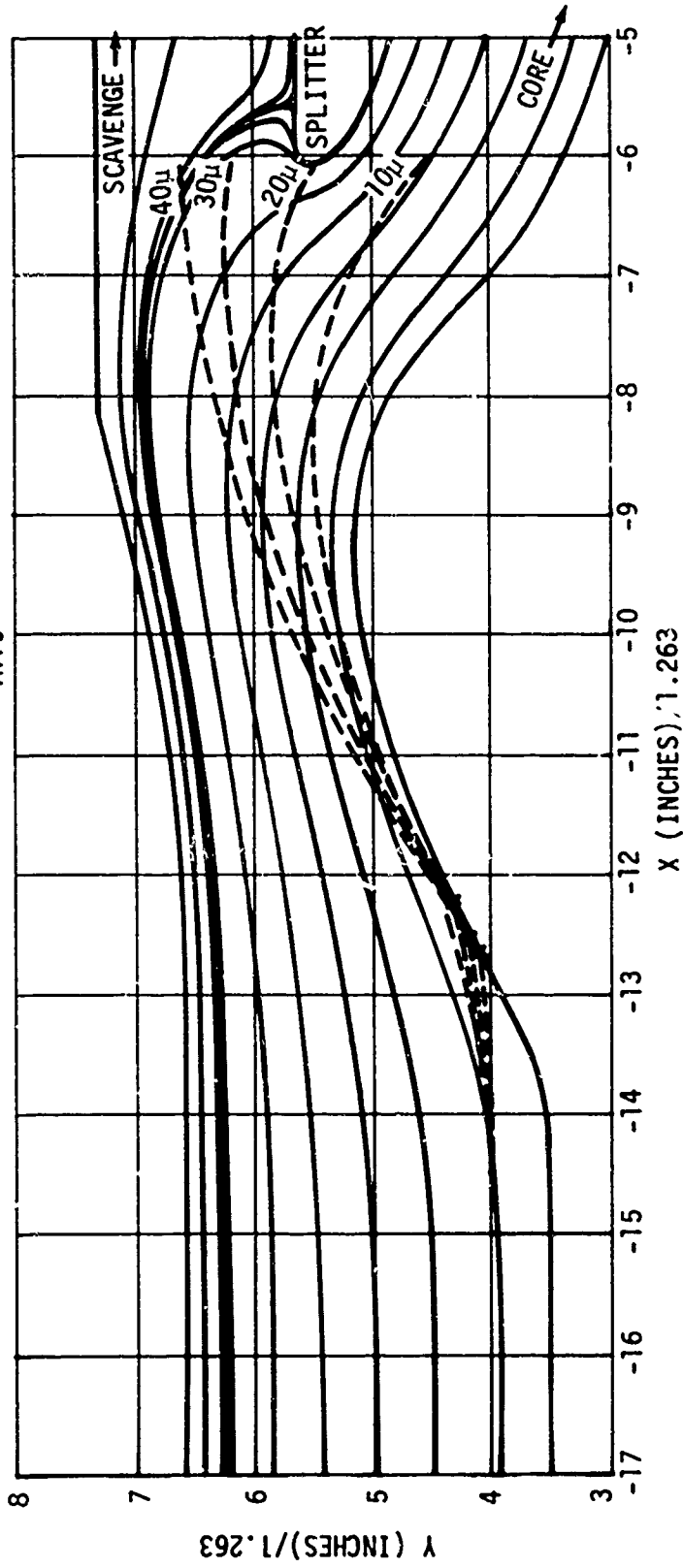


Figure B-3. Trajectories of Particle Injected at $\psi = 0.122$.

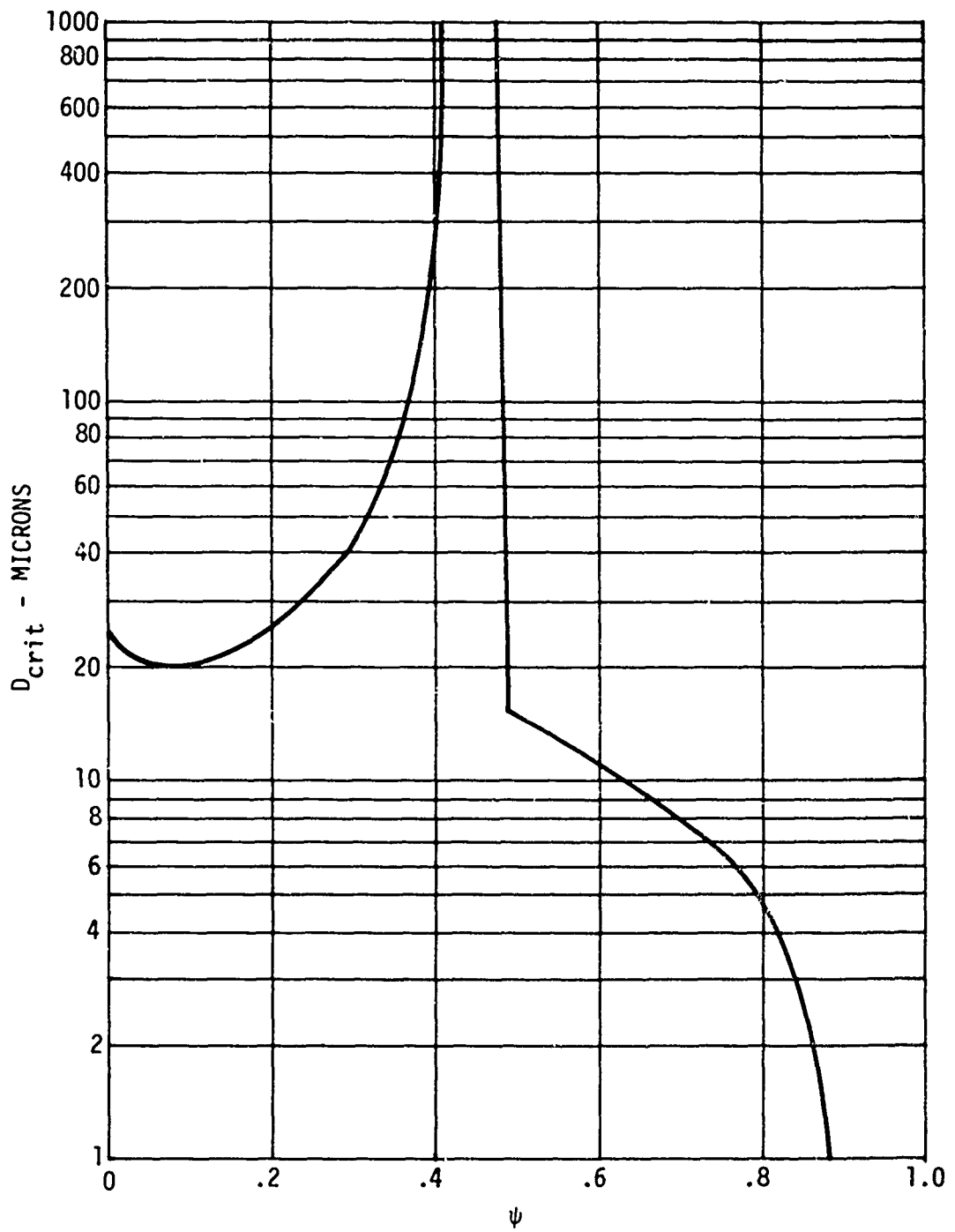


Figure B-4. Critical Diameter Distribution for Figure B-3.

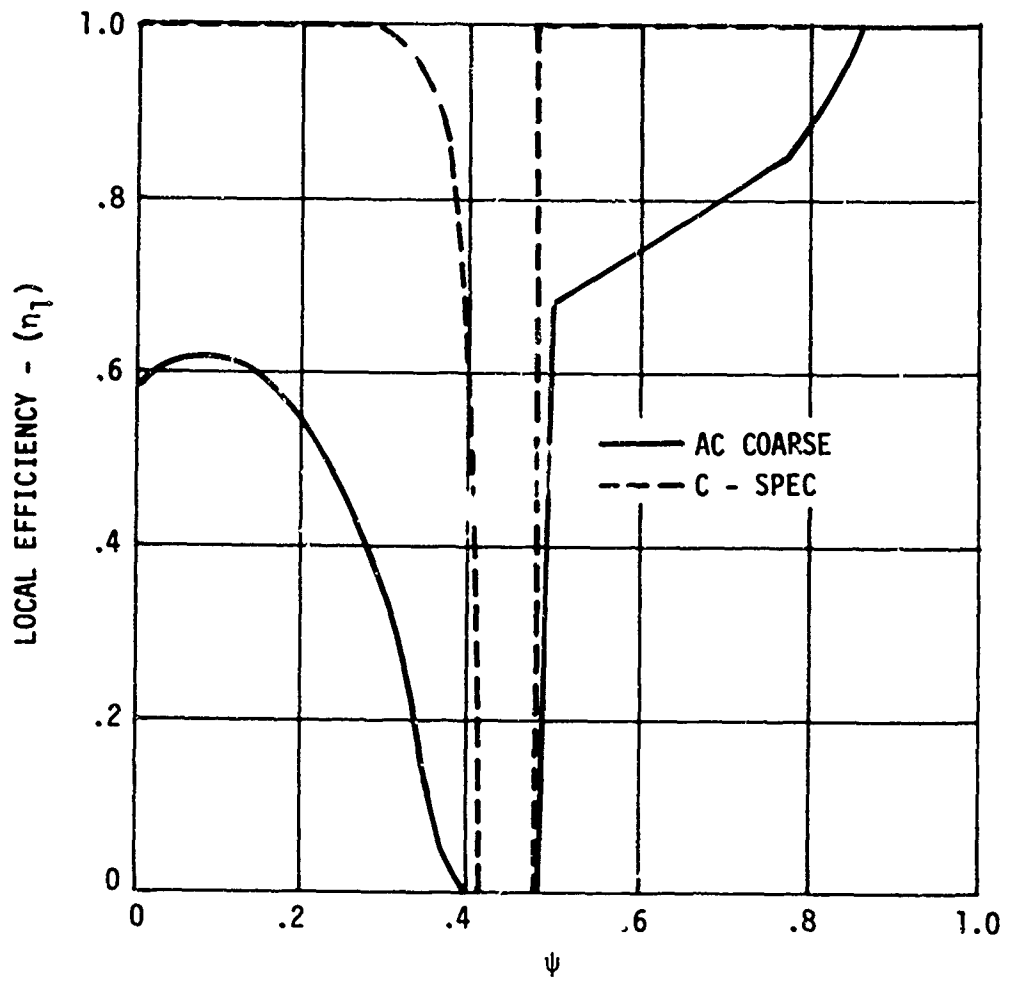


Figure B-5. Local Efficiency Distribution for Figure B-3.

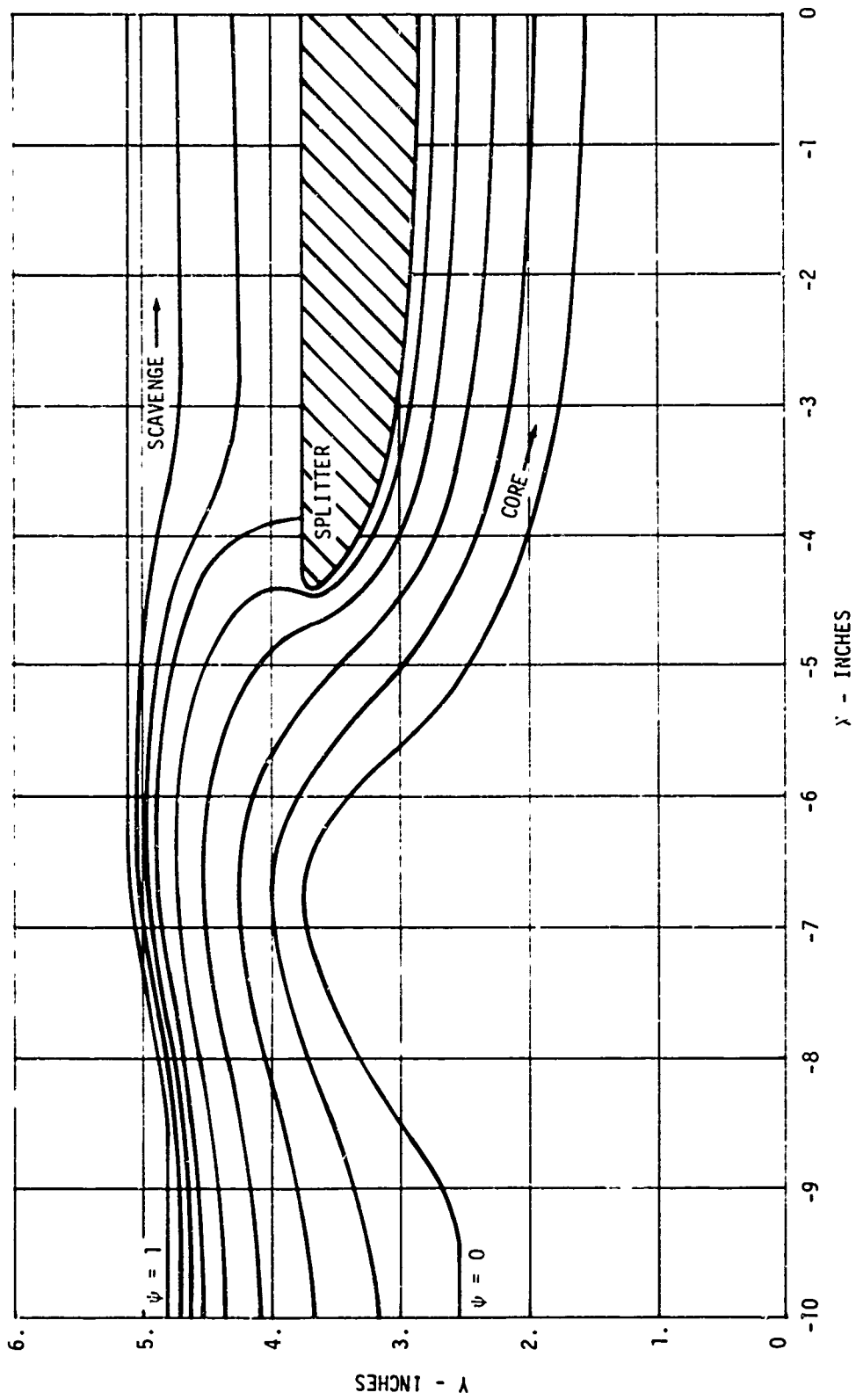


Figure B-6. Hidden Splitter Separator Flux Plot.

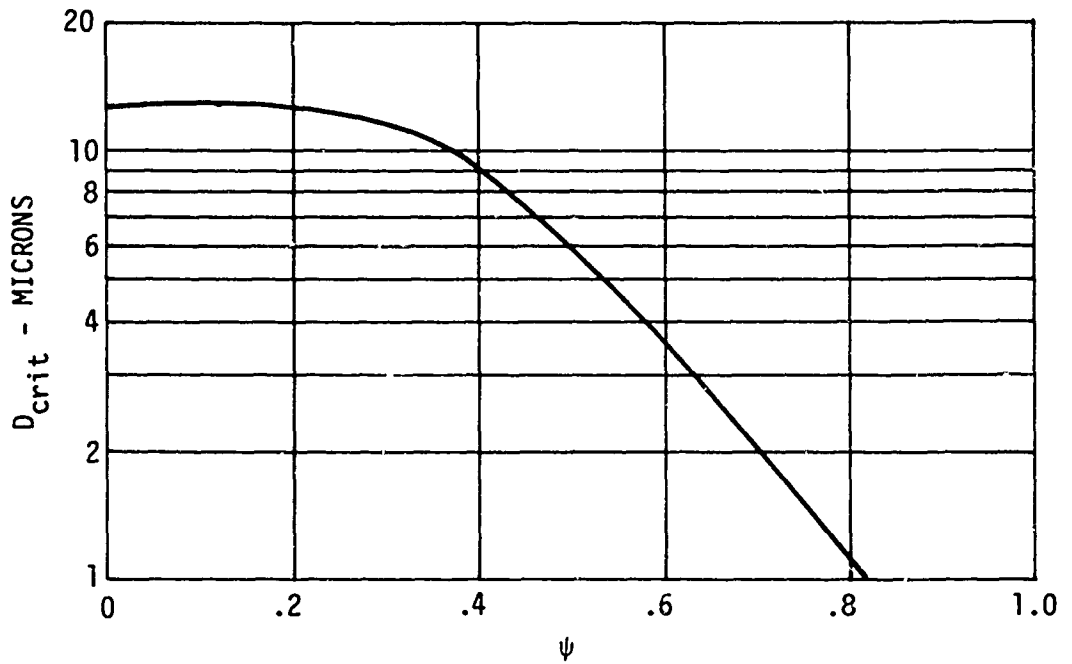


Figure B-7. Critical Diameter Distribution for Figure B-6.

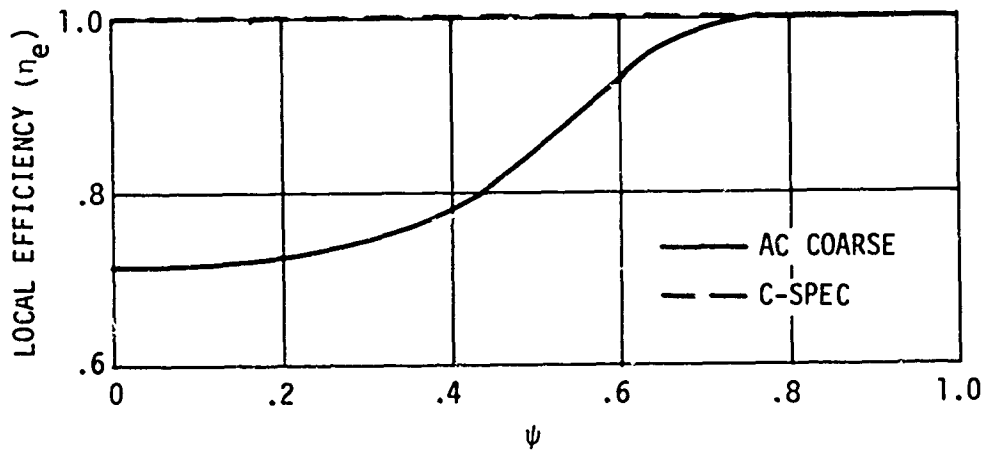


Figure B-8. Local Efficiency Distribution for Figure B-6.

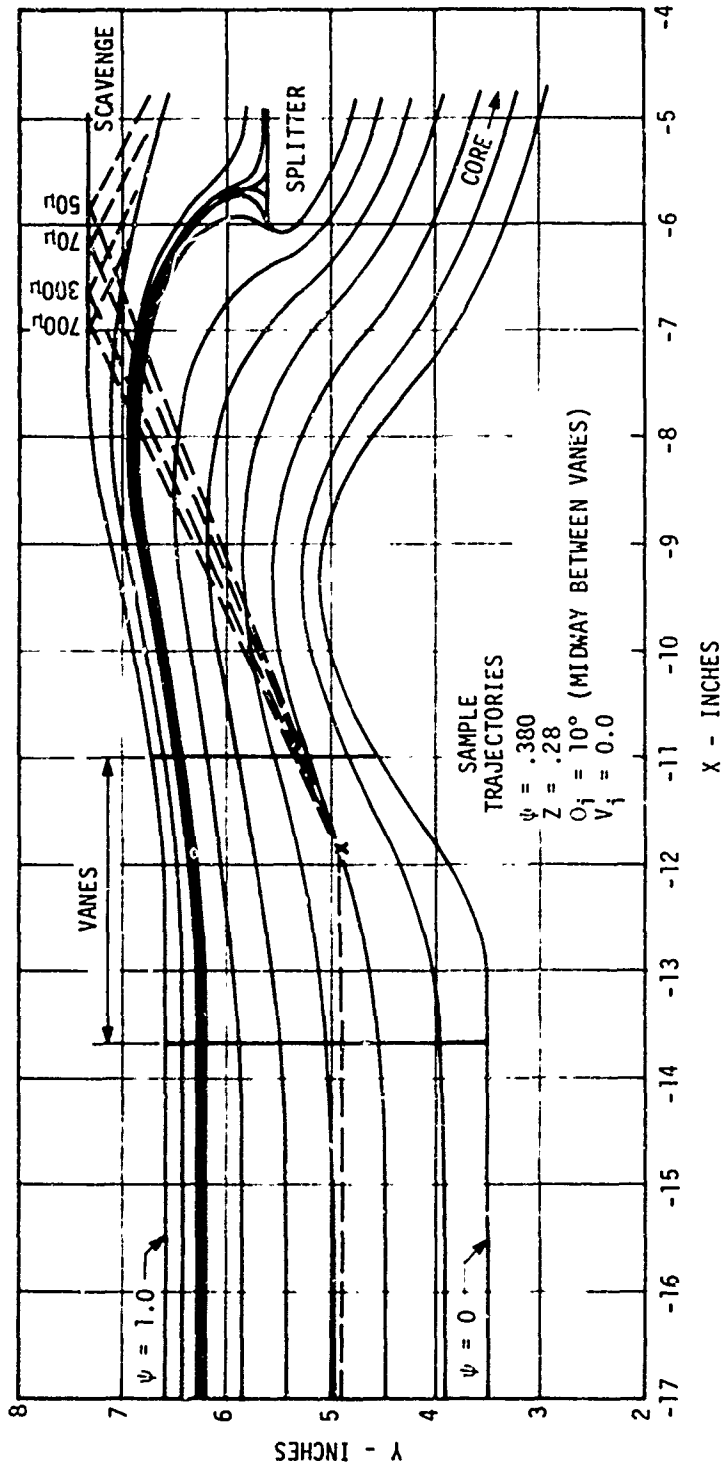


Figure B-9. Trajectories of Particles Injected at $\psi = 0.380$.

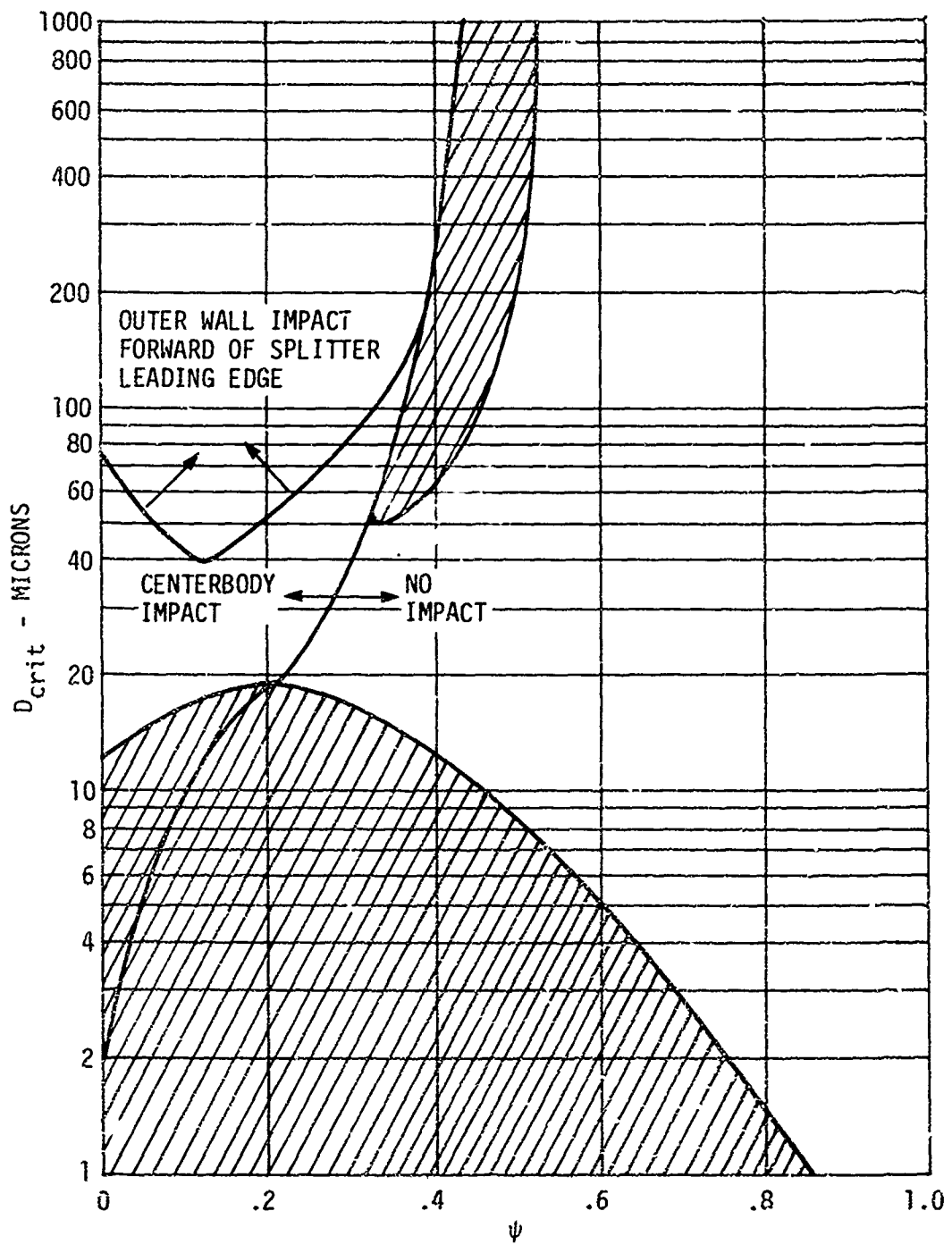


Figure B-10. Critical Diameter Distribution for Figure B-9.

forward of the splitter leading edge. Again particles are started from rest in a cylindrical-walled inlet simulating the bellmouth, and uniform inlet sand distribution is assumed.

The bulk of the analysis of a vaned configuration may be performed by neglecting vane impact phenomena, since the largest effects are due to the imposed swirl field. For $D_p < 20$ microns, the vanes are of little importance since particles of this size follow streamlines quite closely, and only a small number of impacts occur at the vane leading edges. For larger particles, which react much more slowly to streamline curvature changes, vane impact effects are included separately.

The line-of-sight "hole" which would be expected without a swirl field (as in Figure B-4) is reduced to an "island" due to swirl effects. For the smaller size particles, D_c is reduced due to radial acceleration of the swirl field. When vane impacts are included in the analysis, the lower boundary in Figure B-10 remains unchanged. For the larger particles, injection streamlines corresponding to the "island" are of interest. For a certain portion of the island corresponding to injection angle, vane impact occurs, thus imparting a large tangential velocity to the particles. All particles impacting vanes in this region are separated, while particles passing through the vane passage without collision are separated or ingested according to Figure B-10. In order to minimize trajectory calculations, a crossplot may be constructed such as that in Figure B-11, where distance from the vane trailing edge to the particle-vane impact point is plotted versus injection angle. Efficiency of the vanes in this region is then a function of injection angle and essentially independent of particle size. The vane passage efficiency, η_v , is estimated at 0.705. Local efficiency versus injection streamline is plotted on Figure B-12, including the effect of vanes. For the island region of Figure B-10, the local efficiency is

$$\eta_e = 1 - \{ \% (D_{c1}) - \% (D_{c2}) \} \times \eta_v \quad (B-19)$$

where D_{c2} corresponds to the upper boundary in Figure B-10.

D_{c1} corresponds to the lower boundary in Figure B-10.

Analysis Versus Test Results

Results of trajectory analyses performed on three vaneless and one vaned separator are shown in Figure B-13, compared to measured test data. Predicted separation efficiency is consistently high relative to measured efficiency by 0.02 - 0.10 with the assumption of uniform inlet sand density. Agreement between analysis and test could be considerably improved with better definition of initial conditions. Another source of error might lie in the statistical nature of rebound phenomena, an aspect not taken into account in the analysis. Separation efficiencies predicted for the vaned separator where the separation mechanism is mainly aerodynamic are in the closest agreement with measurements.

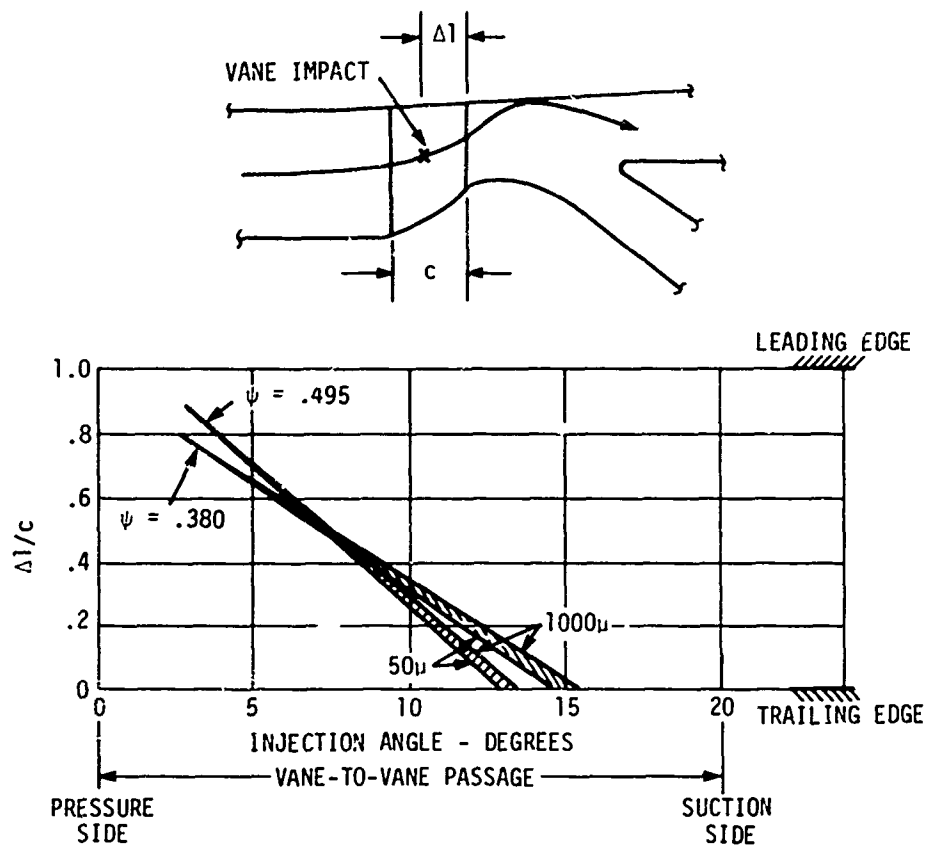


Figure B-11. Vane Impact Profile Crossplot for Figure B-9.

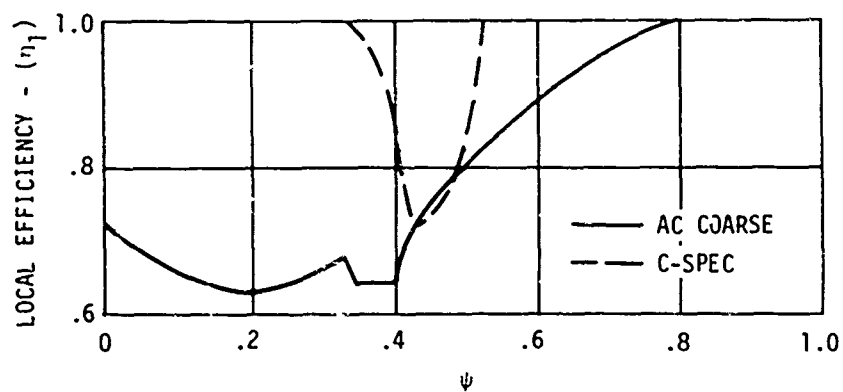


Figure B-12. Local Efficiency Distribution for Figure B-9.

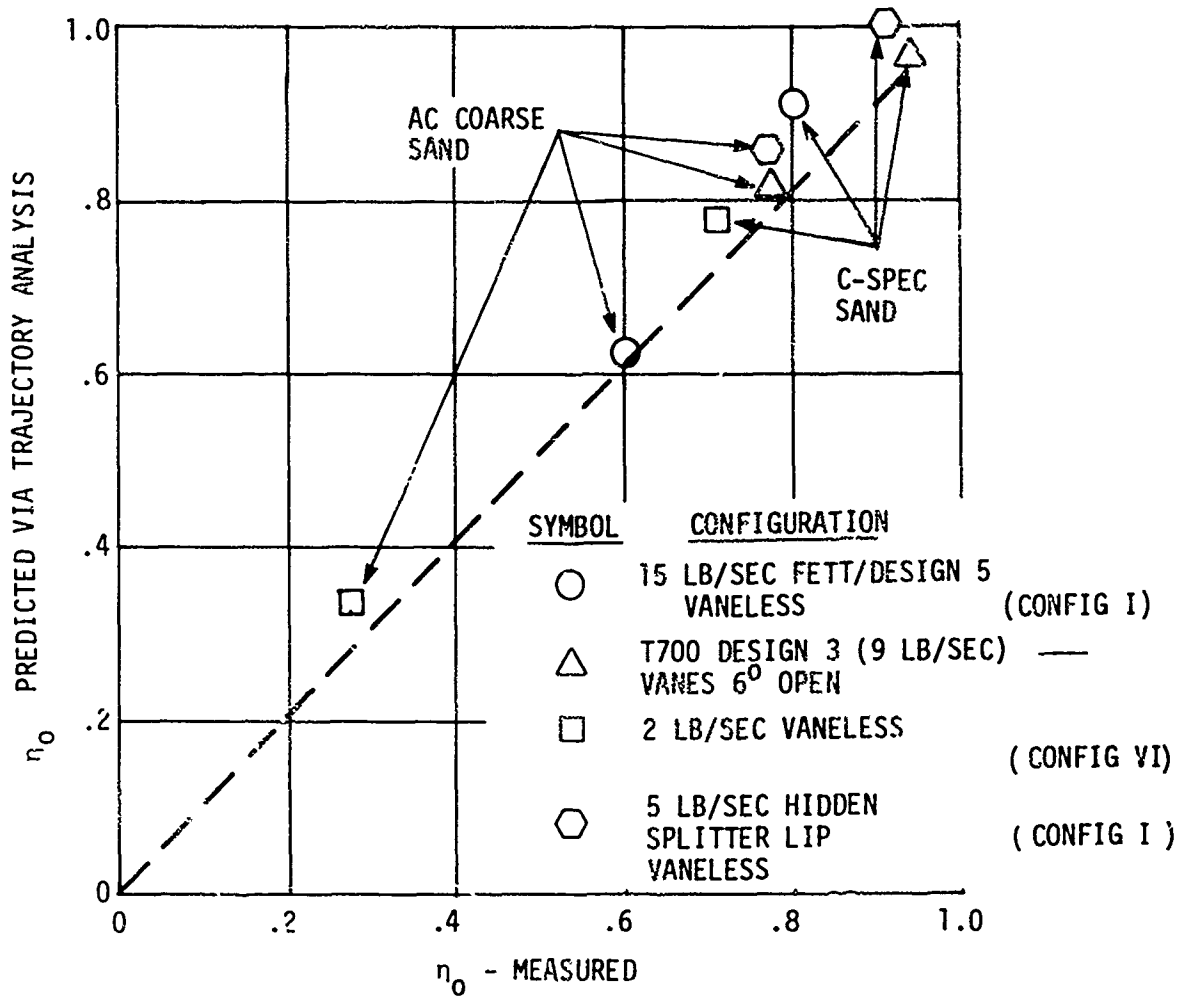


Figure B-13. Comparison of Predicted and Measured Separation Efficiency.

Scaling

If a given separator is scaled by maintaining the velocity field, and altering all physical dimensions by a scale factor (SF), the particle trajectories in the two sizes can be related to the scale factor by

$$D_p/C_d \propto SF \text{ or } D_p \propto SF^a \quad (\text{B-20})$$

for a unique particle trajectory/flow path relationship. In the limit, 0.5 (Stoke's Law) $\leq a \leq$ (C_d independent of Re) for the range or particle sizes and velocities encountered in sand separators, $a \approx 0.62$ based on analytical studies. A trajectory calculated for particle 1, (D_{p1}), for separator 1, is equivalent to the trajectory of particle 2, (D_{p2} = D_{p1} SF^a) in a scaled separator. Hence, D_{c2} = D_{c1} SF^a and separation efficiency can be estimated for the scaled separator by

$$\eta_{e2} = 1 - \% (D_{c1} SF^a) \quad (\text{B-21})$$

and

$$\eta_{o2} = \int_0^1 (C_s/C_o) \eta_{e2} d\psi \quad (\text{B-22})$$

LIST OF SYMBOLS

\bar{a}	acceleration, ft/sec ²
A	area, ft ²
c	chord length, in.
c_o	local sand concentration, mg/ft ³
c_s	average sand concentration, mg/ft ³
C	parameter - $\pi C_d \rho V / 8 \rho_p Z D$
C_d	drag coefficient
d ()	differential
D	diameter, in.
D_{cr}	critical particle diameter, micron
\bar{e}	unit vector
f	function
f_a	depth of erosion, mils
f_d	normalized severity factor
g	acceleration due to gravity, ft/sec ²
h_{is}	isentropic head, ft-lb/lb
l	length, in.
L	axial distance downstream from splitter lip, in.
m	particle mass, lb
M	Mach number
N	speed - rpm
N_s	specific speed
P	pressure, lb/in. ²
Q	volume flow, ft ³ /sec

LIST OF SYMBOLS - Continued

R	radius, in.
R_1	outer wall radius at the separator inlet, in.
Re	Reynolds number
SF	scale factor
t	time, sec
t_m	maximum vane thickness, in.
u	gas velocity, ft/sec
U	blade section tangential velocity, ft/sec
v	particle velocity, ft/sec
v_n	particle velocity normal to impacted surface, ft/sec
v_t	particle velocity tangential to impacted surface, ft/sec
V	relative particle velocity, ft/sec
V_θ	air circumferential velocity, ft/sec
W	mass airflow, lb/sec
z	axial distance downstream from compressor station zero, in.
Z	particle shape factor
β_1	particle incidence angle, deg
β_2	particle rebound angle, deg
ΔP_T	total pressure loss, lb/in. ²
η	separation efficiency
η_c	separation efficiency based on sand concentration
η_w	separation efficiency based on sand weight

LIST OF SYMBOLS - Continued

η_v	vane passage efficiency
μ	air viscosity, lb sec/ft ²
ρ	air density, lb/ft ³
ΣA_t	sum of areas, in ²
ψ	stream function
$\partial()$	partial differential
%	weight fraction of sand with particle diameter less than D_p

SUBSCRIPTS

a	refers to air
c	refers to core
g	refers to gas
l	refers to local conditions
m	indicates maximum
o	refers to average conditions
p	refers to particle
r	radial coordinate
s	refers to sand
t	indicates stagnation conditions
V	refers to relative velocity
Z	axial coordinate
θ	circumferential coordinate